

Characterization Well R-25 Completion Report



*Produced by the Environmental Restoration Project
Groundwater Investigations Focus Area*

Cover photo shows a modified Foremost DR-24 dual-rotary drill rig. The DR-24 is one of several drill-rig types being used for drilling, well installation, and well development in support of the Los Alamos National Laboratory Hydrogeologic Workplan. The Hydrogeologic Workplan is jointly funded by the Environmental Restoration Project and Defense Programs to characterize groundwater flow beneath the 43-square-mile area of the Laboratory and to assess the impact of Laboratory activities on groundwater quality. The centerpiece of the Hydrogeologic Workplan is the installation of up to 32 deep wells in the regional aquifer.

An Affirmative Action/Equal Opportunity Employer

This report was prepared as an account of work sponsored by an agency of the United States Government. Neither the Regents of the University of California, the United States Government nor any agency thereof, nor any of their employees make any warranty, express or implied, or assume any legal liability or responsibility for the accuracy, completeness, or usefulness of any information, apparatus, product, or process disclosed, or represent that its use would not infringe privately owned rights. Reference herein to any specific commercial product, process, or service by trade name, trademark, manufacturer, or otherwise does not necessarily constitute or imply its endorsement, recommendation, or favoring by the Regents of the University of California, the United States Government, or any agency thereof. The views and opinions of authors expressed herein do not necessarily state or reflect those of the Regents of the University of California, the United States Government, or any agency thereof. Los Alamos National Laboratory strongly supports academic freedom and a researcher's right to publish; as an institution, however, the Laboratory does not endorse the viewpoint of a publication or guarantee its technical correctness.

*Characterization Well R-25
Completion Report*

*David Broxton
Rick Warren
Patrick Longmire
Robert Gilkeson
Sue Johnson
David Rogers
William Stone
Brent Newman
Mark Everett
David Vaniman
Steve McLin
Joe Skalski
David Larssen*





A Department of Energy
Environmental Cleanup Program

LA-13909-MS
March 2002
ER2001-0697

Characterization Well R-25 Completion Report



Los Alamos NM 87545

Produced by the Groundwater Investigations Focus Area

Los Alamos National Laboratory, an affirmative action/equal opportunity employer, is operated by the University of California for the United States Department of Energy under contract W-7405-ENG-36.

This report was prepared as an account of work sponsored by an agency of the United States Government. Neither the Regents of the University of California, the United States Government nor any agency thereof, nor any of their employees make any warranty, express or implied, or assume any legal liability or responsibility for the accuracy, completeness, or usefulness of any information, apparatus, product, or process disclosed, or represent that its use would not infringe privately owned rights. Reference herein to any specific commercial product, process, or service by trade name, trademark, manufacturer, or otherwise does not necessarily constitute or imply its endorsement, recommendation, or favoring by the Regents of the University of California, the United States Government, or any agency thereof.

Los Alamos National Laboratory strongly supports academic freedom and a researcher's right to publish; as an institution, however, the Laboratory does not endorse the viewpoint of a publication or guarantee its technical correctness. By acceptance of this article, the publisher recognizes that the U.S. Government retains a nonexclusive, royalty-free license to publish or reproduce the published form of this contribution, or to allow others to do so, for U.S. Government purposes. Los Alamos National Laboratory requests that the publisher identify this article as work performed under the auspices of the U.S. Department of Energy.

TABLE OF CONTENTS

1.0	INTRODUCTION.....	1
PART I: SITE ACTIVITIES.....		1
2.0	SUMMARY OF DRILLING ACTIVITIES.....	1
2.1	Equipment	1
2.2	Schedule.....	3
2.3	Drilling Performance.....	3
2.3.1	Open-Borehole Drilling.....	4
2.3.2	Core Drilling	4
2.3.3	Casing Advancement.....	7
2.3.4	Other Drilling Activities	7
3.0	WELL DESIGN, CONSTRUCTION, AND DEVELOPMENT.....	7
3.1	Well Design	7
3.2	Well Construction	9
3.3	Well Development	12
3.4	Installation of Westbay™ MP55 System	13
3.5	Wellhead Protection	18
4.0	SURVEY ACTIVITIES.....	18
4.1	Geodetic Survey	18
4.2	Surface Radiological Survey	18
PART II: ANALYSES AND PRELIMINARY INTERPRETATIONS		19
5.0	GEOLOGY	19
5.1	Stratigraphic Units	20
5.1.1	Mesa-Top Soil (0- to 1-ft depth)	20
5.1.2	Tshirege Member of the Bandelier Tuff (1- to 384-ft depth)	20
5.1.3	Tephra and Volcaniclastic Sediments of the Cerro Toledo Interval (384- to 509-ft depth).....	28
5.1.4	Otowi Member of the Bandelier Tuff (509- to 843.8-ft depth) and Guaje Pumice Bed (843.8- to 850.5-ft depth).....	28
5.1.5	Puye Formation (Fanglomerate Facies) (850.5 ft to TD of 1942 ft).....	29
5.2	Borehole Geophysics	32
5.2.1	Borehole Logging Activities.....	32
5.2.2	Borehole Geophysical Survey Methods.....	33
5.2.3	Results of Borehole Geophysical Surveys.....	35
6.0	HYDROLOGY	37
6.1	Unsaturated Zone.....	37
6.1.1	Soil-Water Occurrence.....	39
6.1.2	Soil-Water Movement	42
6.1.3	Hydraulic Properties.....	43
6.2	Saturated Zones	44
6.2.1	Groundwater Occurrence.....	44
6.2.2	Groundwater Movement	45

7.0	HYDROCHEMISTRY	48
7.1	Geochemistry of Core and Cuttings	48
7.1.1	HE Compounds, Trace Elements, and Radionuclides.....	48
7.1.2	Anion Profiles and Stable Isotopes	52
7.2	Hydrochemistry of Groundwater	56
7.2.1	Methods	56
7.2.2	Results	57
8.0	MODIFICATIONS TO WORK PLANS.....	67
9.0	SUMMARY OF SIGNIFICANT RESULTS.....	71
9.1	Stratigraphy	71
9.2	Hydrogeology	71
9.3	Geochemistry Results	71
10.0	ACKNOWLEDGEMENTS.....	72
11.0	REFERENCES.....	73

Appendixes

Appendix A	Drilling Chronology
Appendix B	Westbay™ MP55 System Components Installed in Well R-25
Appendix C	Lithologic Log
Appendix D	Descriptions of Geologic Samples
Appendix E	Moisture-Content and Matric-Potential Results
Appendix F	Results of Unsaturated Hydraulic-Property Testing
Appendix G	Groundwater Screening Samples Collected While Drilling R-25 Borehole
Appendix H	Geochemical Calculations and Constraints

List of Figures

Figure 1.0-1	Locations of well R-25 and existing water supply and test wells, with generalized water-level contours	2
Figure 2.3-1	R-25 borehole configuration at total depth.....	8
Figure 3.2-1	As-built well-completion diagram of well R-25	10
Figure 3.2-2	Detail of repaired screen #3 interval in well R-25	11
Figure 3.2-3	Detail from repaired screen #9 to total depth in R-25	12
Figure 5.0-1	Distribution of informal rock units within the Tschicoma Formation, eastern Jemez Mountains.....	19
Figure 5.0-2	Geologic cross-sections through characterization well R-25	21
Figure 5.1-1	Variations in SiO ₂ , Sr, Rb, and Ba in cuttings from the Puye Formation in boreholes R-25, CdV-R15-3, and R-19.....	31
Figure 5.2-1	Results of natural GR surveys conducted on October 14, 1998, and February 27, 1999.....	36

Figure 5.2-2	Results of EM survey conducted on October 14, 1998	38
Figure 6.1-1	Gravimetric moisture content and matric potential in borehole R-25.....	40
Figure 6.1-2	Comparison of moisture-content graphs for boreholes R-25 and R-15.....	41
Figure 6.2-1	Westbay™ versus borehole water-level data for R-25	46
Figure 6.2-2	NW to SE cross-section showing isopotentials and flow near R-25	47
Figure 7.1-1	Pore-water anion concentrations versus depth in R-25.....	54
Figure 7.1-2	Groundwater and pore-water oxygen isotope profile ($\delta^{18}\text{O}$) for borehole R-25	55
Figure 7.2-1	Distribution of HE compounds detected in deep groundwater at borehole R-25.....	60

List of Tables

Table 2.2-1	Comparison of Scoped Versus Actual Completion for Well R-25.....	3
Table 2.3-1	Performance Statistics for Well R-25 Drilling Program	4
Table 2.3-2	Fluids Used During Drilling R-25.....	5
Table 3.1-1	Screen Placements in Well R-25	9
Table 3.2-1	Characteristics of Rod Base Screens Installed in R-25	11
Table 3.4-1	Depths of Key Westbay™ MP55 System Components in Well R-25	15
Table 4.1-1	Geodetic Data for Well R-25	18
Table 5.1-1	Comparison of Stratigraphic Units Encountered in Borehole R-25.....	22
Table 5.1-2	Chemical Analyses of Rock Units Penetrated During Drilling of Borehole R-25	23
Table 5.1-3	Quartz as Percent of Felsic Phenocrysts Within Cooling Units of the Tshirege Member	25
Table 5.1-4	Quantitative X-Ray Diffraction Analyses for Borehole R-25	25
Table 5.1-5	Petrographic Description of Informal Stratigraphic Units Within the Tschicoma Formation in the Eastern Jemez Mountains	29
Table 5.1-6	Percentages of Clasts Within Polished Thin Sections Derived from Different Units Within the Tschicoma Formation.....	30
Table 5.2-1	Borehole Logging Surveys at R-25	33
Table 6.1-1	Samples from R-25 Tested for Hydraulic Properties	43
Table 7.1-1	Core and Cuttings Samples Selected for Contaminant Characterization	49
Table 7.1-2	HE Compound, Trace Element, and Radionuclide Analytes for R-25 Core, Cuttings, and Water Samples.....	49
Table 7.1-3	Estimates of Pore Water Anion Concentrations in R-25 Samples.....	53
Table 7.2-1	R-25 Groundwater Sample Depths, Analyses, and Sampling Zones	56
Table 7.2-2	Field-Measured Parameters for R-25 Groundwater Samples	58
Table 7.2-3	HE Chemistry of R-25 Groundwater Samples	59
Table 7.2-4	Analytical Results for Selected Trace Elements and Major Ions in R-25 Groundwater Samples	61
Table 7.2-5	Tritium Activities in R-25 Groundwater Samples	64

Table 7.2-6	Stable Oxygen and Hydrogen Isotope Data for Water Samples from R-25 and Selected Springs	64
Table 7.2-7	Summary of Nitrogen Chemistry and Nitrogen Isotopes for Water Samples from R-25, Surface Water, and Selected Background Springs.....	65
Table 8.0-1	Activities Planned for R-25 Compared with Work Performed	67

List of Acronyms and Abbreviations

AIT	array induction tool
API	American Petroleum Institute
APS	accelerator porosity sonde
APT	accelerator porosity tool
ASTM	American Society for Testing and Materials
BD	below detection
bgs	below ground surface
CATMS	cations analyzed by mass spectrometry
CMR	combinable magnetic resonance
cps	counts per second
CVAA	cold vapor atomic absorption
DO	dissolved oxygen
DOC	dissolved organic carbon
DR	dual rotation
DX	Dynamic Experimentation (Division)
Eh	decreasing oxidation-reduction potential
EM	electromagnetic induction
EPA	Environmental Protection Agency
FIP	field implementation plan
FMI	formation microimager
foc	fraction of solid organic carbon
FSF	field support facility (part of the Environmental Restoration Project)
ft MSL	feet above mean sea level
FY	fiscal year
GC/MS	gas chromatography/mass spectrometry
GFAA	graphite furnace atomic absorption
GPS	global positioning system
GR	gamma radiation
HA	health advisory
HAA	hydride atomic absorption
HE	high explosive

HMX	octahydro-1,3,5,7-tetranitro-1,3,5,7-tetrazocine
HNGS	hostile environment natural gamma sonde
HPLC	high-performance liquid chromatography
HSA	hollow-stem auger
IC	ion chromatography
ICPES	inductively coupled plasma atomic emission spectroscopy
I.D.	inner diameter
IRMS	isotope ratio mass spectrometry
Kd	distribution coefficient
Koc	organic carbon partition coefficient
LATA	Los Alamos Technical Associates, Inc.
LANL	Los Alamos National Laboratory
LDT	lithodensity tool
LIKPA	laser-induced kinetic phosphorimetric analysis
Ma	mega-annum; million years
MCL	maximum contaminant level
NAD83	North American Datum of 1983
NMED	New Mexico Environment Department
NMR	nuclear magnetic resonance
NMWQCC	New Mexico Water Quality Control Commission
NTU	nephelometric turbidity unit
O.D.	outer diameter
PCB	polychlorinated biphenyl
PID	photoionization detector
PPE	personal protection equipment
QA	quality assurance
RC	reverse circulation
RCRA	Resource Conservation and Recovery Act
RCT	radiological control technician
RDX	hexahydro-1,3,5-trinitro-1,3,5-triazine (research department explosive)
Rf	retardation factor
SAIC	Science Applications International Corporation
SAPP	sodium acid pyrophosphate
SVOC	semivolatile organic compound
TA	technical area
TAL	target analyte list
TD	total depth
TDS	total dissolved solids

3-D	three-dimensional
TOC	total organic carbon
TNT	2,4,6-trinitrotoluene
UTL	upper tolerance limit
VOC	volatile organic compound
WCO	wet chemical oxidation
WCSF	waste characterization strategy form

Metric to English Conversions

Multiply SI (Metric) Unit	by	To Obtain US Customary Unit
kilometers (km)	0.622	miles (mi)
kilometers (km)	3281	feet (ft)
meters (m)	3.281	feet (ft)
meters (m)	39.37	inches (in.)
centimeters (cm)	0.03281	feet (ft)
centimeters (cm)	0.394	inches (in.)
millimeters (mm)	0.0394	inches (in.)
micrometers or microns (μm)	0.0000394	inches (in.)
square kilometers (km^2)	0.3861	square miles (mi^2)
hectares (ha)	2.5	acres
square meters (m^2)	10.764	square feet (ft^2)
cubic meters (m^3)	35.31	cubic feet (ft^3)
kilograms (kg)	2.2046	pounds (lb)
grams (g)	0.0353	ounces (oz)
grams per cubic centimeter (g/cm^3)	62.422	pounds per cubic foot (lb/ft^3)
milligrams per kilogram (mg/kg)	1	parts per million (ppm)
micrograms per gram ($\mu\text{g/g}$)	1	parts per million (ppm)
liters (L)	0.26	gallons (gal.)
milligrams per liter (mg/L)	1	parts per million (ppm)
degrees Celsius ($^{\circ}\text{C}$)	$9/5 + 32$	degrees Fahrenheit ($^{\circ}\text{F}$)

CHARACTERIZATION WELL R-25 COMPLETION REPORT

by

**David Broxton, Rick Warren, Patrick Longmire, Robert Gilkeson, Sue Johnson, David Rogers,
William Stone, Brent Newman, Mark Everett, David Vaniman, Steve McLin,
Joe Skalski, David Larssen**

ABSTRACT

Characterization well R-25, located on the mesa top above Cañon de Valle in the southwestern portion of Los Alamos National Laboratory (LANL, or the Laboratory), is the third well installed as part of the implementation of the "Hydrogeologic Workplan" (LANL 1998, 59599). Well R-25 was funded by the Nuclear Weapons Infrastructure, Facilities, and Construction Program (Defense Program) and installed by the Environmental Restoration Project. Well R-25 is primarily designed to provide water-quality, geochemical, hydrologic, and geologic information that would contribute to the understanding of the hydrogeologic setting beneath the Laboratory.

The R-25 borehole was drilled to a depth of 1942 ft using air-rotary drilling methods. Well R-25 was constructed with nine screened intervals; however, two of the screens, screens #3 and #9, were damaged during well-installation activities. Screens #3 and #9 were restored to partial usefulness, and all well screen intervals were developed prior to installation of a multiport sampling system (WestbayTM).

The geologic strata encountered during borehole advancement included, in descending order, the Tshirege Member of the Bandelier Tuff, tephra and volcanoclastic sediments of the Cerro Toledo interval, the Otowi Member of the Bandelier Tuff, and the Puye Formation. Lithologies and thicknesses were typical for all units except the Cerro Toledo interval and Puye Formation, which were much thicker than expected.

Groundwater occurrences included an upper saturated zone, a zone of alternating wet and dry conditions, and regional saturation. The upper saturated zone was first recognized at a depth of 747 ft within the Otowi Member and had a static level of 711 ft. The zone extended into the Puye Formation to a depth of 1132 ft, making it the thickest perched zone encountered thus far on the Pajarito Plateau. Regional saturation was encountered at a depth of 1286 ft and was continuous to the borehole total depth (TD) of 1942 ft. Hydraulic head measurements in the regional aquifer decreased with depth, suggesting that there is a strong downward vertical gradient, and that well R-25 is located in a recharge area.

Samples of geologic core and cuttings were collected and analyzed for chemical and hydraulic properties. Most analytes were either not detected or their concentrations were within the upper tolerance limits (UTLs) of naturally occurring constituents. Pore-water ion profiles corresponded to moisture content profiles.

Samples of groundwater were collected from the upper saturated zone, the wet/dry zone, and the regional aquifer and analyzed for organic chemicals, inorganic chemicals, and radiochemical components. Significant findings included (1) concentrations of high explosive (HE) compounds in the regional aquifer that were greater than Environmental Protection Agency (EPA) health advisory limits, (2) nitrate concentrations that were greater than those observed at Water Canyon Gallery southwest of well R-25 within the Sierra de los Valles, (3) an isotopic signature for nitrate that was similar to that of nitric acid used during preparation of BaNO₃, RDX, and TNT, and (4) measurable activities of tritium that suggest that travel times to the upper saturated zone are approximately 10 to 50 years. These findings suggest that surface sources of water and contaminants have reached the regional aquifer in the vicinity of well R-25.

1.0 INTRODUCTION

This well completion report describes the drilling, construction, completion, and testing activities performed for characterization well R-25. Well R-25 is located on the south rim of Cañon de Valle, within Technical Area (TA) 16, near the southwestern boundary of the Laboratory, as shown in Figure 1.0-1. It is the third of up to 32 characterization wells to be drilled down to the regional aquifer, as described in the "Hydrogeologic Workplan" (LANL 1998, 59599), in support of the Laboratory's "Groundwater Protection Management Program Plan" (LANL 1996, 70215).

Well R-25 was funded by the Nuclear Weapons Infrastructure, Facilities, and Construction Program (Defense Program) and installed by the Laboratory's Environmental Restoration Project. Well R-25 is designed to provide water-quality and water-level data for intermediate-depth perched groundwater and the regional aquifer in a previously poorly characterized area of the Laboratory. Well R-25 is also intended to provide hydrologic and geologic information that will contribute to the understanding of the hydrogeologic setting beneath the Laboratory. Data collected from the R-25 site will be used, in conjunction with data from other planned characterization boreholes as well as other sources, to evaluate and update sitewide hydrologic and geologic conceptual models.

Preliminary interpretations are presented for some of the data collected, but discussion of other data has been deferred until the data can be evaluated in the context of sitewide information collected from other hydrogeologic characterization wells. A future report will provide an integrated human health and ecological risk assessment and will include groundwater data from other nearby Environmental Restoration Project wells.

PART I: SITE ACTIVITIES

2.0 SUMMARY OF DRILLING ACTIVITIES

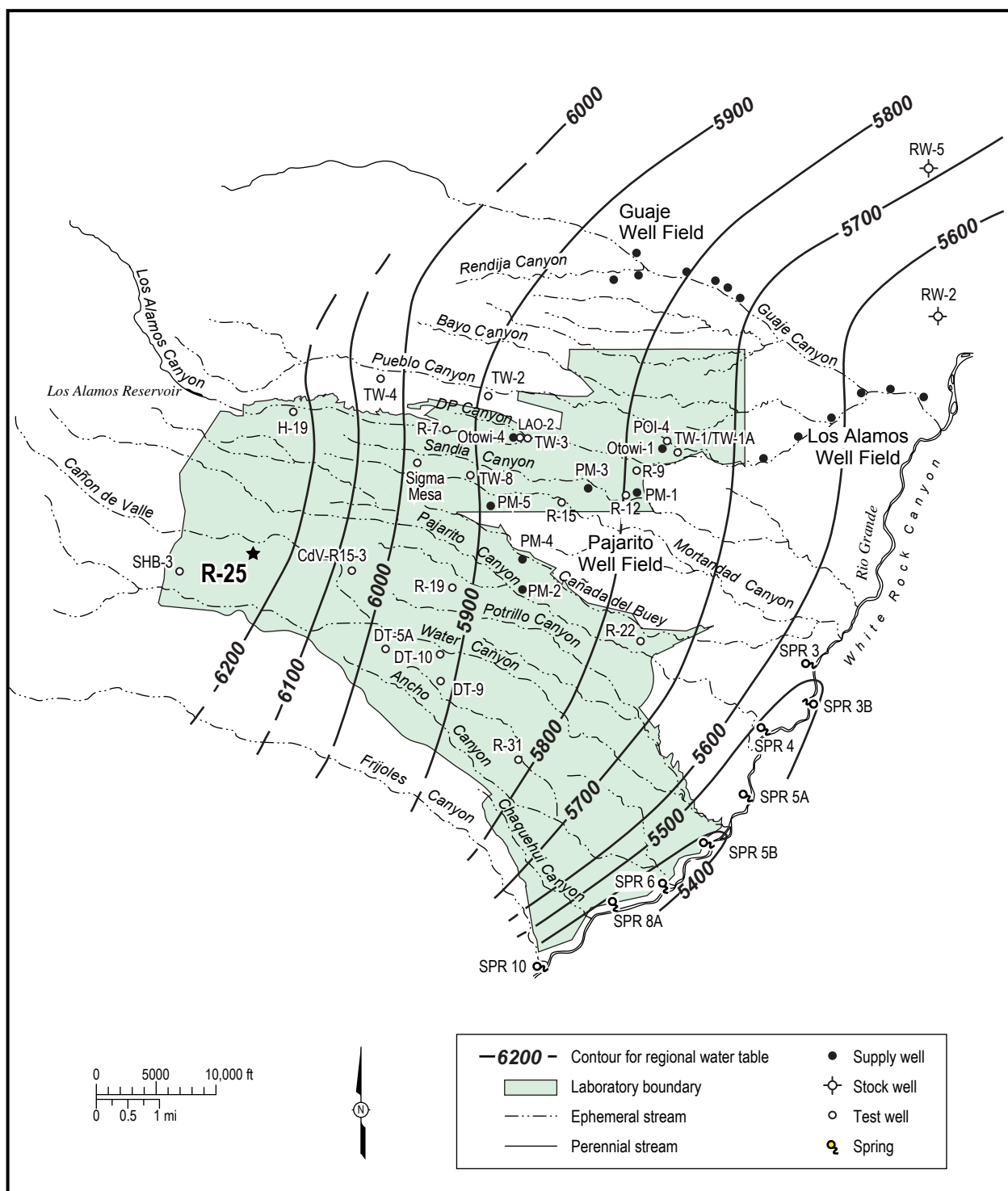
The R-25 borehole was advanced to a depth of 1942 ft, and a nine-screen stainless steel monitoring well was installed. This section summarizes drilling and well construction activities.

2.1 Equipment

Borehole R-25 was drilled by Dynatec Environmental Drilling Company (formerly Tonto) and was the first well at the Laboratory to be drilled using a Foremost™ dual rotation (DR-24) drill rig. Dynatec provided 3-man drilling crews, crew vehicles, drilling hammers and bits, Longyear 134-mm coring and dual-wall rod systems, a 1-ton flatbed truck, and a 5-ton boom truck for handling casing, drill pipe, and heavy support apparatus such as casing jacks.

Two of the nine screens (i.e., screens #3 and #9) in the completed well were damaged during well installation. Repairs to the damaged screens were made with a Universal drill rig 1000 and Longyear HQ (3 1/16-in. inner diameter [I.D.]/3 1/2-in. outer diameter [O.D.]), NQ (2 3/8-in. I.D./2 3/4-in. O.D.), and BQ (1 13/16-in. I.D./2 3/16-in. O.D.) coring systems. TAM and Baski inflatable packers were also used in the repair process.

The Environmental Restoration Project's Field Support Facility (FSF) provided drill casings, drilling bits, a small front-end loader, dust suppression systems, field support trailers for logging and sampling, water containment tanks, drums for cuttings, a Hermit data logger, depth-to-water meters, water sampling bailers, pressure transducers, and a diesel-powered electric generator. The Laboratory's Environmental Science and Waste Technology group provided onsite water sample testing and a filtering apparatus. Both the Geology and Geochemistry group and the FSF provided microscopes for analyzing drill cuttings.



Source: Purtymun 1984, 6513

F1-1 / R-25 WELL COMPLETION RPT / 081399

Figure 1.0-1. Locations of well R-25 and existing water supply and test wells, with generalized water-level contours

2.2 Schedule

Drilling operations began on July 22, 1998. All drilling operations combined, including borehole advancement, coring, sampling, installation of the well casing, plugging of screen #3 and redrilling through the screened interval, installation of the replacement screen for screen #9, installation of the WestbayTM sampling system, and site restoration, required 378 12-hour shifts as of May 17, 2001.

Drilling activities were conducted from approximately 6:00 A.M. to 6:00 P.M. Monday through Friday until May 10, 1999, after which date drilling was conducted 24 hr per day and 7 days per week. Repair and development activities were conducted from approximately 6:00 A.M. to 6:00 P.M. The chronology of drilling operations at the R-25 site is summarized in Appendix A.

Table 2.2-1 compares the scope for well R-25 to the original scope projected in well-installation planning documents. In the planning documents, well R-25 was designed to be 1550 ft deep with a single screened interval. However, the budget estimate was prepared for a single-screen well option and a nine-screen well option. During drilling, the scope and well design were modified to include characterization of the vertical extent of HE contamination encountered. Based on information gathered during drilling, a nine-screen well with a multiport sampling system was selected for the well design.

Table 2.2-1
Comparison of Scoped Versus Actual Completion for Well R-25

	Hydrogeologic Workplan	R-25 Field Implementation Plan	Actual
Completion depth (ft)	1500	1550	1942
Completion design	Single screen	Single screen	Multi-screen (9)

2.3 Drilling Performance

The techniques used to drill R-25 consisted of air-rotary coring, solid-stem auger placement of a surface casing, and air-rotary under-reamer advance of three different casing strings. In addition, other drilling operations involved borehole/corehole/casing drill-out, casing retraction, reaming, and cleaning. Changing drilling systems typically involved tripping out one system, modifying the drilling head and/or circulation plumbing, and tripping in another drilling system from the ground surface to the depth of operations. Telescoping down to the next largest diameter drill casing involved landing the first casing string, changing the table drive jaws, and tripping in the new casing string. Performance statistics are summarized in Table 2.3-1.

From the ground surface to 1942 ft, the total footage drilled using the different drilling techniques and casing sizes was 2100.7 ft. The total footage drilled does not include the footage of one drill system or casing size tripped in or out of another drill system or casing size. The total trip-in footage was 41,722.0 ft, and the total trip-out footage was 47,491.0 ft. Trip-out footage for the casing includes the intervals where the casing was within the next larger casing string. It does not include the intervals where the casing was being retracted for monitoring well completion (i.e., backfilling operations).

Air-rotary advancement of drill casing was performed without fluid assist until 588 ft. After that depth various combinations of water, bentonite, fibrous material, and TORKease® were added for lubricity down to a depth of 1427 ft (Table 2.3-2). From 1507.5 ft to 1547 ft, QUIK-FOAM® and EZ-MUD *plus*® were also added for lubricity.

Table 2.3-1
Performance Statistics for Well R-25 Drilling Program

	Open Hole	Core	9 5/8-in. Casing ^{a,b}	11 3/4-in. Casing ^b	13 3/8-in. Casing ^b	Casing Advance System (4 1/2-in. rods) ^a	Casing Advance System (7-in. rods) ^b	Total (ft)
Total footage drilled (ft)	2	200.5 ^c	751.2	579.0	568	451.2	1415	2100.7
Total footage rate (ft/hr) ^d	1.9	7.5	9.2	19.1	17.1	7.1	16.2	12.2
Tshirege Member footage (ft)	—	84	—	—	351.5	—	351.5	434.6
Tshirege Member rate (ft/hr) ^d	—	7.8	—	—	19.2	—	19.2	15.0
Cerro Toledo footage (ft)	—	24.5	—	—	120.0	—	120.0	149.5
Cerro Toledo rate (ft/hr) ^d	—	13.3	—	—	14.2	—	14.2	14.0
Otowi Member footage (ft)	—	57.5	—	202.0	64.5	—	266.5	321.5
Otowi Member rate (ft/hr) ^d	—	9.0	—	22.2	14.1	—	19.4	16.2
Puye Formation footage (ft)	2	34.5	751.2	377.0	—	451.2	677.0	1162.7
Puye Formation rate (ft/hr) ^d	1.9	4.3	9.2	17.7	—	7.1	17.3	10.5
Trip-in footage (ft)	—	5750.0	1210.0	1590.0	—	16,087.0	17,085.0	41,722.0
Trip-in rate (ft/hr) ^d	—	352.0	138.5	171.6	—	535.3	419.4	396.9
Trip-out footage (ft)	—	5492.0	1230.0	1616.0	—	19,217.0	19,936.0	47,491.0
Trip-out rate (ft/hr) ^d	—	316.2	113.4	128.4	—	453.2	404.4	358.4
Reaming footage (ft)	—	—	560.5	38.0	803.0	—	—	1401.5
Reaming rate (ft/hr) ^d	—	—	28.0	24.0	15.9	—	—	19.5

^a Mitsubishi 9 5/8-in. casing advance systems use 4 1/2-in. reverse circulation (RC) rods.

^b AR Holte 9 5/8-in., 11 3/4-in., and 13 3/8-in. casing advance systems use 7-in. RC rods.

^c TD of borehole is 1942 ft. Total cored footage (200.1 ft) is 10.3% of total borehole footage (1942 ft).

^d Rates are weighted averages over footages drilled or tripped, excluding breaks, repairs, and change-out of tools.

2.3.1 Open-Borehole Drilling

Open-borehole drilling was attempted at a depth of 1153 ft within the Puye Formation. The drilling crew drilled 2 ft of open borehole in loose sand and gravel using a 9 1/4-in.-diameter tricone roller bit. The drilling rate accomplished was 1.9 ft per hour. Because the Puye Formation is an unconsolidated unit, open-borehole drilling proved inefficient and was abandoned.

2.3.2 Core Drilling

Core was collected from the R-25 borehole to provide undisturbed samples for geologic, contaminant, and hydrologic characterization. In addition, core was used to assist in the identification of the perching layer beneath the upper zone of groundwater and to provide information for placing casing seals. A total of 200.5 ft of the R-25 borehole was cored (10.3% of the total 1942-ft depth). Average core recovery was 65.1%. Coring operations were performed with a Longyear 134-mm coring system.

Table 2.3-2
Fluids Used During Drilling R-25

Date	Placement Pathway ^a	Depth(ft)	QUIK-FOAM® (gal.)	EZ-MUD plus® (gal.)	MF-1 floculant (lb)	Ben-seal Bentonite (50-lb bags)	Bentonite Gel (50-lb bags)	Aqua-Guard Bentonite (50-lb bag)	Pel-Plug Bentonite (gal.)	Cellophane (25-lb bag)	Mag Fiber (30-lb bag)	Nylon (1-lb bag)	TORKease® (gal.)	Water (gal.)
22-Sep-98	annulus	588	—	—	—	3	—	—	—	—	—	—	2	100
23-Sep-98	annulus	637	—	—	—	3	1	—	—	—	—	—	3.5	150
25-Sep-98	annulus	667	—	—	—	—	2	—	—	—	—	—	6.5	250
2-Oct-98	annulus	778	—	—	—	3	—	—	—	—	—	—	2.5	150
28-Oct-98	annulus	1066	—	—	—	3	—	—	—	—	—	0.5	—	200
29-Oct-98	annulus	1107	—	—	—	3	—	—	—	—	—	0.5	12.5	200
3-Nov-98	annulus	1137	—	—	—	3	—	—	—	—	—	—	2.5	150
5-Nov-98	rods	1153	—	—	—	0.5	1	3	—	—	0.25	1	2.5	415
7-Nov-98	rods	1155	—	—	—	3	2	6	—	—	0.5	2	—	565
9-Nov-98	rods	1155	—	—	—	7	2	4	—	—	1	4	—	300
10-Nov-98	rods	1155	—	—	—	3	2	—	—	—	0.25	—	2.5	415
11-Nov-98	annulus	1155	—	—	—	4	2	—	—	—	—	4	—	300
13-Nov-98	annulus	1155	—	—	—	16	6	4	—	3	—	2	—	900
14-Nov-98	annulus	1155	—	—	—	12	6	12	—	2	—	6	—	900
16-Nov-98	rods	1157	—	—	—	4	2	4	—	0.66	—	—	—	565
23-Nov-98	rods	1175	—	—	—	11	3	10	5	1	—	—	—	730
9-Dec-98	annulus	1200	—	—	—	3	1	—	—	—	—	—	2.5	150
10-Dec-98	annulus	1211	—	—	—	3	3	—	—	—	—	—	12.5	300
11-Dec-98	annulus	1211	—	—	—	—	2	—	—	—	—	—	5	150
13-Dec-98	annulus	1211	—	—	—	—	3	—	—	—	—	—	5	300
15-Dec-98	annulus	1217	—	—	—	3	1	—	—	0.75	—	—	2.5	150
8-Jan-99	annulus	1427	—	—	—	—	4	—	—	0.5	—	—	—	2575
15-Jan-99	annulus	1507.5	—	—	—	—	—	—	—	—	—	—	—	1300

Table 2.3-2 (continued)

Date	Placement Pathway ^a	Depth(ft)	QUIK-FOAM® (gal.)	EZ-MUD plus® (gal.)	MF-1 flocculant (lb)	Ben-seal Bentonite (50-lb bags)	Bentonite Gel (50-lb bags)	Aqua-Guard Bentonite (50-lb bag)	Pel-Plug Bentonite (gal.)	Cellophane (25-lb bag)	Mag Fiber (30-lb bag)	Nylon (1-lb bag)	TORKease® (gal.)	Water (gal.)
19-Jan-99	rods	1507.5	5	—	—	—	—	—	—	—	—	—	—	6400
20-Jan-99	open casing	1507.5	—	—	1	—	—	—	—	—	—	—	—	14
27-Jan-99	annulus	1507.5	—	—	—	—	3	—	—	0.25	—	—	—	450
28-Jan-99	rods	1507.5	0.25	0.5	—	—	—	—	—	—	—	—	—	250
2-Feb-99	rods	1547	0.1	—	—	—	—	—	—	—	—	—	—	20
Total			5.35	0.5	1	87.5	46	43	5	8.16	2	20	62	18349

^a Rods indicates fluids were introduced downhole at the drill bit via drill rods; annulus indicates fluids were introduced at the surface in the annular space between the drill casing and the borehole wall; open casing indicates fluids were introduced inside drill casing, at the surface, after drill rods were removed from the borehole.

Only 133.3 ft of the 200.1 ft cored were actually recovered: 71.1 ft were recovered from the Tshirege Member at an average rate of 7.8 ft per hour and an average recovery of 84.6%; 7.2 ft were recovered from the Cerro Toledo interval at an average rate of 13.3 ft per hour and an average recovery of 29.4%; 33.1 ft were recovered from the Otowi Member at an average rate of 9.0 ft per hour and an average recovery of 57.6%; and 21.9 ft were recovered from the Puye Formation at an average rate of 4.3 ft per hour and an average recovery of 63.5%.

2.3.3 Casing Advancement

After the 16-in.-diameter surface casing was installed, three telescoped casing strings were installed to advance the borehole and to prevent the upper saturated zone from communicating downhole as the borehole advanced (see Figure 2.3-1). The 13 3/8-in. casing was landed in unsaturated Otowi Member tuff at 578 ft. This casing began to tighten up in the borehole when the Otowi Member was first encountered at 509 ft, and the casing finally became stuck at 578 ft. The 11 3/4-in. casing was then advanced to 1175 ft within a zone of alternating wet and dry conditions. A bentonite grout seal was pressure-injected to seal the casing in place temporarily. The 9 5/8-in. casing was then advanced to the TD of 1942 ft. Table 2.3-1 and Figure 2.3-1 show the casings and casing advance systems used.

2.3.4 Other Drilling Activities

Other drilling activities included reaming the borehole and attempting to free the 13 3/8-in. casing stuck at 578-ft depth. These activities also included cleaning clogged bits, center tubes, and air lines.

A total of 72 hr were spent reaming to keep the casing from binding in the formation. A total of 1401.5 ft of borehole was reamed. Of the total 72 hr, 50 hr were spent reaming with the 13 3/8-in. casing in the variably indurated units of the Bandelier Tuff and the Cerro Toledo interval. Approximately 1.5 hr were spent reaming with the 11 3/4-in. casing, and the remaining 20 hr were spent reaming with the 9 5/8-in. casing in the variable fanglomerates of the Puye Formation.

After the 13 3/8-in. casing became stuck in the hole at 578 ft, the 11 3/4-in. casing was advanced within the 13 3/8-in. casing to 1026 ft. Attempts were then made to free the 13 3/8-in. casing before proceeding further. A retract hammer and spear assembly was deployed down the borehole to loosen the 13 3/8-in. casing. When it became apparent that the entire casing could not be removed, the hammer and spear assembly was used to separate the casing joint at 508 ft, leaving the lowermost 70 ft of casing (508 to 578 ft) in the hole.

3.0 WELL DESIGN, CONSTRUCTION, AND DEVELOPMENT

The R-25 borehole was completed as a nine-screen stainless steel monitoring well. The following sections discuss the design, completion, and development activities.

3.1 Well Design

Geophysical logs, video logs, borehole core and cuttings, water-quality data, water-level data, and drillers' observations were reviewed by the Groundwater Integration Team to plan screen placements for well construction. The number and placement of screens were designed to meet the following criteria:

- to establish the distribution of HE contaminants in the upper zone of saturation and to determine vertical head data for this zone (screens #1, #2, and #3)

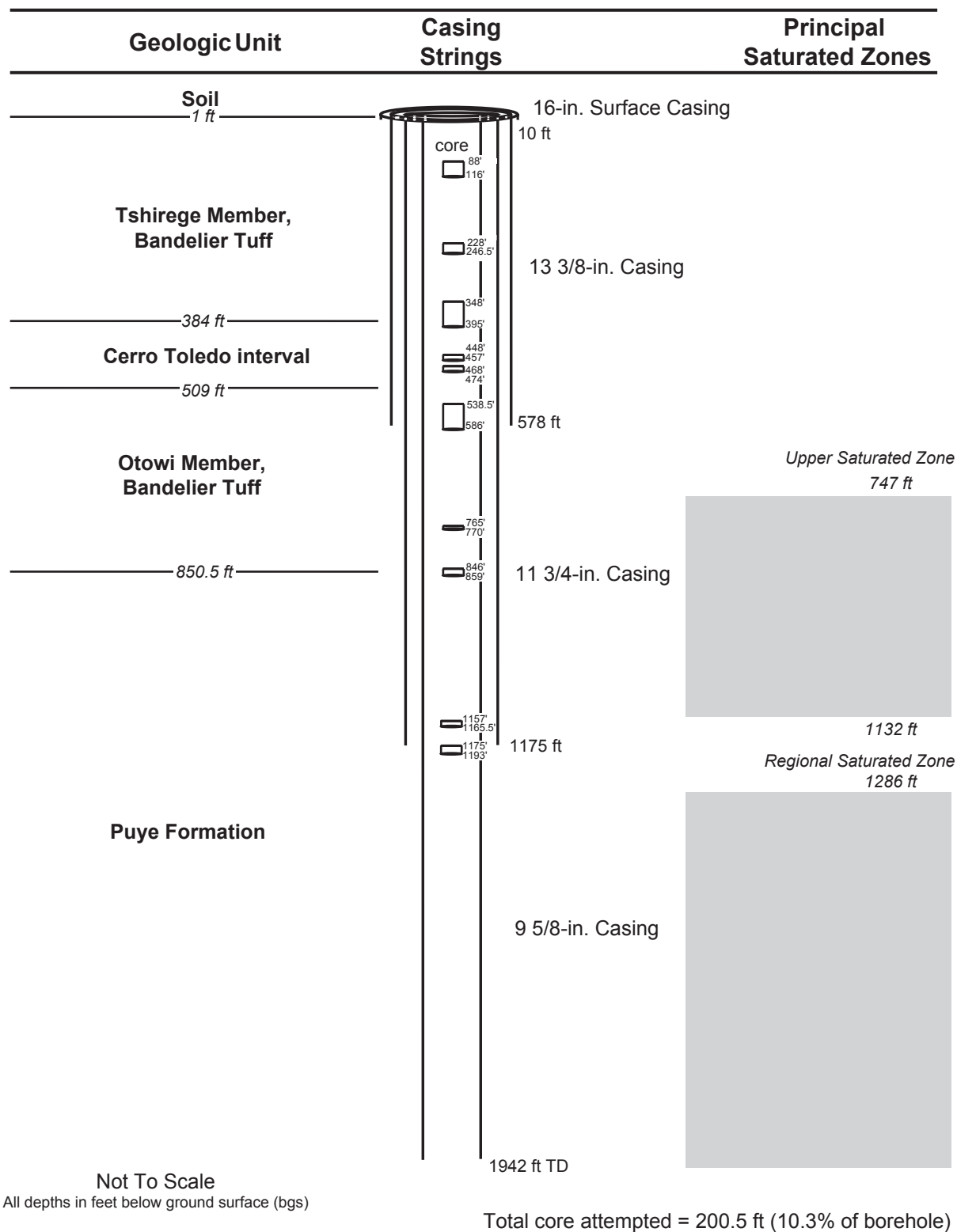


Figure 2.3-1. R-25 borehole configuration at total depth

- to determine whether the alternating wet and dry zone from 1132 to 1286 ft is hydraulically connected to the upper saturated zone and/or the regional zone of saturation (screen #4)
- to determine the water quality and water level at the top of the regional zone of saturation (screen #5)
- to determine the vertical extent of HE contamination and to establish vertical head data for the regional zone of saturation (screens #6, #7, #8, and #9)

The screen placements in well R-25 are given in Table 3.1-1.

Table 3.1-1
Screen Placements in Well R-25

Screen #	Depth (ft)	Geologic/Hydrologic Setting
1	737.6–758.4	Otowi Mbr., uppermost saturation in the upper zone of saturation
2	882.6–893.4	Puye Fm., high HE concentrations in the upper zone of saturation
3	1054.6–1064.6	Puye Fm., zone of highest HE concentrations in the upper zone of saturation
4	1184.6–1194.6	Puye Fm., low HE concentrations in the alternating wet and dry zone
5	1294.7–1304.7	Puye Fm., top of regional zone of saturation; no HE detected during drilling
6	1404.7–1414.7	Puye Fm., highest HE detected in the regional zone of saturation during drilling
7	1604.7–1614.7	Puye Fm., regional zone of saturation; HE detected
8	1794.7–1804.7	Puye Fm., regional zone of saturation; no HE detected
9	1894.7–1904.7	Puye Fm., regional zone of saturation; no HE detected; lowest possible position for a screen above the sump

3.2 Well Construction

The as-built well-completion drawing for well R-25 is shown in Figure 3.2-1. The well was constructed of Schedule 40 304-stainless steel casing with Schedule 80 threaded ends. The lower 900 ft of casing and screen were connected with F480 (American Society for Testing and Materials [ASTM]) threading. The upper 1034 ft were connected with a heavier duty Ventura Flush Joint thread. The well was constructed with rod base screens as described in Table 3.2-1.

The annular space outside each screen was filled with 20/40 sand. An interval of fine sand (30/70) was placed both above and below each screen's sand pack to keep the bentonite grout from infiltrating the 20/40 sand pack. Because of difficulties accurately tagging the top of annular materials at such great depths and under saturated conditions, some 30/70 sand buffers were not installed.

The nine screened intervals were isolated from one another with bentonite seals in the annular space between the outer casing and the borehole wall. The seal was a 50:50 mix, by weight, of 20/40 sand and granular bentonite. The bentonite seal was tremied in either dry or with a transport fluid. From the bottom of the hole up to 1026 ft, the transport fluid consisted of a bentonite, water, and retardant (Catalyst™) mix. The retardant was used to keep the bentonite from expanding in the tremie line within the saturated zone. From 1026 ft up to 610 ft, above the top of the upper saturated zone, the transport fluid was municipal water. Above the saturated zone, the bentonite was introduced dry.

Table 3.2-1
Characteristics of Rod Base Screens Installed in R-25

Screens	I.D. (in.)	O.D. (in.)	Horizontal Wrap Wire (in.)	Vertical Rod (in.)	Number of Rods	Slot Size (in.)	Well Screen Open Area (%)
1 and 2	5.17	5.98	0.118	0.250	32	0.010	7.9
3 through 9	5.17	5.98	0.093	0.093	32	0.010	10.4

Filter-pack sands and bentonite seals were tremied into the annular space between the well casing and the borehole wall as the drill casing was retracted in stages. Placement of annular materials and drill casing retraction were performed concurrently because sloughing of unstable borehole walls could have caused bridging in the annulus and prevented proper placement of sands and bentonite. All drill casing was removed from the borehole during well construction except for the 70-ft section of 13 3/8-in. casing that was stuck and abandoned from 508 to 578 ft.

Screens #3 and #9 were damaged during well construction and were repaired to restore their usefulness. Figure 3.2-2 depicts the final completion of the screen #3 interval. The Westbay™ multiport sampling system was successfully deployed through the repaired screen. The repaired screen provides reliable water head data and access for collection of water samples. The usability of the water chemistry data for the characterization of HE contamination will be determined following the collection of 4 rounds of samples from the well. Figure 3.2-3 depicts the final completion of the screen #9 interval. A transducer installed in screen #9 provides pressure data for the deepest part of the well and will be used with transducers installed in the other well screens to determine vertical head gradients for the TA-16 area.

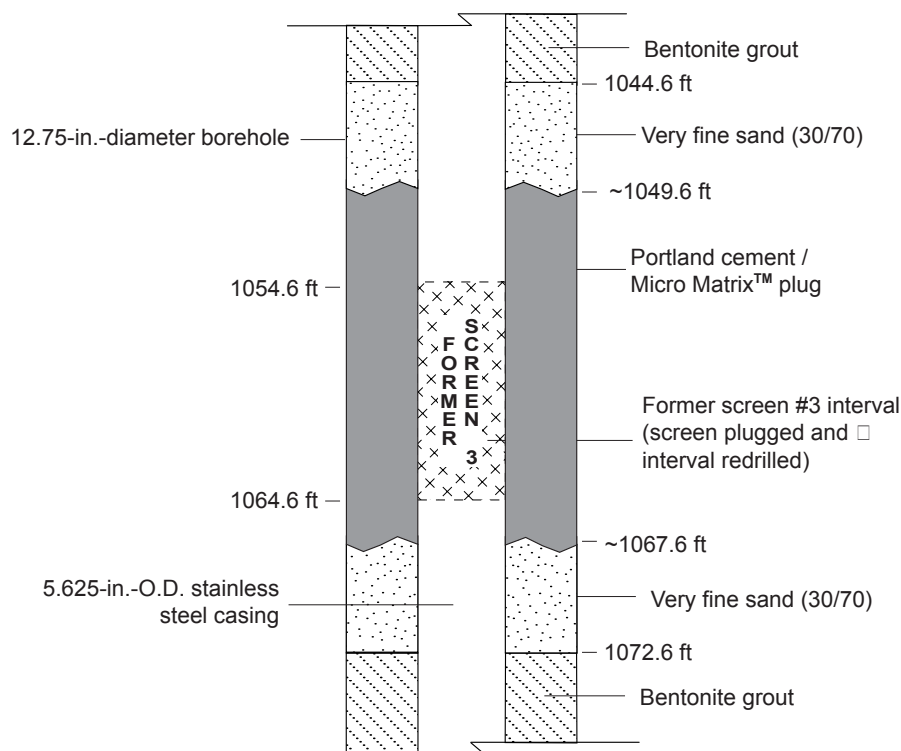


Figure 3.2-2. Detail of repaired screen #3 interval in well R-25

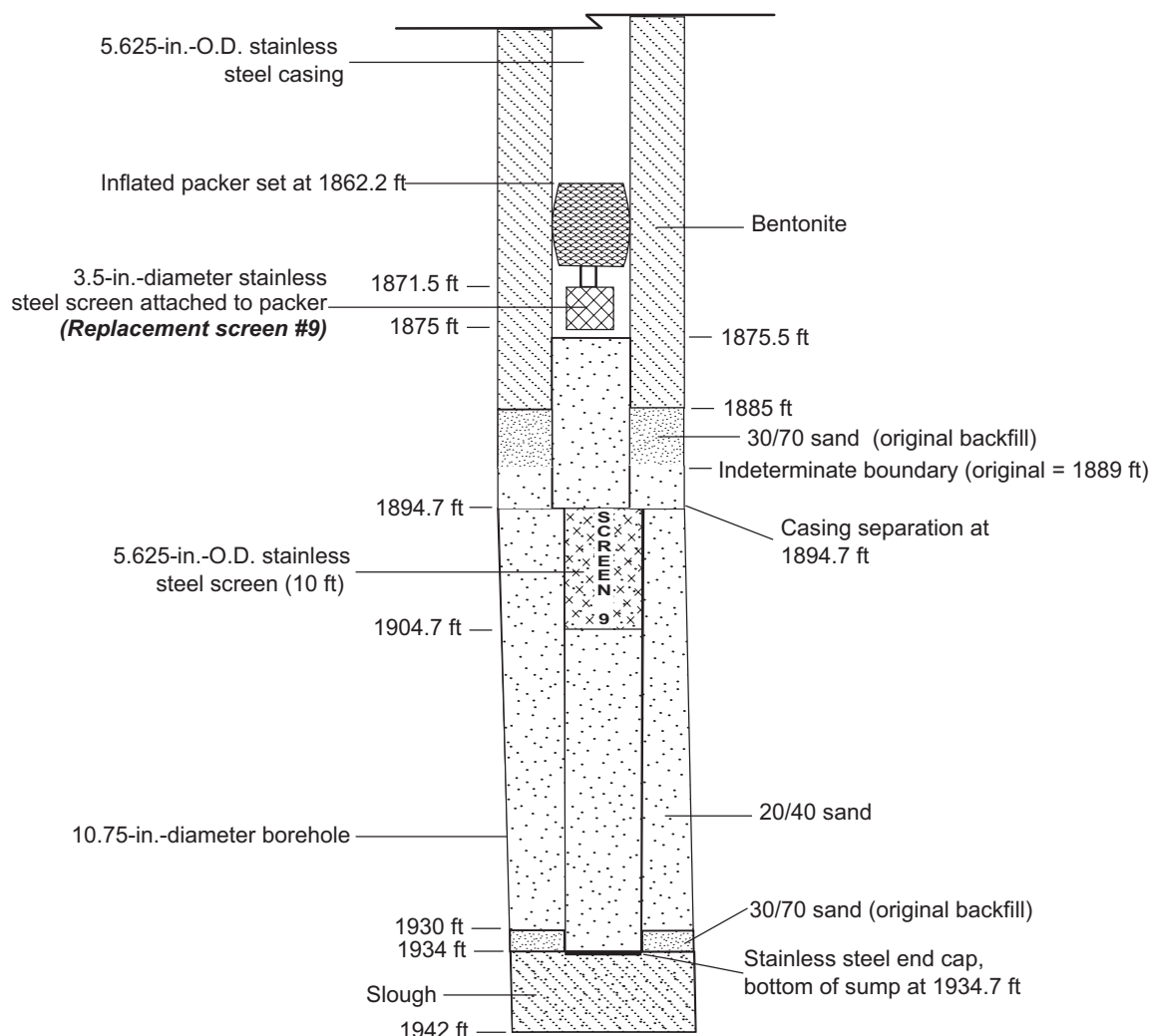


Figure 3.2-3. Detail from repaired screen #9 to total depth in R-25

3.3 Well Development

Prior to screen repair, the following well development activities were performed. Screens #1, #2, #4, #5, #6, #7, and #8 were pressure washed with a water solution containing sodium acid pyrophosphate (SAPP). Some purging of the lower part of the well, below the screen #3 interval, was also conducted. In addition, screens #2 and #8 were partially developed by airlifting water prior to the repairs to screens #3 and #9.

Purging included the introduction of 900 gal. of water into the well and the removal of 1200 gal., 300 gal. of which were formation water. Development included airlifting 39,000 gal. of water from the cased interval between screens #8 and #9. Development also included airlifting 500 gal. from a depth corresponding to screen #2.

After repairs to screens #3 and #9 and injection tests were completed, development activities continued. Starting on January 18, 2000, screens #1 and #2 were scrubbed with a wire brush, and then all screens, except #3 and #9, were jetted. A pump was lowered to 1760 ft, and the well was purged. Pumping continued until February 3, 2000.

Development resumed on April 13, 2000. Screens #1 and #2 were again scrubbed. Water in the well was then airlifted from just above replaced screen #9 (~1850 ft). A submersible pump was then used to target individual screens. Starting with screen #4, the pump was moved down through screened intervals until water-quality parameters were optimized.

Beginning on May 4, 2000, the lower screens (#4 to #8) were scrubbed. The pump was again moved through the screened intervals. The Cerro Grande fire interrupted operations, and development did not resume until September 13, 2000. Pump development continued until the turbidity was as low as attainable, with a final reading of 11.9 NTU. A total of 192,000 gal. of water were removed during development operations following screen repair.

3.4 Installation of Westbay™ MP55 System

Following well development, the Westbay™ MP55 system for groundwater monitoring was installed in the well. The Model 2523 MOSDAX System sampler probe was used to collect groundwater samples from the completed well.

An MP Casing Installation Log, which specifies the location of each Westbay™ MP55 System component, was prepared in the field by Westbay™ in consultation with the Laboratory based on a draft of the well completion diagram. Available geophysical survey results and an as-built video taken of the inside of the well casing were also reviewed before measurement ports, pumping ports, and packers were sited within the well. The final version of the MP Casing Installation Log was approved in the field on September 26, 2000, by the Laboratory prior to installation of the Westbay™ components. The MP Casing Installation Log as approved was used as the installation guide in the field.

A measurement port coupling and associated magnetic location collar were included in each of the eight primary monitoring zones to provide the capability to measure fluid pressures and collect fluid samples. A pumping port coupling was also included in the primary zones to provide purging, sampling and hydraulic conductivity testing capabilities. Additional measurement port couplings were included below the pumping ports in the primary zones to allow future monitoring of hydraulic tests.

Measurement port couplings were included in quality assurance (QA) zones to provide QA testing capabilities. Measurement ports were positioned below each of the packers to permit routine operation of the squeeze relief venting with the packer inflation equipment during the inflation process.

The casing components were set out in sequence according to the MP Casing Installation Log on racks near the borehole. Each casing length was numbered in order, beginning with the lowermost, as an aid in confirming the proper sequence of components. The sequential casing component numbers are given on the MP Casing Installation Log and are used in the following text to identify selected casing components (packers and ports).

The arrangement of the bottom two components was modified in the field just before they were lowered into the well, resulting in an extra component being added. This changed the numbering scheme of the casing. To avoid having to reprint the complete log, the modification was entered by hand on the last page of the log, and the extra piece of casing added was assigned the number 1A. In later printings of the Summary MP Casing Log, the sequential numbers assigned to the casing are in the correct sequence and differ by 1 (the extra piece of casing, No. 1A) from the sequential numbers listed on the MP Casing Installation Log.

The appropriate MP55 System coupling was attached to each piece of casing. Magnetic location collars were attached 2.5 ft below the measurement ports in each of the primary monitoring zones and 2.5 ft below coupling No. 99 near the top of the well.

Abrasion protectors (9-in.-long and 4.3-in.-O.D.) were placed above and below each measurement port, pumping port, and packer installed below screen #3. The purpose was to decrease the possibility of the casing hanging up or suffering damage when passing through the uneven borehole and protruding metal fragments observed by the video log in and below screen #3.

The length of each casing section was measured with a steel tape to confirm nominal lengths, and the data were entered on the MP Casing Installation Log and in the Well Designer file for the well. Each casing component was visually inspected, and serial numbers for each packer, measurement port coupling, and pumping port coupling were recorded on the field copy of the MP Casing Installation Log.

The casing components were lowered into the well in sequence. The first 15 sections of casing were lowered by hand, and a Smeal work-over rig provided by the Laboratory was used to lower the remaining casing components. Each casing joint was tested with a minimum internal pressure of 300 psi for one minute to confirm hydraulic seals. De-ionized water provided by Morrison Knudsen Corp. was used for the joint tests. A record of each successful joint test and the placement of each casing component is on the field copy of the MP Casing Installation Log.

The suspended weight of the casing components was monitored during lowering to confirm that the operating limits of the components were not exceeded. The casing hung up in the well on several occasions during the lowering. On September 28, 2000, the casing hung up for several hours, with No. 144 about 4.5 ft above ground. It was suspected that the bottom of the casing, at about 1087.5 ft, had encountered a section of irregular well pipe or open borehole below screen #3. After repeated attempts, the casing passed by the obstruction. Lowering of the casing to the target position was successfully completed on September 28, 2000.

After the casing was lowered into the borehole, the water level inside the casing was at a depth of more than 1506 ft below the top of the casing, confirming the hydraulic integrity of the casing. The open-hole water level was about 1224 ft below ground level. The casing water level was too deep to measure with the available electric water-level tape. A hydraulic integrity test was conducted by observing the water level inside the casing for one hour during the Pre-Inflation Pressure Profile done on September 29, 2000. With this differential pressure acting on the casing string, the water level inside the casing was stable. The test indicated that the casing was water tight.

After the components were lowered into the well and the hydraulic integrity of the casing had been confirmed, the casing string was positioned as shown in Appendix B. The datum for the borehole was ground level. The casing string was supported with the top of coupling No. 222 at a depth of 6.3 ft. An additional 1.5-m length of casing, identified as No. 223, was added to the casing string for later use during de-stressing of the casing.

The packers were inflated on September 29 to October 2, 2000, using de-ionized water. The packers were inflated in sequence beginning with the lowermost. All of the packers were inflated successfully, and QA tests showed that all of the packer valves were closed and sealed.

The WestbayTM procedure for de-stressing the casing was used after all of the packers had been inflated. The top casing (No. 223) was cut and trimmed to suit the final configuration of the wellhead assembly, and the top completion was installed. The final position of casing No. 223 was 3.18 ft above ground. The final tensile load at the top of the casing was 500 lb. The maximum limit for long-term tensile loading of the casing is 1000 lb (454 kg). A sketch of the as-built top of the casing and final positions of the WestbayTM components is included in Appendix B, and a summary of depth information for key components is provided in Table 3.4-1.

Table 3.4-1
Depths of Key Westbay™ MP55 System Components in Well R-25

Zone No. ^a	Screen Interval (ft) ^b	Sand Pack Interval (ft) ^b	Casing No. (from MP Log)	Packer No.	Packer Serial No. (0612)	Nominal Packer Position ^c (ft)	Magnetic Collar Depth ^b (ft)	Measurement Port Depth ^c (ft)	Pumping Port Depth ^c (ft)	Port Name ^d
QA-1	—	—	186	—	—	—	364.4	361.9	—	QA-1
—	—	—	185	1	120	372.1	—	—	—	—
QA-2	—	—	150	—	—	—	None	710.6	—	QA-2
—	—	—	149	2	118	720.8	—	—	—	—
SQA1	—	—	148	—	—	—	None	725.3	—	SQA1
—	—	—	147	3	060	730.7	—	—	—	—
Zone 1	738.1–757.9	727.6–766.4	144	—	—	—	757.3	754.8	—	MP1A
			143	—	—	—	—	—	760.1	PP1
			142	—	—	—	—	765.8	—	MP1B
—	—	—	141	4	057	769.4	—	—	—	—
LQA1	—	—	140	—	—	—	—	773.9	—	LQA1
—	—	—	131	5	059	862.8	—	—	—	—
SQA2	—	—	130	—	—	—	—	867.3	—	SQA2
—	—	—	129	6	157	872.6	—	—	—	—
Zone 2	883.1–892.9	872.6–903.4	126	—	—	—	894.3	891.8	—	MP2A
			125	—	—	—	—	—	897.2	PP2
			124	—	—	—	—	902.8	—	MP2B
—	—	—	123	7	142	906.5	—	—	—	—
LQA2	—	—	122	—	—	—	—	911.0	—	LQA2
—	—	—	109	8	173	1034.4	—	—	—	—
SQA3	—	—	108	—	—	—	—	1038.8	—	SQA3
—	—	—	107	9	155	1044.2	—	—	—	—
Zone 3	1055.1–1064.1	1044.6–1072.6	104	—	—	—	—	1063.4	—	MP3A
			103	—	—	—	1065.9	—	1068.8	PP3
			101	—	—	—	—	1084.2	—	MP3B
—	—	—	100	10	147	1089.6	—	—	—	—

Table 3.4-1 (continued)

Zone No. ^a	Screen Interval (ft) ^b	Sand Pack Interval (ft) ^b	Casing No. (from MP Log)	Packer No.	Packer Serial No. (0612)	Nominal Packer Position ^c (ft)	Magnetic Collar Depth ^b (ft)	Measurement Port Depth ^c (ft)	Pumping Port Depth ^c (ft)	Port Name ^d
LQA3	—	—	99	—	—	—	—	1094.1	—	LQA3
—	—	—	91	11	146	1168.3	—	—	—	—
SQA4	—	—	90	—	—	—	—	1172.8	—	SQA4
—	—	—	89	12	162	1178.1	—	—	—	—
Zone 4	1185.9–1194.1	1174.6–1202.6	87	—	—	—	1194.9	1192.4	—	MP4A
			86	—	—	—	—	—	1197.8	PP4
			85	—	—	—	—	1203.4	—	MP4B
—	—	—	84	13	073	1207.2	—	—	—	—
LQA4	—	—	83	—	—	—	—	1211.6	—	LQA4
—	—	—	75	14	104	1279.3	—	—	—	—
SQA5	—	—	74	—	—	—	—	1283.7	—	SQA5
—	—	—	73	15	058	1289.1	—	—	—	—
Zone 5	1295.1–1304.1	1284.6–1312.6	71	—	—	—	1305.9	1303.4	—	MP5A
			70	—	—	—	—	—	1308.8	PP5
			69	—	—	—	—	1314.4	—	MP5B
—	—	—	68	16	055	1318.2	—	—	—	—
LQA5	—	—	67	—	—	—	—	1322.6	—	LQA5
—	—	—	60	17	171	1387.0	—	—	—	—
SQA6	—	—	59	—	—	—	—	1391.5	—	SQA6
—	—	—	58	18	145	1396.9	—	—	—	—
Zone 6	1405.1–1414.1	1394.6–1422.6	56	—	—	—	1408.8	1406.3	—	MP6A
			55	—	—	—	—	—	1411.7	PP6
			54	—	—	—	—	1417.3	—	MP6B
—	—	—	53	19	154	1421.1	—	—	—	—
LQA6	—	—	52	—	—	—	—	1425.6	—	LQA6
—	—	—	35	20	061	1586.8	—	—	—	—
SQA7	—	—	34	—	—	—	—	1591.3	—	SQA7
—	—	—	33	21	108	1596.6	—	—	—	—

Table 3.4-1 (continued)

Zone No. ^a	Screen Interval (ft) ^b	Sand Pack Interval (ft) ^b	Casing No. (from MP Log)	Packer No.	Packer Serial No. (0612)	Nominal Packer Position ^c (ft)	Magnetic Collar Depth ^b (ft)	Measurement Port Depth ^c (ft)	Pumping Port Depth ^c (ft)	Port Name ^d
Zone 7	1605.1–1614.1	1594.6–1622.6	31	—	—	—	1608.5	1606.0	—	MP7A
			30	—	—	—	—	—	1611.4	PP7
			29	—	—	—	—	1617.1	—	MP7B
—	—	—	28	22	063	1620.8	—	—	—	—
LQA7	—	—	27	—	—	—	—	1625.3	—	LQA7
—	—	—	11	23	165	1776.7	—	—	—	—
SQA8	—	—	10	—	—	—	—	1781.2	—	SQA8
—	—	—	9	24	024	1786.6	—	—	—	—
Zone 8	1795.1–1804.1	1784.6–1812.6	7	—	—	—	1798.5	1796.0	—	MP8A
			6	—	—	—	—	—	1801.4	PP8
			5	—	—	—	—	1807.0	—	MP8B
—	—	—	4	25	163	1810.7	—	—	—	—
SQA9	—	—	3	—	—	—	—	1815.2	—	SQA9
—	—	—	2	26	030	1820.6	—	—	—	—
Zone 9	1895.1–1904.1	1884.6–1912.6	1	—	—	—	1827.6	1825.1	—	MP9
				—	—	—	—	—	—	—
				—	—	—	—	—	—	—

^a QA = quality assurance zone or port, LQA = long quality assurance zone or port, SQA = short quality assurance zone or port.

^b All depths are with respect to ground surface.

^c All depths of MP55 System casing components are the depth to the top of the respective coupling.

^d MP = measurement port, PP = pumping port.

After packer inflation was completed, fluid pressures were measured at each measurement port. The fluid pressure profile measurements were taken on October 3 and 4, 2000. At that time, the in-situ formation pressures may not have recovered from the pre-installation and installation activities. Longer term monitoring may be required to establish representative fluid pressures.

Plots of the piezometric levels in all zones, including QA zones, based on the September 29, October 3, and October 4 pressure measurements, were examined to confirm proper operation of the measurement ports and as a check on the presence of annular seals between adjacent monitoring zones. All of the measurement ports operated normally. Each of the packers was supporting a differential hydraulic pressure, indicating the presence of packer seals.

3.5 Wellhead Protection

After the well was completed and the Westbay™ sampling system installed, a 10-ft x 5-ft x 6-in., 3000-psi concrete surface pad was poured. A coupling pipe for a solar panel energy source was set in the concrete. Bollards were cemented 2 ft into the ground with a 3-ft stickup on all four sides of the pad. Drill cuttings were used to recontour the site to approximate the original grade. The ground was reseeded with native grasses and fertilized. Erosion control structures (straw bales) destroyed in the Cerro Grande fire were replaced.

4.0 SURVEY ACTIVITIES

4.1 Geodetic Survey

The location of well R-25 was determined by geodetic survey on April 20, 2001, using a Wild/Leica TC 1000 total station. Control for the survey was provided by Stations 1420 and 1421 from the 1992 Laboratory-wide control network. Field measurements were reduced using LisCad Plus® 5.0 surveying software.

The survey located the brass cap monument in the southeast corner of the concrete pad at the well and measured elevations at the top of the well casing and the top of the Westbay™ sampling system aluminum plate (Table 4.1-1). Horizontal well coordinates are New Mexico State Plane Grid Coordinates, Central Zone (North American Datum of 1983 [NAD 83]) and are expressed in feet. Elevation is expressed in feet above mean sea level relative to the National Geodetic Vertical Datum of 1929. The Facility for Information Management, Analysis, and Display (FIMAD) location number for well R-25 is 16-05961.

Table 4.1-1
Geodetic Data for Well R-25

Point	Easting (ft)	Northing (ft)	Elevation (ft)
Brass monument	1615178.42	1764060.50	7516.1
Top of stainless steel well casing	1615177.17	1764063.00	7518.8
Top of Westbay™ plate	1615177.11	1764062.93	7518.0

4.2 Surface Radiological Survey

A surface radiological survey was conducted before drilling activities began at the R-25 site. The predrilling radiation survey was conducted on July 7, 1998, and consisted of collecting alpha and beta/gamma background measurements and conducting statistical analysis to calculate action levels.

Calculated background values for the drill site were 0.4 cpm for alpha, 216.8 cpm for beta/gamma, and 17.2 μ R/hr for dose rate.

Established action levels are used as a basis to determine if borehole materials screened during drilling exhibit radioactivity above surface background values. The survey area consisted of 15 points spaced out in a grid pattern projected over the work area. Each point was surveyed using direct-reading alpha, beta/gamma, and dose rate meters. Alpha was measured using a Ludlum Model 139 with air proportional probe; beta/gamma was measured using an ESP-1 with an HP-260 probe; dose rate was measured using a Ludlum Model 19 μ R/hr meter.

PART II: ANALYSES AND PRELIMINARY INTERPRETATIONS

5.0 GEOLOGY

Well R-25 is located near the western edge of the Pajarito Plateau, 1.9 km east of the Pajarito fault zone that separates the plateau from the Jemez Mountains to the west. Generally dacitic lavas of the Tschicoma Formation form bedrock within the higher terrain of the eastern Jemez Mountains (Smith et al. 1970, 09752). The Tschicoma Formation, emplaced mostly during the Early Pliocene epoch, consists of overlapping volcanic dome complexes and associated lava flows that aggregate to thicknesses that probably exceed 5000 ft locally. Several individual units, described below, have been characterized just west of well R-25 (Figure 5.0-1). These units of the Tschicoma Formation are the subject of on-going field and laboratory investigations and are not yet defined as formal stratigraphic units.

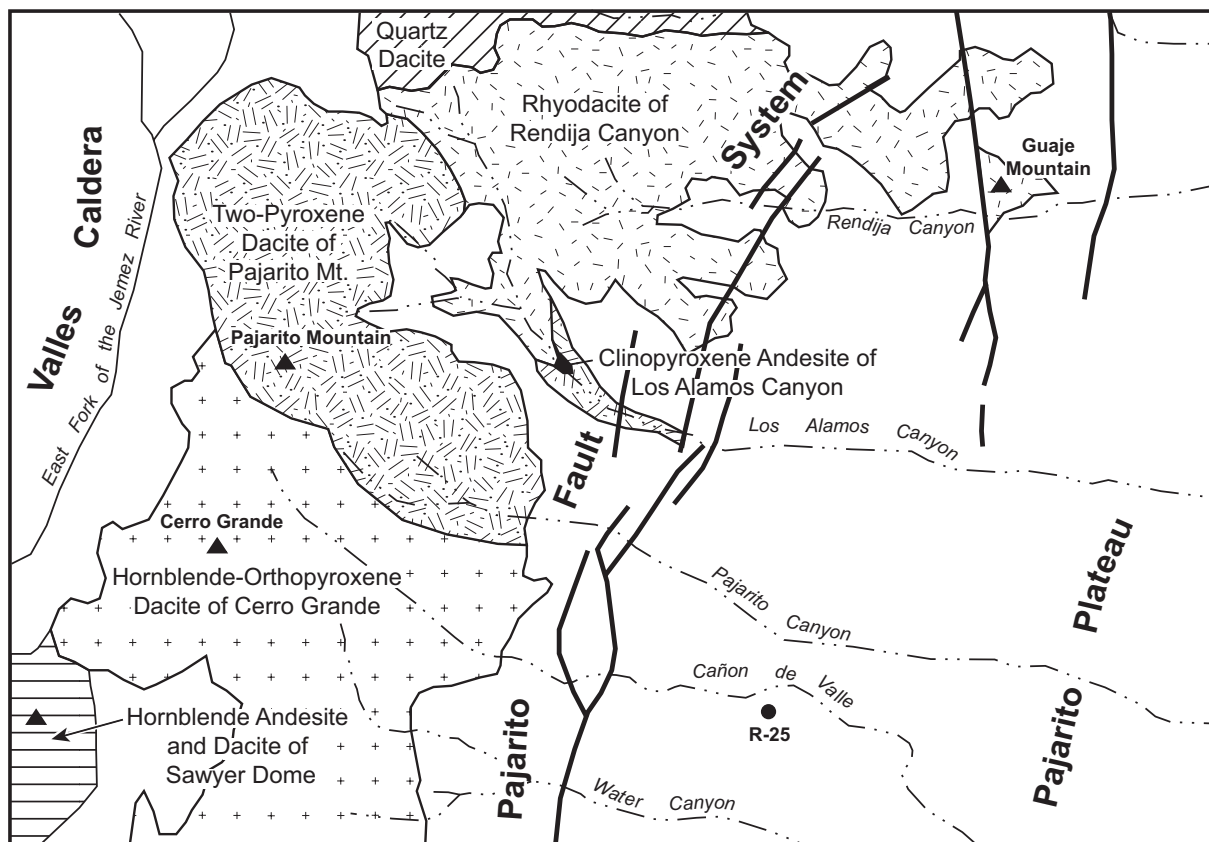


Figure 5.0-1. Distribution of informal rock units within the Tschicoma Formation, eastern Jemez Mountains

The Pajarito Plateau was formed by outflow sheets of the Bandelier Tuff that erupted from the Valles caldera in the central part of the Jemez Mountains. Two major eruptions emplaced the Otowi and Tshirege Members of the Bandelier Tuff 1.61 and then 1.22 million years ago (Ma), respectively (Izett and Obradovich 1994, 48817). In the western part of the Laboratory, these ignimbrites buried the Puye Formation, a fanglomerate unit derived from erosion of the Tschicoma Formation (Griggs 1964, 8795; Waresback 1986, 58715). Puye deposits onlap and interfinger with the Tschicoma Formation in the subsurface near the western edge of the Pajarito Plateau. The Puye Formation is the upper part of the regional aquifer in the western and central part of the plateau. Cross-sections through well R-25 (Figure 5.0-2) illustrate these features.

5.1 Stratigraphic Units

The R-25 borehole penetrated the stratigraphic units shown in Figure 2.3-1 and listed in Table 5.1-1. Identification of these units was based on examination of core and cuttings, geophysical logs, drilling information, geochemical and mineralogic data, and narrative descriptions for 28 polished thin sections. A lithologic log for R-25 is provided in Appendix C. Unit contacts were forecasted with moderate success within the Bandelier Tuff, primarily due to control provided by drill hole SHB-3, which is located 2 km southwest of R-25. SHB-3 bottomed in the Puye Formation, 20 ft beneath the base of the Bandelier Tuff. Sitewide geologic model predictions that R-25 might intersect Tschicoma lavas and Santa Fe Group sediments proved to be incorrect. Instead, sands and gravels of the Puye Formation were encountered beneath the Bandelier Tuff and extended to the TD of 1942 ft in the R-25 borehole.

5.1.1 Mesa-Top Soil (0- to 1-ft depth)

A thin layer of soil was penetrated from the surface to a depth of 1 ft. The soil consisted of unconsolidated silt, clay, and sand-sized fragments of sanidine and quartz derived from underlying bedrock.

5.1.2 Tshirege Member of the Bandelier Tuff (1- to 384-ft depth)

The Pleistocene Tshirege Member is 383 ft thick in R-25. It is a chemically-zoned ignimbrite that exhibits complex zones of welding and crystallization subdivided into four cooling units. Definition and nomenclature for these units were based on Broxton and Reneau (1995, 49726), Warren et al. (1997, 59180), and Gardner et al. (2001, 70106). In general, tuff compositions become more chemically evolved downsection through the Tshirege Member. Concentrations of SiO_2 , P_2O_5 , Rb, Y, and Nb tend to increase with depth whereas TiO_2 , Al_2O_3 , total iron, Ca, Sr, and Ba tend to decrease (Table 5.1-2). Petrographic characteristics also vary as a function of depth. For example, phenocryst abundances, particularly quartz, increase from the upper units to the lower units of the Tshirege Member (Table 5.1-3).

5.1.2.1 Qbt 4 (1- to 84-ft depth)

Qbt 4 is made up of a series of variably welded vitric to devitrified ash-flow tuffs that extend from 1 to 84 ft depth. Several systems of nomenclature have been applied to these tuffs (see for example Rogers 1995, 54419; Warren et al. 1997, 59180; Gardner et al. 2001, 70106). In this report, the name Qbt 4 is retained because ongoing petrologic studies suggest that these tuffs are genetically related. The occurrence of these tuffs is restricted to the western side of the Pajarito Plateau, and their unique petrographic and chemical characteristics indicate that latter stages of the Tshirege eruption tapped magmas that were significantly less evolved than the high-silica rhyolites that form the bulk of the Tshirege Member.

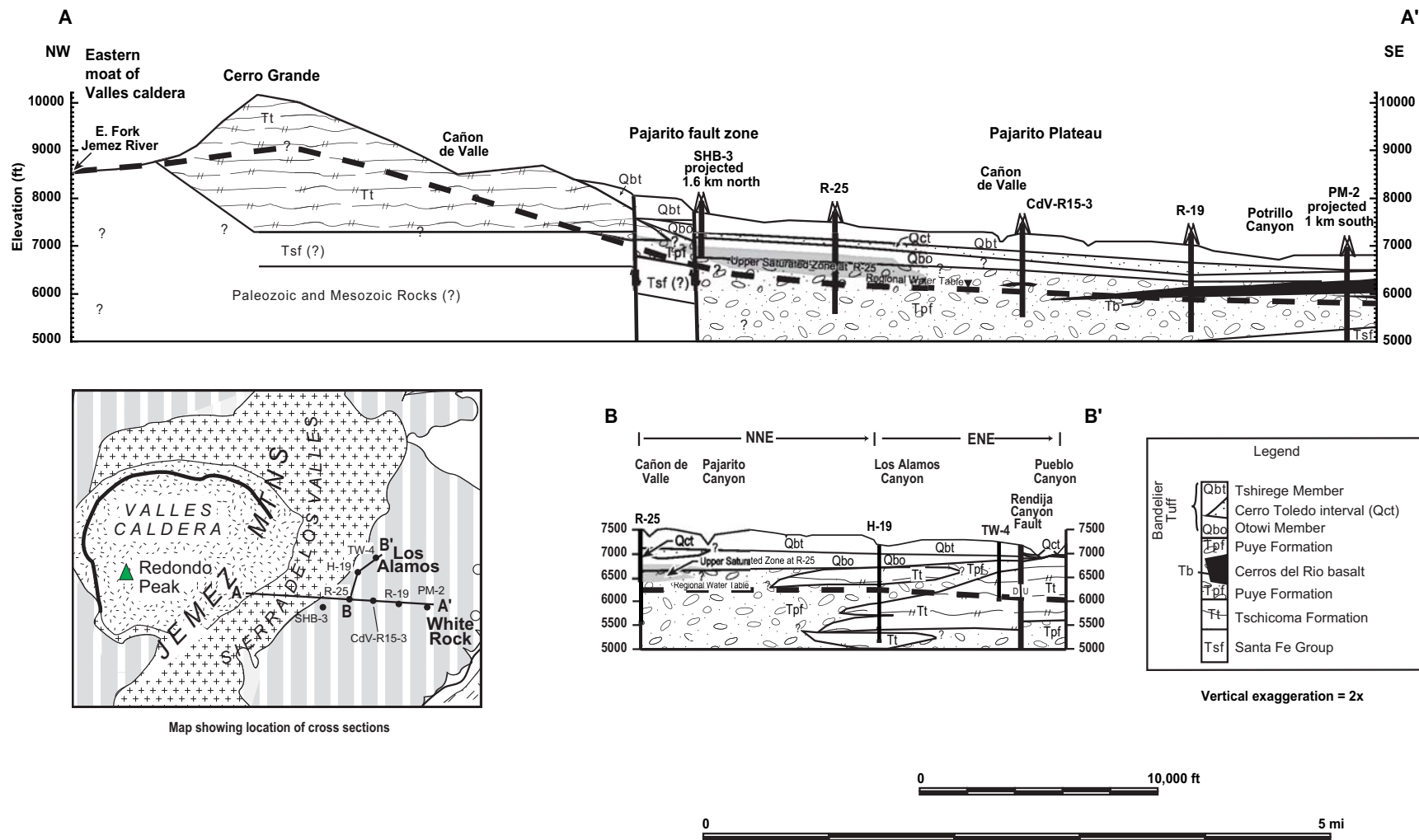


Figure 5.0-2. Geologic cross-sections through characterization well R-25

Table 5.1-1
Comparison of Stratigraphic Units Encountered in Borehole R-25

Stratigraphic Unit	Symbol	Drilled			Forecast Depth ^{a,b} (ft)	
		Elevation ^b (ft)	Depth ^b (ft)	Thickness (ft)	FIP ^c	FY 98
Soil	—	7517	1	1	—	—
Tshirege Member, Unit 4	Qbt 4	7434	84	83	93	92
Tshirege Member, Unit 3t	Qbt 3t	7363	155	71	—	—
Tshirege Member, Unit 3	Qbt 3	7289	229	74	272	192
Tshirege Member, Unit 2	Qbt 2	7186	332	103	349	233
Tshirege Member, Unit 1v	Qbt 1v	7156.5	361.5	29.5	376	290
Tshirege Member, Unit 1g	Qbt 1g	7136.2	381.8	20.3	435	354
Tshirege Member, Tsankawi Pumice Bed	Qbtt	7134	384	2.2	440	359
Sediments of the Cerro Toledo interval	Qct	7009	509	125	508	446
Otowi Member, ash flow tuff	Qbo	6674.2	843.8	334.8	899	768
Otowi Member, Guaje Pumice Bed	Qbog	6667.5	850.5	6.7	906	794
Puye Fanglomerate	Tpf	<5576	>1942	>1091	—	1115
Latite of SHB-1	TPcl4	—	abs ^d	—	abs	1567
Puye Formation	Tpf	—	—	—	1023	1656
Tschicoma Formation	Tt	—	abs	—	1267	abs
Puye Formation	Tpf	—	—	>1090	1929	abs
Totavi Formation	Tpt	—	—	—	1983	1721
Santa Fe Group	Tsf	—	—	—	—	1721

^a Forecast depths are taken from R-25 field implementation plan (FIP) and from 1998 version of sitewide geologic model (FY 98).

^b All data are for base of unit; elevations in feet above mean sea level and depths in feet below ground surface.

^c Geologic contacts are based on projections from geologic cross-sections.

^d abs = absence of unit.

Table 5.1-2
Chemical Analyses of Rock Units Penetrated During Drilling of Borehole R-25

Sample Number ^a	R25-5D	R25-30.5D	R25-59D	R25-93.2	R25-144D	R25-165.5D	R25-188D	R25-231.35	R25-264D	R25-318D	R25-352.4	R25-373.5	R25-428DP
Depth (ft)	5	30.5	59	93.2	144	165.5	188	231.35	264	318	352.4	373.5	428
Stratigraphic Unit	Tshirege Member, Qbt 4	Tshirege Member, Qbt 4	Tshirege Member, Qbt 4	Tshirege Member, Qbt 3t	Tshirege Member, Qbt 3t	Tshirege Member, Qbt 3	Tshirege Member, Qbt 3	Tshirege Member, Qbt 2	Tshirege Member, Qbt 2	Tshirege Member, Qbt 2	Tshirege Member, Qbt 1v	Tshirege Member, Qbt 1g	Cerro Toledo, Qct
Sample Type	Cuttings	Cuttings	Cuttings	Core	Cuttings	Cuttings	Cuttings	Core	Cuttings	Cuttings	Core	Core	Pumice Separates from Cuttings
SiO ₂ %	71.9	71.2	73.5	76.0	73.4	74.9	80.1 ^b	78.9	75.6	74.9	78.4	74.4	73.8
TiO ₂ %	0.26	0.35	0.32	0.19	0.18	0.16	0.13	0.09	0.11	0.16	0.08	0.08	0.12
Al ₂ O ₃ %	13.3	13.8	13.2	13.1	13.7	13.3	10.8	11.8	12.5	12.9	11.5	12.7	12.9
FeO % ^c	0.53	0.91	0.88	0.52	0.38	0.38	0.38	0.17	0.24	0.21	0.12	0.52	0.61
Fe ₂ O ₃ % ^c	1.86	2.06	1.85	1.47	1.68	1.52	1.05	1.21	1.48	2.05	1.38	1.11	0.61
MnO %	0.08	0.09	0.09	0.08	0.08	0.08	0.05	0.03	0.07	0.11	0.06	0.08	0.06
MgO %	0.19	0.33	0.38	NA ^d	NA	NA	NA	NA	NA	0.20	NA	NA	NA
CaO %	0.64	0.81	0.93	0.38	0.33	0.30	0.30	0.17	0.17	0.48	0.21	0.19	0.43
Na ₂ O %	4.06	4.33	4.36	4.50	4.48	4.56	3.74	3.98	4.44	4.32	3.98	3.62	2.70
K ₂ O %	5.01	4.38	4.23	4.80	4.89	4.90	3.85	4.38	4.79	4.56	4.12	4.60	5.61
P ₂ O ₅ %	0.05	0.04	0.05	0.02	0.02	0.02	0.01	<0.01 ^e	0.01	0.03	<0.01	<0.01	<0.01
LOI % ^f	2.22	1.59	0.32	0.18	0.31	0.19	0.08	0.25	0.21	0.24	0.24	1.94	3.33
Total %	100.2	100.1	100.3	101.4	99.5	100.4	100.5	101.0	99.7	100.2	100.2	99.4	100.3
V ppm	<10	16	13	<9	<10	<10	<10	12	<10	<11	14	<10	<10
Cr ppm	<8	<8	11	<7	11	<8	<8	<8	<8	<8	<8	<8	13
Ni ppm	<11	<11	<11	<11	<11	<11	<11	<11	<11	<11	<11	<11	<11
Zn ppm	71	92	123	76	73	84	57	45	75	121	69	115	67
Rb ppm	88	64	74	108	113	131	71	121	158	170	169	215	172
Sr ppm	67	95	123	37	40	41	38	21	19	74	22	15	24
Y ppm	38	34	26	38	51	42	18	45	49	64	68	88	46
Zr ppm	390	409	338	388	278	289	191	191	262	246	197	271	163
Nb ppm	46	43	41	54	59	69	35	51	89	84	82	131	67
Ba ppm	285	438	417	209	155	126	174	99	98	225	89	<47	50

Table 5.1-2 (continued)

Sample Number ^a	R25-456	R25-484DP	R25-568	R25-798DP	R25-846.1P10	R25-864D10	R25-1082D10	R25-1302D10	R25-1587D10	R25-1647D10	R25-1802D10	R25-1927DP
Depth (ft)	456	484	568	798	846.1	864	1082	1302	1587	1647	1802	1927
Stratigraphic Unit	Cerro Toledo, dacite clast	Cerro Toledo, Qct	Otowi Member, Qbo	Otowi Member, Qbo	Guaje Pumice Bed, Qbog	Puye Formation, Tpf	Puye Formation, Tpf	Puye Formation, Tpf	Puye Formation, Tpf	Puye Formation, Tpf	Puye Formation, Tpf	Puye Formation, Tpf
Sample Type	Core	Pumice Separates from Cuttings	Core	Pumice Separates from Cuttings	Pumice Separates (>2 mm)	Cuttings (>2 mm)	Cuttings (>2 mm)	Cuttings (>2 mm)	Cuttings (>2 mm)	Cuttings (>2 mm)	Cuttings (>2 mm)	Pumice Separates from Cuttings
SiO ₂ %	65.8	72.1	77.1	73.5	72.7	67.5	67.8	68.2	68.0	69.5	69.6	76.9
TiO ₂ %	0.61	0.15	0.13	0.05	0.06	0.51	0.49	0.50	0.44	0.47	0.43	0.20
Al ₂ O ₃ %	16.2	13.2	12.0	13.1	12.7	15.2	15.3	15.3	14.9	15.3	14.6	11.8
FeO %	1.13	0.90	0.32	0.59	0.60	1.23	1.05	1.27	1.24	1.37	0.41	<0.01
Fe ₂ O ₃ %	3.25	0.88	0.98	0.87	0.90	2.48	2.59	2.49	2.11	2.05	2.66	0.62
MnO %	0.08	0.07	0.05	0.09	0.09	0.06	0.06	0.06	0.06	0.07	0.06	0.03
MgO %	1.45	0.12	0.12	NA	NA	1.52	1.28	1.58	1.44	1.39	1.18	
CaO %	4.12	0.41	0.47	0.21	0.31	3.27	3.21	3.39	3.11	3.14	2.46	0.51
Na ₂ O %	4.14	2.51	3.20	4.02	3.63	3.89	3.84	3.85	3.62	3.82	3.88	3.08
K ₂ O %	2.69	5.39	4.54	4.42	4.50	3.15	3.22	3.18	3.31	3.35	3.80	4.73
P ₂ O ₅ %	0.22	0.01	0.02	<0.01	<0.01	0.18	0.16	0.17	0.15	0.15	0.13	0.02
LOI %	0.29	4.40	1.91	2.87	3.80	0.65	0.61	0.58	0.75	0.30	0.70	0.87
Total %	100.3	100.2	101.0	99.8	99.5	99.9	99.9	100.9	99.4	101.2	100.1	98.9
V ppm	63	<10	<10	<10	<10	38	52	55	41	46	39	<10
Cr ppm	45	<8	<8	<8	<8	44	34	43	34	35	41	<8
Ni ppm	22	<11	<11	<11	<11	22	23	26	19	15	28	<11
Zn ppm	64	74	49	132	122	57	61	58	54	52	57	<13
Rb ppm	44	143	115	370	344	64	64	50	63	63	93	180
Sr ppm	590	19	42	5	10	440	441	467	395	428	352	72
Y ppm	18	36	27	122	112	13	14	11	11	15	21	11
Zr ppm	170	283	180	272	263	181	170	183	173	175	156	119
Nb ppm	19	54	42	187	198	13	20	12	16	19	34	58
Ba ppm	1234	<47	183	<47	54	1305	1249	1345	1289	1329	928	268

Note: All analyses determined by x-ray fluorescence; Emily Kluk, analyst. Values reported in percent or parts per million by weight. Analytical errors (2σ) are SiO₂, 0.7; TiO₂, 0.01; Al₂O₃, 0.2; FeO and Fe₂O₃, 0.06; MnO, 0.01; MgO, 0.08; CaO, 0.1; Na₂O, 0.1; K₂O, 0.05; P₂O₅, 0.01; V, 10; Cr, 8; Ni, 10; Zn, 12; Rb, 5; Sr, 25; Y, 6; Zr, 30; Nb, 7; and Ba, 50.

^a Number listed after R25- indicates depth in feet. Drill cuttings are indicated by D and the depth listed is the top of the cuttings run, pumice is indicated by P, and all others are core.

The number 10 at the end of the sample number indicates >10 mesh (>2 mm) size fraction.

^b This SiO₂ concentration is greater than normally expected for the Tshirege Member and may reflect concentration of quartz phenocrysts in cutting samples.

^c Ferrous/ferric ratio determined by digestion and titration.

^d NA = not analyzed.

^e Values indicated are less than detection limit with the detection limit indicated by the number.

^f LOI = loss on ignition; determined gravimetrically by Emily Kluk.

Table 5.1-3
Quartz as Percent of Felsic Phenocrysts Within Cooling Units of the Tshirege Member

Cooling Unit	Number of Analyses ^a	Average (vol. %)	Range (vol. %)
4	6	11	2–22
3t	4	18	14–24
3	33	37	23–51
2	18	41	26–55
1v	4	41	34–45
1g	9	39	27–48

^a Data are taken primarily from Broxton et al. (1995, 58207; 1995, 54709), Broxton et al. (1996, 54948), and Warren et al. (1997, 59180).

From 1 ft to 5 ft, Qbt 4 consists of moderate orange pink partially-welded vitric ignimbrite that forms a thin caprock at the R-25 site. From 5 ft to 35 ft, Qbt 4 consists of light brown nonwelded vitric ignimbrite. From 35 to 51 ft, it consists of pinkish gray nonwelded devitrified ignimbrite, and from 51 to 84 ft, it consists of light brownish gray nonwelded devitrified ignimbrite. The lowermost tuffs of Qbt 4 in R-25 are a distinct lithology that is characterized by fewer and smaller pumices, fewer phenocrysts, and iron-stained pumices and lithics; these lower tuffs are equivalent to the Qbt 4 tuffs capping Pajarito Mesa described by Broxton et al. (1995, 54709).

Table 5.1-4 shows mineralogic data by x-ray diffraction for selected samples collected from Qbt 4. These data show that the upper part of the unit contains primary volcanic glass whereas the lower part of the unit is dominated by alkali feldspar, quartz, and cristobalite (Table 5.1-4). Whole-rock SiO₂ concentrations (71–74 wt% SiO₂) for Qbt 4 are significantly lower than for underlying Tshirege units (Table 5.1-2). Petrographic studies indicate that Qbt 4 is characterized by phenocrysts and glomerocrysts consisting of anorthoclase, sanidine, subordinate quartz, and minor plagioclase and clinopyroxene. Glomerophyric clots tend to be more abundant in the upper part of the unit.

Table 5.1-4
Quantitative X-Ray Diffraction Analyses for Borehole R-25

Sample ^a	Smectite	Kaolinite ^b	Tridymite	Cristobalite	Opal-CT	Quartz	Feldspar	Glass	Mica	Hematite	Hornblende	Total
R25-5D Tshirege Mbr, Qbt 4	—	—	—	—	2 ± 1	2 ± 1	29 ± 4	67 ± 4	—	Trc.	—	100 ± 4
R25-30.5D Tshirege Mbr, Qbt 4	Trc.	—	—	—	6 ± 3	10 ± 1	54 ± 8	29 ± 8	Trc.	1 ± 1	—	100 ± 9
R25-59D Tshirege Mbr, Qbt 4	Trc.	—	1 ± 1	16 ± 1	—	19 ± 1	68 ± 10	—	Trc.	—	Trc.	104 ± 10
R25-93.2 Tshirege Mbr, Qbt 3t	Trc.	—	20 ± 2	7 ± 3	—	7 ± 1	67 ± 9	—	—	—	—	101 ± 10
R25-144D Tshirege Mbr, Qbt 3t	Trc.	—	17 ± 2	9 ± 4	—	5 ± 1	66 ± 9	—	—	—	Trc.	97 ± 10

Table 5.1-4 (continued)

Sample ^a	Smectite	Kaolinite ^b	Tridymite	Cristobalite	Opal-CT	Quartz	Feldspar	Glass	Mica	Hematite	Hornblende	Total
R25-165.5D Tshirege Mbr, Qbt 3	—	—	14 ± 1	11 ± 1	—	7 ± 1	68 ± 10	—	Trc.	—	—	100 ± 10
R25-188D Tshirege Mbr, Qbt 3	—	—	9 ± 1	4 ± 2	—	30 ± 2	61 ± 9	—	—	—	—	104 ± 9
R25-231.35 Tshirege Mbr, Qbt 2	—	—	16 ± 2	6 ± 3	—	21 ± 2	61 ± 9	—	—	—	—	104 ± 10
R25-264D Tshirege Mbr, Qbt 2	—	—	11 ± 1	18 ± 2	—	10 ± 1	60 ± 8	—	—	Trc.	—	99 ± 8
R25-318D Tshirege Mbr, Qbt 2	—	—	17 ± 2	12 ± 2	—	9 ± 1	64 ± 9	—	Trc.	1 ± 1	Trc.	103 ± 10
R25-352.4D Tshirege Mbr, Qbt 1v	—	—	4 ± 1	12 ± 1	—	27 ± 2	61 ± 9	—	1 ± 1	Trc.	—	105 ± 9
R25-373.5 Tshirege Mbr, Qbt 1g	—	1 ± 1	—	—	7 ± 2	13 ± 1	30 ± 4	49 ± 4	Trc.	Trc.	—	100 ± 5
R25-428DP Cerro Toledo	—	—	—	—	—	Trc.	2 ± 1	98 ± 1	—	—	Trc.	100 ± 1
R25-456 Cerro Toledo	1 ± 1	—	1 ± 1	21 ± 2	—	1 ± 1	74 ± 10	—	Trc.	1 ± 1	2 ± 1	101 ± 10
R25-484DP Cerro Toledo	Trc.	Trc.	—	—	—	1 ± 1	5 ± 1	94 ± 1	—	—	—	100 ± 1
R25-568 Otowi Mbr.	Trc.	—	—	—	8 ± 3	12 ± 1	28 ± 4	52 ± 5	Trc.	Trc.	—	100 ± 5
R25-798DP Otowi Mbr.	—	—	—	—	—	2 ± 1	5 ± 1	93 ± 1	—	—	—	100 ± 1
R25-846.1P10 Guaje Pumice Bed	—	—	—	—	—	10 ± 1	11 ± 2	79 ± 2	Trc.	—	—	100 ± 2
R25-864D10 Puye Formation	1 ± 1	—	12 ± 1	10 ± 1	—	1 ± 1	60 ± 8	15 ± 8	Trc.	1 ± 1	—	100 ± 8
R25-1082D10 Puye Formation	2 ± 1	—	11 ± 1	9 ± 4	—	6 ± 1	60 ± 8	11 ± 9	Trc.	1 ± 1	Trc.	100 ± 9
R25-1302D10 Puye Formation	—	—	11 ± 1	13 ± 1	—	1 ± 1	66 ± 9	8 ± 9	Trc.	1 ± 1	Trc.	100 ± 9
R25-1587D10 Puye Formation	—	—	8 ± 1	13 ± 1	—	1 ± 1	57 ± 8	20 ± 8	—	1 ± 1	—	100 ± 8
R25-1647D10 Puye Formation	—	—	18 ± 2	11 ± 2	—	—	61 ± 9	10 ± 9	Trc.	Trc.	—	100 ± 9
R25-1802D10 Puye Formation	1 ± 1	—	12 ± 1	12 ± 1	—	1 ± 1	55 ± 8	17 ± 8	1 ± 1	1 ± 1	—	100 ± 8
R25-1927DP Puye Formation	1 ± 1	—	4 ± 1	30 ± 2	—	4 ± 1	52 ± 7	9 ± 7	—	—	—	100 ± 7

Note: All values are reported in weight percent. Steve Chipera, analyst. Analytical uncertainties ($\pm 2\sigma$) are listed for all measurements except trace (Trc.) detection ($<1\%$).

^a Number listed after R25- indicates depth in feet. Drill cuttings are indicated by D and the depth listed is the top of the cuttings run, pumice is indicated by P, and all others are core. The number 10 at the end of the sample number indicates >10 mesh (>2 mm) size fraction.

^b Kaolinite or chlorite.

5.1.2.2 Qbt 3t (84- to 155-ft depth)

Qbt 3t is a devitrified ignimbrite and grades from partially welded at the top to moderately welded at the base. The use of "t" in the unit symbol refers to the transitional nature of this unit; Qbt 3t chemical and petrographic characteristics are transitional between Qbt 4 and Qbt 3. Although welded, cores of Qbt 3t were poorly consolidated, probably due to pervasive vapor phase crystallization. The bulk rock mineralogy of Qbt 3t is similar to that for lower Qbt 4 except that tridymite is the dominant silica phase in Qbt 3t (Table 5.1-4). The abundance of quartz phenocrysts is intermediate between that of Qbt 4 and Qbt 3 (Table 5.1-3). Polished thin sections of Qbt 3t contain 15% and 20% quartz in downward sequence (Appendix D). Qbt 3t thins rapidly eastward. In R-25 it is 74 ft thick, but in outcrops only 1000 ft to the east it is only about 20 ft thick (Warren et al. 1997, 59180).

The contact between Qbt 3t and Qbt 3 was difficult to assign based on the cuttings from the borehole. Placement of the contact at 155 ft depth was based on a slight welding break at about 155 ft and petrographic data showing that quartz makes up 35% of felsic phenocrysts in a sample from 165.5 ft depth (Appendix D). Chemical analyses of TiO_2 and Zr for samples of the tuff suggest that the contact may occur between 165.5 and 188 ft depth (Table 5.1-2), but the high relative quartz content of the sample at 165.5 ft is considered more reliable for identifying Qbt 3.

5.1.2.3 Qbt 3 (155- to 229-ft depth)

Qbt 3 is a devitrified ignimbrite that grades from moderately welded at the top to nonwelded at the base. Cuttings were poorly consolidated throughout, probably due to pervasive vapor phase crystallization. Tridymite abundances were slightly less than in Qbt 3t (Table 5.1-4). Quartz in Qbt 3 makes up 35% to 20% felsic phenocrysts in downward sequence (Appendix D). A similar reversal in the normal trend of increasing quartz downsection was found in stratigraphic sections 1106-2 and 1085-2 in the central part of the Laboratory sampled by Broxton et al. (1995, 58207; 1995, 54709).

5.1.2.4 Qbt 2 (229- to 332-ft depth)

Qbt 2 is a moderately welded, well indurated, devitrified ignimbrite. Welding grades from moderately welded at the top of the unit to partially welded at the base. The bulk rock mineralogy of Qbt 2 is generally similar to Qbt 3, with the dominant mineral phases consisting of alkali feldspar, quartz, tridymite, and cristobalite (Table 5.1-4).

5.1.2.5 Qbt 1v (332- to 361.5-ft depth)

Qbt 1v is a nonwelded, devitrified ignimbrite. The use of "v" in the unit symbol refers to vapor-phase crystallization in the upper part of cooling unit Qbt 1. The mineralogy of Qbt 1v is generally similar to that of Qbt 2, except that tridymite is less abundant in Qbt 1v (Table 5.1-4). The contact between Qbt 1v and Qbt 2 is gradational and was placed where compaction of pumices was no longer apparent downsection of the flattened pumices in Qbt 2. The base of Qbt 1v was placed at the first appearance of the vitric pumices that mark the contact with Qbt 1g.

5.1.2.6 Qbt 1g (361.5- to 381.8-ft depth) and Tsankawi Pumice Bed (381.8- to 384-ft depth)

Qbt 1g is a nonwelded ignimbrite at the base of the Tshirege Member in R-25. This unit consists of massive, poorly consolidated, vitric ash-flow tuff. The use of "g" in the unit symbol refers to the presence of primary volcanic glass that is preserved with little or no alteration. A sample from a depth of 373.5 ft contained 49% glass and 7% opal-CT (Table 5.1-4). The Tsankawi Pumice Bed, a plinian fall deposit, occurs from 381.8 to 384 ft.

5.1.3 Tephras and Volcaniclastic Sediments of the Cerro Toledo Interval (384- to 509-ft depth)

The Pleistocene Cerro Toledo interval is 125 ft thick in R-25, extending from 384 to 509 ft. The interval is typically well bedded where exposed in outcrops on the eastern side of the Laboratory (Broxton and Reneau 1995, 49726), but the fabric of the rock in R-25 could not be determined from cuttings. The Cerro Toledo interval in R-25 consists of vitric, tuffaceous, sandy silt, probably deposited within a fluvial environment. Numerous large lithics include dacite lava of Sawyer Dome (Figure 5.0-1), a unit of the Tschicoma Formation. Vitric pumices common within the unit have uniform petrographic characteristics within individual beds. However, the petrographic character of the pumices differs between the upper and lower parts of the unit (Appendix D), suggesting multiple sources for these deposits. Though vitric, the pumices are partly filled with two generations of smectite. Perhaps the earlier clay was deposited by soil illuviation prior to deposition of the Tshirege Member, and the later clay resulted from limited glass alteration under saturated conditions.

The Cerro Toledo interval in R-25 is twice as thick as that predicted by the sitewide geologic model. Cerro Toledo deposits in boreholes CdV-R15-3 and R-19, both located east of R-25, were also thicker than predicted. These deposits probably fill paleo-drainages developed on the eroded top of the underlying Otowi Member. Revision to the sitewide geologic model is needed to better reflect the significant thickness of Cerro Toledo deposits under the western side of the Pajarito Plateau.

5.1.4 Otowi Member of the Bandelier Tuff (509- to 843.8-ft depth) and Guaje Pumice Bed (843.8- to 850.5-ft depth)

Ash-flow tuffs of the Pleistocene Otowi Member were encountered from 509 to 852 ft in R-25. The Otowi Member consists of massive, poorly consolidated, vitric, nonwelded ash-flow tuff. The most important mineralogic component of the tuff is glass, ranging from 52% to 93% (Table 5.1-4). The Otowi Member is chemically zoned, particularly for trace elements. Comparison of samples from depths of 568 ft and 798 ft (Table 5.1-2) shows that concentrations of Rb, Y, and Nb increase downsection, and TiO₂, CaO, Sr, and Ba increase upsection.

The ignimbrite is featureless in downhole video except for faint horizontal layering observed at 790, 819, 827, and 832.8 ft. These features, especially at the 790-ft depth, may represent flow unit boundaries or surge beds. Narrative descriptions for two polished thin sections (Appendix D) confirm the vitric nature of the unit as well as a typical phenocryst assemblage dominated by sanidine and quartz, and with scarce mafics dominated by clinopyroxene. A lithic-rich zone occurs between 573 and 600 ft.

The downhole video also reveals seepage and continuous flow of groundwater along open, near vertical fractures. This groundwater is described further in Section 6.2.1.1.

The Guaje Pumice Bed forms the lowermost 6.7 ft of the Otowi Member in R-25. This is much thinner than other occurrences of the Guaje Pumice Bed further to the east and north, suggesting that the location of R-25 was either south of the main dispersal axis for this fall deposit, or this deposit was partly eroded prior to or during emplacement of the Otowi ignimbrite. The deposit consists of stratified pumice beds, lithic beds that include quartzose sandstone, and fine ash beds. Two cycles of pumice fall, each capped by a 1-in.-thick ash layer with tops at 843.8 ft and 844.4 ft, were noted in the downhole video. The phenocryst mineralogy for the pumices is indistinguishable from that of the overlying ignimbrite (Appendix D).

5.1.5 Puye Formation (Fanglomerate Facies) (850.5 ft to TD of 1942 ft)

The Puye Formation in R-25 is an alluvial fan deposit made up primarily of coarse clastic rocks derived from dacitic to rhyodacitic units of the Tschicoma Formation that crop out in the Jemez Mountains west of the Pajarito fault. Due to the proximity of the source rocks, these fanglomerate deposits consist of poorly consolidated and poorly sorted boulders, cobbles, gravels, and sands. Downhole video for depths of 852 and 863 ft, 1175 and 1180 ft, and 1472 and 1482 ft reveals clast-supported boulder conglomerate, with boulders up to 2 ft in diameter. Moderately well-rounded pebbles and cobbles predominate, with some lenses of granules. The bulk mineralogy of the Puye Formation is dominated by varying proportions of feldspar, glass, tridymite, cristobalite, and quartz (Table 5.1-4).

The Puye Formation in R-25 is more than 1090 ft thick, extending from 852 ft to below the TD of 1942 ft. Two units recognized by the provenance of their dominant clasts are (1) the upper Pajarito Mountain unit from 852 to 1657 ft, and (2) the Rendija Canyon unit from 1657 to 1942 ft. The bedrock units within the Tschicoma Formation that were the likely sources for clasts in the Puye Formation are described in Table 5.1-5, and their outcrop distribution is shown in Figure 5.0-1. Examination of clasts within polished thin sections (Appendix D) indicates that the upper Pajarito Mountain unit represents a fan shed eastward, contemporaneous with eruption of upper dacite of Pajarito Mountain, whereas the Rendija Canyon unit represents the southern part of a fan that was contemporaneous with eruption of rhyodacite of Rendija Canyon.

Table 5.1-5
Petrographic Description of Informal Stratigraphic Units
Within the Tschicoma Formation in the Eastern Jemez Mountains

Unit Name	N ^a	Phenocrysts ^b	Characteristic Petrographic Features ^b
Dacite of Coleman Dome	2	22% PL, 8% HN, 0.9% OX	Very abundant HN
Dacite of Pajarito Mountain (upper)	5	18% PL, 4.3% OX, 1.0% CX	Abundant PX, OX strongly dominant
Dacite of Pajarito Mountain (lower)	4	9% PL, 2.2% OX, 1.6% CX	Common PX, subequal OX and CX
Dacite of Cerro Grande (upper)	1	15% PL, 3% HN, 1.7% OX	Common HN, dominant over OX
Rhyodacite of Rendija Canyon	6	6% PL, 5% KF, 4% QZ, 0.4% BT, 0.1% CX	Wormy QZ and highly resorbed PL
Andesite of Los Alamos Canyon	2	11% PL, 4.7% CX, 2.3% OX	Abundant PX, CX strongly dominant

Note: Outcrop extents are shown in Figure 5.0-1. Units are listed by inferred order of age (with oldest at the bottom), although stratigraphic positions are uncertain.

^a N = number of analyses.

^b PL = plagioclase, HN = hornblende, OX = orthopyroxene, PX = pyroxene, CX = clinopyroxene, KF = potassium feldspar, QZ = quartz, and BT = biotite.

5.1.5.1 Late Miocene Paleosol (850.5- to 852-ft depth)

Downhole video reveals a brown, massive, generally fine-grained sediment with highly scattered pebbles between the depths of 850.5 and 852.0 ft. The upper contact is wavy, with an amplitude of 0.5 in., and the lower contact has 4 in. of relief, extending up to 851.7 ft on the opposite side of the borehole. This layer represents a paleosol developed atop the Puye Formation.

5.1.5.2 Puye Formation – Upper Pajarito Mountain Fan Deposits (852- to 1657-ft depth)

The upper Pajarito Mountain fan deposits of the Puye Formation in R-25 are 805 ft thick, extending from 852 to 1657 ft. This unit consists mostly of sand and gravel, with cobbles and boulders prevalent within the upper 341 ft (Appendix C). Vitric lava clasts within this unit are common (Table 5.1-6), suggesting that the sediments are relatively unaltered. High proportions of clasts derived from upper dacite of Pajarito Mountain occur within cuttings from this interval, as summarized in Table 5.1-6. Immediately below this interval, no clasts of upper dacite of Pajarito Mountain can be recognized. The abrupt appearance of clasts derived predominantly from a single source area suggests that this fan complex was contemporaneous with eruption of upper dacite of Pajarito Mountain to the northwest of R-25 (Figure 5.0-1). Clasts derived from upper dacite of Pajarito Mountain are not recognized within the Puye Formation at either R-9 (Broxton et al. 2001, 71250) or R-12 (Broxton et al. 2001, 71252), so this fan evidently does not extend to the northeastern part of the Pajarito Plateau.

Table 5.1-6
Percentages of Clasts Within Polished Thin Sections
Derived from Different Units Within the Tschicoma Formation

Depth (ft)	Source Unit of Clast					Vitric Clasts (%)
	Dacite of Pajarito Mt. (upper)	Dacite of Pajarito Mt. (lower)	Dacite of Cerro Grande	Rhyodacite of Rendija Canyon	Miocene Basalt	
864	95	—	—	5	—	10
1082	100	—	—	—	—	20
1302	100	—	—	—	—	10
1517	85	—	15	—	—	35
1587	100	—	—	—	—	30
1647	90	—	10	—	—	0
1682	—	43	19	38	—	38
1802	—	14	5	81	—	0
1927	—	—	—	100	—	0
1937	—	—	26	68	5	5

Note: Values in the second through sixth columns represent vol. % of clasts within a polished thin section. Each thin section of cuttings contains approximately 20 separate clasts, each with long dimensions >2 mm. Data are taken from Appendix D. Depths represent the lower depth of the 5-ft-thick cuttings interval sampled. The sample from the 1927-ft depth represents a polished section of 45 individual pumices.

5.1.5.3 Puye Formation – Rendija Canyon Fan Deposits (1657 to ~1870 ft) and High-Rb, Low-Sr Fan Deposits (~1870 ft to TD of 1942 ft)

The Rendija Canyon fan deposits of the Puye Formation in R-25 are >285 ft thick, extending from 1657 to 1942 ft (the total drilled depth in R-25). This unit consists mostly of sand and gravel, with boulders prevalent between 1870 and 1925 ft (Appendix C). A large fraction of clasts near the top of this unit are vitric (Table 5.1-6), suggesting that sediments here are unaltered. Rhyodacite of Rendija Canyon is the dominant clast type in these deposits, although clasts derived from other sources are also present (Table 5.1-6). A polished thin section of pumices separated from cuttings collected at 1927 ft is monolithologic and may represent a primary pumice fall.

Chemical data from cuttings collected from the Puye Formation in R-25 are summarized in Table 5.1-2. Four constituents (SiO_2 , Sr, Rb, and Ba) are plotted against elevations for boreholes R-25, CdV-R15-3, and R-19 in Figure 5.1-1. The interpretation of chemical data from cuttings is limited by several factors. Drill cuttings represent composite samples that may include several lithologies from a limited depth range. Additionally, the return of cuttings to the surface often results in the loss of fine fractions of the materials sampled. Analysis of cuttings from R-19 suggests that chemical variations within different size fractions are generally small in the Puye Formation (Broxton et al. 2000, 71253). The following discussion recognizes the limitations imposed on the interpretation of the geochemical data by the nature of the materials sampled.

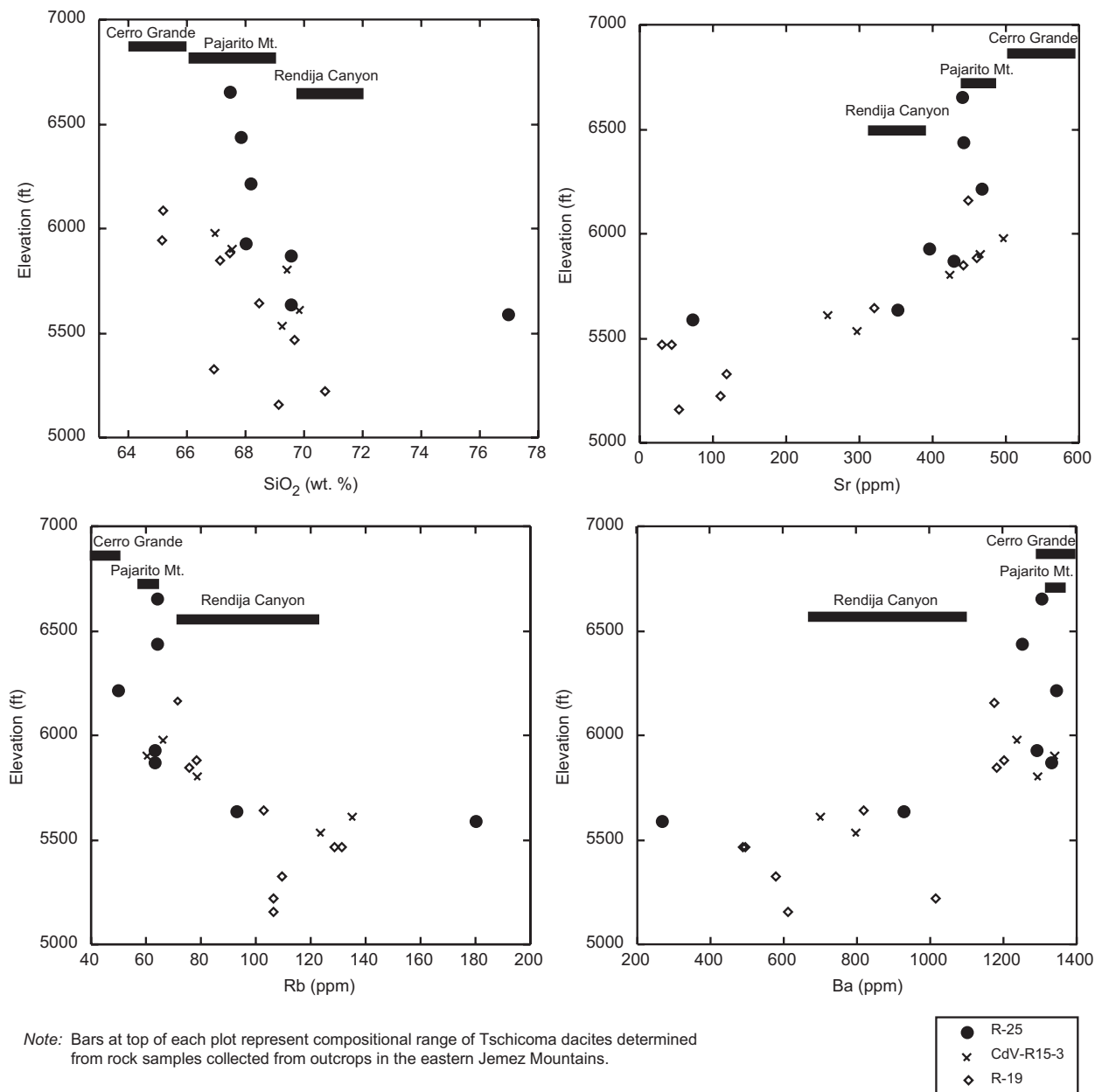


Figure 5.1-1. Variations in SiO_2 , Sr, Rb, and Ba in cuttings from the Puye Formation in boreholes R-25, CdV-R15-3, and R-19

The chemical data indicate a general trend of increasing SiO₂ and Rb and decreasing Sr and Ba with depth in boreholes R-25, CdV-R15-3, and R-19. The trends are consistent with the dacite of Pajarito Mountain as an important source of clasts in the upper part of the Puye Formation and the rhyodacite of Rendija Canyon as an important source in the lower part for this part of the Pajarito Plateau. The Rendija Canyon fan deposits of the Puye Formation are represented by a single sample (depth 1802 ft and elevation 5715 ft) in Table 5.1-2 and Figure 5.1-1. The chemical data shown in Figure 5.1-1 (particularly for Sr and Ba) also suggest that the lowermost Puye deposits in all three wells were derived from source rocks other than the rhyodacite of Rendija Canyon. These lowermost Puye deposits were apparently derived from older source rocks that were more chemically evolved than the Rendija Canyon rhyodacite. The locations and ages of these older source rocks are not known at this time but are possibly related to the Bearhead Rhyolite and Canovas Canyon Rhyolite (Smith et al. 1970, 09752). It appears that the R-25 borehole barely penetrated the top of these older fan deposits before reaching TD; these deposits are currently included in the Rendija Canyon fan deposits of the Puye Formation in R-25 because of their limited characterization.

5.2 Borehole Geophysics

Borehole geophysical surveys were conducted in the R-25 borehole during drilling, and through stainless steel casing and annular fill after the well was installed. This section describes the borehole geophysical survey methods that were employed and presents the results obtained from the logging.

5.2.1 Borehole Logging Activities

Borehole geophysical data were obtained from two sources: (1) Laboratory and subcontractor personnel conducted borehole video, natural gamma radiation (GR), and electromagnetic induction (EM) surveys using Laboratory geophysical logging equipment, and (2) Schlumberger, Inc., personnel obtained a suite of borehole geophysical logs. Table 5.2-1 lists the borehole video and geophysical surveys that were obtained from each source.

On October 14, 1998, GR and EM logs were run by Laboratory subcontractors through cased hole from 0 to 580 ft and open hole from 580 to 980 ft. On October 17, 1998, Laboratory borehole logging equipment was used to obtain an open-hole video log from 580 to 863 ft using a 4-in.-diameter side-viewing camera. On January 4, 1999, the Laboratory's 4-in.-diameter side-viewing camera was used to log open borehole from 1175 to 1180 ft, and on January 21, 1999, the 4-in.-diameter camera was used to log the open borehole from 1472 to 1482 ft. On February 27, 1999, a GR log was run in cased borehole from 0 to 1942 ft using Laboratory equipment.

Schlumberger, Inc., initially logged R-25 on April 21, 1999. Logging took place inside the 5-in.-I.D. stainless steel well casing and was designed to evaluate the position of the tremie pipe lost in the annular fill during well construction. This geophysical logging suite was also designed to evaluate the placement of sand packs around screens and bentonite seals between screens. Five separate logs through the well casing were obtained; the geophysical logs obtained during each run are listed in Table 5.2-1. The Schlumberger logging tools tagged the bottom of the well at 1894 ft bgs, and the water level was 1216 ft bgs.

Schlumberger, Inc., re-logged the completed well on March 16, 2000, after the repairs to screens #3 and #9 were completed. Four separate logging runs were made (Table 5.2-1). These logs were designed to document the as-built condition of the well and its annular fill prior to installation of the WestbayTM sampling system.

Table 5.2-1
Borehole Logging Surveys at R-25

Operator	Date	Depth (ft) ^a	Survey
Laboratory and subcontractor personnel using Laboratory equipment	10/14/98	0–980 (580–980 open hole)	Natural GR and EM
	10/17/98	0–863 (580–863 open hole)	Borehole video survey (side-viewing)
	1/4/99	0–1180 (1175–1180 open hole)	Borehole video survey (side-viewing)
	1/21/99	0–1482 (1472–1482 open hole)	Borehole video survey (side-viewing)
	2/27/99	0–1942 (all cased hole)	Natural GR
Schlumberger, Inc.	4/21/99	0–1942 (inside well casing with partial annular fill)	Survey #1:
			Cement bond log
			Multifinger caliper
			Compensated neutron
			Natural gamma spectroscopy
			Ultrasonic imager
	3/16/00	0–1942 (inside well casing after screen #3 repair)	Survey #2:
			Natural gamma spectroscopy
			Multifinger caliper
			Neutron porosity
			Hole deviation

^a Depth range for logging run.

5.2.2 Borehole Geophysical Survey Methods

5.2.2.1 Gross Gamma Radiation

The GR survey employs a scintillation detector to measure the gross GR activity of the formation; the information is used for determination of lithology and for depth correlation between different geophysical surveys. Naturally occurring GR comes from the decay of potassium-40 plus the uranium and thorium decay series. Often, these elements occur in higher concentrations within clay minerals; hence, GR surveys are used to estimate lithology. At the Laboratory, the GR log was strongly affected by primary volcanic lithology.

5.2.2.2 Electromagnetic Induction

The EM logging tool is used to measure formation electrical conductivity 8 to 39 in. from the borehole axis. EM measurements are sensitive to the electrical properties of the rocks and the quantity and quality of contained groundwater.

5.2.2.3 Epithermal Neutron (CNT-G or APT)

The epithermal neutron tool provides information about moisture content in the unsaturated zone and porosity in the saturated zone. The epithermal neutron-neutron logging tool measures the amount of

hydrogen in the formation in either a water- or air-filled borehole. The hydrogen content typically provides a good measure of moisture content in the unsaturated zone and porosity in the saturated zone. However, the tool can overestimate either value if there is a significant amount of hydrogen in the matrix minerals (e.g., clay).

The CNT-G neutron tool uses a 16-Ci source of americium-beryllium to generate neutrons and has a lateral depth of investigation of 9 in. with a vertical resolution of 18 in. The accelerator porosity tool (APT) uses thermal excitation of tritium as a neutron source and provides a calibrated moisture content with parameters similar to those for the CNT-G tool. In addition, the APT provides uncalibrated moisture measurement (slowing-down time) with both a 3-in. vertical resolution and depth of investigation. The CNT-G tool was used for the April 21, 1999, geophysical logging, and the APT was used for the March 16, 2000, logging.

5.2.2.4 Natural Gamma Spectroscopy

The hostile natural gamma ray sonde (HNGS) uses two bismuth germanate scintillation detectors to measure the natural GR of the formation. The HNGS makes similar measurements to the GR tool (Section 5.2.2.1), but the HNGS is capable of gamma ray energy discrimination. Gamma ray spectra recorded on both detectors are analyzed with a full-spectrum procedure based on a least-squares fitting technique. The procedure uses a set of standard responses for each contributor to the gamma ray signal—potassium-40, uranium, and thorium—and converts the signal to concentrations of each element based on their isotopic abundance and assuming secular equilibria for uranium and thorium.

Filtering techniques are used to reduce the statistical noise by comparing and averaging counts at a certain depth with counts sampled just before and after. The final outputs are the total gamma ray measurement; a uranium-free gamma-ray measurement; and the concentrations of potassium-40, thorium, and uranium. The radius of investigation depends on several factors: hole size, mud density, formation bulk density (denser formations display slightly lower radioactivity), and the energy of the gamma rays (a higher energy gamma ray can reach the detector from deeper in the formation). For a gamma ray of 1.46 MeV (potassium-40), 90% of the signal is from a shell 7 in. thick.

5.2.2.5 Multifinger Caliper

The multifinger caliper is used to measure borehole or well casing rugosity. The caliper used by Schlumberger, Inc., has 36 arms that are reported in 6 sectors. Maximum and minimum readings are recorded for each sector.

5.2.2.6 Sonic Logs

The ultrasonic imager uses velocity and attenuation of high frequency sound waves to image well casing to determine casing thickness and corrosion characteristics. The ultrasonic imager was used in R-25 to determine if the tremie pipe lost in the annular fill could be located adjacent to the well casing. Attempts to image the tremie pipe were unsuccessful.

A cement-bond log uses sound waves to determine the bonding characteristics of annular materials in contact with the outer wall of well casing. In R-25, a cement-bond log was used to determine if the position of the dropped tremie pipe could be detected if the rod were in contact with the well casing. The cement-bond log was not successful in determining the position of the tremie pipe.

5.2.2.7 Hole Deviation

A gyroscope survey was conducted to determine the hole deviation as a function of depth in R-25. The survey uses a wire-line gyroscope to map the drilled path of boreholes and wells.

5.2.3 Results of Borehole Geophysical Surveys

5.2.3.1 GR and EM Results Obtained Using Laboratory Borehole Survey Tools

Figure 5.2-1 shows the results of natural GR surveys conducted in R-25 on October 14, 1998, and February 27, 1999. The October 14 survey was conducted through 16-in. surface casing to 20 ft, through 13 3/8-in. casing to 578 ft, and in open borehole from 580 to 980 ft. The February 27 survey was conducted entirely through telescoped, heavy-walled drill casing: 16-in. casing to 20 ft, 13 3/8-in. casing to 578 ft, 11 3/4-in. casing to 1175 ft, and 9 5/8-in. casing to the TD of 1942 ft.

Some of the most significant changes in gamma activity shown in R-25 logs are associated with attenuation of gamma rays by multiple telescoping drill casings. The most significant geologic features revealed by the gamma log include the following:

- Natural GR increases slightly downsection within the Tshirege Member of the Bandelier Tuff with the highest gamma activity associated with Qbt 1g. This reflects the chemical zonation within the Tshirege Member, with U and Th concentrations increasing downsection in the unit.
- Gamma activity is highly variable through the Cerro Toledo interval. This probably reflects varying proportions of tuff and dacite detritus that make up individual beds within this epiclastic deposit.
- The open-hole log shows that the Otowi Member undergoes several distinct step-wise increases and decreases in gamma activity as a function of depth. Increases occur at the top of the unit (about 600 ft), at 650 ft, and at 725 ft. A significant decrease in gamma activity occurs at 790 ft, and a smaller decrease occurs at 840 ft near the upper contact of the Guaje Pumice Bed. The sharp decrease in gamma activity at 790 ft is coincident with faint horizontal layering observed in downhole video and may represent a depositional break within the Otowi Member.
- The gamma signature for Otowi Member ash-flow tuffs is similar for R-25, CdV-R15-3, and R-19. All three wells show an overall pattern of increasing gamma activity downsection to a maximum two-thirds to three-quarters of the way through the unit before decreasing near the base of the ignimbrite. As noted above, the increases and decreases are step-wise in R-25. The gamma activity varies more systematically in CdV-R15-3 and R-19.
- The open-hole log shows that the Guaje Pumice Bed exhibits a low gamma spike just above the abrupt gamma decrease associated with the geologic contact at the top of the Puye Formation. The borehole video shows that this spike is coincident with lithic-rich beds from 844 to 846 ft within the Guaje Pumice Bed. These fall deposits contain a high proportion of intermediate composition lava clasts that have significantly lower U and Th concentrations than adjacent beds dominated by rhyolitic pumice. Similar low-gamma spikes are found in the Guaje Pumice Bed deposits of CdV-R15-3 and R-19, and they may represent similar lithic-rich fall deposits.
- The natural gamma activity in the upper part of the Puye Formation varies little down to a depth of 1180 ft. Gamma activities decrease systematically from 1180 to 1450 ft and then remain constant to about 1655 ft. At 1655 ft, there is an increase in gamma activity that corresponds with the top of the Rendija Canyon fan deposits. Another increase in gamma activity at about 1870 ft may mark the top of older fan deposits that are discussed in Section 5.1.5.3.

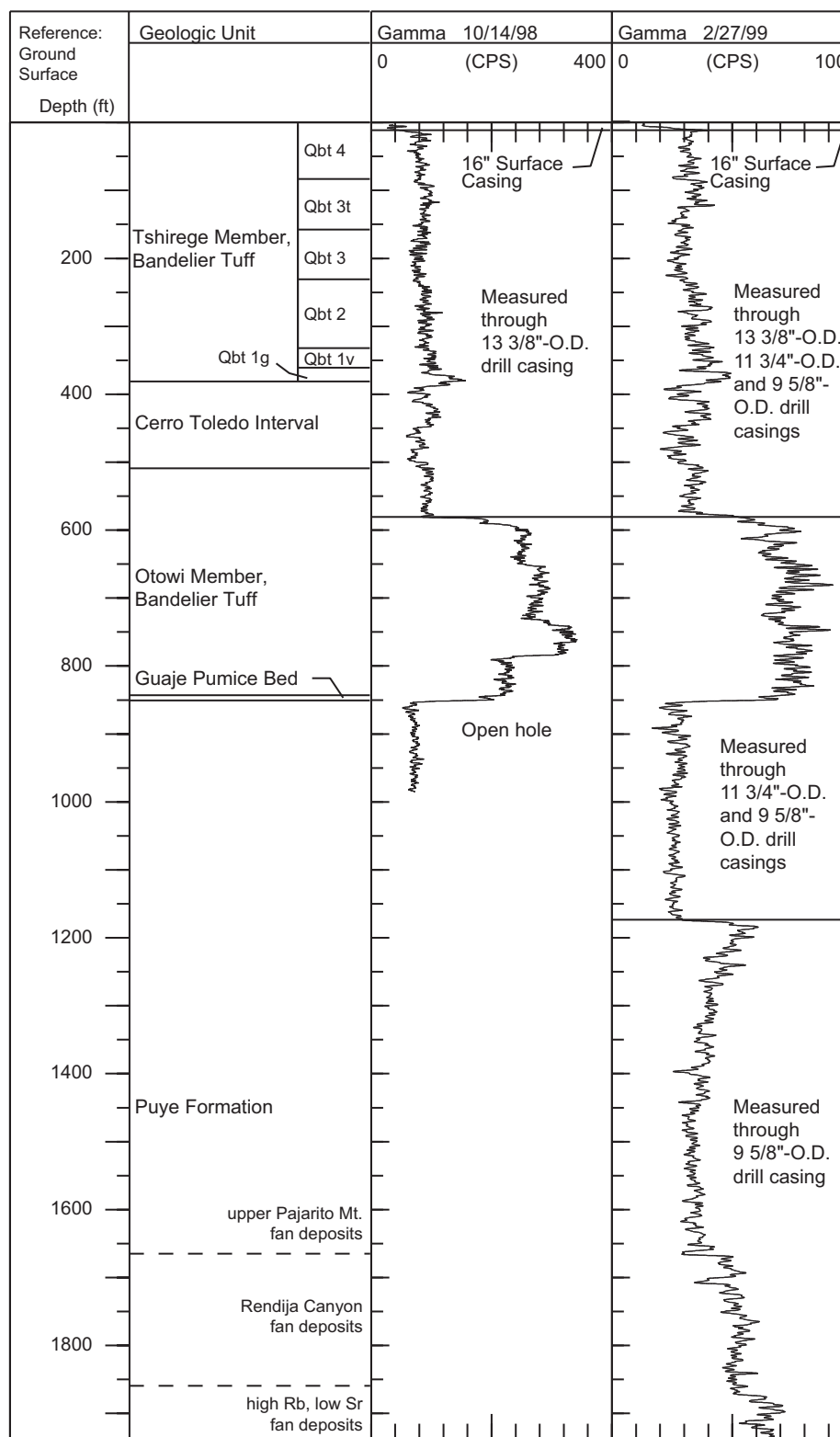


Figure 5.2-1. Results of natural GR surveys conducted on October 14, 1998, and February 27, 1999

Figure 5.2-2 shows the results of the EM survey along with the gamma log collected on October 14, 1998. These logs were conducted in open hole from depths of 580 to 980 ft. The water level in the borehole at the time of the EM survey was at 785.5 ft and is indicated by a shift to higher conductivity and lower resistivity. The conductivity log shows six maxima from 840 to 980 ft. The highest conductivity values occur from 844 to 850 ft and correspond to the Guaje Pumice Bed. The other conductivity maxima are associated with the broad zone of higher conductivities that extend from 780 ft in the Otowi Member to 980 ft in the Puye Formation. This interval is part of the upper saturated zone of groundwater identified during drilling. However, conductivities in the upper part of this saturated zone (i.e., below 711 ft) are indistinguishable from conductivities in the unsaturated rocks above.

5.2.3.2 Results of Schlumberger Geophysical Logging

The Schlumberger logging that took place on April 21, 1999, was unsuccessful in determining the location of the tremie pipe in the well's annular fill. Neither the ultrasonic imager nor the cement-bond log was able to detect the tremie pipe adjacent to the well casing.

The results of the Schlumberger logs that were run to determine the placement of annular fill materials outside the stainless steel well were mixed. The neutron log identified zones of high water content that may indicate intervals of bridging in the annular fill. Intervals of possible bridging include: 1250 to 1256 ft, 1398 to 1404 ft, 1444 to 1446 ft, and 1668 to 1672 ft. These intervals are relatively limited in extent and do not compromise the isolation of any of the well screens. Subsequent pressure readings within each of the screen intervals using the WestbayTM sampling system confirmed the isolation of all screens.

Attempts to confirm the placement of sand filter packs and bentonite seals with geophysical surveys were unsuccessful. The natural gamma spectroscopy was unable to determine natural radiation differences between quartz sand and bentonite. The bentonite used in R-25 was a variety that provided a poor signal contrast to the filter pack. Subsequent wells installed as part of the "Hydrogeologic Workplan" used bentonite with greater potassium concentrations; this has improved the ability to determine the placement of annular fill materials using natural gamma tools.

The borehole deviation survey was conducted by Scientific Drilling International under subcontract to Schlumberger, Inc. The log shows that R-25 is nearly vertical to a depth of about 900 ft. The well then deviates to the southeast along an azimuth of 127°. The total deviation at TD is 22.8 ft.

6.0 HYDROLOGY

Unsaturated, perched-saturation, and regional-saturation zones occur in R-25. The following sections discuss analyses performed for hydrologic characterization of water occurrence and movement in each type of zone.

6.1 Unsaturated Zone

Unsaturated conditions occur between the ground surface and a depth of 711 ft, where perched saturation was encountered. Within the unsaturated zone, pore-water occurrence and pore-water movement are parameters of interest. The presence of soil-water, coupled with the hydraulic properties of the geologic material, suggests potential pathways for recharge and movement of contaminants.

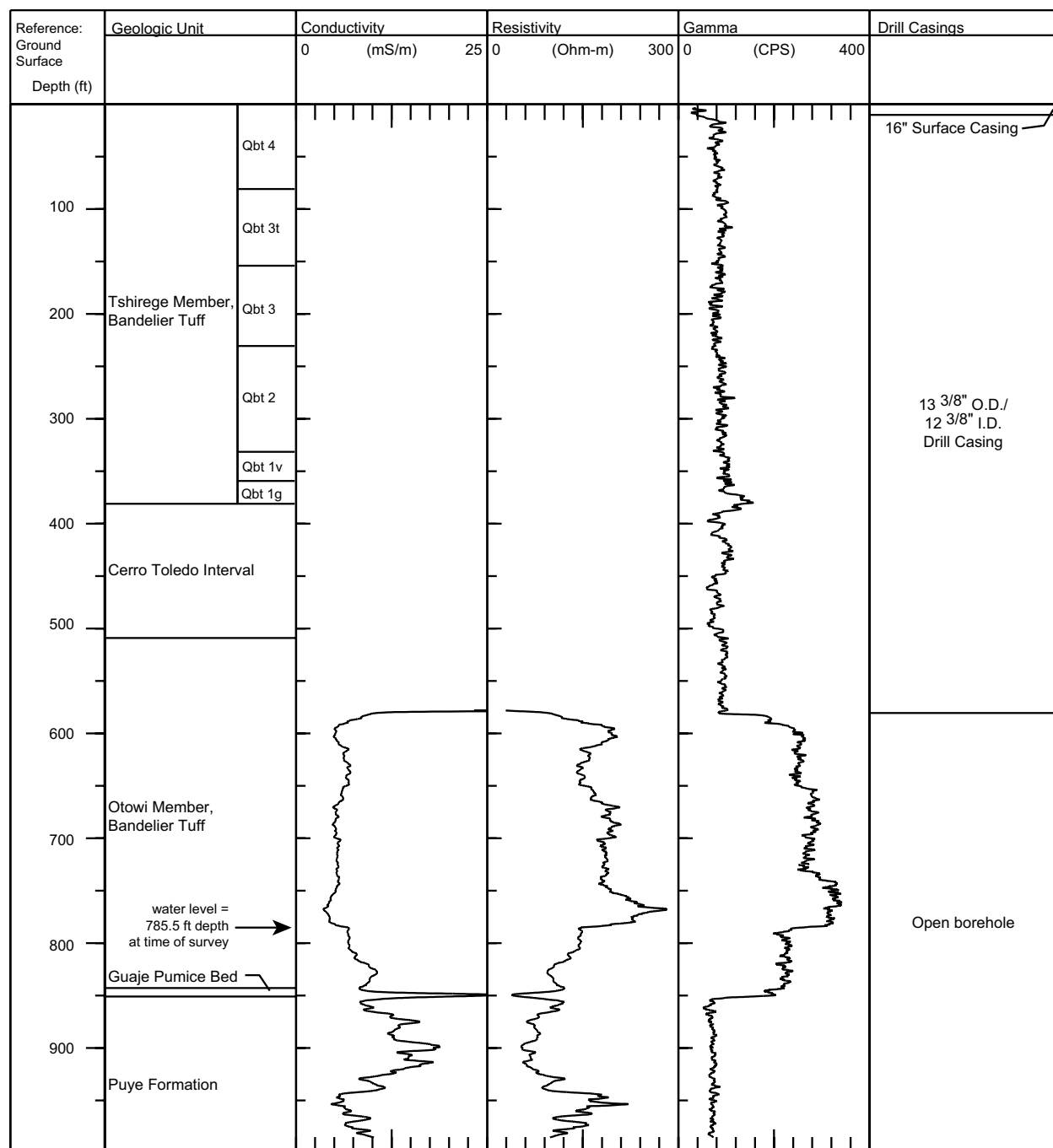


Figure 5.2-2. Results of EM survey conducted on October 14, 1998

6.1.1 Soil-Water Occurrence

6.1.1.1 Methods

Moisture content was determined from drill cuttings and core samples collected from the uppermost 664 ft of borehole R-25. R-25 was drilled dry from 0 to 588 ft (Table 2.3-2). From 588 to 664 ft, small amounts of water were introduced into the annulus at ground surface when new 20-ft rods were tripped into the hole. The cuttings quickly dried out as the hole advanced, and samples were collected from the 588- to 664-ft interval to determine moisture content when the deeper part of the rod run was being drilled. Because an increase in moisture content corresponds with the initial introduction of fluids into the borehole, data from samples collected below the 588-ft depth should be treated as suspect. After 664 ft, water was introduced on a continuous basis to facilitate drilling, and no further samples were collected for moisture-content analysis.

After core or cuttings were screened for radioactivity, samples were immediately placed in pre-weighed and pre-labeled jars with tightly fitting lids. The moisture content was determined gravimetrically by drying the samples in an oven in accordance with ASTM method D2216-90. Samples collected for determination of moisture content are listed with the analytical results in Appendix E. Moisture content is given as the ratio of the weight of water to the weight of the dry sample.

6.1.1.2 Results

Moisture content in the Tshirege Member is about 5% gravimetric near the surface and declines, with some fluctuation, to about 2% gravimetric at 340 ft near the top of Qbt 1v (Figure 6.1-1). Below 340 ft, moisture content increases through Qbt 1v and Qbt 1g to 21% in the top of the Cerro Toledo interval. No data were collected for the Tsankawi Pumice Bed. This pattern of increasing moisture content at the base of the Tshirege Member is also seen in Cañada del Buey well CDBM-1 (Rogers and Gallaher 1995, 49824), in several wells in MDA G (Rogers and Gallaher 1995, 49824; Neeper and Gilkeson 1996, 70104), in LADP-4 in TA-21 (Broxton et al. 1995, 58207), in several wells in TA-49 (Neeper and Gilkeson 1996, 70104), and in R-15 in Mortandad Canyon (Figure 6.1-2) (Longmire et al. 2001, 70103).

Moisture content falls with depth within the Cerro Toledo interval to below 5%, above and below a second maximum of 24% at 437 ft. The two moisture maxima of 21% and 24% may represent saturations of about 60%, assuming a bulk density of 1.29 gm/cm^3 and a porosity of 47%, which are the median values for the combined Tsankawi Pumice Bed and the Cerro Toledo interval (Rogers and Gallaher 1995, 49824).

These moisture maxima probably relate to changes in the pore sizes of the rock at interfaces between layers. Even in the case of no vertical flow, rock with finer grains will hold more moisture than adjacent rock with larger pore sizes. In the event that moisture is moving downward, it may increase at an interface where pore size changes. Where a fine-grained rock overlies a coarser grained rock, moisture builds up above the boundary in the finer grained unit until sufficient water pressure exists to force water into the larger pores of the underlying coarser grained material (Hillel 1980, 71306).

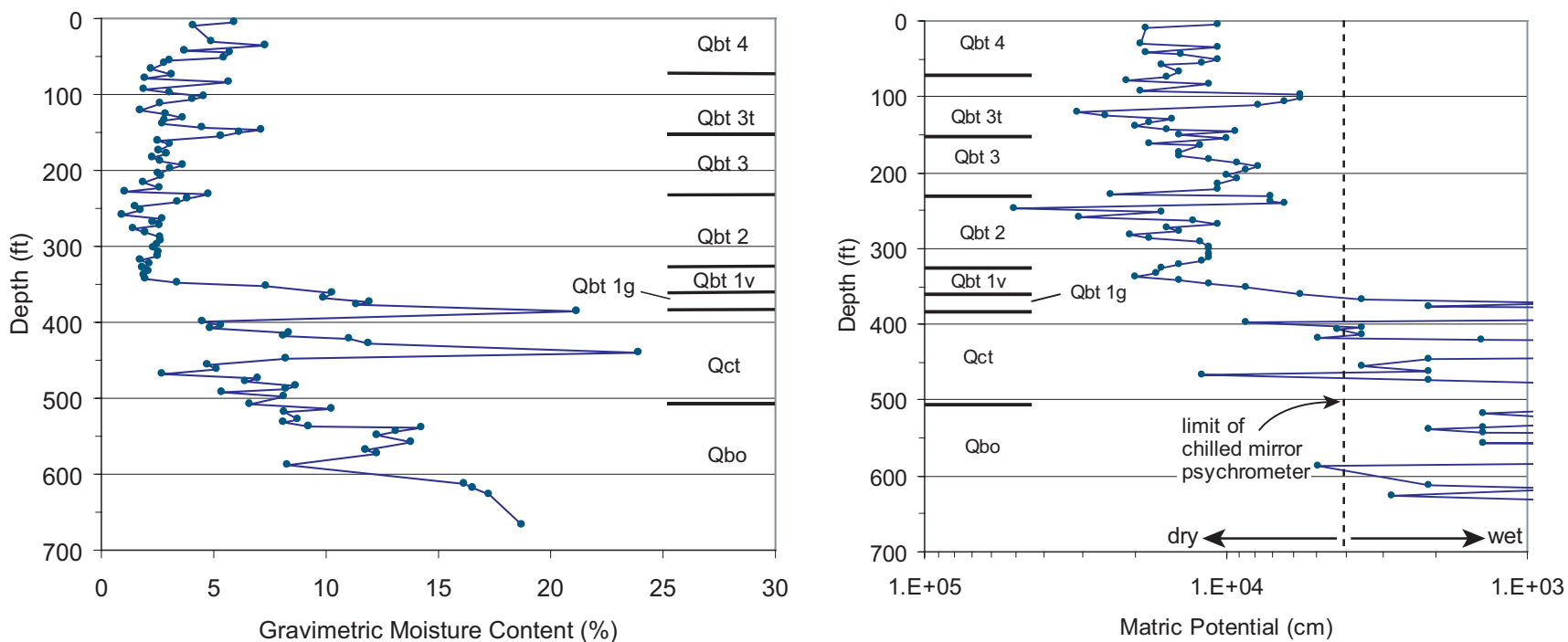


Figure 6.1-1. Gravimetric moisture content and matric potential in borehole R-25

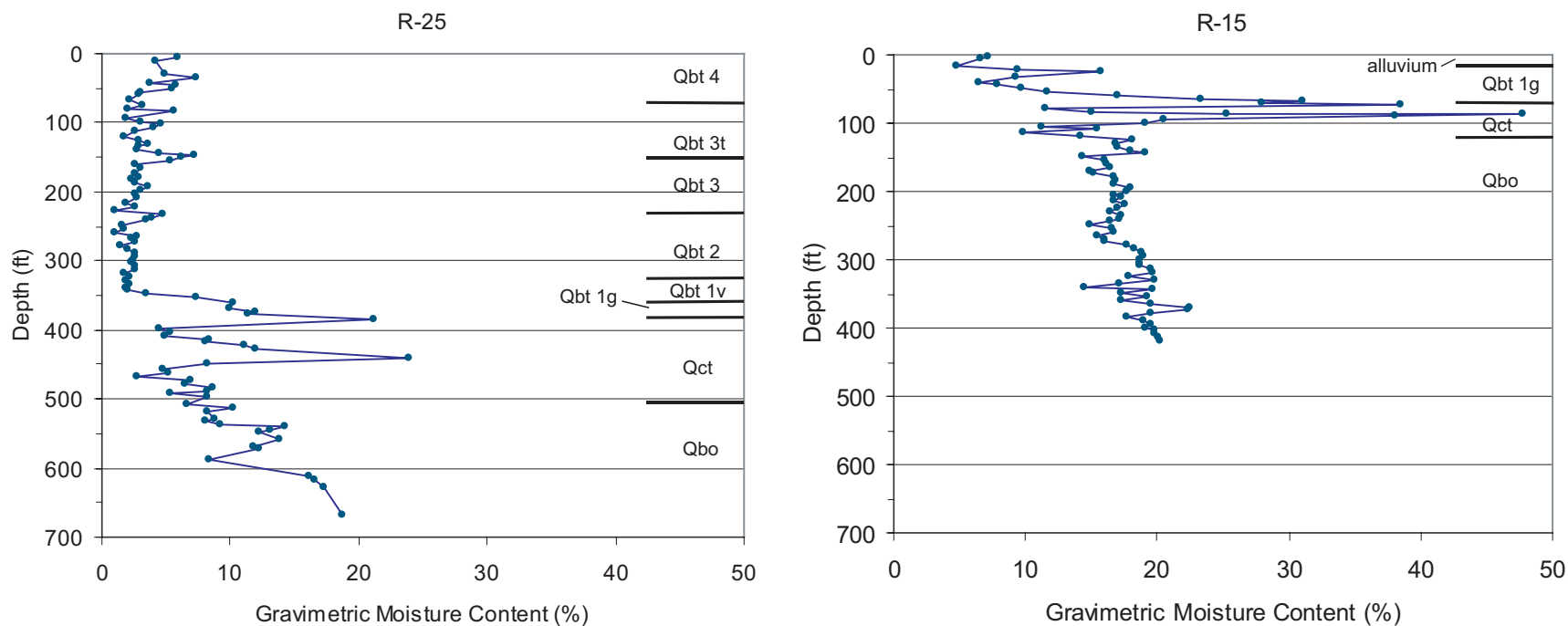


Figure 6.1-2. Comparison of moisture-content graphs for boreholes R-25 and R-15

In the lower part of the Cerro Toledo interval and the underlying Otowi Member, moisture content increases with depth, from about 5% to above 15%, although there is fluctuation in this pattern. A pattern of downwardly increasing moisture for the Otowi Member, similar to that found in R-25, was also seen in core samples collected from R-15 in Mortandad Canyon (Figure 6.1-2) (Longmire et al. 2001, 70103), LADP-3 in Los Alamos Canyon (Broxton et al. 1995, 50119), and R-12 in Sandia Canyon (Broxton et al. 2001, 71252). In R-15, moisture content decreases from 17% at the top of the Otowi Member to about 15% near the center of the unit, and then generally rises to 20% at the base of the unit (Figure 6.1-2). In R-12, gravimetric moisture content in the Otowi Member systematically increases with depth, from 6% near the top to 20% near the base of the unit. In LADP-3, moisture content for the Otowi Member ranges from 10% to 23%, although, in the upper part, moisture first decreases with depth. These wells are all located in canyon bottoms.

On the other hand, moisture content in the Otowi Member decreases with depth at two mesa-top locations: TA-49 (Neeper and Gilkeson 1996, 70104) and LADP-4 (Broxton et al. 1995, 50119). It also decreases in the canyon bottom location of Cañada del Buey well CDBM-1 (Rogers and Gallaher 1995, 49824).

6.1.2 Soil-Water Movement

When the pores in a rock are not water-filled, the hydrostatic pressure (or matric potential) is less than atmospheric pressure. The pressure potential is negative, meaning that work is required to remove water from the rock. The energy making up matric potential arises from capillary forces holding water in the pores and from adsorption that holds water to particle surfaces. In Figure 6.1-1, the absolute value of the matric potential is shown.

6.1.2.1 Methods

The chilled mirror psychrometer (or water activity meter) measures water activity in very dry soils or rocks (Gee et al. 1992, 58717). The water activity can then be converted to matric potential. The units of matric potential may be given as pressure in Pascals (Pa), or as the height of an equivalent column of water, in cm (10,200 cm H₂O = 1 MPa). The working range for the meter is in soils with a water activity of less than 0.003 (-0.4 MPa or -4080 cm H₂O) (Gee et al. 1992, 58717). As a result of measurement uncertainty, some materials near a water activity of 1 (that is, near saturation and outside of the instrument's working range) produce water activity measurements greater than 1.

Despite the inability of the chilled mirror psychrometer to measure water activity in rocks with higher moisture content, the method has advantages. The method is inexpensive, and it gives more detailed vertical information than would laboratory measurements of available core samples. For the profile in dry rock, such as in R-25 (discussed below) the chilled mirror psychrometer provides a picture of vertical matric-potential fluctuations over a 350-ft depth that would not otherwise be apparent. In selected cases, laboratory measurements were collected over a wider range of moisture content from core samples preserved for that purpose (Section 6.1.3).

Samples were double-sealed in zipper bags and wrapped in packing tape immediately following screening for radioactivity. Holding times ranged from 3 to 13 days, except for six samples collected from the 586- to 667-ft depth, which were held for 23 to 24 days. Measurements were made in duplicate within 10 min after loading sample material into plastic vials with tight-fitting lids that were inserted directly into the psychrometer. Core was crushed into mm-sized fragments as quickly as possible after breaking the seal in order to load the vials.

Repeat measurements demonstrated that samples produced the same results as long as the measurements were made within 3 hr after loading the vials and securing the lids. All analytical runs were bracketed by measurements of standards that demonstrated a 2 sigma reproducibility of .0026 water activity units for 114 analyses of the matric potential of distilled water. This is close to the instrument precision stated in Gee et al. (1992, 58717) of 0.003 water activity units (-0.4 MPa or -4080 cm H₂O). Data listed in Appendix E for matric-potential analyses represent the average of two (three, in one case) measurements made on a sample.

6.1.2.2 Results

A profile of matric potential versus depth appears beside a profile of moisture content versus depth in Figure 6.1-1. The axis of the matric-potential plot is reversed so that drier values appear on the left of the plot, corresponding to the direction of the drier values for moisture content. In general, the dry values for matric potential correspond to dry values for moisture content. The exact correspondence of matric potential and moisture content depends on rock texture as well as moisture content. Samples collected above a depth of 360 ft (Qbt 1v and above) have matric potentials within the working range of the psychrometer. These samples generally have gravimetric moisture contents below 5%. Higher moisture content below this depth resulted in few measurements within the psychrometer's working range. The variation in matric potential with depth within the Tshirege Member reflects the variation in moisture content with depth, as well as the variation in porosity and pore-size distribution.

6.1.3 Hydraulic Properties

Core and cuttings samples were collected in the unsaturated zone and are preserved and stored at the FSF. Four samples from the unsaturated zone were selected for hydraulic-properties testing based on data needs identified for modeling and other purposes. These samples were analyzed for a full suite of hydraulic properties: moisture content, porosity, bulk density, saturated hydraulic conductivity, and determination of moisture characteristics. A listing of the samples tested is given in Table 6.1-1.

Table 6.1-1
Samples from R-25 Tested for Hydraulic Properties

Sample Number	Geologic Unit	Depth Interval (ft)	Test
CACV-98-0039	Qbt 2 (densely-welded tuff) ^a	239.2–239.5	H Pkg ^b
CACV-98-0043	Qbt 1g (nonwelded tuff) ^c	371.2–371.5	H Pkg
CACV-98-0046	Tsankawi Pumice Bed	383.5–384	H Pkg
CACV-98-0049	Qbo (nonwelded tuff) ^d	546.8–547.5	H Pkg
CACV-99-0021	Qbo (nonwelded tuff)	767.5–768	Ksat ^e

Source: Stone 2000, 66781.

^a Qbt 2 = Unit 2, Tshirege Member, Bandelier Tuff.

^b H Pkg = hydraulic package (full range of unsaturated-zone characteristics).

^c Qbt 1g = Unit 1 glassy, Tshirege Member, Bandelier Tuff.

^d Qbo = Otowi Member, Bandelier Tuff.

^e Ksat = saturated hydraulic conductivity only.

6.1.3.1 Methods

Samples for hydraulic-properties testing were collected as soon as possible after core extraction and were protected from moisture loss by the following methods:

- Samples were collected in 6-in.-diameter Lexan plastic or stainless steel liners loaded into the core tube.
- If a core sample collected without a liner was deemed to warrant hydraulic testing, it was quickly inserted into a liner, intact if possible.
- The ends of the Lexan plastic or stainless steel liners containing core to be preserved were capped with tight-fitting plastic caps and sealed with Teflon nonstick-coated tape.
- The capped ends of the liner were wrapped with clear packing tape.
- The footage interval of the sample, as well as the time and date of sample collection, were recorded on the liner with indelible ink.
- The capped and labeled liner was inserted into a Coreprotec aluminized sleeve labeled with the same sampling information.
- The ends of the Coreprotec sleeve were melted together with an electric heat sealer, creating an airtight seal.
- The protected cores were documented as samples for hydraulic testing, stored to prevent freezing, and transported to the FSF as soon as possible after they were collected.
- Custody of the samples was transferred from the Canyons Focus Area field support team to the FSF using a Microsoft® Access database and electronic chain-of-custody form.

6.1.3.2 Results

Results of hydraulic-properties testing of core from the unsaturated zone in R-25 are presented in Appendix F as reported by Stone (2000, 66781).

6.2 Saturated Zones

Two saturated zones were projected to occur in R-25: one perched near the base of the Bandelier Tuff (as in SHB-3) and one associated with the regional zone of saturation in the Puye Formation.

6.2.1 Groundwater Occurrence

Groundwater occurred in R-25 essentially as predicted. However, the great vertical extent of the perched saturation (711 to 1132 ft) was unexpected.

6.2.1.1 First Saturation

The first water encountered in R-25 was that perched in the Otowi Member of the Bandelier Tuff (see Figure 2.3-1). Saturation was first noted in cuttings from a depth of 747 ft. Before drilling continued, depth to water was measured by electric probe first at 734 ft and finally at 711 ft. This 36-ft water-level rise should not be taken as a response to confinement, but rather as a reflection of the normal lag time

required for water to fill the hole after a saturated zone is opened up by drilling. The borehole video shows an abrupt increase in moisture on the borehole walls at a depth of 718 ft. Saturation persisted into the underlying Puye Formation to a depth of 1132 ft.

6.2.1.2 Alternating Wet and Dry Zone

Underlying the perched saturation is a zone of alternating wet and dry materials. Excerpts from the field log for the portion of the R-25 borehole in the Puye Formation at and below a depth of 1132 ft document this as follows:

- dry cuttings at 1132 ft
- unsaturated conditions from 1172 ft to 1173 ft
- saturated conditions from 1173 ft to 1175 ft
- dry zone from 1175.4 ft to 1176.4 ft
- saturated core from 1180 ft to 1182 ft
- moist core from 1182 ft to 1182.5 ft
- slightly moist core from 1184 to 1185 ft
- dry core from 1188 to 1193 ft
- relatively dry cuttings from 1192 to 1200.5 ft

This wet and dry zone continues to a depth of 1286 ft, where it is believed that regional saturation is encountered. The unsaturated intervals seem to be associated with coarse sedimentary deposits expected to have low permeability under less than saturated conditions. This zone is apparently responsible for perching the water encountered in the Otowi Member.

6.2.1.3 Deep Saturation

At a depth of 1286 ft (64 ft shallower than predicted) the R-25 borehole penetrates groundwater believed to be associated with the regional zone of saturation. This saturation occurs in the Puye Formation and continues to the TD at 1942 ft. Although R-25 is completed in the Puye Formation, the deep saturation presumably extends into underlying sediments of the Santa Fe Group.

6.2.2 Groundwater Movement

The two components of groundwater movement are direction and rate. Although data for evaluating horizontal flow direction are not provided by a single well, vertical flow direction can be determined by analysis of head distribution along the borehole, especially if casing is advanced while drilling. Flow rate (i.e., Darcy velocity) is the product of hydraulic conductivity and horizontal gradient. Hydraulic conductivity is obtained by field or laboratory tests, as discussed in Section 6.2.2.2 below.

6.2.2.1 Vertical Head Distribution

The sense of the vertical gradient, that is, whether water movement in the saturated zone is up or down, is best determined by examining the vertical water-level or head distribution. If water-level depth increases or head decreases with borehole depth, the gradient is downward. Conversely, if water-level depth decreases or head increases with borehole depth, the gradient is upward.

Piezometers are open-bottom tubes set at discrete depths in the saturated zone for determining hydraulic head. Theoretically, when casing is advanced during drilling, as in R-25, the well may be thought of as an infinite set of piezometers. More specifically, if the casing is sufficiently tight, static water levels observed during such drilling can be used to construct the isopotential field in the area. In practice, however, there may be some space between the casing and borehole wall and the water at the bottom of the casing may be in contact with water behind the casing. In this case, water-level measurement yields a composite value. Furthermore, water soundings are made only when drilling activities permit. As a result, not all observations made are static water levels. For example, if the casing has been withdrawn to expose a sizable length of open borehole at the time of measurement, the casing is no longer a piezometer interrogating a discrete interval and sounding again yields a composite water level. Also, if the drilling activity immediately preceding measurement is particularly disruptive of fluid in the borehole or not enough time has been allowed for the water level to recover from that activity, measurements will be misleading. Thus, water-level data taken while the hole is being drilled tend to be "noisy."

An electronic database was constructed to record water levels and the conditions at the time they were measured. Noise in the water-level data for R-25 was filtered out by considering three factors: (1) the length of open hole at the time of measurement (was the hole a true piezometer at the time?), (2) the pre-measurement activity in the well (was it especially disruptive of water level?), and (3) the elapsed time between that activity and the water-level measurement (had there been enough time for recovery to a static level?). Several of the water levels that seemed to be static based on these criteria were selected for analysis of vertical head distribution. A plot of depth to water versus depth of the borehole at the time of measurement for the static water levels selected is given in Figure 6.2-1. Water levels selected in the way described compare favorably with those obtained by pressure transducers in the Westbay™ multiport monitoring system installed in the completed well.

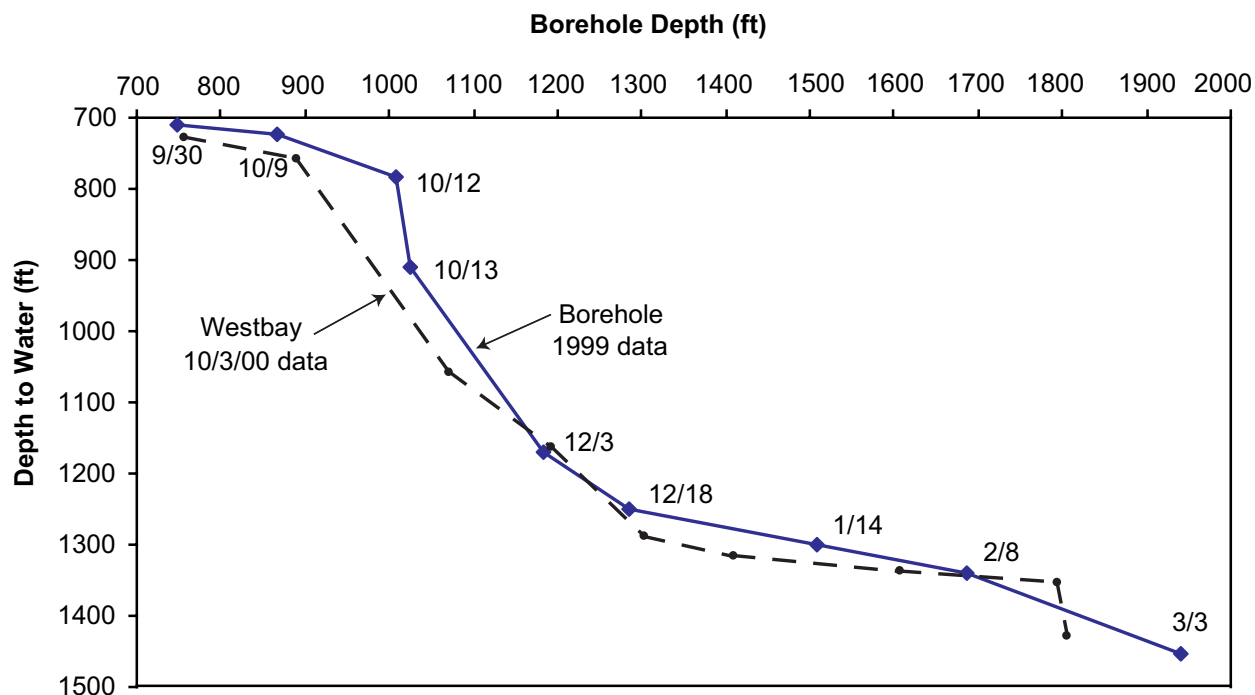


Figure 6.2-1. Westbay™ versus borehole water-level data for R-25

These water-level depths were converted to head values (subtracted from the ground-surface elevation at R-25) and plotted at the depths where they were observed (Figure 6.2-2). Because the isopotentials decrease downward, and groundwater moves from higher to lower head, the vertical gradient in both zones of saturation is downward. The head distribution confirms that R-25 is located in a recharge area, as suggested by its location near the mountains at the western edge of the Laboratory.

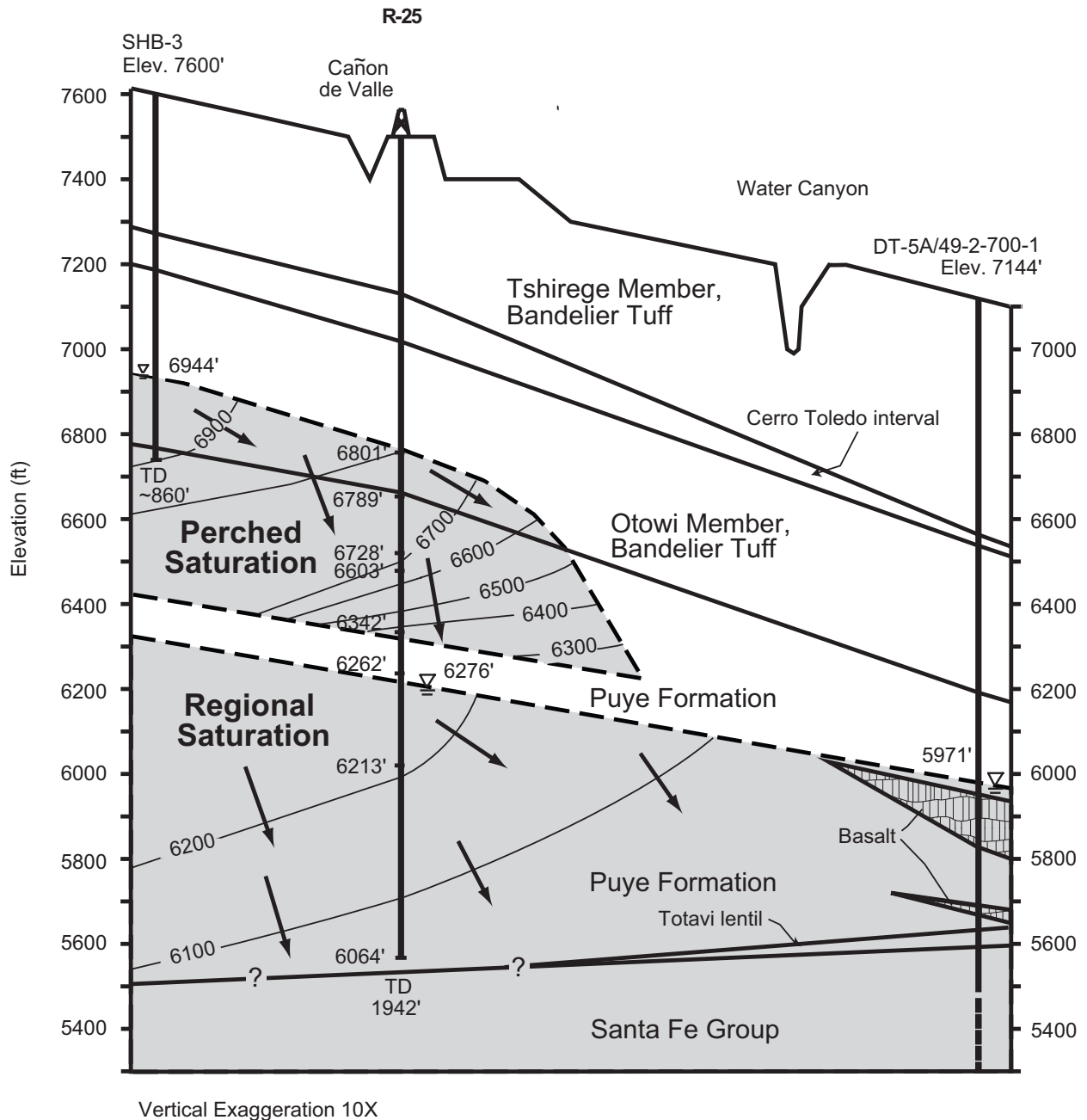


Figure 6.2-2. NW to SE cross-section showing isopotentials and flow near R-25
See Figure 1.0-1 for locations of wells used in figure.

6.2.2.2 Hydraulic Properties

Both field and laboratory measurements can provide data on the hydraulic properties of saturated materials. However, slug-injection testing was unsuccessful in R-25; the screened intervals simply would not accept the injected water. One core sample of nonwelded tuff from the Otowi Member of the Bandelier Tuff was analyzed in the laboratory for saturated hydraulic conductivity (Table 6.1-1). Analysis by the constant-head method gave a value of 2.7×10^{-4} cm/sec (Stone 2000, 66781).

7.0 HYDROCHEMISTRY

This section summarizes the results of geochemical characterization investigations conducted at borehole R-25. Samples of groundwater, core, and cuttings were collected from the R-25 borehole and analyzed for contaminants of concern identified for TA-16 (LANL 1998, 59891).

7.1 Geochemistry of Core and Cuttings

Thirteen samples of core and cuttings were collected from R-25 and analyzed for HE compounds and associated degradation products, trace elements, major anions, and radionuclides as generally required by the Resource Conservation and Recovery Act (RCRA) and for constituents appropriate for characterization purposes. One sample was also analyzed for organic content. Table 7.1-1 provides sample information and correlation to the hydrogeology encountered during drilling. Screening for radioactivity (rad van) was performed prior to shipping samples to analytical laboratories.

7.1.1 HE Compounds, Trace Elements, and Radionuclides

7.1.1.1 Methods

Approximately 500 to 1000 g of core or cuttings samples were placed in appropriate sample jars in protective plastic bags before they were shipped to analytical laboratories. Samples were shipped to Paragon Analytics, Inc., in Fort Collins, Colorado, and analyzed using methods specified by EPA (1987, 57589). Sample duplicates were collected and analyzed in accordance with EPA procedures. Solid samples were partially digested using HCl, H₂O₂, and hot HNO₃ (EPA Method 3050) before analysis for metals. Table 7.1-2 provides the list of analytes and the analytical methods and techniques. Analytical techniques included high-pressure liquid chromatography (HPLC) for analysis of HE compounds and associated degradation products; inductively coupled plasma emission spectroscopy (ICPES) for metals and trace elements; cold vapor atomic absorption (CVAA) for mercury; alpha spectrometry for americium-241 and uranium and plutonium isotopes; gamma spectroscopy for cesium-137 and other gamma-emitting isotopes; and gas proportional counting for strontium-90.

Field screening for volatile organic compounds (VOCs) was conducted using a photoionization detector (PID). No VOCs were detected with the PID.

7.1.1.2 Results

Data quality validation was performed on the analytical results. No serious deficiencies in data quality were identified. These data were validated through the ER Project.

Table 7.1-1
Core and Cuttings Samples Selected for Contaminant Characterization

Sample Interval	Geologic Unit	Sample Type	Analyses ^a	Sampling Zone
110.25 to 110.65 ft	Tshirege Member	Core	gross- α , - β , - γ , HE, TOC, TAL metals, rad van	Unsaturated
223 to 225 ft	Tshirege Member	Cuttings	gross- α , - β , - γ , HE, TOC, TAL metals, isotopic U, rad van, SVOCs	Unsaturated
243.7 to 244.7 ft	Tshirege Member	Core	gross- α , - β , - γ , HE, TAL metals, rad van, isotopic U, SVOCs	Unsaturated
318 to 319 ft	Tshirege Member	Cuttings	gross- α , - β , - γ , HE, TAL metals, rad van, isotopic U, SVOCs	Unsaturated
353 to 354 ft	Tshirege Member	Core	gross- α , - β , - γ , HE, TAL metals, rad van, isotopic U, SVOCs	Unsaturated
366 to 366.8 ft	Tshirege Member	Core	gross- α , - β , - γ , HE, TAL metals, rad van, isotopic U, SVOCs	Unsaturated
387.2 to 388.2 ft	Cerro Toledo interval	Core	gross- α , - β , - γ , HE, TAL metals, rad van, isotopic U, SVOCs	Unsaturated
440 to 445 ft	Cerro Toledo interval	Cuttings	gross- α , - β , - γ , HE, TAL Metals, rad van, isotopic U, SVOCs	Unsaturated
448 to 449 ft	Cerro Toledo interval	Core	gross- α , - β , - γ , HE, TAL metals, rad van, isotopic U, SVOCs	Unsaturated
550.2 to 551.2 ft	Otowi Member	Core	gross- α , - β , - γ , HE, TAL metals, rad van, SVOCs, isotopic U, CATMS, VOCs, anions	Unsaturated
687 to 695 ft	Otowi Member	Cuttings	gross- α , - β , - γ , HE, TAL metals, rad van, isotopic U, SVOCs, CATMS	Unsaturated
768.5 to 769.45 ft	Otowi Member	Core	gross- α , - β , - γ , HE, TAL metals, rad van, SVOCs, isotopic U, VOCs, anions, % organic carbon	Upper saturated
1132 to 1137 ft.	Puye Formation	Cuttings	gross- α , - β , - γ , HE, TAL metals, rad van, isotopic U, SVOCs, VOCs	Wet/dry

^a HE = high explosives, TOC = total organic carbon, TAL = target analyte list, rad = radionuclides, SVOC = semivolatile organic compounds, VOCs = volatile organic compounds, CATMS = cations analyzed by mass spectrometry.

Table 7.1-2
HE Compound, Trace Element, and
Radionuclide Analytes for R-25 Core, Cuttings, and Water Samples

Analyte	Analytical Method	Analytical Technique ^{a,b}
Hexahydro-1,3,5-trinitro-1,3,5-triazine (RDX)	EPA Method 8330	HPLC
Nitrobenzene	EPA Method 8330	HPLC
Octahydro-1,3,5,7-tetranitro-1,3,5,7-tetrazocine (HMX)	EPA Method 8330	HPLC
1,3-dinitrobenzene	EPA Method 8330	HPLC
1,3,5-trinitrobenzene (TNB)	EPA Method 8330	HPLC
2-amino-4,6 dinitrotoluene (2-A-4,6-DNT)	EPA Method 8330	HPLC
2-nitrotoluene	EPA Method 8330	HPLC

Table 7.1-2 (continued)

Analyte	Analytical Method	Analytical Technique ^{a,b}
2,4-dinitrotoluene	EPA Method 8330	HPLC
2,4,6-trinitrotoluene (TNT)	EPA Method 8330	HPLC
2,6-dinitrotoluene	EPA Method 8330	HPLC
3-nitrotoluene	EPA Method 8330	HPLC
4-amino-2,6 dinitrotoluene (4-A-2,6-DNT)	EPA Method 8330	HPLC
4-nitrotoluene	EPA Method 8330	HPLC
Tetryl	EPA Method 8330	HPLC
Total organic carbon	EPA Method 415.1	WCO
Aluminum	EPA Method 6010B	ICPES
Antimony	EPA Method 6010B	ICPES, HAA
Arsenic	EPA Method 7060A	ICPES, HAA
Barium	EPA Method 6010B	ICPES
Beryllium	EPA Method 6010B	ICPES
Cadmium	EPA Method 6010B	ICPES, GFAA
Calcium	EPA Method 6010B	ICPES
Chromium	EPA Method 6010B	ICPES, GFAA
Cobalt	EPA Method 6010B	ICPES, GFAA
Copper	EPA Method 6010B	ICPES, GFAA
Iron	EPA Method 6010B	ICPES
Lead	EPA Method 6010B	ICPES, GFAA
Magnesium	EPA Method 6010B	ICPES
Manganese	EPA Method 6010B	ICPES
Mercury	EPA Method 7470A	ICPES, CVAA
Nickel	EPA Method 6010B	ICPES, GFAA
Potassium	EPA Method 6010B	ICPES
Selenium	EPA Method 6010B	ICPES, HAA
Silver	EPA Method 6010B	ICPES, GFAA
Sodium	EPA Method 6010B	ICPES
Thallium	EPA Method 6010B	ICPES, GFAA
Uranium	No EPA Method	LIKPA
Vanadium	EPA Method 6010B	ICPES
Zinc	EPA Method 6010B	ICPES
Americium-241	No EPA Method	chemical separation/ alpha spectrometry
Plutonium-238	No EPA Method	chemical separation/ alpha spectrometry
Plutonium-239,240	No EPA Method	chemical separation/ alpha spectrometry
Uranium-234	No EPA Method	chemical separation/ alpha spectrometry

Table 7.1-2 (continued)

Analyte	Analytical Method	Analytical Technique ^{a,b}
Uranium-235	No EPA Method	chemical separation/ alpha spectrometry
Uranium-238	No EPA Method	chemical separation/ alpha spectrometry
Cesium-137	No EPA Method	chemical separation/ gamma spectrometry
Strontium-90	No EPA Method	gas proportional counting
Gamma-emitting isotopes	No EPA Method	chemical separation/ gamma spectrometry
Tritium	No EPA Method	direct counting
Volatile organic compounds	EPA Method 8260B	GC/MS
Semivolatile organic compounds	EPA Method 8081A, 8082, 8270C	GC/MS
Anions		
Bromide	EPA Method 9056	IC
Chlorate	EPA Method 9056	IC
Chloride	EPA Method 9056	IC
Fluoride	EPA Method 9056	IC
Nitrate	EPA Method 9056	IC
Nitrite	EPA Method 9056	IC
Orthophosphate	EPA Method 9056	IC
Sulfate	EPA Method 9056	IC
Other Inorganic Chemicals		
Silica	EPA Method 370.1	Colorimetry
Total cyanide	EPA Method 9012A	Colorimetry

^a HPLC = high-pressure liquid chromatography, ICPES = inductively coupled plasma emission spectroscopy, CVAA = cold vapor atomic absorption, IC = ion chromatography, HAA = hydride atomic absorption, GFAA = graphite furnace atomic absorption, WCO = wet chemical oxidation, GC/MS = gas chromatography/mass spectrometry, LIKPA = laser-induced kinetic phosphorimetric analysis. EES-6 used GFAA and HAA on screening water samples collected from R-25.

^b EPA SW-846 or equivalent.

HE compounds and degradation products were not detected in core and cuttings samples collected from the R-25 borehole. These compounds poorly adsorb onto the Bandelier Tuff and Puye Formation due to the near absence of solid organic matter (<0.05 wt%).

Results for trace element analyses show that concentrations of trace elements, including barium and uranium, were within LANL background UTLs for the Bandelier Tuff. Some elements were not present or were present at concentrations less than quantitation limits. These included antimony, arsenic, cadmium, cobalt, copper, lead, mercury, nickel, selenium, silver, thallium, and vanadium.

Isotopes of uranium (uranium-234, uranium-235, and uranium-238), gross alpha, gross beta, and gross gamma were detected in samples from the R-25 borehole. Activities of gross alpha, gross beta, and gross gamma in samples of core and cuttings were greater than 1 pCi/g, where measurable, and varied with depth. Activities of isotopic uranium were higher in samples collected from the Bandelier Tuff, reflecting

the high total uranium in this volcanic rock (Ryti et al. 1998, 58093). Lower activities of uranium-234, uranium-235, and uranium-238 were generally found in samples collected from the Puye Formation. Activities of total isotopic uranium were not elevated above Laboratory background for the Bandelier Tuff. Activities of americium-241; cesium-137; plutonium-238; plutonium-239,240; and strontium-90 were less than the detection limits in the samples of core and cuttings, indicating that no Laboratory-derived contamination from the isotopes is detectable in core samples collected from R-25.

The organic carbon content was measured in one core sample from the Otowi Member and was less than 0.05 wt%. The near absence of organic carbon, which is a dominant adsorbent for HE compounds, is consistent with the analytical results for HE compounds presented above.

7.1.2 Anion Profiles and Stable Isotopes

Anion profiles (bromide, chloride, nitrate, nitrite, phosphate, oxalate, and sulfate) and stable oxygen (oxygen-18 [^{18}O] and oxygen-16 [^{16}O]) and hydrogen (deuterium [^3H or D] and [H] protium) isotopes were determined for 30 core and cuttings samples collected from the upper part of the R-25 borehole. The samples were co-located with selected samples analyzed for moisture content and matric potential.

7.1.2.1 Methods

Samples were washed with deionized water at EES-6 for 16 hr before analysis for anions (Broxton et al. 2001, 71252). The precision limits for major anions were generally within 10%.

Pore-water anion concentrations for bromide, chloride, fluoride, nitrate, nitrite, phosphate, and sulfate were determined for the same samples collected for moisture-content analysis from the unsaturated zone, as described in Section 6.1. Anion concentrations in leachates were determined by IC. Pore-water anion concentrations were then calculated using leachate concentrations, gravimetric moisture contents, and estimated bulk densities (i.e., from Daniel B. Stephens and Associates [1999, 70105] for the upper units of the Tshirege Member, and from Rogers and Gallaher [1995, 49824] for deeper units).

Analyses for both $\delta^{18}\text{O}$ and δD were performed on core samples from the unsaturated zone. Samples were sent to the New Mexico Institute of Mining and Technology in Socorro, New Mexico, for analysis. Analyses were performed on moisture-protected samples using the vacuum distillation method of Shurbaji and Campbell (1997, 64063) and the $\delta^{18}\text{O}$ and δD extraction methods of Socki et al. (1992, 64064) and Kendall and Coplen (1985, 64061) respectively. The analytical precision for analyses by mass spectrometry was better than 0.2 ‰ for $\delta^{18}\text{O}$ and 6 ‰ for δD .

7.1.2.2 Results

Estimates of pore water anion concentrations (screening analyses) are given in Table 7.1-3. Many of the concentrations were below detection limits, which may be a result of dilution associated with the sample preparation method.

In general, the anions all showed similar behavior, with multi-peaked profiles with depth, although some differences and the magnitude of concentrations (especially for chloride and sulfate) were not always consistent. Vertical profiles for chloride, oxalate, phosphate, and sulfate are presented in Figure 7.1-1.

A chloride spike occurred at about 50 ft within the lower part of Qbt 4. The chloride spike that occurred between about 231 and 332 ft corresponds to a region of moderately welded tuff of Qbt 2 that lies between non- to poorly welded tuff units. The increase in chloride below 600 ft in the Otowi Member may be related to the upper perched zone at 711 ft. In other boreholes (e.g., R-9), a spike in anion

concentrations was observed above perched saturated zones. The chloride increase also corresponds to an increase in moisture content in the Otowi Member. However, anion results for depths below 588 ft may have been affected by the addition of drilling fluids (Section 6.1.1.1).

Table 7.1-3
Estimates of Pore Water Anion Concentrations in R-25 Samples

Depth (ft)	Bromide (mg/L)	Chloride (mg/L)	Nitrate (mg/L)	Nitrite (mg/L)	Oxalate (mg/L)	Phosphate (mg/L)	Sulfate (mg/L)
5	2	69	BD	BD	BD	7	561
9.5	2	121	BD	BD	BD	7	325
30.5	0	61	BD	BD	23	BD	271
51.5	1	322	BD	BD	9	BD	100
74	BD ^a	84	BD	BD	48	BD	50
93.2	BD	47	BD	BD	BD	BD	9
112	BD	21	BD	BD	BD	BD	4
131	BD	20	BD	BD	21	BD	21
150	BD	84	BD	BD	12	2	17
174	BD	62	BD	BD	BD	17	8
198	BD	48	BD	BD	BD	6	11
228	BD	67	BD	BD	53	BD	72
252.5	BD	463	BD	BD	17.9	7	17
277	BD	219	BD	BD	36	20	22
302	BD	212	BD	BD	34	5	14
328	BD	136	BD	BD	30	27	17
352.4	BD	16	BD	BD	6	BD	6
373.5	BD	8	BD	BD	BD	BD	1
399	BD	10	BD	BD	17	BD	21
422	BD	9	BD	BD	4	BD	6
440	BD	13	BD	BD	3	BD	6
462	BD	12	BD	BD	18	BD	23
484	BD	6	BD	BD	19	BD	19
508	BD	12	BD	BD	12	BD	25
532	BD	7	BD	BD	4	BD	8
558	BD	5	BD	BD	BD	1	5
588	BD	11	BD	BD	38	BD	47
613	BD	15	0.3	BD	7	BD	27
627	BD	94	BD	BD	5	BD	176
667	BD	311	0.59	BD	8	BD	553

Note: These data are used for screening purposes only.

^a BD = below detection.

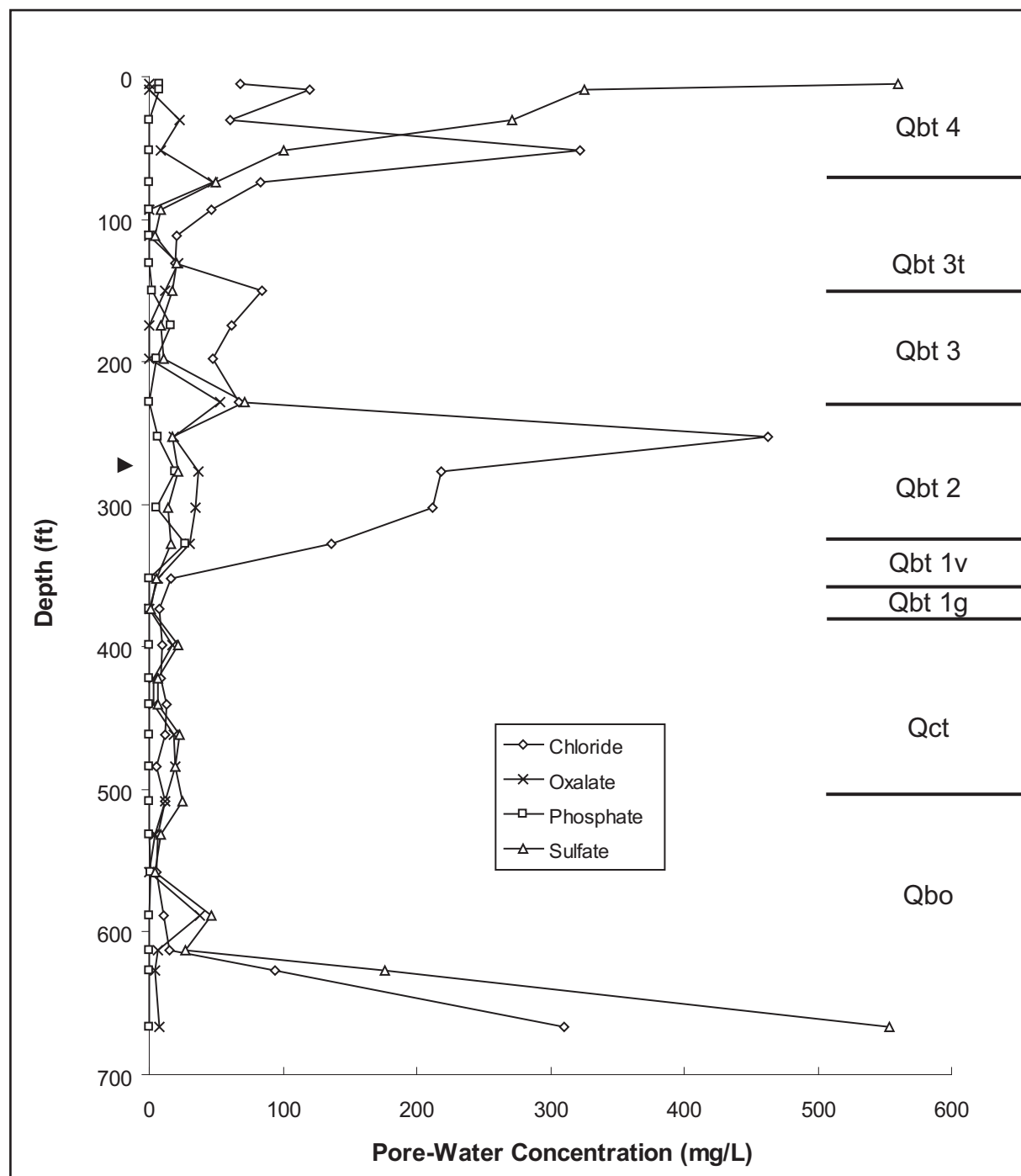


Figure 7.1-1. Pore-water anion concentrations versus depth in R-25

The $\delta^{18}\text{O}$ and δD results were similar and showed a noisy but decreasing trend down to 566 ft. Figure 7.1-2 shows the $\delta^{18}\text{O}$ results. The results plotted at 1158 and 1184 ft correspond to samples from the perching unit for the upper saturated zone, and the decreasing trend is also supported by the results of the δD analyses. No samples were taken between 566 and 1158 ft.

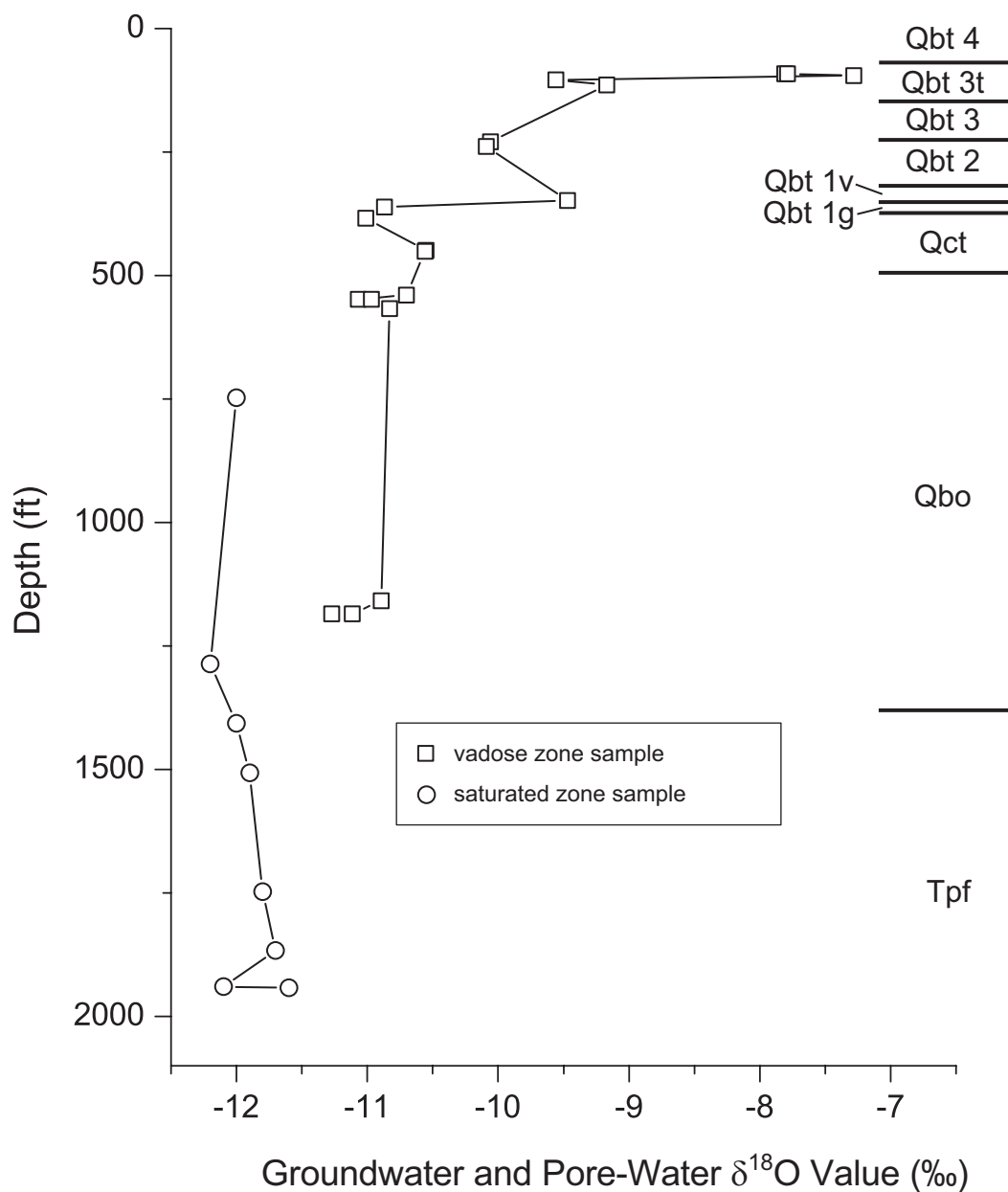


Figure 7.1-2. Groundwater and pore-water oxygen isotope profile ($\delta^{18}\text{O}$) for borehole R-25
(See Table 7.2-6 for $\delta^{18}\text{O}$ values for the saturated zones.)

There may be a systematic bias between the unsaturated and saturated zone isotopic analyses. The analysis of the unsaturated zone samples are the least accurate and precise, and the results are typically isotopically lighter than those for samples collected from the upper saturated zone. The absolute difference, however, is only about 1‰. In general, borehole R-25 has a fairly consistent isotopic signature below Tshirege Qbt 2. This observation suggests that either the recharge source of the two saturated zones is similar or the zones have some connectivity, although not necessarily in the vicinity of R-25. Results of stable isotope analyses for the upper saturated zone and regional aquifer suggest that both groundwaters are well mixed.

7.2 Hydrochemistry of Groundwater

Fourteen screening groundwater samples were collected during drilling from two saturated zones encountered in the R-25 borehole and analyzed to determine natural solute and contaminant distributions. Samples were analyzed for HE compounds and degradation products, major cations and anions, metals, organic compounds, radionuclides, stable isotopes, and dissolved organic carbon (DOC). One screening sample collected from 1938 ft was analyzed only for HE compounds and degradation products. Table 7.2-1 provides information on sample depths and analyses performed. Two replicate groundwater samples were collected from 1940 ft, consisting of one bailer sample and one airlifted sample.

Table 7.2-1
R-25 Groundwater Sample Depths, Analyses, and Sampling Zones

Sample Depth (ft)	Analyses	Sampling Zone
Otowi Member		
747	Full suite ^a	Upper saturated
Puye Formation		
867	Full suite	Upper saturated
1047	Full suite	Upper saturated
1137	Full suite	Wet/dry zone
1184	Full suite	Wet/dry zone
1286	Full suite	Regional aquifer
1407	Full suite	Regional aquifer
1507	Full suite	Regional aquifer
1607	Full suite	Regional aquifer
1747	Full suite	Regional aquifer
1867	Full suite	Regional aquifer
1938	Full suite	Regional aquifer
1940	Full suite	Regional aquifer
1942	HE and degradation products	Regional aquifer

^a The full suite of analyses includes HE compounds and their degradation products, metals, major cations and anions, organic compounds, radionuclides, stable isotopes, and DOC.

7.2.1 Methods

Groundwater samples were mostly collected using a clean stainless steel bailer. Some samples collected from the regional aquifer were airlifted to minimize “down time” of the drill rig. Field measurements for temperature, dissolved oxygen (DO), turbidity, pH, and specific conductance were determined onsite. Screening for RDX and TNT using DTech instruments was performed at a field laboratory. Both filtered and unfiltered samples were collected. Samples to be analyzed for metals and radionuclides were filtered through a 0.45-µm filter and acidified with analytical-grade HNO₃ to a pH of 2.0 or less. Samples to be analyzed for DOC were filtered with a special 0.45-µm silver filter to eliminate biodegradation of organic solutes. All samples were stored at 4°C until they were analyzed. Alkalinity was determined in the laboratory using standard titration techniques shortly after sample collection (within 24 hr).

Concentrations of HE compounds and degradation products in nonfiltered groundwater samples were determined using HPLC (EPA Method 8330). Concentrations of VOCs and SVOCs (polychlorinated biphenyls [PCBs] and pesticides) were determined using GC/MS. Analyses were performed by Paragon Analytics, Inc.

Concentrations of inorganic analytes were determined at both Paragon Analytics, Inc., and EES-6 using techniques specified in EPA SW-846 (EPA 1987, 57589). These included IC for anions (bromide, chloride, fluoride, nitrate, nitrite, oxalate, phosphate, and sulfate), colorimetry for total cyanide, CVAA for mercury, and ICPEES for aluminum, antimony, arsenic, barium, beryllium, boron, cadmium, calcium, chromium, cobalt, copper, iron, lead, magnesium, manganese, nickel, potassium, selenium, sodium, thallium, vanadium, and zinc. HAA (antimony, arsenic, and selenium), GFAA (cadmium, chromium, cobalt, copper, lead, nickel, silver, and thallium), and ion selective electrode (ammonium) analytical techniques were used by EES-6 in addition to ICPEES. Charge balance errors calculated from filtered groundwater samples analyzed by EES-6 ranged from -0.16 to +12.22% (Appendix G), predominantly within the EPA recommended range of $\pm 10.00\%$.

Radionuclide analyses were performed by Paragon Analytics, Inc., Teledyne, and the University of Miami (low-level tritium). The activity of tritium in groundwater samples was determined by direct counting and electrolytic enrichment (low-level tritium, < 2 pCi/L). LIKPA was used to analyze groundwater samples for uranium; alpha spectrometry for americium, plutonium, and uranium isotopes; gamma spectrometry for cesium isotopes; and gas proportional counting for strontium-90.

Samples were analyzed for stable isotopes of oxygen (oxygen-18 and oxygen-16) and hydrogen (hydrogen and deuterium) by Geochron Laboratories and for nitrogen (nitrogen-15 and nitrogen-14) by Coastal Sciences Laboratories, Inc., using the isotope ratio mass spectrometry (IRMS) technique. Analytical errors associated with δD and $\delta^{18}O$ measurements were ± 4 and 1% , respectively.

Laboratory blanks were analyzed in accordance with EPA and Laboratory procedures. The precision limits for major ions and trace elements were generally less than 10%.

7.2.2 Results

7.2.2.1 Field Parameters

Field-measured parameters for the 13 groundwater samples collected from borehole R-25 (excluding the sample from 1938 ft), including pH, temperature, specific conductance, and turbidity, are provided in Table 7.2-2. These parameters were measured at the time of sample collection when groundwater was in contact with the atmosphere. DO was also measured; however, DO values are not reported because of potential atmospheric contamination (oxygen diffusion into water samples) from the electrode and interference from suspended particles contributing to very high turbidity values.

7.2.2.2 Organic and HE Compounds

VOCs and SVOCs were not detected in the screening groundwater samples from the R-25 borehole. The samples were obtained using a stainless steel bailer, and volatilization may have taken place during field sampling.

Table 7.2-2
Field-Measured Parameters for R-25 Groundwater Samples

Sample Depth (ft)	Sampling Zone	Sample Date	pH (standard units)	Temperature (°C)	Specific Conductance (μS/cm)	Turbidity (NTU)
Otowi Member						
747	Upper saturated	09/30/98	6.80	12.2	174	os ^a
Puye Formation						
867	Upper saturated	10/09/98	6.52	9.4	166	622
1047	Upper saturated	10/28/98	7.24	13.0	165	455
1137	Wet/dry zone	1/03/98	8.07	15.2	151	os
1184	Wet/dry zone	12/03/98	7.50	10.1	133	os
1286	Regional aquifer	12/18/98	7.67	11.0	102	os
1407	Regional aquifer	01/07/99	6.83	10.6	160	os
1507	Regional aquifer	01/13/99	7.95	8.8	109	os
1607	Regional aquifer	02/03/99	7.67	11.4	109	207
1747	Regional aquifer	02/12/99	7.28	14.0	116	os
1867	Regional aquifer	02/20/99	6.84	15.0	84	328
1940	Regional aquifer	02/23/99	6.80	13.7	145	os
1942	Regional aquifer	02/26/99	7.23	11.8	92	421

^a os = off scale because of very high turbidity values for open borehole groundwater samples.

Table 7.2-3 provides analytical results for HE compounds and degradation products present in nonfiltered groundwater samples collected from the R-25 borehole. RDX and TNT are the two contaminants of most concern because their concentrations exceeded the EPA health advisory (HA) limits for drinking water of 0.61 μg/L for RDX and 2.2 μg/L for TNT (EPA 2000, 70122). The EPA HA limit for HMX is 1800 μg/L.

Figure 7.2-1 shows the distribution of HE compounds detected in groundwater samples from R-25. The highest concentrations of RDX (84 μg/L) and HMX (12 μg/L) were measured in a groundwater sample collected from 1047 ft, whereas the highest concentration of TNT (19 μg/L) was measured in a sample from 867 ft. Degradation products of TNT that were detected include 4-A-2,6-DNT and 2-A-4,6-DNT, which are stable under anaerobic conditions. Other HE-related compounds analyzed for but not detected included 1,3-dinitrobenzene, tetra, nitrobenzene, 2,6-dinitrotoluene, 2,4-dinitrotoluene, 2-nitrotoluene, 4-nitrotoluene, and 3-nitrotoluene. Nitrotoluene isomers are additional degradation products of TNT. The detection limit for these compounds typically is 1 μg/L or less using the HPLC method.

Because concentrations of RDX and TNT found in the upper saturated zone and possibly the regional aquifer at the R-25 site exceeded EPA HA limits for drinking water, mobilities of these compounds in aquifer materials were estimated so that preliminary predictions could be made regarding their travel times to the nearest water supply well. A brief discussion of the results of mobility calculations for these two compounds is given here. Full calculations and supporting assumptions are provided in Appendix H.

Table 7.2-3
HE Chemistry of R-25 Groundwater Samples

Sample Depth (ft)	Sampling Zone	RDX (µg/L)	HMX (µg/L)	4-A-2,6-DNT (µg/L)	2-A-4,6-DNT (µg/L)	TNB (µg/L)	TNT (µg/L)
Otowi Member							
747	Upper saturated	12	<1	0.38	0.51	<0.26	<0.25
Puye Formation							
867	Upper saturated	63	8.3	3.7	5.2	2.2	19
1047	Upper saturated	84	12	4.6	5.7	<2.5	5.3
1137	Wet/dry zone	50	9.2	4.3	2.9	<1.3	<1.3
1184	Wet/dry zone	4.2	<1	<0.25	0.43	<0.26	<0.25
1287	Regional aquifer	<0.84	<1.0	<0.25	<0.25	<0.26	<0.25
1407	Regional aquifer	62	9.7	<1.3	2	<1.3	7.1
1507	Regional aquifer	4.4	<1	<0.25	<0.26	<0.26	<0.25
1607	Regional aquifer	15	2.6	5	0.46	<0.26	0.84
1747	Regional aquifer	<0.84	<1	<0.25	<0.25	<0.25	<0.25
1867	Regional aquifer	0.97	<1	<0.25	<0.25	<0.26	<0.25
1938	Regional aquifer	<0.84	<1	<0.25	<0.25	<0.26	<0.25
1940 (air lifted)	Regional aquifer	8.8	1.5	1.7	0.69	<0.26	0.77
1940 (bailer)	Regional aquifer	9.6	1.6	1.8	0.79	<0.26	1.1
1942	Regional aquifer	5.9	<1	1.1	<0.25	<0.26	0.64
EPA HA ^a		0.61	1800	no HA	no HA	no HA	2.2

Note: RDX (hexahydro-1,3,5-trinitro-1,3,5-triazine), HMX (octahydro-1,3,5,7-tetranitro-1,3,5,7-tetrazocine), 4-A-2,6-DNT (4-amino-2,6-dinitrotoluene), 2-A-4,6-DNT (2-amino-4,6-dinitrotoluene), TNB (1,3,5-trinitrobenzene), and TNT (2,4,6-trinitrotoluene). HE compounds analyzed by HPLC (EPA Method 8330) at Paragon Analytics, Inc., Fort Collins, Colorado.

^a EPA (Region 6) lifetime HA limit, October 2000.

Distribution coefficients (K_d) for RDX and TNT were calculated using an organic carbon partition coefficient taken from literature (K_{oc}) for each compound (Burrows et al. 1989, 71319) and a value for the fraction of solid organic carbon (f_{oc} , 0.0001) estimated from a core sample from the Otowi Member. The low K_d s for RDX (0.01 cm³/g) and TNT (0.052 cm³/g) suggest that these compounds remain in the aqueous phase and do not adsorb to aquifer materials. This is also consistent with the lack of detected HE in core and cuttings samples.

Retardation factors (R_f) ($R_f = 1 + \rho K_d/n$) for RDX and TNT were calculated using their respective K_d s, and bulk density (ρ) (1.18 g/cm³) and effective porosity (n) (0.47) values for the Otowi Member. Both RDX and TNT, with R_f values of 1.03 and 1.13, respectively, are predicted to migrate at nearly the same rate as groundwater.

The travel time for groundwater (regional aquifer) at the R-25 site to reach the nearest water supply well, PM-2, is estimated between 50 and 200 years. This is based on plateau-wide average groundwater flow rates of between 95 and 345 ft per year determined by Purtymun (1995, 45344).

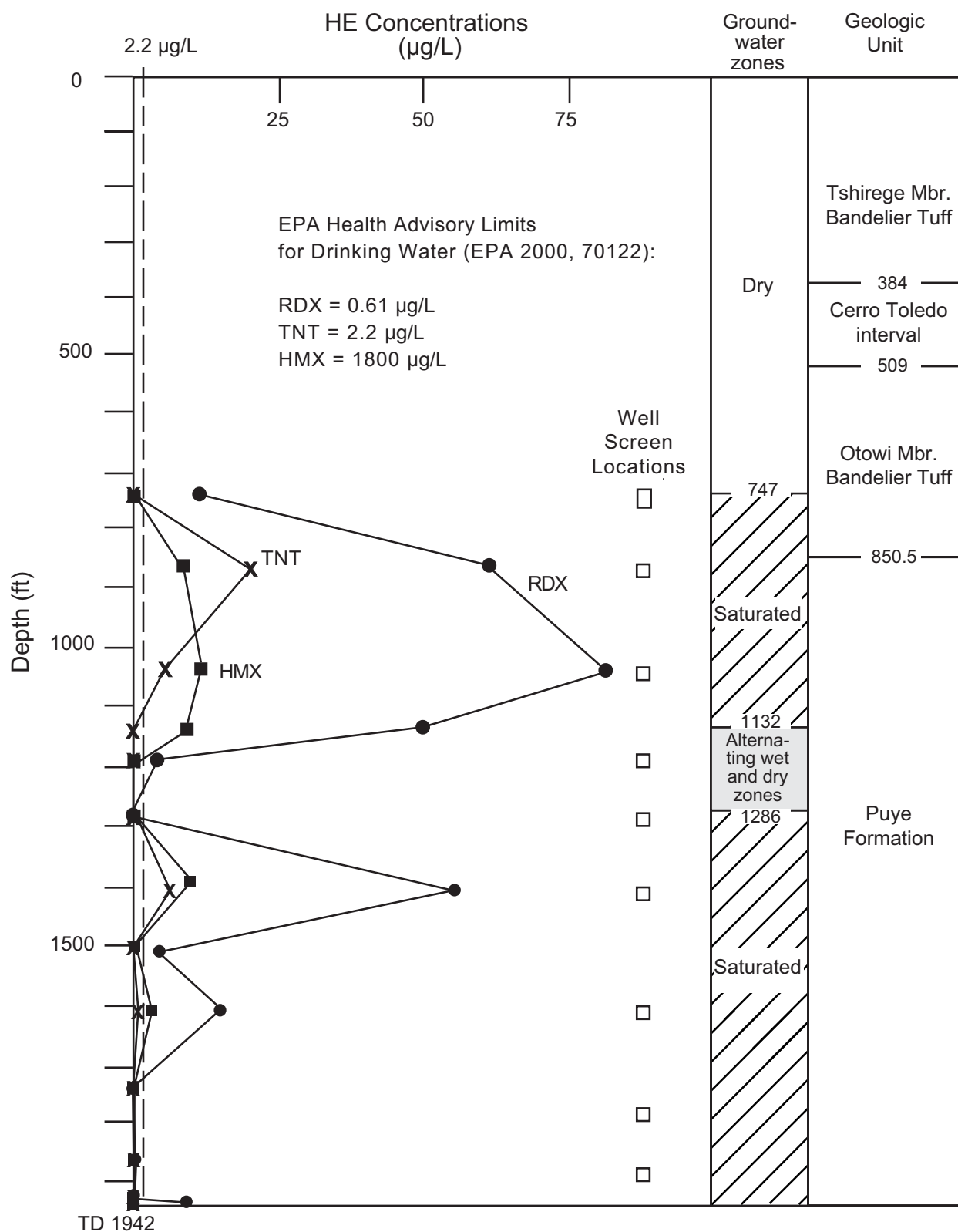


Figure 7.2-1. Distribution of HE compounds detected in deep groundwater at borehole R-25

Although these calculations imply that RDX and TNT will remain in the aqueous phase and migrate at the same rate as groundwater, they do not take into account hydrolysis reactions, biodegradation, or mixing, which are dependent on the site-specific conditions of the dynamic groundwater-aquifer material-biochemical system present at the R-25 site.

7.2.2.3 Major Ions and Trace Elements

Analytical results for 17 major ions, 30 trace elements, and 5 other water quality parameters in filtered and nonfiltered groundwater screening samples collected from the R-25 borehole are given in Appendix G. Results for selected analytes are given in Table 7.2-4 to support the discussion presented here. The precision limits for major ions and trace elements were within 10%.

Table 7.2-4
Analytical Results for Selected Trace Elements and Major Ions in R-25 Groundwater Samples

Depth (ft)	Sampling Zone	Barium (mg/L)	Chloride (mg/L)	Boron (mg/L)	Nitrate (mg/L)	Manganese (mg/L)
Otowi Member						
747	Upper saturated	0.006	11.1	0.12	4.17	1.39
Puye Fm						
867	Upper saturated	0.005	9.80	0.058	4.02	0.27
1047	Upper saturated	0.007	9.13	0.090	3.55	0.19
1137	Wet/dry zone	0.005	8.04	0.074	3.84	0.11
1184	Wet/dry zone	0.008	5.79	0.027	3.32	0.18
1286	Regional aquifer	0.014	1.09	0.014	1.70	0.25
1407	Regional aquifer	0.016	8.03	0.087	2.38	0.21
1507	Regional aquifer	0.010	3.80	0.037	1.31	0.19
1607	Regional aquifer	0.014	2.49	0.027	1.86	0.19
1747	Regional aquifer	0.013	1.54	0.011	1.86	0.10
1867	Regional aquifer	0.009	1.65	0.010	1.93	0.11
1940	Regional aquifer	0.015	2.15	0.013	1.81	0.14
1942	Regional aquifer	0.006	1.77	0.016	1.53	0.30

The upper saturated zone is characterized by a mixed calcium-sodium-bicarbonate ionic composition as shown by two samples, one from the Otowi Member at a depth of 747 ft and one from the Puye Formation at a depth of 867 ft. Values for field pH were 6.80 in the Otowi Member sample and 6.52 in the Puye Formation sample. Values for total dissolved solids (TDS) were 265 mg/L in the Otowi Member sample and 223 mg/L in the Puye Formation sample.

The alternating wet and dry zone above the regional aquifer is characterized by a sodium-bicarbonate ionic composition as shown by one sample from the Puye Formation at a depth of 1137 ft. The field pH value was 8.07, and the TDS value was 209 mg/L.

The regional aquifer is dominantly a calcium-sodium-bicarbonate type as represented by the samples collected at depths of 1286, 1407, 1507, 1607, 1747, 1867, 1940, and 1942 ft in the Puye Formation.

Field pH values ranged from 6.80 to 7.95, and TDS values ranged from 135 mg/L to 207 mg/L. TDS values decreased with depth, probably due to mixing.

Most of the groundwater samples collected from the R-25 borehole have very similar major ion compositions, in addition to similar values for stable isotopes and detectable tritium, suggesting that the upper saturated zone and the regional aquifer are hydraulically connected. This is consistent with the downward vertical pressure gradients measured in R-25 (Section 6.2). Major ion compositions of groundwater samples collected from R-25 are also similar to those of water samples collected from Peter Seep, SWSC Spring, Burning Ground Spring, Martin Spring, upper Cañon de Valle surface water, and upper Cañon de Valle alluvial groundwater (LANL 1998, 59891). Dissolved concentrations of nitrate, sulfate, and chloride in R-25 screening groundwater samples are similar to those found in springs and surface water around TA-16, suggesting recharge from surface water sources. The presence of HE compounds and degradation products also confirms recharge from surface water sources to groundwater at the R-25 site.

Inorganic chemicals used at TA-16 for HE manufacturing and research include barium, boron, nitrogen-bearing HE compounds, and other materials. Barium nitrate (baratol) is used in the preparation of HE compounds. The solubility of barium nitrate is 897 mg/L at 20°C (Dean 1985, 71312). Residues of HE compounds and barium nitrate are known to have been discharged to upper Cañon de Valle, and concentrations of barium in surface water in upper Cañon de Valle exceed 1 mg/L (LANL 1998, 59891). Barium, however, has precipitated from solution in the forms of barium sulfate and barium carbonate in upper Cañon de Valle, resulting in a decrease in barium concentrations in surface water downstream from the 260 outfall (LANL 1998, 59891).

Concentrations of dissolved barium in water samples from R-25 ranged from 0.005 to 0.007 mg/L in samples from the upper saturated zone and from 0.006 to 0.016 mg/L in samples from the regional aquifer (Table 7.2-4). The New Mexico Water Quality Control Commission (NMWQCC) groundwater standard for dissolved barium is 1 mg/L. The upper saturated zone and regional aquifer at R-25 are predicted to be undersaturated with respect to barium sulfate and barium carbonate, and precipitation of these two minerals from solution is not likely, based on results of model simulations using the computer code MINTEQA2 (Allison et al. 1991, 49930). Adsorption of barium onto aquifer material is considered to be the dominant process controlling the fate and transport of barium at the R-25 site.

Concentrations of dissolved chloride in water samples from R-25 ranged from 9.13 to 11.1 mg/L in samples from the upper saturated zone, from 5.79 to 8.04 mg/L in samples from the wet/dry zone, and from 1.09 to 8.03 mg/L in samples from the regional aquifer (Table 7.2-4). Chloride concentrations at Water Canyon Gallery were approximately 1 mg/L in 1993 (Blake et al. 1995, 49931). Dissolved concentrations of chloride decreased with depth in both saturated zones. The NMWQCC groundwater standard for dissolved chloride is 250 mg/L (secondary, or aesthetic, standard).

Concentrations of dissolved boron (stable as $B(OH)_3^0$) in water samples from R-25 ranged from 0.027 mg/L in samples from the wet/dry zone to 0.12 mg/L in samples from the top of the saturated zone. Dissolved boron concentrations in samples from the regional aquifer ranged from 0.010 mg/L in a sample from 1867 ft to 0.087 mg/L in a sample from 1407 ft (Table 7.2-4). Dissolved concentrations of boron decreased with depth in both saturated zones. Concentrations of boron at Water Canyon Gallery were 0.13 mg/L in 1993 (Blake et al. 1995, 49931). The NMWQCC groundwater standard for dissolved boron is 0.75 mg/L.

Concentrations of dissolved nitrate (as nitrate) in water samples from R-25 ranged from 3.32 mg/L (0.75 mg/L as nitrogen) in a sample from the wet/dry zone to 4.17 mg/L (0.95 mg/L as nitrogen) in a sample from the upper saturated zone (Table 7.2-4). Concentrations of dissolved nitrate decreased with

depth in both the upper saturated zone and the regional aquifer. Dissolved nitrate concentrations in samples from the regional aquifer ranged from 1.31 mg/L (0.30 mg/L as nitrogen) to 2.38 mg/L (0.54 mg/L as nitrogen). Concentrations of nitrate at Water Canyon Gallery were 0.98 mg/L in 1993 (Blake et al. 1995, 49931). The NMWQCC groundwater standard for dissolved nitrate (as nitrate) is 44 mg/L, or 10 mg/L as nitrogen. The dissolution of $\text{Ba}(\text{NO}_3)_2$ used in HE processing at TA-16 may constitute a potential source of nitrate.

Concentrations of dissolved manganese (predominantly stable as Mn^{2+}) in water samples from the R-25 borehole ranged from 0.11 mg/L in a sample from the wet/dry zone to 1.39 mg/L in a sample from the upper saturated zone. Dissolved manganese concentrations in samples from the regional aquifer ranged from 0.10 to 0.30 mg/L (Table 7.2-4). Dissolved concentrations of manganese generally decreased with depth in both saturated zones, suggesting that an oxidation-reduction gradient or decreasing oxidation-reduction potential (Eh) occurs with depth. Concentrations of manganese at Water Canyon Gallery were less than 0.01 mg/L in 1993 (Blake et al. 1995, 49931). The NMWQCC groundwater standard for dissolved manganese is 0.2 mg/L (secondary or aesthetic standard).

Concentrations of dissolved manganese and iron in screening water samples from the R-25 borehole could be enhanced by the oxidation of DOC and/or the biodegradation of TNT and RDX. DOC concentrations were greater than 1 mg/L, which is sufficient to enhance the reduction of TNT to 4-A-2,6-DNT or 2-A-4,6-DNT ($\mu\text{g/L}$ range). The biological reduction of TNT to either 4-A-2,6-DNT or 2-A-4,6-DNT acts as an additional reducing agent for Mn(IV) mineral species (electron acceptor) dissolving to form aqueous Mn(II) species. This reduction increases the concentration of dissolved manganese. The same is true for the reduction of Fe(III) solids to aqueous Fe(II) species. Oxidation-reduction processes associated with these transformations are described in further detail in Appendix H.

7.2.2.4 Tritium Activities in Groundwater

Activities of tritium in groundwater samples collected from R-25 are provided in Table 7.2-5. Groundwater in the upper saturated zone contains a component of surface water and/or alluvial water that is between 10 and 50 years old (Blake et al. 1995, 49931; Adams et al. 1995, 47192) based on measurable tritium activities at 747 ft. Groundwater was first encountered at this depth in R-25 and did not consist of a mixture of waters due to drilling operations. The age of groundwater at 747 ft was determined by the following expression: $a_t^3\text{H} = a_o^3\text{H}e^{-\lambda t}$, where $a_t^3\text{H}$ is the measured tritium activity (77.2 pCi/L), $a_o^3\text{H}$ is the initial tritium activity of rainwater collected at S-Site (127 pCi/L) in 1990 (Adams et al. 1995, 47192), $-\lambda$ is the decay constant ($\ln 2/t_{1/2}$ [12.43 yr for tritium]), and t is time in years. Solving for $a_t^3\text{H}$ in 1998 and using $t_{1/2}$ equal to 12.43 yr for tritium, the calculated activity is 81.5 pCi/L, which is in close agreement with the measured activity (77.2 pCi/L). This calculation does not take into account dispersion and mixing or the fact that activities of tritium in rainwater vary seasonally at S-Site. This calculation provides a minimum age of the groundwater encountered within the upper saturated zone. This is also true for the upper saturated portion of the regional aquifer at a depth of 1286 ft. Potential downward movement of groundwater in borehole R-25 during drilling, however, may have resulted in elevated tritium activities at 1407, 1607, 1940, and 1942 ft.

7.2.2.5 Stable Isotopes of Hydrogen, Oxygen, and Nitrogen

Stable isotope ratios for hydrogen and oxygen, provided in Table 7.2-6, were measured to evaluate source(s) of groundwater encountered in R-25. These values plot close to, but below, the Jemez Mountain meteoric ($\delta\text{D} = 8\delta^{18}\text{O} + 12$) and global meteoric ($\delta\text{D} = 8\delta^{18}\text{O} + 10$) water lines provided by Blake et al. (1995, 49931). This suggests that these groundwaters were derived from a meteoric or atmospheric source, and that evaporation has not affected their isotopic composition. The stable isotopic compositions

of R-25 groundwater and springs west of the Laboratory are similar, suggesting similar sources. Results of stable isotope analyses suggest that the groundwater at R-25 is well mixed and that residence times are short within the upper saturated zone and possibly the regional aquifer.

Table 7.2-5
Tritium Activities in R-25 Groundwater Samples

Depth (ft)	Sampling Zone	Sample Date	Activity (pCi/L) ^a
Otowi Member			
747	Upper saturated zone	09/30/98	77.2 ± 2.9
Puye Formation			
867	Upper saturated zone	10/09/98	81.4 ± 2.9
1184	Wet/dry zone	12/03/98	44.7 ± 1.6
1286	Regional aquifer	12/18/98	3.77 ± 0.35
1407	Regional aquifer	01/07/99	72.8 ± 2.6
1607	Regional aquifer	02/03/99	32.6 ± 1.3
1747	Regional aquifer	02/12/99	1.02 ± 0.32
1867	Regional aquifer	02/20/99	1.85 ± 0.29
1940	Regional aquifer	02/23/99	14.46 ± 0.54
1942	Regional aquifer	02/26/99	8.11 ± 0.41

^a Analytical error is 1 standard deviation. University of Miami used both direct counting and electrolytic enrichment methods to measure tritium activities in these groundwater samples.

Table 7.2-6
Stable Oxygen and Hydrogen Isotope Data for Water Samples from R-25 and Selected Springs

Depth (ft)	Formation	δD (‰)	δ ¹⁸ O (‰)
747	Otowi Member	-77	-12.0
1286	Puye Formation	-82	-12.2
1407	Puye Formation	-79	-12.0
1507	Puye Formation	-80	-11.9
1747	Puye Formation	-76	-11.8
1867	Puye Formation	-76	-11.7
1940	Puye Formation	-79	-12.1
1942	Puye Formation	-80	-11.6
Upper Cañon de Valle Spring	Tschicoma Fm/Bandelier Tuff	-75	-11.9
Water Canyon Gallery	Bandelier Tuff	-74	-11.9
Apache Spring	Tschicoma Fm/Bandelier Tuff	-76	-12.2

Note: Analysis of the R-25 samples was performed by Geochron Laboratories, Cambridge, Massachusetts. Analysis of the spring samples was performed by Western Michigan University. δD standard = 0.000316, and δ¹⁸O standard = 0.0039948 (double atom ratio for both standards) provided by Geochron.

Stable isotopes of nitrogen were measured to evaluate source(s) of nitrate found at the R-25 site. Concentrations of ammonium were insufficient to determine nitrogen isotopes associated with this cation. The main sources of nitrate found in groundwater and surface water at the Laboratory include (1) natural organic nitrogen in soils and sediments, (2) dissolved nitric acid and HE containing $\text{Ba}(\text{NO}_3)_2$ discharges, (3) fertilizers, and (4) treated septic/effluent discharges. Of these possible sources, aqueous discharges of both dissociated nitric acid, HE discharges, and treated septic/effluent probably exceed naturally- and fertilizer-derived nitrate. The dominant source of nitrate at the R-25 site is most probably a combination of dissolution of $\text{Ba}(\text{NO}_3)_2$, and biodegradation of RDX, HMX, and TNT. Sewage sources probably contribute minimally. Elevated concentrations of nitrate have been measured at TA-16, including Martin Spring, Burning Ground Spring, and SWSC Spring (LANL 1998, 59891).

The isotopic standard for $\delta^{15}\text{N}$ is nitrogen in air, which has a value of 0 ‰ (Clark and Fritz 1997, 59168). Reacting ammonia gas with oxygen gas produces nitric acid. Ammonia is oxidized to nitrate through a series of reactions involving nitrous oxide, nitric oxide, and nitric dioxide, which eventually produce nitric acid. Ammonia is initially produced by reacting nitrogen gas, having a $\delta^{15}\text{N}$ value of 0 ‰, with hydrogen gas. Consequently, the $\delta^{15}\text{N}$ value for nitric acid is close to 0 ‰ or is slightly enriched with nitrogen-15. A nitric acid standard prepared by EES-6 personnel has an average $\delta^{15}\text{N}$ value of 1.0 ‰ (Table 7.2-7).

Table 7.2-7
Summary of Nitrogen Chemistry and Nitrogen Isotopes
for Water Samples from R-25, Surface Water, and Selected Background Springs

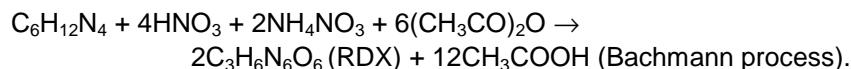
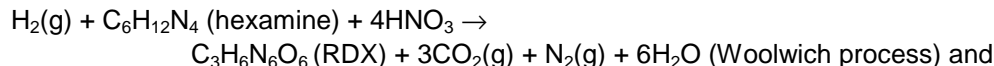
Location	$\text{NO}_3\text{-N}$ (ppm)	$\text{NH}_4\text{-N}$ (ppm)	$\delta^{15/14}\text{N-NO}_3^a$ (‰)	Water Type
R-25 (747 ft)	0.95	0.03	+3.1	Upper saturated zone
R-25 (867 ft)	0.90	0.03	+2.8	Upper saturated zone
R-25 (1286 ft)	0.32	0.02	+2.6	Regional aquifer
R-25 (1407)	0.51	<0.02	+4.3	Regional aquifer
R-25 (1607 ft)	0.42	<0.02	+2.5	Regional aquifer
R-25 (1747 ft)	0.31	<0.02	-0.6	Regional aquifer
R-25 (1867 ft)	0.20	<0.02	+1.1	Regional aquifer
R-25 (1942 ft)	0.25	<0.02	+0.3	Regional aquifer
Los Alamos Canyon Reservoir	0.04	—	-2.4	Surface
Upper Pajarito Canyon	0.01	—	-2.4 (2)	Surface
Water Canyon Gallery	0.10	—	0	Spring
Apache Spring	0.35	—	-0.5 (2)	Spring
HNO_3 Std. ^b	5.7	<0.02	+1.0 (4)	Dilute acid

^a Analysis for nitrogen isotopes was performed by Coastal Sciences Laboratories, Inc., Austin, Texas. The number of analyses for each sample is given in parentheses.

^b Laboratory HNO_3 standard (5.7 ppm nitrate as nitrogen) prepared at EES-6.

Water samples were collected from R-25, the Los Alamos Canyon reservoir, and Laboratory springs and analyzed for ammonium, nitrate, and nitrogen-15/nitrogen-14. Analytical results for nitrogen species and isotopes are presented in Table 7.2-7. The analytical error associated with the $\delta^{15}\text{N}$ analyses is less than ± 1.0 ‰ using IRMS at nitrate (as nitrogen) concentrations of less than 0.5 ppm.

The HE compounds and $\text{Ba}(\text{NO}_3)_2$ were prepared at different army depot sites and shipped to the Laboratory for use at TA-16. Treated HE effluents sampled at TA-16 are characterized by low $\delta^{15}\text{N}$ values ($<+6\text{‰}$) derived from the nitric acid used in the preparation of $\text{Ba}(\text{NO}_3)_2$ and HE compounds. For example, RDX is produced by reacting nitric acid with hexamine and ammonium nitrate as shown in the following two reactions (Card and Autenrieth 1998, 71308):



Water samples collected from upgradient Laboratory springs, the Los Alamos Canyon reservoir, and upper Pajarito Canyon have $\delta^{15}\text{N}\text{-NO}_3$ values ranging from -2.4 to 0‰ (Table 7.2-7). These nitrogen isotope values are consistent with nitrate (inorganic and organic) associated with sediments and volcanic deposits (Clark and Fritz 1997, 59168). Upgradient concentrations of dissolved nitrate (as nitrate) west of TA-16 are less than 0.4 ppm .

Groundwater samples collected from R-25 have $\delta^{15}\text{N}\text{-NO}_3$ values ranging from -0.6 to $+4.3\text{‰}$ (Table 7.2-7). Possible sources of nitrate in R-25 groundwater, based on nitrogen isotopic analyses, include discharges containing dissociated $\text{Ba}(\text{NO}_3)_2$ and residues of HE. This is consistent with known sources of treated effluent discharged from the 260 and other outfalls at TA-16 west of R-25. It is possible that a shift in nitrogen isotope composition to heavier values at the R-25 site is due to both barium nitrate (denitrification) and biodegradation (reduction of nitro functional groups to amino functional groups) of HE compounds (RDX and TNT) in the upper saturated zone.

Within the regional aquifer at the R-25 site, nitrogen isotope values become less enriched with nitrogen-15, producing less positive $\delta^{15}\text{N}$ values with depth. This may represent an increase in mixing of native groundwater with smaller portions of surface water and alluvial groundwater at TA-16.

At other sites around the Laboratory, nitrate discharges are due to treated sewage effluent. Nitrate derived from treated septic effluent, as determined at R-12 (Broxton et al. 2001, 71252), is enriched in nitrogen-15 and depleted in nitrogen-14 and is characterized by positive $\delta^{15}\text{N}$ values (7 to $>30\text{‰}$; Clark and Fritz 1997, 59168). During denitrification, which is the reduction of nitrate to nitrogen gas in the presence of organic carbon, residual nitrate becomes enriched in nitrogen-15. Subsequently, $\delta^{15}\text{N}$ values become increasingly more positive with increasing denitrification as observed at R-12 and in Pueblo Canyon and lower Los Alamos Canyon east of the Bayo sewage treatment plant.

7.2.2.6 Radionuclides and Uranium

Activities of uranium-238, uranium-235, and uranium-234 are less than 1 pCi/L in both filtered and nonfiltered groundwater samples collected from R-25. Activities of gross alpha, gross beta, and gross gamma are greater than 1 pCi/L in both filtered and nonfiltered samples, which is due to decay products within the uranium-238 and uranium-235 decay series (gross alpha and gross gamma). Activities of americium-241; cesium-137; plutonium-238; plutonium-239,240; and strontium-90 are less than detectable levels in samples from both the upper saturated zone and the regional aquifer. Actinides and fission products are not constituents of concern at TA-16.

Dissolved uranium concentrations in groundwater samples collected from R-25 are less than $1\text{ }\mu\text{g/L}$. Concentrations of dissolved uranium in samples from R-25 are below the proposed EPA maximum contaminant level (MCL) ($0.020\text{ }\mu\text{g/L}$) and the NMWQCC standard (5 mg/L).

8.0 MODIFICATIONS TO WORK PLANS

Table 8.0-1 compares the planned characterization activities as presented in the Hydrogeologic Workplan (LANL 1998, 59599), the Core Document for Canyons Investigations (LANL 1997, 55622), and the R-25 FIP (LANL 1998, 59162) with actual characterization activities performed at R-25.

Table 8.0-1
Activities Planned for R-25 Compared with Work Performed

	Hydrogeologic Workplan and Core Document for Canyons Investigations	R-25 Field Implementation Plan	Actual Work
Planned Depth	100 to 500 ft into the regional aquifer	1550 ft	1942 ft
Drilling Method	Methods may include, but are not limited to, hollow-stem auger, air-rotary/Odex/Stratex, air-rotary/Barber rig, mud-rotary drilling	Air-rotary methods, including downhole percussion hammers on 4.5-in.- and 7-in.-O.D. dual-wall casings to drill open hole; air-rotary 101-mm Geobarrel system to collect continuous core; air-rotary Holte and Stratex casing advance systems and downhole percussion hammers to drill and advance casing in the borehole simultaneously	Same as FIP except coring system used instead of 101-mm Geobarrel
Amount of Core	100% of the borehole	Approximately 53% of the borehole	10% of the borehole
Lithologic Log	Log to be prepared from core, cuttings, drilling performance	Log to be prepared from core, cuttings, drilling performance	Log prepared from core, cuttings, drilling performance, petrography, and x-ray diffraction and fluorescence analyses
Number of Water Samples Collected for Contaminant Analysis	A water sample to be collected from each saturated zone	A water sample to be collected from discrete intervals from both saturated zones; 5 water samples planned	14 water samples collected from 2 saturated zones

Table 8.0-1 (continued)

	Hydrogeologic Workplan and Core Document for Canyons Investigations	R-25 Field Implementation Plan	Actual Work
Water Sample Analytes	Radiochemistry I, II, and III analytes; ³ H, gamma spectroscopy scan; general inorganic chemicals; metals; stable isotopes	Trace Elements/Metals: Al, Sb, As, Ba, Be, B, Cd, Ca, Cr, Co, Cu, Fe, Pb, Mg, Mn, Hg, Ni, K, Se, Ag, Na, Ti, U, V, Zn, NH ₄ Anions: Br, CO ₃ , Cl, F, NO ₃ , NO ₂ , PO ₄ , HCO ₃ , SO ₄ Other Chemicals: Si, cyanide, TOC Radionuclides: ³ H, ⁹⁰ Sr, ¹³⁷ Cs, ²⁴¹ Am, ²³⁴ U, ²³⁵ U, ²³⁸ U, ²³⁸ Pu, ^{239,240} Pu, gamma spectroscopy, gross alpha, gross beta, gross gamma Organic Compounds: HE compounds and degradation products, VOCs, SVOCs Other Analyses: ¹⁴ C, ¹³ C, ¹⁸ O/ ¹⁶ O, δD, DOC	Same as FIP and with nitrogen isotopes added to analytical suite
Water Sample Field Measurements	Alkalinity, pH, specific conductance, temperature, turbidity	Alkalinity, DO (completed well only), pH, specific conductance, temperature, turbidity	pH, specific conductance, DO, temperature, turbidity, and DTech for RDX and TNT; alkalinity was measured in the laboratory
Number of Core/Cuttings Samples Collected for Contaminant Analysis	20 samples of core or cuttings from each borehole	Up to 37 core/cuttings samples planned; number of samples assumes 5 saturated zones are present	13 samples of core/cuttings collected
Core Sample Analytes	Uppermost sample to be analyzed for a full range of compounds; deeper samples to be analyzed for Radiochemistry I, II, and III analytes, ³ H, and metals; 4 samples to be analyzed for VOCs	Trace Elements/Metals: Al, Sb, As, Ba, Be, Cd, Cr, Co, Cu, Fe, Pb, Mn, Hg, Mo, Ni, Se, Ag, Ti, U, V, Zn Anions: Br, Cl, F, SO ₄ , NO ₃ Other Chemicals: HE compounds and degradation products, cyanide Radionuclides: ³ H, ⁹⁰ Sr, ¹³⁷ Cs, ²⁴¹ Am, ²³⁴ U, ²³⁵ U, ²³⁸ U, ²³⁸ Pu, ^{239,240} Pu, gamma spectroscopy, gross alpha, gross beta, gross gamma VOCs and SVOCs to be determined in 4 samples and where PID detections occur	Same as FIP

Table 8.0-1 (continued)

	Hydrogeologic Workplan and Core Document for Canyons Investigations	R-25 Field Implementation Plan	Actual Work
Hydraulic Property Analyses	Physical properties to be determined on 5 samples typically including moisture content, porosity, particle density, bulk density, saturated hydraulic conductivity, and water retention characteristics	Physical properties to be determined in each of the major stratigraphic units, including particle size (sedimentary units), moisture content, matric potential, porosity, particle density, bulk density, saturated hydraulic conductivity, and water retention characteristics	A total of 5 core samples selected for hydraulic properties analysis; 4 core samples from the unsaturated zone analyzed for full suite of hydraulic properties, including moisture content, porosity, bulk density, saturated hydraulic conductivity, and determination of moisture characteristics; one core sample from the saturated zone analyzed for saturated hydraulic conductivity only; a total of 105 samples analyzed for moisture content and matric potential
Geology	Approximately 10 samples of core or cuttings to be collected for mineralogy, petrography, and rock chemistry	Geology task leader to determine the number of samples needed to resolve stratigraphic and lithologic uncertainties; a maximum of 30 samples to be collected	39 samples analyzed for mineralogy, petrography, and chemistry
Geophysics	In general, open-hole geophysics to include caliper, EM, GR, magnetic susceptibility, color borehole video, fluid temperature (saturated), fluid resistivity (saturated), single-point resistivity (saturated), and spontaneous potential (saturated) logs; cased-hole geophysics to include gamma-gamma density, GR, and thermal neutron logs	In stable open borehole environments, geophysics measurements to include caliper, EM, GR, magnetic susceptibility, color borehole video, gamma-gamma, and thermal/epithermal neutron logs; in cased borehole, geophysics measurements to include gamma-gamma density, GR, and thermal neutron logs	Same as FIP plus compensated neutron, spectral gamma, multifinger caliper, hole deviation, cement bond, and ultrasonic imager logs
Water-Level Measurements	Not included	Water levels to be determined for each saturated zone by water-level meter or by pressure transducer	Water levels determined for each saturated zone by water-level meter or by pressure transducer
Slug Tests	Not included	Slug tests planned for all zones of saturation encountered	Slug injection tests unsuccessful; screen intervals of well would not accept injected water

Table 8.0-1 (continued)

	Hydrogeologic Workplan and Core Document for Canyons Investigations	R-25 Field Implementation Plan	Actual Work
Air Permeability/ Borehole Anemometry	Conducted in Bandelier Tuff at 10-ft intervals after removing the hollow-stem auger and/or Odex/Stratex casing	In unsaturated environments, borehole anemometry and straddle packer air permeability measurements may be made in stable open borehole environments at locations determined in the field	Anemometry and air permeability not measured
Surface Casing	Approximately 20-in.-O.D. casing extending from land surface to 10-ft depth in underlying competent layer and grouted in place	10-in.-diameter low carbon steel casing set to a minimum depth of 20 ft with a 3-ft stickup	16-in. surface casing to 20 ft
Minimum Well Casing Size	6-5/8-in. O.D.	5-in. I.D.	5-in.-I.D., 5.625-in.-O.D., Schedule 40 304-stainless steel casing
Well Screen	Machine-slotted (0.01-in.) stainless steel screen(s) with flush-jointed threads; number and length of screens to be determined on a site-specific basis and proposed to NMED	60 ft of prepacked, 6.68-in.-diameter, machine-slotted (0.01-in.) stainless steel screen with flush-jointed threads	5-in.-I.D. flush-threaded, 0.010-in.-slot, stainless steel screen
Filter Material	>90% silica sand, properly sized for the 0.010-in. slot size of the well screen, extending 2 ft above and below the well screen	>98% silica sand, properly sized for the 0.010-in. slot size of the well screen, extending 2 ft above and below the well screen	>98% silica sand; 20/40 sand at screen; 30/70 sand in transition to bentonite above and below screen
Backfill materials (exclusive of filter materials)	Uncontaminated drill cuttings below sump and bentonite above sump	Bentonite in borehole below well; fine sand in transition zone 10 ft above and 3 ft below filter pack; bentonite above transition zone to bottom of surface casing; cement grout between surface casing and borehole wall and between surface casing and well casing	Granular bentonite and 20/40 sand (50:50 mix)
Sump	Stainless steel casing	5.56-in.-diameter stainless steel casing 10 ft long	5.625-in.-O.D. stainless steel casing 30 ft long

The planned depth for R-25 was originally 1550 ft; however, during drilling, a decision was made to extend the total depth to 1942 ft in order to characterize the vertical extent of HE contamination in the regional aquifer. Because of the HE contamination, more groundwater samples were collected than planned for in the FIP.

The Hydrogeologic Workplan specified that R-25 would be continuously cored. The amount of projected core was reduced to 53% in the FIP, and only 10% was actually collected during drilling. The amount of core collected during drilling was reduced because of the slower-than-expected coring rates and the associated high costs of collecting core in zones that would be redrilled by the casing advance system.

9.0 SUMMARY OF SIGNIFICANT RESULTS

9.1 Stratigraphy

R-25 provides new geologic control for stratigraphic units in the southwest part of the Laboratory. In descending order, geologic units penetrated in R-25 include the Tshirege Member of the Bandelier Tuff, tephra and volcanoclastic sediments of the Cerro Toledo interval, the Otowi Member of the Bandelier Tuff, and the Puye Formation. The Cerro Toledo interval was thicker than predicted, probably because of deposition in paleo-valleys cut into the underlying Otowi Member. The Puye Formation was also significantly thicker than predicted by the site-wide geologic model. Tschicoma dacitic lavas and Santa Fe Group sedimentary deposits were expected to occur in the lower part of the borehole; neither unit was present.

At R-25, the Puye Formation consists of bouldery fanglomerate, reflecting deposition close to source rocks exposed west of the Pajarito fault zone, about 1.9 mi to the west. Based on narrative descriptions from polished thin sections, the uppermost 805 ft of the Puye Formation in R-25 was derived mostly from upper dacite of Pajarito Mountain, which lies northwest of R-25. Below the 1657-ft depth, Puye deposits were derived mostly from rhyodacite of Rendija Canyon, which lies north-northwest of R-25. The lowermost parts of these deposits appear to be derived from high-silica rhyolite sources that pre-date the Rendija Canyon rhyodacite.

9.2 Hydrogeology

An upper groundwater system was encountered from depths of 711 to 1132 ft within the lower part of the Otowi Member and upper part of the Puye Formation. Alternating wet and dry zones were encountered from 1132 to 1286 ft within the Puye Formation. The saturated thickness of the upper groundwater body is approximately 421 ft, making it the thickest intermediate-depth perched groundwater body identified on the Pajarito Plateau.

The regional aquifer was encountered at a depth of 1286 ft in the Puye Formation, and continuous saturation occurs to the total borehole depth of 1942 ft. Based on preliminary water-level observations during drilling and pressure transducer readings in the completed well, the vertical head distribution is downward in both the upper saturated zone and the regional aquifer.

9.3 Geochemistry Results

Discharges from past HE manufacturing activities at TA-16 are the probable source of HE constituents found in the groundwater at R-25. The manufacturing activities and discharges at TA-16 have occurred since the 1940s. Historically, the Laboratory discharged more than 12 million gal. of HE-contaminated wastewater a year at TA-16. These discharges were reduced to 120,000 gal. per year by 1997 due to the installation of a new HE waste treatment plant and elimination of 19 of 21 HE wastewater outfalls at TA-16.

HE compounds and their degradation products were present in most of the groundwater samples collected from the borehole during the drilling of R-25. No elevated activities of radionuclides or elevated concentrations of dissolved trace metals, excluding manganese and iron (secondary, or aesthetic, standards), were detected in groundwater samples collected from borehole R-25. Activities of tritium were measured within the upper saturated zone and regional aquifer, suggesting that a portion of groundwater is less than 50 years of age. Concentrations of solutes including chloride, iron, manganese, nitrate, and sulfate measured at borehole R-25 are higher than those reported by Blake et al. (1995, 49931) at Water Canyon Gallery.

RDX and TNT are the two contaminants of most concern because their concentrations exceeded EPA HA limits (0.6 µg/L, RDX; 2.2 µg/L, TNT) for drinking water (EPA 2000, 70122). HMX was found, but in concentrations well below the EPA HA limit of 1800 µg/L (EPA 2000, 70122). The highest concentrations of RDX (84 µg/L or 84 ppb) and HMX (12 µg/L) were measured in a groundwater sample collected from 1047 ft, whereas the highest concentration of TNT (19 µg/L) was measured in a sample from 867 ft. Known degradation products of TNT include 4-A-2,6-DNT and 2-A-4,6-DNT, which were also detected in some water samples.

The nearest drinking water supply well (PM-2) is about 3 mi east of R-25. HE compounds and degradation products were not present in any of the supply wells sampled during 1999. Earlier hydrology studies of the regional aquifer indicate that the groundwater moves laterally at a rate of between 95 and 345 ft per year, but the exact rate still remains unknown. The groundwater travel time and concentrations of HE between R-25 and the nearest water supply well are unknown (Purtymun 1995, 45344). RDX and TNT are predicted to migrate at the same rate as the average groundwater flow velocity or speed. Recent drilling results from wells CdV-R15-3 (report in preparation) and R-19 (Broxton et al. 2001, 71253) 1.6 mi and 2.9 mi east of R-25, respectively, demonstrate that the regional aquifer is not affected by HE contamination.

10.0 ACKNOWLEDGEMENTS

Allyn Pratt, Deba Daymon, and John McCann supported all phases of this investigation as the ER focus area leaders responsible for execution of the drilling program.

Charlie Nylander of ESH-18 is Program Manager for the Groundwater Characterization Program and chairman for the Groundwater Integration Team. He participated in planning and decisions regarding drilling methods, well design, and evaluation of data collection.

Tonto Environmental Drilling Company provided drilling services under the direction of John Eddy and Larry Thoren, the drilling supervisors. The drilling crew consisted of Glen Woodward, Casy Howe, Juan Rivera, John van Horn, and Gray Rich.

Horace Patillo of Morrison-Knudsen Corp. was one of the site safety officers and radiological control technicians for drilling activities. He also performed HE spot testing and radiological screening.

Ken McFadden of Morrison-Knudsen Corp. was one of the site safety officers and radiological control technicians for drilling activities. He also performed HE spot testing and radiological screening.

Trung Nguyen of ESH-5 provided Laboratory oversight for health and safety.

Richard Bjarke of ESH-1 provided Laboratory oversight for radiological controls.

Dewight Bazzell of E-ER performed HE screening on cuttings, core, and groundwater samples.

Steve Bolivar of EES-13 provided contract oversight for drilling activities, field support, sample management and curation, and analytical support.

Stephanie Hagelberg of E-ER provided contract oversight for drilling activities, field support, sample management and curation, and analytical support.

Augusta Garcia of E-ER provided data management support.

Dale Counce of EES-1 was the analyst for water chemistry analyses used to screen groundwater samples. Emily Kluk of EES-6 provided x-ray fluorescence analysis, and Steve Chipera of EES-6 provided x-ray diffraction analysis of geologic samples.

Joe Beveridge provided equipment and field support for water-level measurements.

Gene Turner of the Department of Energy (DOE), Los Alamos Area Office, and Bob Enz of ENZ, Inc., provided DOE oversight.

John Young of the NMED Hazardous and Radioactive Materials Bureau provided regulatory oversight during drilling operations.

Michael Dale and Chris Hanlon-Meyer of the New Mexico Environment Department DOE Oversight Bureau collected sample splits from groundwater zones and acted as liaisons with the regulators.

Bill McCormick provided TA-16 health and safety oversight, HE spot test screening, and HE release tags for materials leaving the R-25 drill site.

Andy Kilbury of Tetra Tech EMI, Inc., was editor for this document; Pamela Maestas of Neptune and Company, Inc., was compositor.

11.0 REFERENCES

Adams, A. I., F. Goff, and D. Counce, February 1995. "Chemical and Isotopic Variations of Precipitation in the Los Alamos Region, New Mexico," Los Alamos National Laboratory Report LA-12895-MS, Los Alamos, New Mexico. (Adams et al. 1995, 47192)

Allison, J. D., D. S. Brown, and K. J. Novo-Gradac, March 1991. "MINTEQA2/PRODEFA2, A Geochemical Assessment Model for Environmental Systems: Version 3.0 User's Manual," EPA/600/3-91/021, Office of Research and Development, Athens, Georgia. (Allison et al. 1991, 49930)

Blake, W. D., F. Goff, A. I. Adams, and D. Counce, May 1995. "Environmental Geochemistry for Surface and Subsurface Waters in the Pajarito Plateau and Outlying Areas, New Mexico," Los Alamos National Laboratory report LA-12912-MS, Los Alamos, New Mexico. (Blake et al. 1995, 49931)

Broxton, D. E., P. A. Longmire, P. G. Eller, and D. Flores, June 1995. "Preliminary Drilling Results for Boreholes LADP-3 and LADP-4," in *Earth Science Investigation for Environmental Restoration—Los Alamos National Laboratory Technical Area 21*, Los Alamos National Laboratory report LA-12934-MS, Los Alamos, New Mexico, pp. 93–109. (Broxton et al. 1995, 50119)

Broxton, D. E., G. H. Heiken, S. J. Chipera, and F. M. Byers, Jr., June 1995. "Stratigraphy, Petrography, and Mineralogy of Bandelier Tuff and Cerro Toledo Deposits," in *Earth Science Investigation for Environmental Restoration—Los Alamos National Laboratory Technical Area 21*, Los Alamos National Laboratory report LA-12934-MS, Los Alamos, New Mexico, pp. 33–63. (Broxton et al. 1995, 58207)

Broxton, D. E., and S. L. Reneau, August 1995. "Stratigraphic Nomenclature of the Bandelier Tuff for the Environmental Restoration Project at Los Alamos National Laboratory," Los Alamos National Laboratory report LA-13010-MS, Los Alamos, New Mexico. (Broxton and Reneau 1995, 49726)

Broxton, D. E., D. Vaniman, F. M. Byers, Jr., S. J. Chipera, E. C. Kluk, and R. G. Warren, December 1995. "Stratigraphy, Mineralogy, and Chemistry of Bedrock Tuffs at Pajarito Mesa," in *Geological Site Characterization for the Proposed Mixed Waste Disposal Facility, Los Alamos National Laboratory*, S. L. Reneau and R. R. Raymond, Jr., eds., Los Alamos National Laboratory report LA-13089-MS, Los Alamos, New Mexico, pp. 5–30. (Broxton et al. 1995, 54709)

Broxton, D. E., R. T. Rytí, D. Carlson, R. G. Warren, E. C. Kluk, and S. J. Chipera, March 1996. "Natural Background Geochemistry of the Bandelier Tuff at MDA P, Los Alamos National Laboratory, New Mexico," Los Alamos National Laboratory report LA-UR-96-1151, Los Alamos, New Mexico. (Broxton et al. 1996, 54948)

Broxton D. E., R. Gilkeson, P. Longmire, J. Marin, R. Warren, D. Vaniman, A. Crowder, B. Newman, B. Lowry, D. Rogers, W. Stone, S. McLin, G. WoldeGabriel, D. Daymon, and D. Wycoff, May 2001. "Characterization Well R-9 Completion Report," Los Alamos National Laboratory report LA-13742-MS, Los Alamos, New Mexico. (Broxton et al. 2001, 71250)

Broxton, D. E., R. Warren, D. Vaniman, B. Newman, A. Crowder, M. Everett, R. Gilkeson, P. Longmire, J. Marin, W. Stone, S. McLin, and D. Rogers, May 2001. "Characterization Well R-12 Completion Report," Los Alamos National Laboratory report LA-13822-MS, Los Alamos, New Mexico. (Broxton et al. 2001, 71252)

Broxton, D. E., D. Vaniman, W. Stone, S. McLin, J. Marin, R. Koch, R. Warren, P. Longmire, D. Rogers, and N. Tapia, May 2001. "Characterization Well R-19 Completion Report," Los Alamos National Laboratory report LA-13823-MS, Los Alamos, New Mexico. (Broxton et al. 2001, 71253)

Card, R. E. Jr. and R. Autenrieth, March 1998. "Treatment of HMX and RDX Contamination," Amarillo National Resource Center for Plutonium, ANRCTP-1998-2, 48 p. (Card and Autenrieth 1998, 71308)

Clark, I. D., and P. Fritz, 1997. *Environmental Isotopes in Hydrogeology*, Lewis Publishers, New York, New York. (Clark and Fritz 1997, 59168)

Dalrymple, G. B., A. Cox, R. R. Doell, and C. S. Gromme, 1967. "Pliocene Geomagnetic Polarity Epochs," *Earth Planet. Sci. Lett.*, Vol. 2, pp. 163–173. (Dalrymple et al. 1967, 49924)

Daniel B. Stephens and Associates, January 1999. "Laboratory Analysis of Soil Hydraulic Properties for TA-16 Boreholes 2667, 2668, 2669, Project No. 8844.01," prepared for Los Alamos National Laboratory, Los Alamos, New Mexico. (Daniel B. Stephens and Associates 1999, 70105)

Dean, J. A., 1985. *Lange's Handbook of Chemistry*, 13th ed. McGraw-Hill Book Company, New York, New York, p. 5-7, Table 5-6. (Dean 1985, 71312)

Environmental Surveillance and Compliance Programs, September 1997. "Environmental Surveillance and Compliance at Los Alamos during 1996," Los Alamos National Laboratory report LA-13343-ENV, Los Alamos, New Mexico. (Environmental Surveillance and Compliance Programs 1997, 56684)

EPA (US Environmental Protection Agency), May 1987. "Test Methods for Evaluating Solid Waste, Laboratory Manual, Physical/Chemical Methods," SW-846, Third Edition, Update III, Washington, D.C. (EPA 1987, 57589)

EPA (US Environmental Protection Agency), 2000. "Drinking Water Standards and Health Advisories," EPA 822-B-00-001, Office of Water, U.S. Environmental Protection Agency, Washington, D.C. (EPA 2000, 70122)

Freeze, R.A., and J. A. Cherry, 1979. *Groundwater*, ISBN 0-13-365312, Prentice Hall, Englewood Cliffs, New Jersey. (Freeze and Cherry 1979, 64057)

Gardner, J. N., S. Reneau, C. Lewis, A. Lavine, D. Krier, G. WoldeGabriel, and G. Guthrie, July 2001. "Geology of the Pajarito Fault Zone in the Vicinity of S-Site (TA-16), Los Alamos National Laboratory, Rio Grande Rift, New Mexico," Los Alamos National Laboratory report LA-13831-MS, Los Alamos, New Mexico. (Gardner et al. 2001, 70106)

Gee, G. W., M. D. Campbell, G. S. Campbell, and J. H. Campbell, 1992. "Rapid Measurement of Low Soil Water Potentials Using a Water Activity Meter," *Soil Science Society of America Journal*, Vol. 56, pp. 1068–1070. (Gee et al. 1992, 58717)

Griggs, R. L., 1964. "Geology and Ground-Water Resources of the Los Alamos Area, New Mexico," with a section on "Quality of Water" by John D. Hem, U.S. Geological Survey Water-Supply Paper 1753, Washington, D.C. (Griggs 1964, 8795)

Heiken, G., F. Goff, J. Stix, S. Tamanyu, M. Shafiqullah, S. Garcia, and R. Hagan, 1986. "Intracaldera Volcanic Activity, Toledo Caldera and Embayment, Jemez Mountains, New Mexico," *Journ. Geophys. Res.*, Vol. 91, No. B2, pp. 1799–1815. (Heiken et al. 1986, 48638)

Hillel, D., 1980. *Applications of Soil Physics*, Academic Press, San Diego, California, 385 pp. (Hillel 1980, 71306)

Hofstetter, T. B., C. G. Heijman, S. B. Haderlein, C. Holliger, and R. P. Schwarzenbach, 1999. "Complete Reduction of TNT and Other (Poly)nitroaromatic Compounds Under Iron-Reducing Subsurface Conditions," *Environmental Science and Technology*, Vol. 33, No. 9, pp. 1479–1487. (Hofstetter et al. 1999, 71307)

Izett, G. A., and J. D. Obradovich, February 10, 1994. "⁴⁰Ar/³⁹Ar Age Constraints for the Jaramillo Normal Subchron and the Matuyama-Brunhes Geomagnetic Boundary," *Journal of Geophysical Research*, Vol. 99, No. B2, pp. 2925–2934. (Izett and Obradovich 1994, 48817)

Kendall, C., and T. B. Coplen, 1985. "Multisample Conversion of Water to Hydrogen by Zinc for Stable Isotope Determination," *Analytical Chemistry*, Vol. 57, pp. 1437–1446. (Kendall and Coplen 1985, 64061)

Langmuir, D., 1997. *Aqueous Environmental Geochemistry*, Prentice-Hall, Inc., Upper Saddle River, New Jersey. (Langmuir 1997, 56037)

LANL (Los Alamos National Laboratory), September 1998. "RFI Report for Potential Release Site 16-021(c)," Volume I, Los Alamos National Laboratory report LA-UR-98-4101, Los Alamos, New Mexico. (LANL 1998, 59891)

LANL (Los Alamos National Laboratory), November 1995. "Task/Site Work Plan for Operable Unit 1049: Los Alamos Canyon and Pueblo Canyon," Los Alamos National Laboratory report LA-UR-95-2053, Los Alamos, New Mexico. (LANL 1995, 50290)

LANL (Los Alamos National Laboratory), January 31, 1996. "Groundwater Protection Management Program Plan," rev. 2.0, Los Alamos, New Mexico. (LANL 1996, 70215)

LANL (Los Alamos National Laboratory), April 1997. "Core Document for Canyons Investigations," Los Alamos National Laboratory report LA-UR-96-2083, Los Alamos, New Mexico. (LANL 1997, 55622)

LANL (Los Alamos National Laboratory), September 1997. "Work Plan for Mortandad Canyon," Los Alamos National Laboratory report LA-UR-97-3291, Los Alamos, New Mexico. (LANL 1997, 56835)

LANL (Los Alamos National Laboratory), March 1998. "Field Implementation Plan for the Drilling and Testing of LANL Regional Characterization Well R-12," Los Alamos, New Mexico. (LANL 1998, 59162)

LANL (Los Alamos National Laboratory), May 22, 1998. "Hydrogeologic Workplan," rev. 1.0, Los Alamos, New Mexico. (LANL 1998, 59599)

Longmire, P. A., D. Broxton, W. Stone, B. Newman, R. Gilkeson, J. Marin, D. Vaniman, D. Counce, D. Rogers, R. Hull, S. McLin, and R. Warren, May 2001. "Characterization Well R-15 Completion Report," Los Alamos National Laboratory report LA-13749-MS, Los Alamos, New Mexico. (Longmire et al. 2001, 70103)

Neeper, D. A. and R. H. Gilkeson, 1996. "The Influence of Topography, Stratigraphy, and Barometric Venting on the Hydrology of Unsaturated Bandelier Tuff," New Mexico Geological Society, Jemez Mountains Region, pp. 427–433. (Neeper and Gilkeson 1996, 70104)

Purtymun, W. D., January 1984. "Hydrologic Characteristics of the Main Aquifer in the Los Alamos Area: Development of Ground Water Supplies," Los Alamos National Laboratory report LA-9957-MS, Los Alamos, New Mexico. (Purtymun 1984, 6513)

Purtymun, W. D., January 1995. "Geologic and Hydrologic Records of Observation Wells, Test Holes, Test Wells, Supply Wells, Springs, and Surface Water Stations in the Los Alamos Area," Los Alamos National Laboratory report LA-12883-MS, Los Alamos, New Mexico. (Purtymun 1995, 45344)

Rogers, D. B., and B. M. Gallaher, September 1995. "The Unsaturated Hydraulic Characteristics of the Bandelier Tuff," Los Alamos National Laboratory report LA-12968-MS, Los Alamos, New Mexico. (Rogers and Gallaher 1995, 49824)

Rogers, D. B., July 1998. "Impact of Tritium Disposal on Surface Water and Groundwater at Los Alamos National Laboratory Through 1997," Los Alamos National Laboratory report LA-13465-SR, Los Alamos, New Mexico. (Rogers 1998, 59169)

Rogers, M. A., 1995. "Geologic Map of Los Alamos National Laboratory Reservation," New Mexico Environment Department, scale 1:4800. (Rogers 1995, 54419)

Burrows, E. P., D. H. Rosenblatt, W. R. Mitchell, and D. L. Parmer, 1989. "Organic Explosives and Related Compounds: Environmental and Health Considerations," Technical Report 8901, U.S. Army Biomedical Research and Development Laboratory, Fort Detrick, Frederick, Maryland. (Burrows et al. 1989, 71319)

Ryti, R. T., P. A. Longmire, D. E. Broxton, S. L. Reneau, and E. V. McDonald, May 7, 1998. "Inorganic and Radionuclide Background Data for Soils, Canyon Sediments, and Bandelier Tuff at Los Alamos National Laboratory" (draft), Los Alamos National Laboratory report, Los Alamos, New Mexico. (Ryti et al. 1998, 58093)

Schwarzenbach, R. P., P. M. Gschwend, and D. M. Imboden, 1993. *Environmental Organic Chemistry*, John Wiley and Sons, Inc., New York, New York, 681 p. (Schwarzenbach et al. 1993, 71318)

Shurbaji, A. R., and A. R. Campbell, February 1997. "Study of Evaporation and Recharge in Desert Soil Using Environmental Tracers, New Mexico USA," *Environmental Geology*, Vol. 29, pp. 147–151. (Shurbaji and Campbell 1997, 64063)

Socki, R. A., H. R. Karlsson, and E. K. Gibson, 1992. "Extraction Technique for Determination of Oxygen-18 in Water Using Preevacuated Glass Vials," *Analytical Chemistry*, Vol. 64, pp. 829–831. (Socki et al. 1992, 64064)

Smith, R. L., R. A. Bailey, and C. S. Ross, 1970. "Geologic Map of the Jemez Mountains, New Mexico," US Geological Survey Miscellaneous Geological Investigations Map I-571, scale 1:125 000. (Smith et al. 1970, 09752)

Spain, J. C., J. B. Hughes, and H.-J. Knackmuss, 2000. *Biodegradation of Nitroaromatic Compounds and Explosives*, Lewis Publishers, Boca Raton, Florida, 434 p. (Spain et al. 2000, 71317)

Spell, T. L., P. R. Kyle, and J. Baker, 1996. "Geochronology and Geochemistry of the Cerro Toledo Rhyolite," in *New Mexico Geological Society Guidebook, 47th Field Conference, Jemez Mountains Region*, F. Goff, B. S. Kues, M. A. Rogers, L. D. McFadden, and J. N. Gardner, eds., pp. 263–268. (Spell et al. 1996, 55542)

Stimac, J. A., D. E. Broxton, E. C. Kluk, and S. J. Chipera, 1998. "Preliminary Stratigraphy of Tuffs from Borehole 49-2-700-1 at Technical Area 49, Los Alamos National Laboratory, New Mexico," Los Alamos National Laboratory unnumbered report, Los Alamos, New Mexico. (Stimac et al. 1998, 59161)

Stone, W. J., 2000. "Laboratory-Derived Hydraulic Properties of Selected Materials from Wells R-9, R-12, and R-25," Los Alamos National Laboratory report LA-UR-00-3587, Los Alamos, New Mexico. (Stone 2000, 66781)

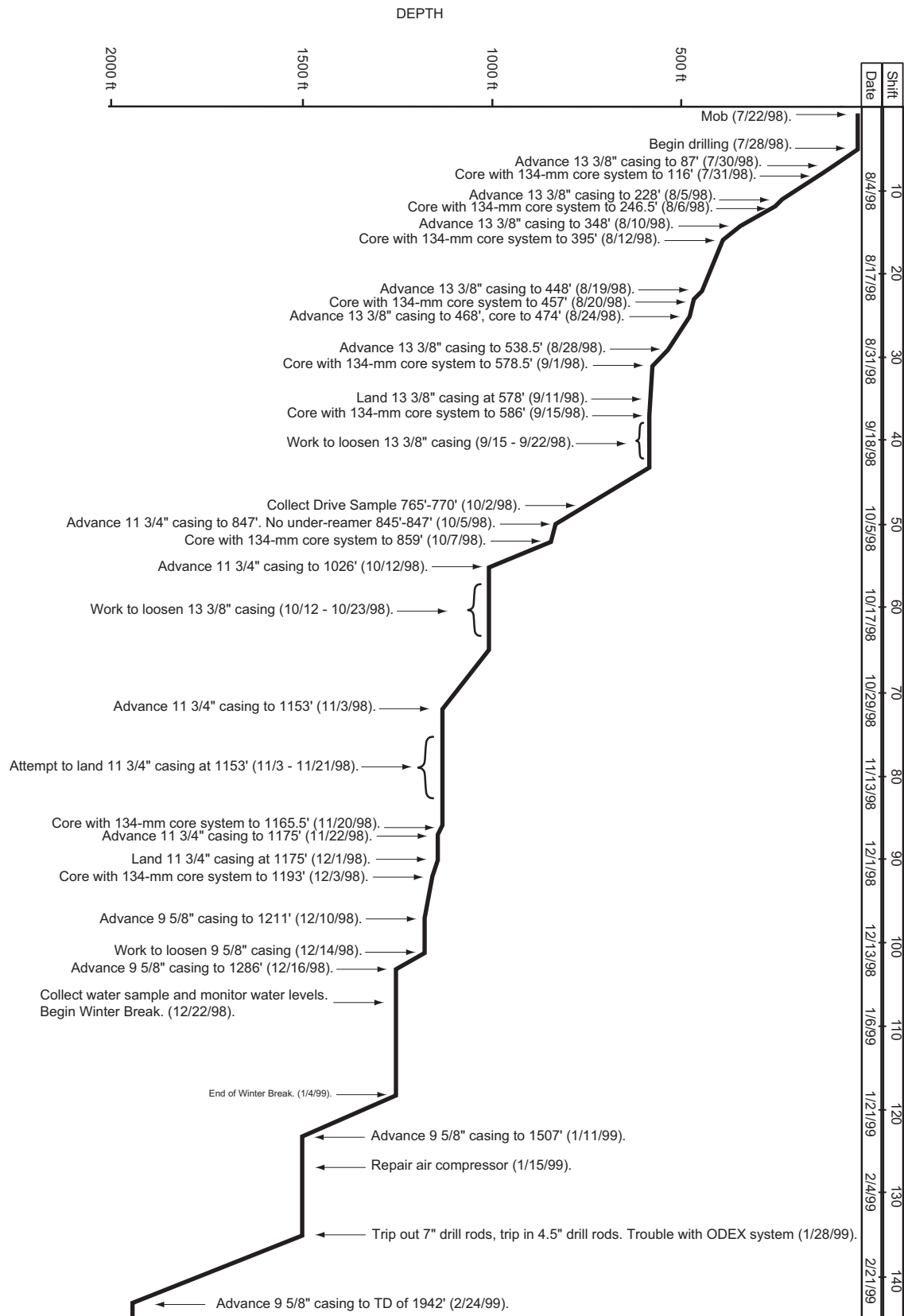
van Genuchten, M. Th., F. J. Leij, and S. R. Yates, December 1991. "The RETC Code for Quantifying the Hydraulic Functions of Unsaturated Soils," EPA/600/2-91/065, prepared by the U.S. Salinity Laboratory, U.S. Department of Agriculture, Agricultural Research Service, Riverside, California. (van Genuchten et al. 1991, 65419)

Waresback, D. B., August 1986. "The Puye Formation, New Mexico: Analysis of a Continental, Rift-Filling, Volcaniclastic Alluvial-Fan Sequence," Master of Science in Geology thesis, University of Texas, Arlington, Texas. (Waresback 1986, 58715)

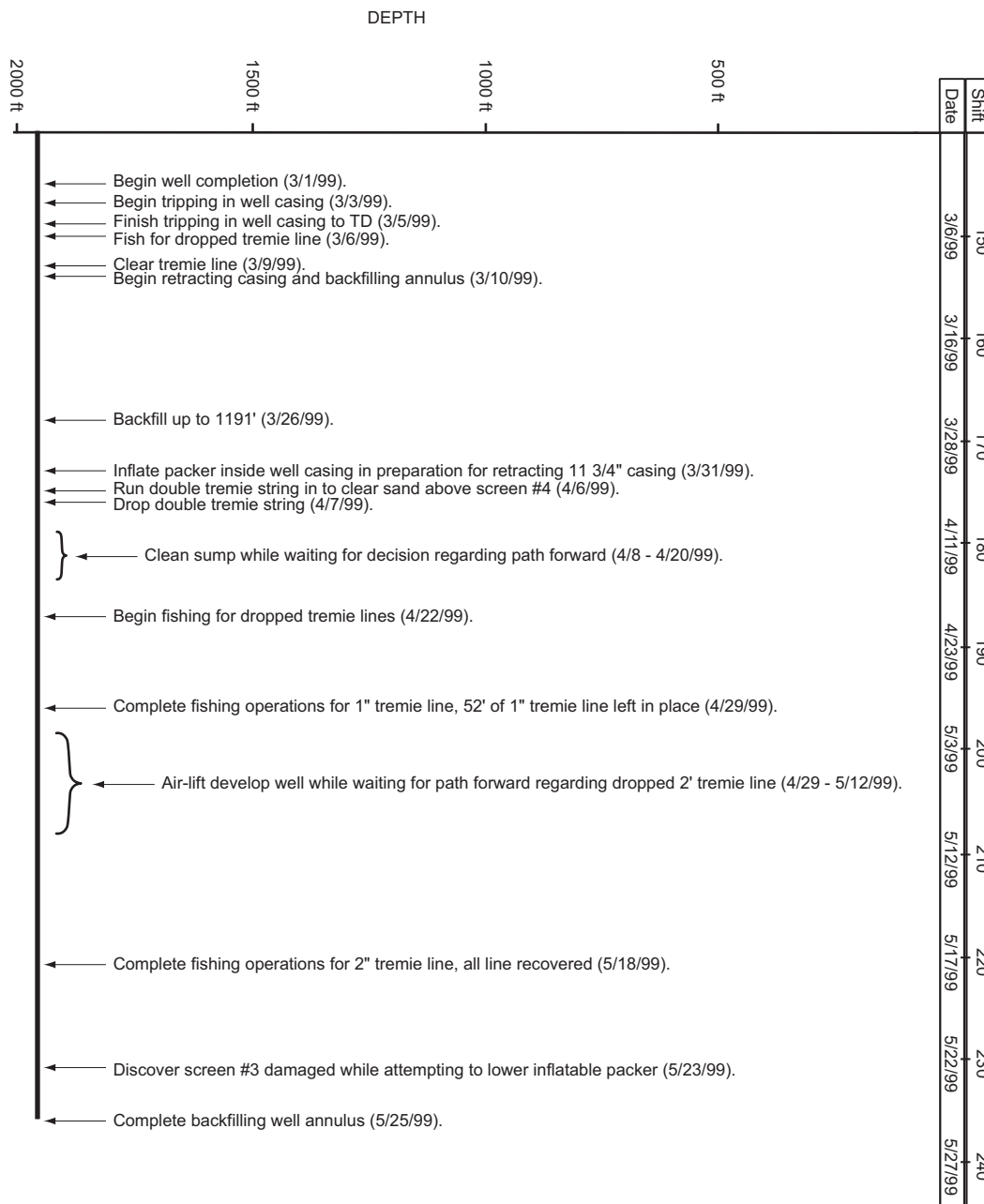
Warren, R. G., E. V. McDonald., and R. T. Rytí, August 1997. "Baseline Geochemistry of Soil and Bedrock, Tshirege Member of the Bandelier Tuff at MDA-P," Los Alamos National Laboratory report LA-13330-MS, Los Alamos, New Mexico. (Warren et al. 1997, 59180)

Appendix A

Drilling Chronology



(Continued on Next Page)



Appendix B

WestbayTM MP55 System Components Installed in Well R-25

Summary MP Casing Log

Company: LANL
Well: R25
Site:
Project: Hydrogeology Characterization

Job No: WB777
Author: DL

Well Information

Reference Datum:
Elevation of Datum: 0.00 ft.
MP Casing Top: 0.00 ft.
MP Casing Length: 1835.44 ft.
Depth Adjusted For:

Field De-Stressing

Well Description:

Plastic in 5-inSS well casing

Other References:

Screens + zones LANL Mar 5, 1999

Z3 screen damaged. See att'd drift diag.

Abrasion Protectors see Installation Log

Borehole Depth: 1942.00 ft.

Borehole Inclination:

Borehole Info: (# - start - end - diameter)

Diameter #1 - 0.00 20.00 20.00 in.

Diameter #2 - 20.00 580.00 14.50 in.

Diameter #3 - 580.00 1175.00 12.75 in.

Diameter #4 - 1175.00 1942.00 10.75 in.

File Information

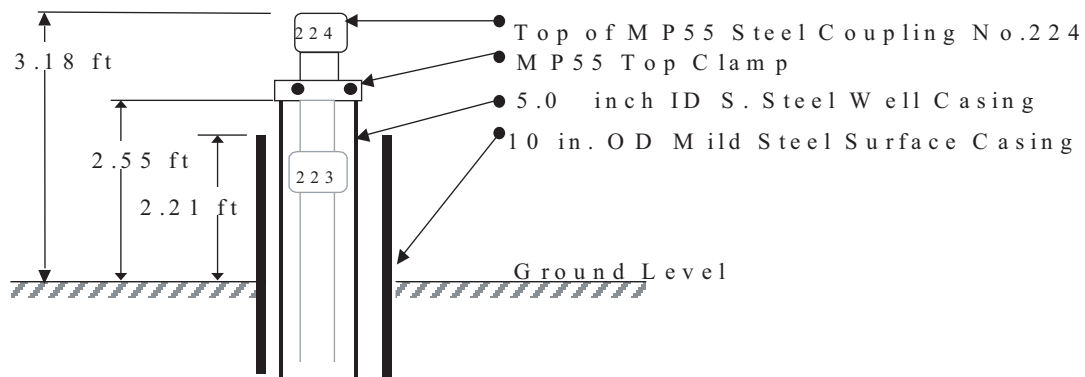
File Name: 777_R25.WWD

File Date: Oct 03 17:54:05 2000

Report Date: Tue Oct 03 18:01:31 2000

Sketch of Wellhead Completion




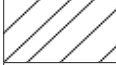





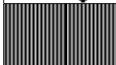

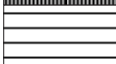




R 2 5 - S u r f a c e C o m p l e t i o n



Summary MP Casing Log
LANL

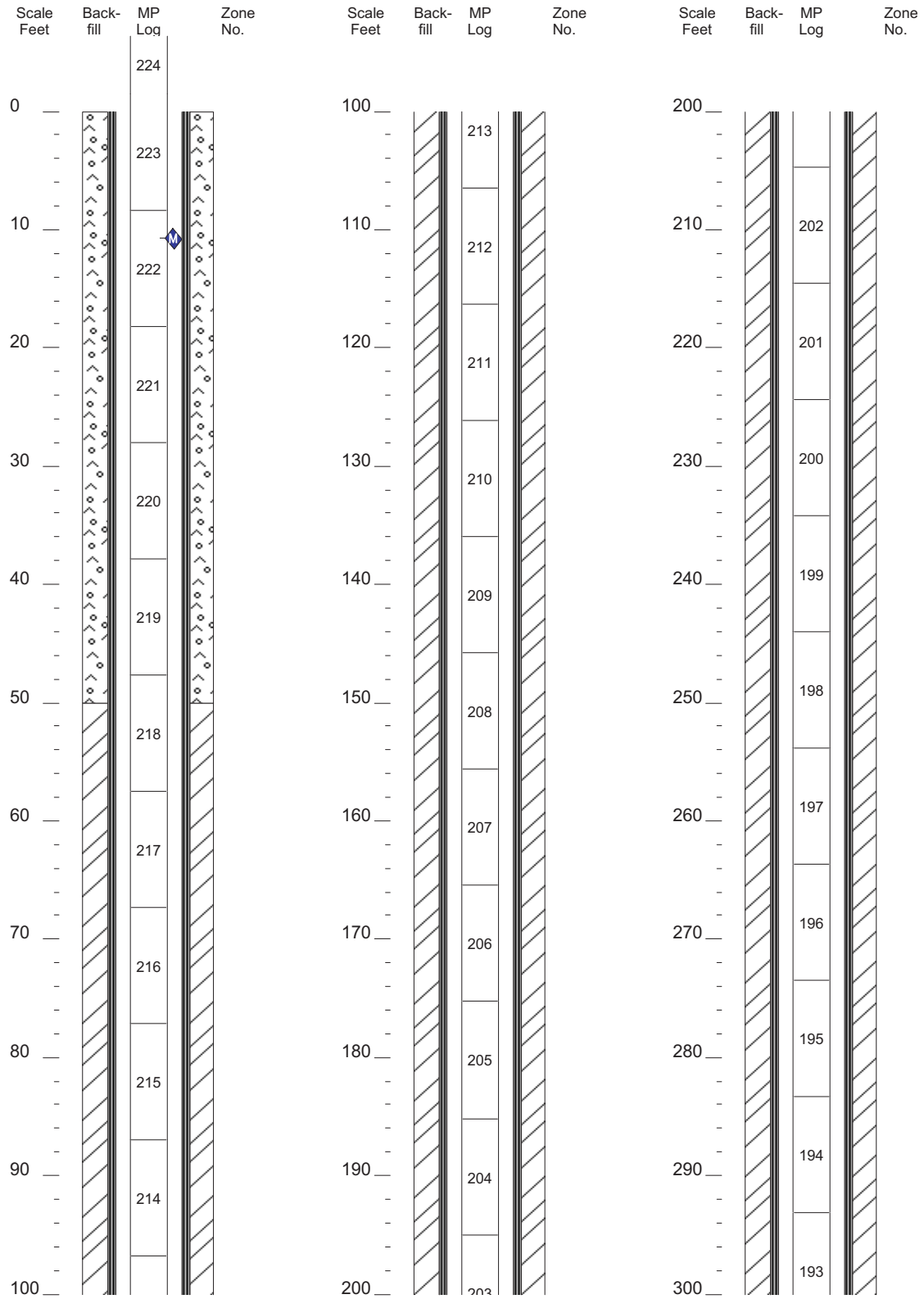
Job No: WB777
Well: R25

Legend

(Qty) MP Components	Geology	Backfill/Casing
 (2) 0603 - MP55 End Plug		 Concrete
 (36) 0601M15 - MP55 Casing, PVC, 1.5m		 Bentonite
 (152) 0601M30 - MP55 Casing, PVC, 3.0m		 Sand Fine
 (26) 0612M15 - MP55 Packer with stiffeners		 Sand Coarse
 (10) 0601M10 - MP55 Casing, PVC, 1.0m		 Stainless Steel
 (183) 0602 - MP55 Regular Coupling		 Well Screen
 (35) 0605 - MP55 Measurement Port		
 (8) 0607 - MP55 Hydraulic Pumping Port		
 (12) 0608 - MP55 Magnetic Location Collar		
 (37) ABRAS - Abrasion Protector		

Summary MP Casing Log
LANL

Job No: WB777
Well: R25



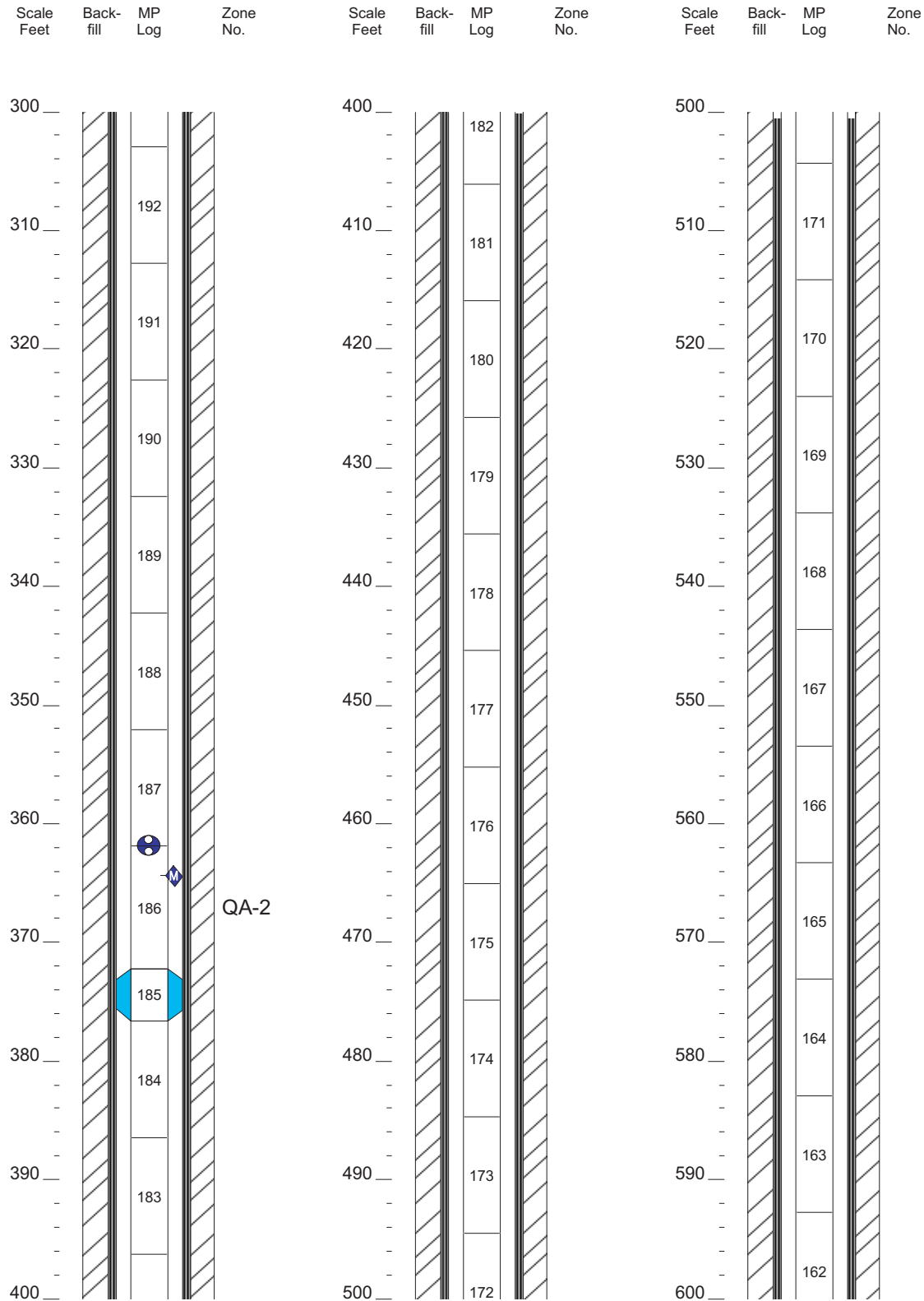
(c) Westbay Instruments Inc. 1998

Tue Oct 03 18:01:31 2000

Page: 3

Summary MP Casing Log
LANL

Job No: WB777
Well: R25



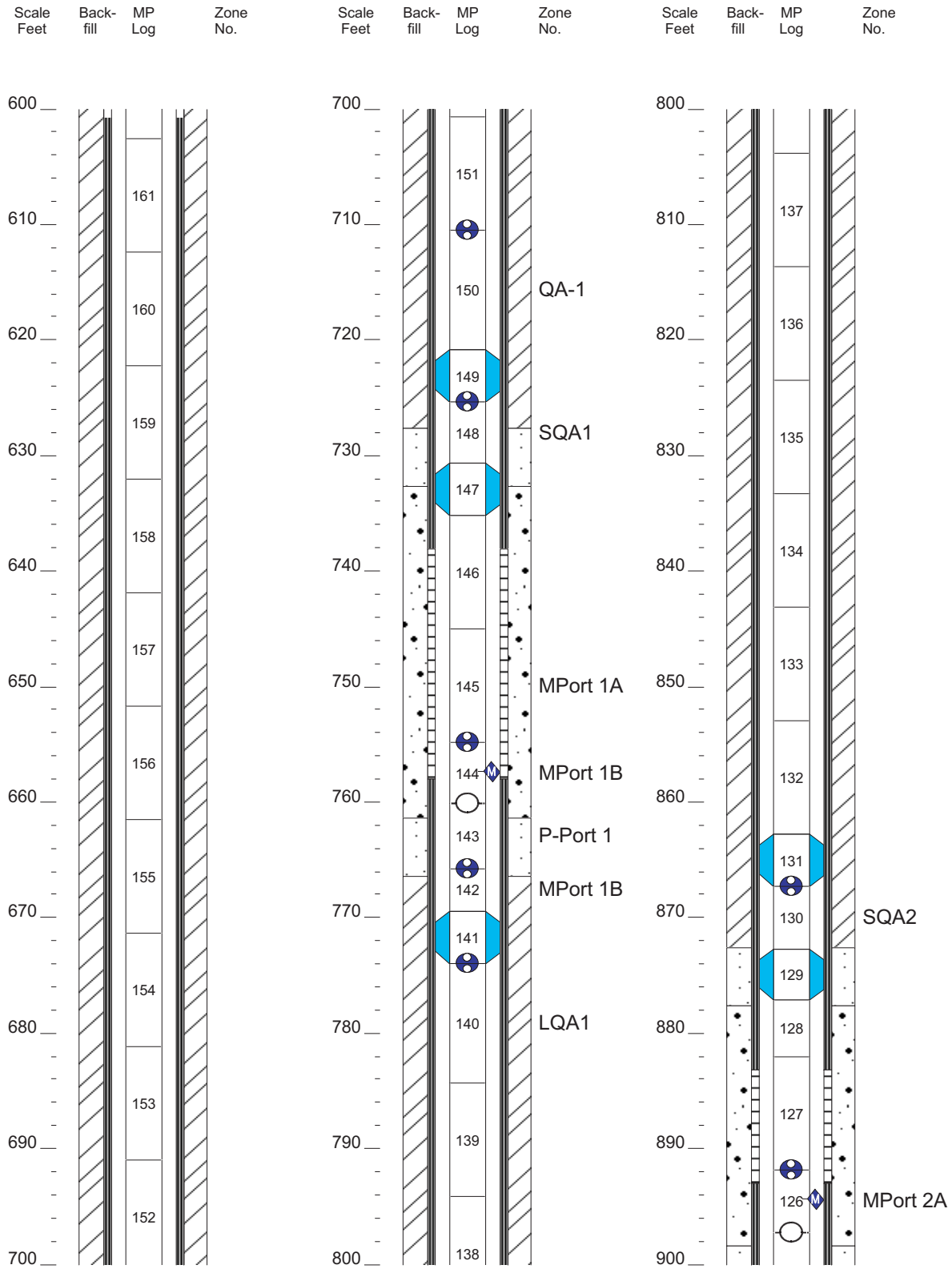
(c) Westbay Instruments Inc. 1998

Tue Oct 03 18:01:36 2000

Page: 4

Summary MP Casing Log
LANL

Job No: WB777
Well: R25



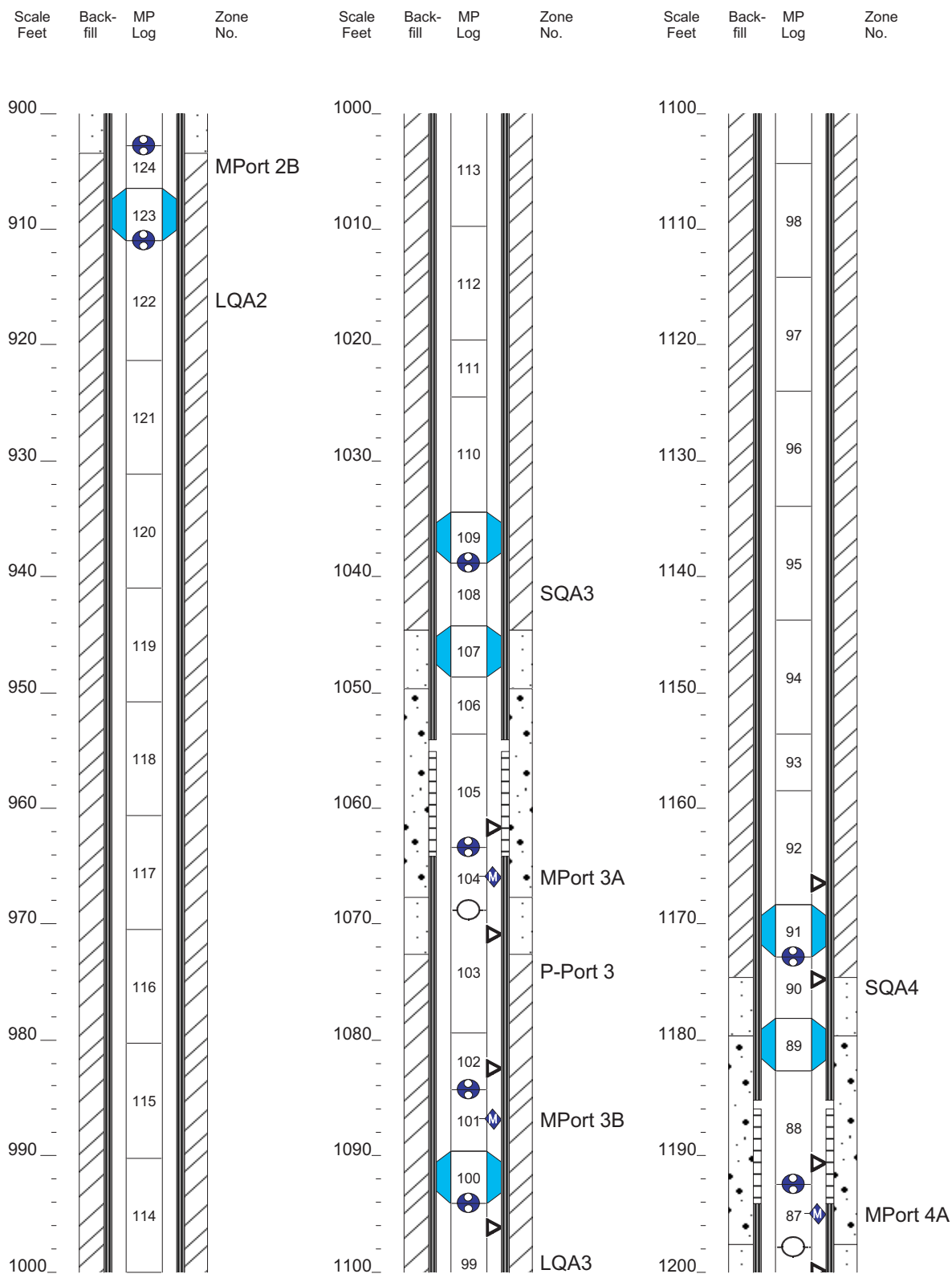
(c) Westbay Instruments Inc. 1998

Tue Oct 03 18:03:17 2000

Page: 5

Summary MP Casing Log
LANL

Job No: WB777
Well: R25



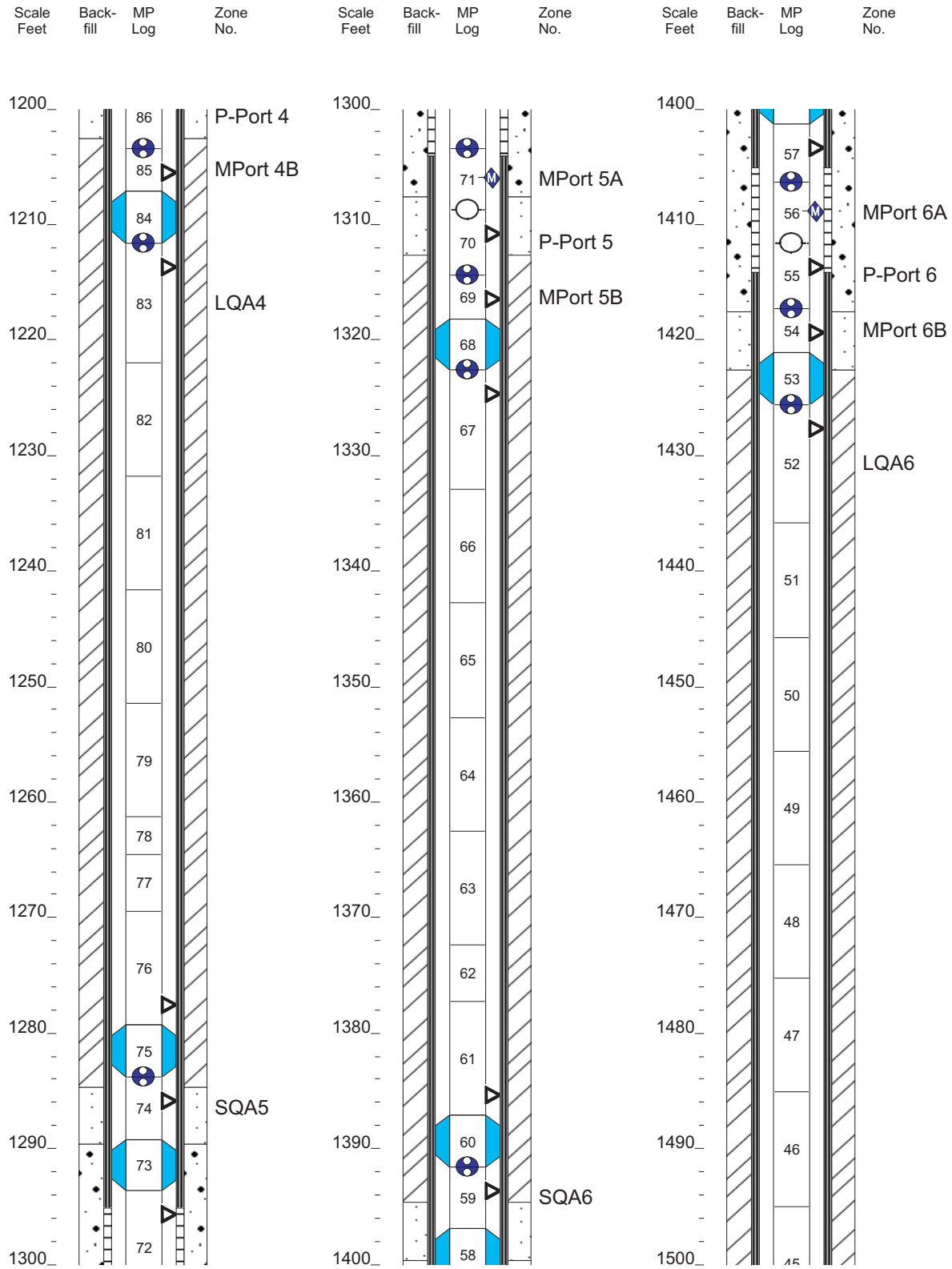
(c) Westbay Instruments Inc. 1998

Tue Oct 03 18:03:22 2000

Page: 6

Summary MP Casing Log
LANL

Job No: WB777
Well: R25



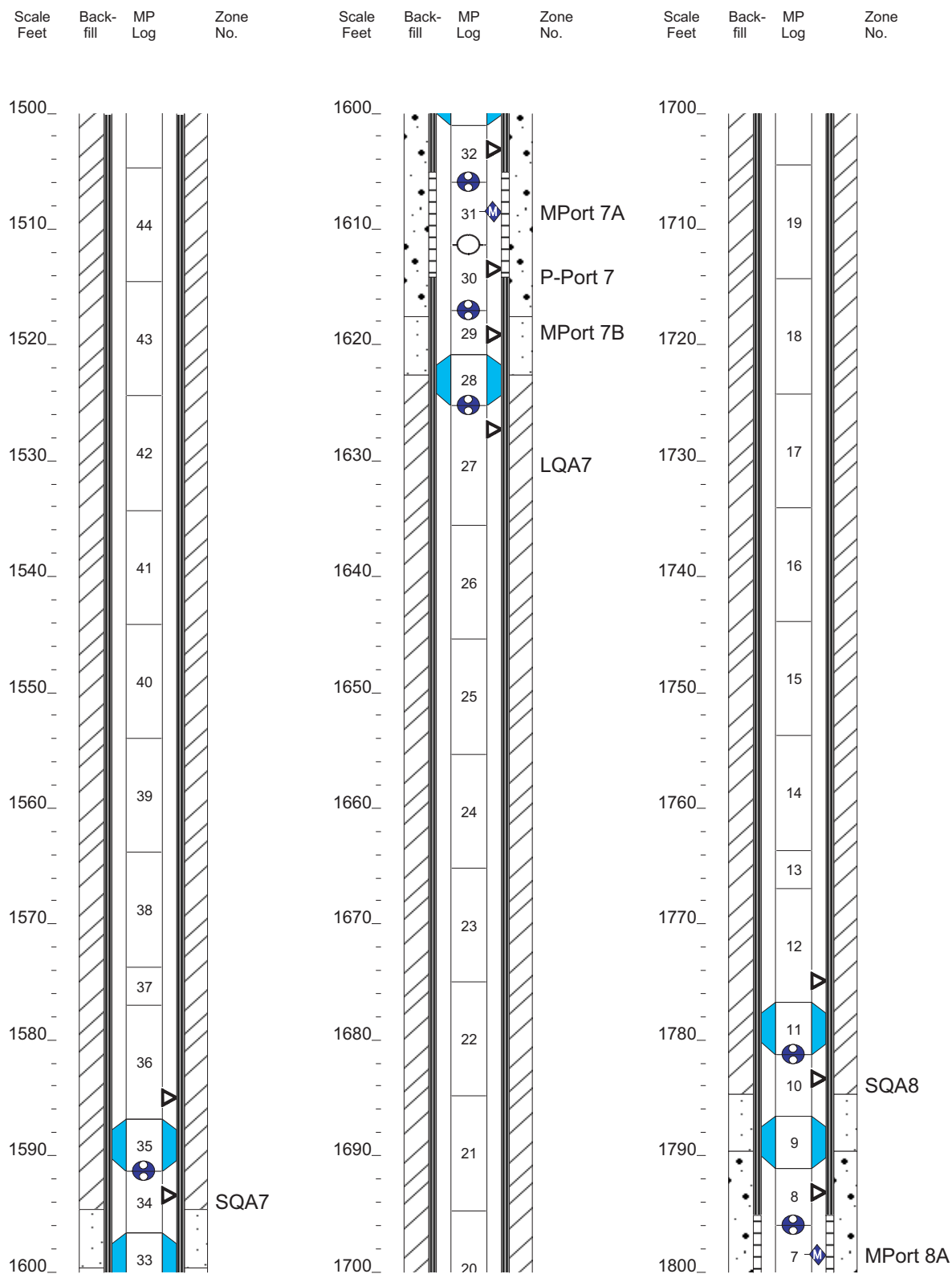
(c) Westbay Instruments Inc. 1998

Tue Oct 03 18:03:27 2000

Page: 7

Summary MP Casing Log
LANL

Job No: WB777
Well: R25



(c) Westbay Instruments Inc. 1998

Tue Oct 03 18:03:32 2000

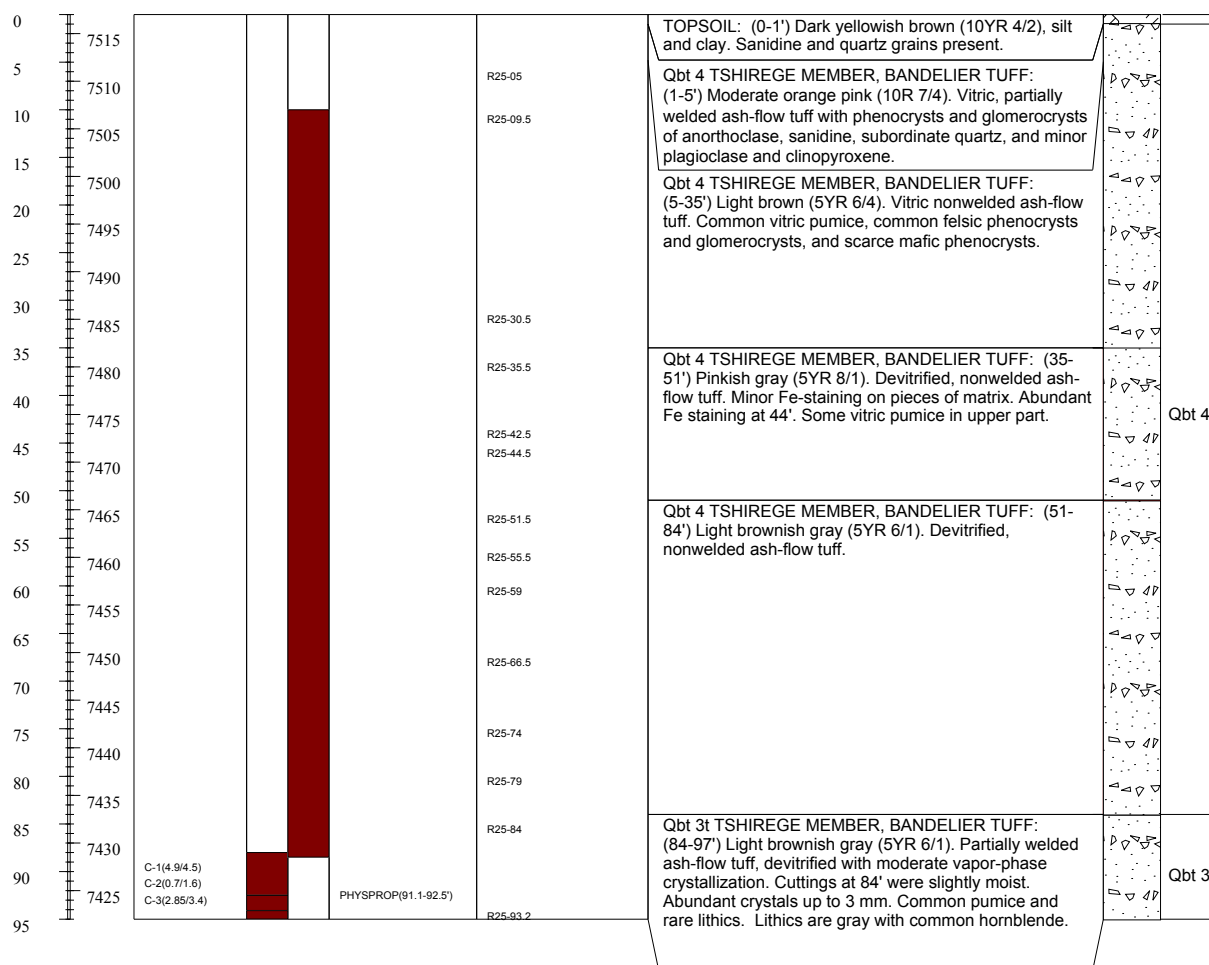
Page: 8

Appendix C

Lithologic Log

LOS ALAMOS NATIONAL LABORATORY
REGIONAL HYDROGEOLOGIC CHARACTERIZATION PROJECT
ENVIRONMENTAL RESTORATION, GROUNDWATER FOCUS AREA
BOREHOLE LOG

BOREHOLE ID: R-25				TA/OU: TA-16				Page 1 of 20			
DRILLING COMPANY: Tonto Drilling Co.				START DATE: July 22, 1998/0930				END DATE: February 24, 1999			
DRILLING EQ/METHOD: Foremost DR24				SAMPLING EQ/METHOD: Wireline core barrel sampling							
GROUND ELEVATION: 7516.1'				TOTAL DEPTH = 1942' bgs							
DRILLER: Larry Thoren				GEOLOGY P.I.: Rick Warren				SITE GEOLOGIST: Mark Everett			
Depth (ft)	Elevation (ft)	Core Run # (amt.-recov./amt. attemp.)	Core Run	Cuttings Collected	Hydrologic Property (Physprop) and Geochemical (Geochem) Samples (CACV-9x-xxxx)	Moisture/Matric Pot. R25-depth (ft)	Lithology	Graphic Log	Lithologic Symbol		



LOS ALAMOS NATIONAL LABORATORY
REGIONAL HYDROGEOLOGIC CHARACTERIZATION PROJECT
ENVIRONMENTAL RESTORATION, GROUNDWATER FOCUS AREA
BOREHOLE LOG

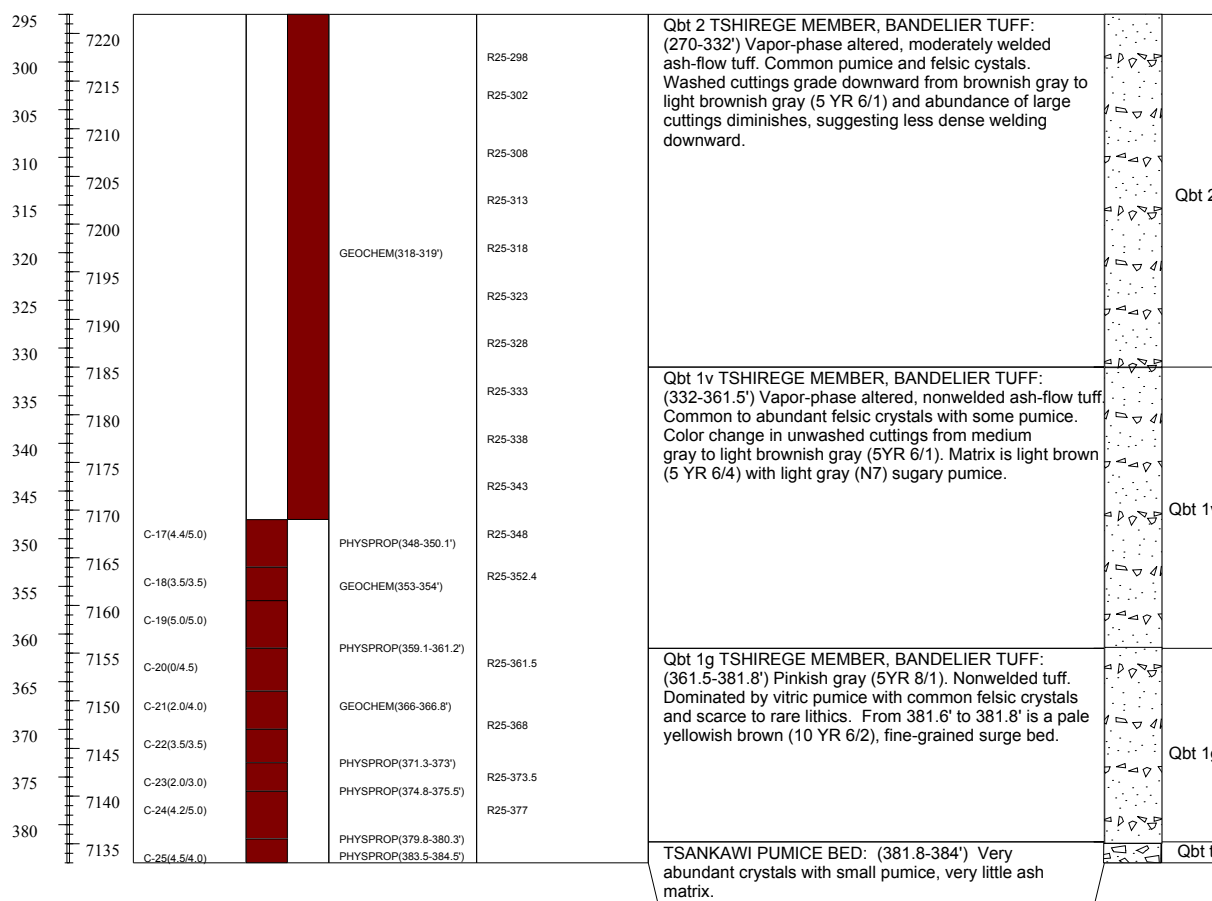
BOREHOLE ID: R-25			TA/OU: TA-16			Page 2 of 20			
DRILLING COMPANY: Tonto Drilling Co.			START DATE: July 22, 1998/0930			END DATE: February 24, 1999			
DRILLING EQ/METHOD: Foremost DR24			SAMPLING EQ/METHOD: Wireline core barrel sampling						
GROUND ELEVATION: 7516.1'			TOTAL DEPTH = 1942' bgs						
DRILLER: Larry Thoren			GEOLOGY P.I.: Rick Warren			SITE GEOLOGIST: Mark Everett			
Depth (ft)	Elevation (ft)	Core Run # (amt.-recov./amt. attemp.)	Core Run	Cuttings Collected	Hydrologic Property (Physprop) and Geochemical (Geochem) Samples (CACV-9x-xxxx)	Moisture/Matric Pot. R25-depth (ft)	Lithology	Graphic Log	Lithologic Symbol
95	7420	C-4(3.2/3.5)			PHYSPROP(95.42-96.42')	R25-97.8	Qbt 3t TSHIREGE MEMBER, BANDELIER TUFF: (84-97') Light brownish gray (5YR 6/1). Partially welded ash-flow tuff, devitrified with moderate vapor-phase crystallization. Cuttings at 84' were slightly moist. Abundant crystals up to 3 mm. Common pumice and rare lithics. Lithics are gray with common hornblende.		
100	7415	C-5(0.6/0.8)			PHYSPROP(96.58-96.95')	R25-102.3			
105	7410	C-6(4.6/4.2)			GEOCHEM(103.35-103.7') PHYSPROP(104.68-106')	R25-106.8			
110	7405	C-7(4.65/5.0)			PHYSPROP(108.6-110.65') GEOCHEM(110.25-110.65')	R25-112			
115	7400	C-8(4.1/5.0)			PHYSPROP(113.35-115.05')		Qbt 3t TSHIREGE MEMBER, BANDELIER TUFF: (97-102') Light gray (N7). Densely welded ash-flow tuff.		
120	7395					R25-121	Qbt 3t TSHIREGE MEMBER, BANDELIER TUFF: (102-116') Medium light gray (N6). Devitrified, moderately welded ash-flow tuff. Fracture with wet clay at 106.6'. Fracture with minor free water at 110.4'. Core dry 112' to 116'.		
125	7390					R25-126			
130	7385					R25-131	Qbt 3t TSHIREGE MEMBER, BANDELIER TUFF: (116-155') Light gray (N8) to pale yellowish brown (10YR 6/2) to grayish orange pink (5YR 7/2). Devitrified, moderately welded ash-flow tuff. Common pumice and scarce to rare lithics. Common phenocrysts from 143' to 155'.		
135	7380					R25-134.5			
140	7375					R25-139			
145	7370					R25-144 R25-146.6			
150	7365					R25-150			
155	7360					R25-155	Qbt 3 TSHIREGE MEMBER, BANDELIER TUFF: (155-229') Grayish orange pink (5YR 7/2). Vapor-phase altered, moderately welded ash-flow tuff, grading to pale yellowish brown (10YR 6/2), partially welded tuff. Common phenocrysts and rare lithics.		
160	7355					R25-161			
165	7350					R25-165.5			
170	7345								
175	7340					R25-174 R25-178			
180	7335					R25-183			
185	7330					R25-188			
190	7325					R25-193			
195									

LOS ALAMOS NATIONAL LABORATORY
REGIONAL HYDROGEOLOGIC CHARACTERIZATION PROJECT
ENVIRONMENTAL RESTORATION, GROUNDWATER FOCUS AREA
BOREHOLE LOG

BOREHOLE ID: R-25					TA/OU: TA-16		Page 3 of 20		
DRILLING COMPANY: Tonto Drilling Co.					START DATE: July 22, 1998/0930		END DATE: February 24, 1999		
DRILLING EQ/METHOD: Foremost DR24					SAMPLING EQ/METHOD: Wireline core barrel sampling				
GROUND ELEVATION: 7516.1'					TOTAL DEPTH = 1942' bgs				
DRILLER: Larry Thoren			GEOLOGY P.I.: Rick Warren		SITE GEOLOGIST: Mark Everett				
Depth (ft)	Elevation (ft)	Core Run # (amt.-recov./amt. attemp.)	Core Run	Cuttings Collected	Hydrologic Property (Physprop) and Geo-chemical (Geochem) Samples (CACV-9x-xxxx)	Moisture/Matric Pot. R25-depth (ft)	Lithology	Graphic Log	Lithologic Symbol
195	7320					R25-198	Qbt 3 TSHIREGE MEMBER, BANDELIER TUFF: (155-229') Grayish orange pink (5YR 7/2). Moderately welded ash-flow tuff. Vapor-phase crystallization. Grades to pale yellowish brown (10YR 6/2), nonwelded to partially welded ash-flow tuff at base of unit. Common phenocrysts and rare lithics.		Qbt 3
200	7315					R25-204			
205	7310					R25-208			
210	7305					R25-216			
215	7300					R25-223			
220	7295				GEOCHEM(223-225')	R25-228	Qbt 2 TSHIREGE MEMBER, BANDELIER TUFF: (229-270') Light brownish gray (5YR 6/1). Moderately welded ash-flow tuff, approaching densely welded at the top. Minor vapor-phase crystallization. Common felsic crystals, lithics, and pumice.		Qbt 2
225	7290	C-9(4.3/5.0)			PHYSPROP(229-231')	R25-231.35			
230	7285	C-10(2.0/3.1)				R25-237.5			
235	7280	C-10.5(0/0.9)			PHYSPROP(238.2-240.2')	R25-241.7			
240	7275	C-11(2.3/2.3)			GEOCHEM(243.7-244.7')	R25-248			
245	7270	C-12(2.3/2.0)			PHYSPROP(246-246.5')	R25-252.5	Qbt 2 TSHIREGE MEMBER, BANDELIER TUFF: (270-332') Vapor-phase altered, moderately welded ash-flow tuff. Common pumice and felsic crystals. Washed cuttings grade downward from brownish gray to light brownish gray (5 YR 6/1) and abundance of large cuttings diminishes, suggesting less welding downward.		Qbt 2
250	7265	C-13(2.2/1.4)				R25-258.5			
255	7260	C-14(2.0/2.0)				R25-264			
260	7255	C-15(0.75/1.3)				R25-268			
265	7250	C-16(0.5/0.5)				R25-272.5			
270	7245					R25-277			
275	7240					R25-282			
280	7235					R25-288			
285	7230					R25-293			
290	7225								
295									

LOS ALAMOS NATIONAL LABORATORY
REGIONAL HYDROGEOLOGIC CHARACTERIZATION PROJECT
ENVIRONMENTAL RESTORATION, GROUNDWATER FOCUS AREA
BOREHOLE LOG

BOREHOLE ID: R-25				TA/OU: TA-16				Page 4 of 20			
DRILLING COMPANY: Tonto Drilling Co.				START DATE: July 22, 1998/0930				END DATE: February 24, 1999			
DRILLING EQ/METHOD: Foremost DR24				SAMPLING EQ/METHOD: Wireline core barrel sampling							
GROUND ELEVATION: 7516.1'				TOTAL DEPTH = 1942' bgs							
DRILLER: Larry Thoren				GEOLOGY P.I.: Rick Warren				SITE GEOLOGIST: Mark Everett			
Depth (ft)	Elevation (ft)	Core Run # (amt.-recov./amt. attemp.)	Core Run	Cuttings Collected	Hydrologic Property (Physprop) and Geochemical (Geochem) Samples (CACV-9x-xxxx)	Moisture/Matric Pot. R25-depth (ft)	Lithology			Graphic Log	Lithologic Symbol

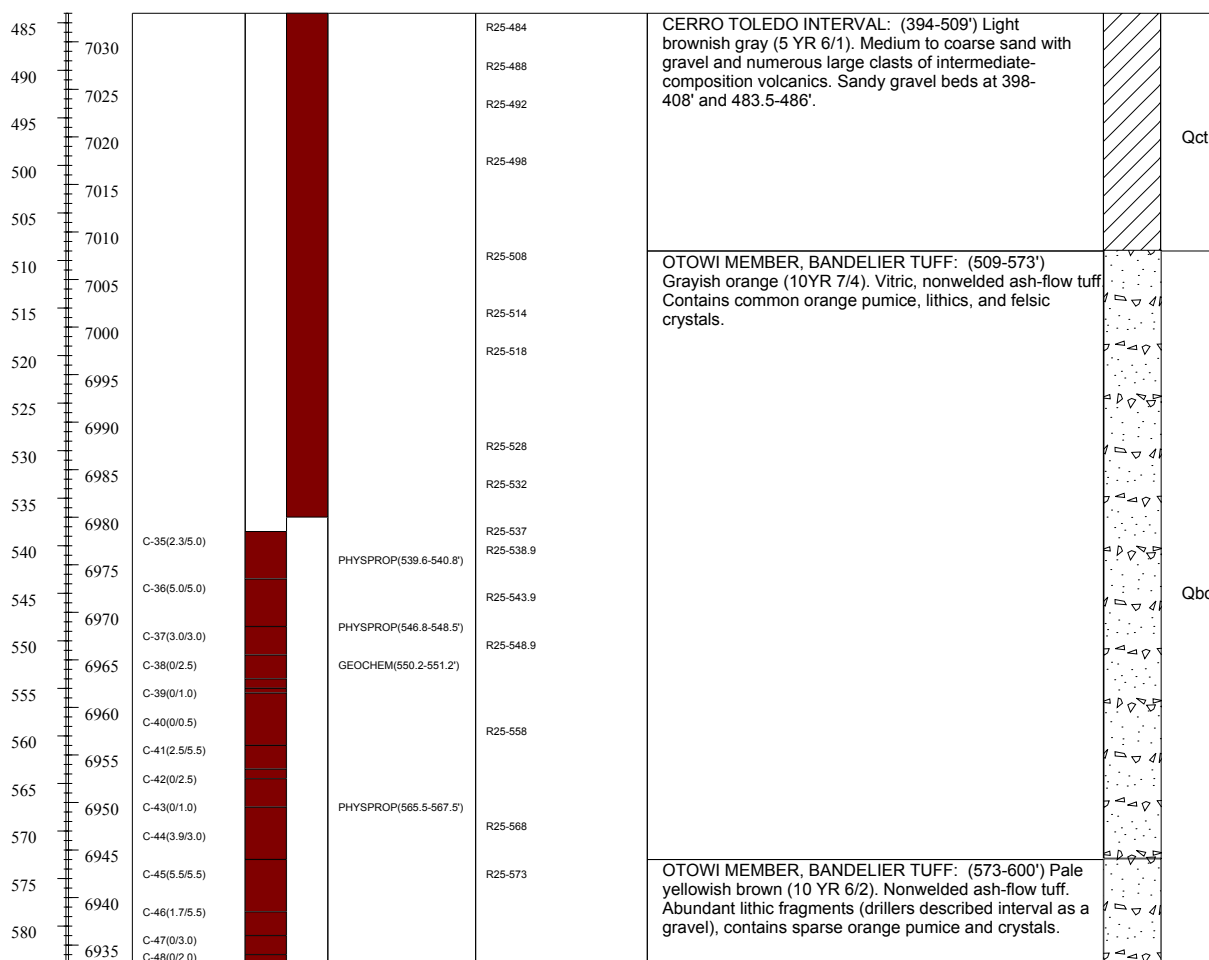


LOS ALAMOS NATIONAL LABORATORY
REGIONAL HYDROGEOLOGIC CHARACTERIZATION PROJECT
ENVIRONMENTAL RESTORATION, GROUNDWATER FOCUS AREA
BOREHOLE LOG

BOREHOLE ID: R-25			TA/OU: TA-16			Page 5 of 20			
DRILLING COMPANY: Tonto Drilling Co.			START DATE: July 22, 1998/0930			END DATE: February 24, 1999			
DRILLING EQ/METHOD: Foremost DR24			SAMPLING EQ/METHOD: Wireline core barrel sampling						
GROUND ELEVATION: 7516.1'			TOTAL DEPTH = 1942' bgs			SITE GEOLOGIST: Mark Everett			
DRILLER: Larry Thoren			GEOLOGY P.I.: Rick Warren						
Depth (ft)	Elevation (ft)	Core Run # (amt.- recov./amt. attemp.)	Core Run	Cuttings Collected	Hydrologic Property (Physprop) and Geo- chemical (Geochem) Samples (CACV-9x-xxxx)	Moisture/Matric Pot. R25-depth (ft)	Lithology	Graphic Log	Lithologic Symbol
385	7130	C-26(2.7/3.0)			PHYSPROP(383.5-384.5')	R25-385.5	CERRO TOLEDO INTERVAL: (384-394') Light brown (5 YR 5/6). Clayey fine sand with relict pumice clasts up to 4 mm. Pumice is mostly altered to clay, glassy where preserved. Possible soil horizon.		
390	7125	C-27(0/1.5)			GEOCHEM(387.2-388.2')				
395	7120	C-28(0.2/5.0)					CERRO TOLEDO INTERVAL: (394-509') Light brownish gray (5 YR 6/1). Medium to coarse sand with gravel and numerous large clasts of intermediate-composition volcanics. Sandy gravel beds at 398-408' and 483.5-486'.		Qct
400	7115					R25-399			
405	7110					R25-404			
410	7105					R25-408			
415	7100					R25-414			
420	7095					R25-418			
425	7090					R25-422			
430	7085					R25-428			
435	7080								
440	7075					R25-440			
445	7070	C-29(3.4/4.0)			GEOCHEM(440-445')				
450	7065	C-30(0/2.5)			GEOCHEM(448-449')	R25-448			
455	7060	C-31(0.3/1.0)			PHYSPROP(449-450.8')				
460	7055	C-32(0.5/1.5)				R25-456			
465	7050					R25-462			
470	7045	C-33(0.1/5.0)				R25-468			
475	7040	C-34(0/1.0)				R25-474			
480	7035					R25-478			
						R25-484			

LOS ALAMOS NATIONAL LABORATORY
REGIONAL HYDROGEOLOGIC CHARACTERIZATION PROJECT
ENVIRONMENTAL RESTORATION, GROUNDWATER FOCUS AREA
BOREHOLE LOG

BOREHOLE ID: R-25				TA/OU: TA-16				Page 6 of 20			
DRILLING COMPANY: Tonto Drilling Co.				START DATE: July 22, 1998/0930				END DATE: February 24, 1999			
DRILLING EQ/METHOD: Foremost DR24				SAMPLING EQ/METHOD: Wireline core barrel sampling							
GROUND ELEVATION: 7516.1'				TOTAL DEPTH = 1942' bgs							
DRILLER: Larry Thoren				GEOLOGY P.I.: Rick Warren				SITE GEOLOGIST: Mark Everett			
Depth (ft)	Elevation (ft)	Core Run # (amt.-recov./amt. attemp.)	Core Run	Cuttings Collected	Hydrologic Property (Physprop) and Geochemical (Geochem) Samples (CACV-9x-xxxx)	Moisture/Matric Pot. R25-depth (ft)	Lithology	Graphic Log	Lithologic Symbol		



LOS ALAMOS NATIONAL LABORATORY
REGIONAL HYDROGEOLOGIC CHARACTERIZATION PROJECT
ENVIRONMENTAL RESTORATION, GROUNDWATER FOCUS AREA
BOREHOLE LOG

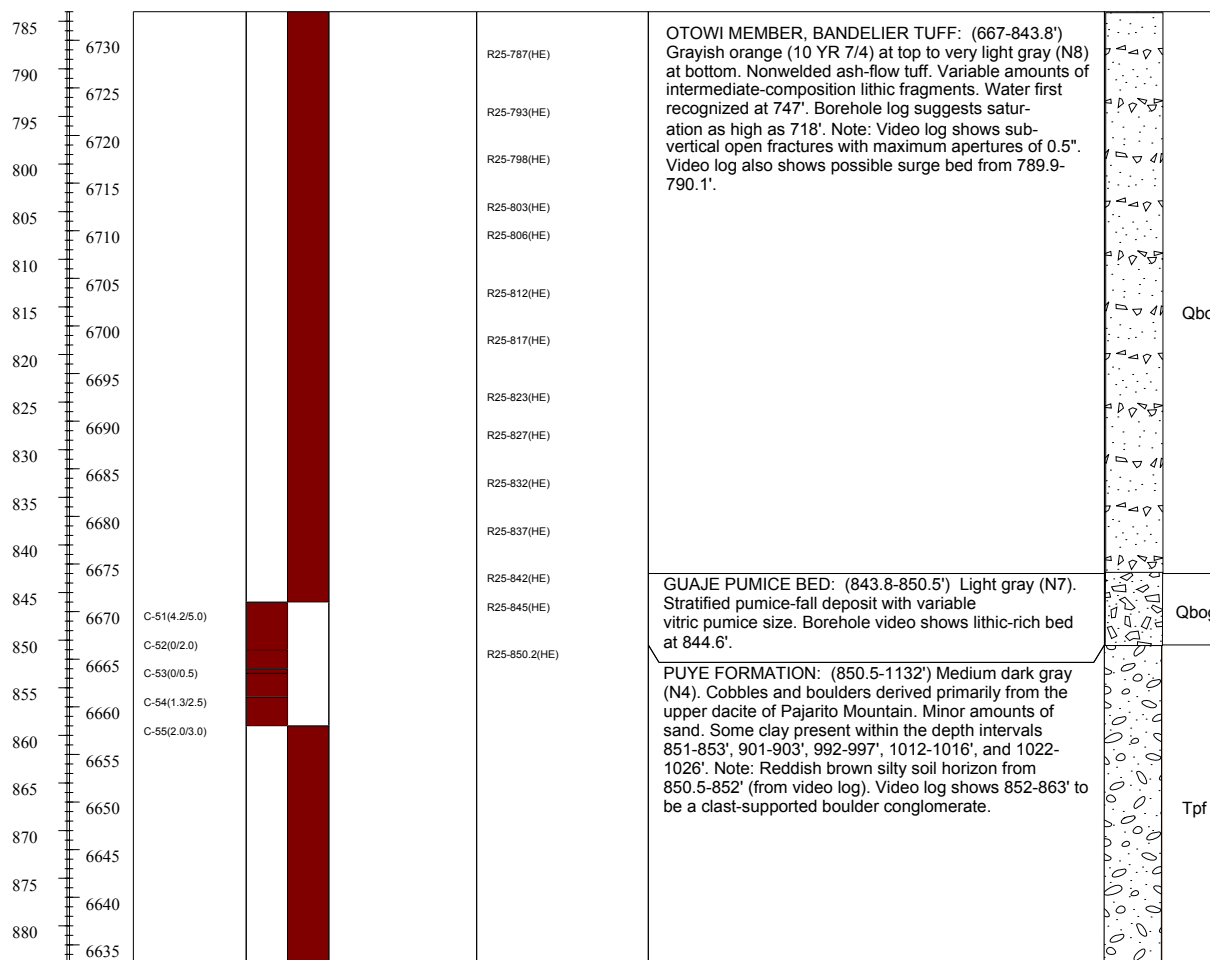
BOREHOLE ID: R-25				TA/OU: TA-16		Page 7 of 20			
DRILLING COMPANY: Tonto Drilling Co.				START DATE: July 22, 1998/0930		END DATE: February 24, 1999			
DRILLING EQ/METHOD: Foremost DR24				SAMPLING EQ/METHOD: Wireline core barrel sampling					
GROUND ELEVATION: 7516.1'				TOTAL DEPTH = 1942' bgs					
DRILLER: Larry Thoren		GEOLOGY P.I.: Rick Warren		SITE GEOLOGIST: Mark Everett					
Depth (ft)	Elevation (ft)	Core Run # (amt.-recov./amt. attemp.)	Core Run	Cuttings Collected	Hydrologic Property (Physprop) and Geochemical (Geochem) Samples (CACV-9x-xxxx)	Moisture/Matric Pot. R25-depth (ft)	Lithology	Graphic Log	Lithologic Symbol
585	6930	C-49(0/1.0)					OTOWI MEMBER, BANDELIER TUFF: (573-600') Pale yellowish brown (10 YR 6/2). Nonwelded ash-flow tuff. Abundant lithic fragments (drillers described interval as a gravel). Contains sparse orange pumice and crystals.		
590	6925	C-50(0/2.0)					OTOWI MEMBER, BANDELIER TUFF: (600-667') Pale yellowish brown (10 YR 6/2). Nonwelded ash-flow tuff. Contains abundant fine grained (<5 mm) orange pumice, common lithics, and abundant crystals.		
595	6920								
600	6915								
605	6910								
610	6905								
615	6900								
620	6895								
625	6890								
630	6885								
635	6880								
640	6875								
645	6870								
650	6865								
655	6860								
660	6855								
665	6850								
670	6845						OTOWI MEMBER, BANDELIER TUFF: (667-843.8') Grayish orange (10 YR 7/4) at top to very light gray (N8) at bottom. Nonwelded ash-flow tuff. Variable amounts of intermediate-composition lithic fragments. Water first recognized at 747'. Borehole log suggests saturation as high as 718'. Note: Video log shows sub-vertical open fractures with maximum apertures of 0.5". Video log also shows possible surge bed from 789.9-790.1'.		
675	6840								
680	6835								

C-8

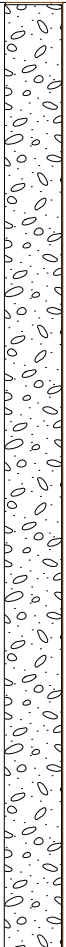
ER2001-0697

LOS ALAMOS NATIONAL LABORATORY
REGIONAL HYDROGEOLOGIC CHARACTERIZATION PROJECT
ENVIRONMENTAL RESTORATION, GROUNDWATER FOCUS AREA
BOREHOLE LOG


BOREHOLE ID: R-25			TA/OU: TA-16			Page 9 of 20			
DRILLING COMPANY: Tonto Drilling Co.			START DATE: July 22, 1998/0930			END DATE: February 24, 1999			
DRILLING EQ/METHOD: Foremost DR24			SAMPLING EQ/METHOD: Wireline core barrel sampling						
GROUND ELEVATION: 7516.1'			TOTAL DEPTH = 1942' bgs						
DRILLER: Larry Thoren			GEOLOGY P.I.: Rick Warren			SITE GEOLOGIST: Mark Everett			
Depth (ft)	Elevation (ft)	Core Run # (amt.-recov./amt. attemp.)	Core Run	Cuttings Collected	Hydrologic Property (Physprop) and Geochemical (Geochem) Samples (CACV-9x-xxxx)	Moisture/Matric Pot. R25-depth (ft)	Lithology	Graphic Log	Lithologic Symbol



LOS ALAMOS NATIONAL LABORATORY
REGIONAL HYDROGEOLOGIC CHARACTERIZATION PROJECT
ENVIRONMENTAL RESTORATION, GROUNDWATER FOCUS AREA
BOREHOLE LOG

BOREHOLE ID: R-25				TA/OU: TA-16		Page 10 of 20			
DRILLING COMPANY: Tonto Drilling Co.				START DATE: July 22, 1998/0930			END DATE: February 24, 1999		
DRILLING EQ/METHOD: Foremost DR24				SAMPLING EQ/METHOD: Wireline core barrel sampling					
GROUND ELEVATION: 7516.1'				TOTAL DEPTH = 1942' bgs					
DRILLER: Larry Thoren		GEOLOGY P.I.: Rick Warren			SITE GEOLOGIST: Mark Everett				
Depth (ft)	Elevation (ft)	Core Run # (amt.-recov./amt. attemp.)	Core Run	Cuttings Collected	Hydrologic Property (Physprop) and Geochemical (Geochem) Samples (CACV-9x-xxxx)	Moisture/Matric Pot. R25-depth (ft)	Lithology	Graphic Log	Lithologic Symbol
885	6630						PUYE FORMATION: (850.5-1132') Medium dark gray (N4). Cobbles and boulders derived primarily from the upper dacite of Pajarito Mountain. Minor amounts of sand. Some clay present within the depth intervals 851-853', 901-903', 992-997', 1012-1016', and 1022-1026'. Note: Reddish brown silty soil horizon from 850.5-852' (from video log). Video log shows 852-863' to be a clast-supported boulder conglomerate.		Tpf
890	6625								
895	6620								
900	6615								
905	6610								
910	6605								
915	6600								
920	6595								
925	6590								
930	6585								
935	6580								
940	6575								
945	6570								
950	6565								
955	6560								
960	6555								
965	6550								
970	6545								
975	6540								
980	6535								

LOS ALAMOS NATIONAL LABORATORY
REGIONAL HYDROGEOLOGIC CHARACTERIZATION PROJECT
ENVIRONMENTAL RESTORATION, GrOUNDWATER FOCUS AREA
BOREHOLE LOG

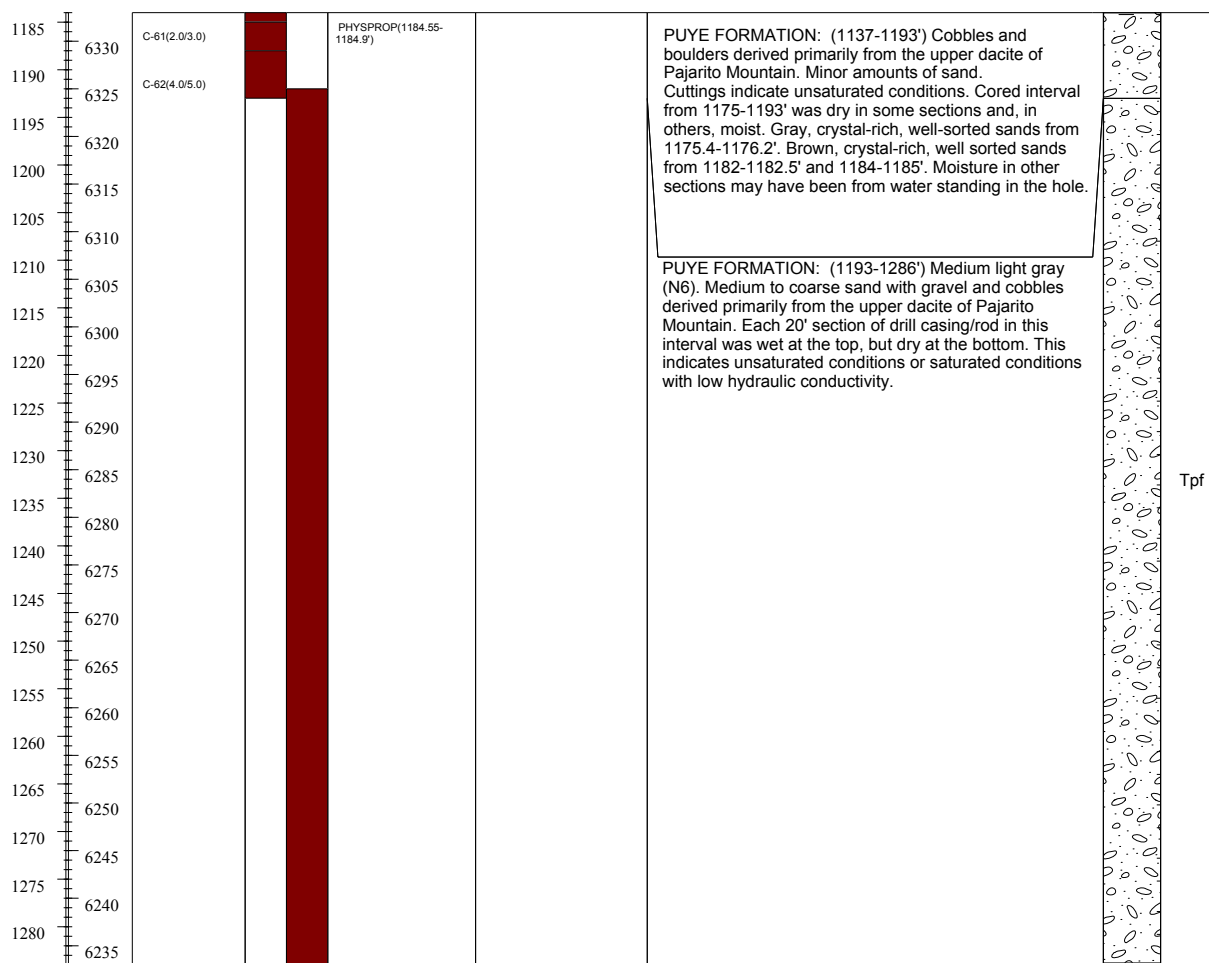
BOREHOLE ID: R-25				TA/OU: TA-16		Page 11 of 20			
DRILLING COMPANY: Tonto Drilling Co.				START DATE: July 22, 1998/0930		END DATE: February 24, 1999			
DRILLING EQ/METHOD: Foremost DR24				SAMPLING EQ/METHOD: Wireline core barrel sampling					
GROUND ELEVATION: 7516.1'				TOTAL DEPTH = 1942' bgs					
DRILLER: Larry Thoren		GEOLOGY P.I.: Rick Warren		SITE GEOLOGIST: Mark Everett					
Depth (ft)	Elevation (ft)	Core Run # (amt. - recov./amt. attemp.)	Core Run	Cuttings Collected	Hydrologic Property (Physprop) and Geochemical (Geochem) Samples (CACV-9x-xxxx)	Moisture/Matric Pot. R25-depth (ft)	Lithology	Graphic Log	Lithologic Symbol
985 990 995 1000 1005 1010 1015 1020 1025 1030 1035 1040 1045 1050 1055 1060 1065 1070 1075 1080	6530 6525 6520 6515 6510 6505 6500 6495 6490 6485 6480 6475 6470 6465 6460 6455 6450 6445 6440 6435						PUYE FORMATION: (850.5-1132') Medium dark gray (N4). Cobbles and boulders derived primarily from the upper dacite of Pajarito Mountain. Minor amounts of sand. Some clay present within the depth intervals 851-853', 901-903', 992-997', 1012-1016', and 1022-1026'. Note: Reddish brown silty soil horizon from 850.5-852' (from video log). Video log shows 852-863' to be a clast-supported boulder conglomerate.		Tpf

LOS ALAMOS NATIONAL LABORATORY
REGIONAL HYDROGEOLOGIC CHARACTERIZATION PROJECT
ENVIRONMENTAL RESTORATION, GROUNDWATER FOCUS AREA
BOREHOLE LOG

BOREHOLE ID: R-25			TA/OU: TA-16			Page 12 of 20			
DRILLING COMPANY: Tonto Drilling Co.			START DATE: July 22, 1998/0930			END DATE: February 24, 1999			
DRILLING EQ/METHOD: Foremost DR24			SAMPLING EQ/METHOD: Wireline core barrel sampling						
GROUND ELEVATION: 7516.1'			TOTAL DEPTH = 1942' bgs						
DRILLER: Larry Thoren			GEOLOGY P.I.: Rick Warren			SITE GEOLOGIST: Mark Everett			
Depth (ft)	Elevation (ft)	Core Run # (amt.-recov./amt. attemp.)	Core Run	Cuttings Collected	Hydrologic Property (Physprop) and Geochemical (Geochem) Samples (CACV-9x-xxxx)	Moisture/Matric Pot. R25-depth (ft)	Lithology	Graphic Log	Lithologic Symbol
1085	6430						PUYE FORMATION: (850.5-1132') Medium dark gray (N4). Cobbles and boulders derived primarily from the upper dacite of Pajarito Mountain. Minor amounts of sand. Some clay present within the depth intervals 851-853', 901-903', 992-997', 1012-1016', and 1022-1026'. Note: Reddish brown silty soil horizon from 850.5-852' (from video log). Video log shows 852-863' to be a clast-supported boulder conglomerate.		
1090	6425								
1095	6420								
1100	6415								
1105	6410								
1110	6405								
1115	6400								
1120	6395								
1125	6390								
1130	6385								
1135	6380				GEOCHEM(1132-1137')		PUYE FORMATION: (1132-1137') Medium light gray (N6). Relatively high fraction of fine-grained sand and silt mixed with gravel and cobbles derived primarily from the upper dacite of Pajarito Mountain. Cuttings indicate unsaturated conditions.		Tpf
1140	6375						PUYE FORMATION: (1137-1193') Cobbles and boulders derived primarily from the upper dacite of Pajarito Mountain. Minor amounts of sand. Cuttings indicate unsaturated conditions. Cored interval from 1175-1193' was dry in some sections and, in others, moist. Gray, crystal-rich, well-sorted sands from 1175.4-1176.2'. Brown, crystal-rich, well sorted sands from 1182-1182.5' and 1184-1185'. Moisture in other sections may have been from water standing in the hole.		
1145	6370								
1150	6365								
1155	6360	C-56(5.0/5.0)			PHYSPROP(1158.6-1159.6')				
1160	6355	C-57(1.4/3.5)							
1165	6350								
1170	6345	C-58(1.2/5.0)							
1175	6340								
1180	6335	C-60(1.0/1.0)							

LOS ALAMOS NATIONAL LABORATORY
REGIONAL HYDROGEOLOGIC CHARACTERIZATION PROJECT
ENVIRONMENTAL RESTORATION, GROUNDWATER FOCUS AREA
BOREHOLE LOG

BOREHOLE ID: R-25			TA/OU: TA-16			Page 13 of 20			
DRILLING COMPANY: Tonto Drilling Co.			START DATE: July 22, 1998/0930			END DATE: February 24, 1999			
DRILLING EQ/METHOD: Foremost DR24			SAMPLING EQ/METHOD: Wireline core barrel sampling						
GROUND ELEVATION: 7516.1'			TOTAL DEPTH = 1942' bgs						
DRILLER: Larry Thoren			GEOLOGY P.I.: Rick Warren			SITE GEOLOGIST: Mark Everett			
Depth (ft)	Elevation (ft)	Core Run # (amt.-recov./amt. attemp.)	Core Run	Cuttings Collected	Hydrologic Property (Physprop) and Geochemical (Geochem) Samples (CACV-9x-xxxx)	Moisture/Matric Pot. R25-depth (ft)	Lithology	Graphic Log	Lithologic Symbol



LOS ALAMOS NATIONAL LABORATORY
REGIONAL HYDROGEOLOGIC CHARACTERIZATION PROJECT
ENVIRONMENTAL RESTORATION, GROUNDWATER FOCUS AREA
BOREHOLE LOG

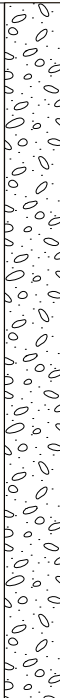



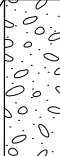

BOREHOLE ID: R-25				TA/OU: TA-16				Page 14 of 20			
DRILLING COMPANY: Tonto Drilling Co.				START DATE: July 22, 1998/0930				END DATE: February 24, 1999			
DRILLING EQ/METHOD: Foremost DR24				SAMPLING EQ/METHOD: Wireline core barrel sampling							
GROUND ELEVATION: 7516.1'				TOTAL DEPTH = 1942' bgs							
DRILLER: Larry Thoren				GEOLOGY P.I.: Rick Warren				SITE GEOLOGIST: Mark Everett			
Depth (ft)	Elevation (ft)	Core Run # (amt.-recov./amt. attemp.)	Core Run	Cuttings Collected	Hydrologic Property (Physprop) and Geo-chemical (Geochem) Samples (CACV-9x-xxxx)	Moisture/Matric Pot. R25-depth (ft)	Lithology	Graphic Log	Lithologic Symbol		

1285	6230						PUYE FORMATION: (1193-1286') Medium light gray (N6). Medium to coarse sand with gravel and cobbles derived primarily from the upper dacite of Pajarito Mountain. Each 20' section of drill casing/rod in this interval was wet at the top, but dry at the bottom. This indicates unsaturated conditions or saturated conditions with low hydraulic conductivity.		
1290	6225						PUYE FORMATION: (1286-1387') Medium gray (N5). Medium to coarse sand with minor gravel derived primarily from the upper dacite of Pajarito Mountain. Every 20' section of drill casing/rod drilled through this interval and below was uniformly wet, indicating saturated conditions.		
1295	6220								
1300	6215								
1305	6210								
1310	6205								
1315	6200								
1320	6195								
1325	6190								
1330	6185								
1335	6180								
1340	6175								
1345	6170								
1350	6165								
1355	6160								
1360	6155								
1365	6150								
1370	6145								
1375	6140								
1380	6135								

LOS ALAMOS NATIONAL LABORATORY
REGIONAL HYDROGEOLOGIC CHARACTERIZATION PROJECT
ENVIRONMENTAL RESTORATION, GROUNDWATER FOCUS AREA
BOREHOLE LOG

BOREHOLE ID: R-25				TA/OU: TA-16		Page 15 of 20			
DRILLING COMPANY: Tonto Drilling Co.				START DATE: July 22, 1998/0930		END DATE: February 24, 1999			
DRILLING EQ/METHOD: Foremost DR24				SAMPLING EQ/METHOD: Wireline core barrel sampling					
GROUND ELEVATION: 7516.1'				TOTAL DEPTH = 1942' bgs					
DRILLER: Larry Thoren		GEOLOGY P.I.: Rick Warren		SITE GEOLOGIST: Mark Everett					
Depth (ft)	Elevation (ft)	Core Run # (amt.- recov./amt. attemp.)	Core Run	Cuttings Collected	Hydrologic Property (Physprop) and Geo- chemical (Geochem) Samples (CACV-9x-xxxx)	Moisture/Matric Pot. R25-depth (ft)	Lithology	Graphic Log	Lithologic Symbol
1385	6130						PUYE FORMATION: (1286-1387") Medium gray (N5). Medium to coarse sand with minor gravel derived primarily from the upper dacite of Pajarito Mountain. Every 20' section of drill casing/rod drilled through this interval and below was uniformly wet, indicating saturated conditions.		
1390	6125						PUYE FORMATION: (1387-1397") Medium gray (N5). Medium to coarse sand.		
1395	6120						PUYE FORMATION: (1397-1557") Medium dark gray (N4). Coarse gravel and sand derived primarily from the upper dacite of Pajarito Mountain. Very fine sand at 1507' was probably derived from a single vitric boulder, either mechanically weathered in place or disaggregated by drilling. Note: Video log shows 1467-1472' is primarily clast-supported boulder conglomerate. Boulders present up to 2' in diameter.		
1400	6115								
1405	6110								
1410	6105								
1415	6100								
1420	6095								
1425	6090								
1430	6085								
1435	6080								
1440	6075								
1445	6070								
1450	6065								
1455	6060								
1460	6055								
1465	6050								
1470	6045								
1475	6040								
1480	6035								

LOS ALAMOS NATIONAL LABORATORY
REGIONAL HYDROGEOLOGIC CHARACTERIZATION PROJECT
ENVIRONMENTAL RESTORATION, GROUNDWATER FOCUS AREA
BOREHOLE LOG

BOREHOLE ID: R-25			TA/OU: TA-16			Page 16 of 20			
DRILLING COMPANY: Tonto Drilling Co.			START DATE: July 22, 1998/0930			END DATE: February 24, 1999			
DRILLING EQ/METHOD: Foremost DR24			SAMPLING EQ/METHOD: Wireline core barrel sampling						
GROUND ELEVATION: 7516.1'			TOTAL DEPTH = 1942' bgs						
DRILLER: Larry Thoren			GEOLOGY P.I.: Rick Warren			SITE GEOLOGIST: Mark Everett			
Depth (ft)	Elevation (ft)	Core Run # (amt. - recov./amt. attemp.)	Core Run	Cuttings Collected	Hydrologic Property (Physprop) and Geochemical (Geochem) Samples (CACV-9x-xxxx)	Moisture/Matric Pot. R25-depth (ft)	Lithology	Graphic Log	Lithologic Symbol
1485	6030						PUYE FORMATION: (1397-1557") Medium dark gray (N4). Coarse gravel and sand derived primarily from the upper dacite of Pajarito Mountain. Very fine sand at 1507' was probably derived from a single vitric boulder, either mechanically weathered in place or disaggregated by drilling. Note: Video log shows 1467-1472' is primarily clast-supported boulder conglomerate. Boulders present up to 2' in diameter.		
1490	6025								
1495	6020								
1500	6015								
1505	6010								
1510	6005								
1515	6000								
1520	5995								
1525	5990								
1530	5985								
1535	5980								
1540	5975								
1545	5970								
1550	5965								
1555	5960								
1560	5955						PUYE FORMATION: (1557-1567") Medium light gray (N6). Predominantly very fine to medium sand with minor coarse sand. Moderate amounts of black glassy grains in >60 mesh fraction.		
1565	5950								
1570	5945								
1575	5940						PUYE FORMATION: (1567-1627") Medium light gray (N6). Medium sand to gravel derived primarily from the upper dacite of Pajarito Mountain.		
1580	5935								

LOS ALAMOS NATIONAL LABORATORY
REGIONAL HYDROGEOLOGIC CHARACTERIZATION PROJECT
ENVIRONMENTAL RESTORATION, GROUNDWATER FOCUS AREA
BOREHOLE LOG

BOREHOLE ID: R-25			TA/OU: TA-16			Page 17 of 20			
DRILLING COMPANY: Tonto Drilling Co.			START DATE: July 22, 1998/0930			END DATE: February 24, 1999			
DRILLING EQ/METHOD: Foremost DR24			SAMPLING EQ/METHOD: Wireline core barrel sampling						
GROUND ELEVATION: 7516.1'			TOTAL DEPTH = 1942' bgs						
DRILLER: Larry Thoren			GEOLOGY P.I.: Rick Warren			SITE GEOLOGIST: Mark Everett			
Depth (ft)	Elevation (ft)	Core Run # (amt.- recov./amt. attemp.)	Core Run	Cuttings Collected	Hydrologic Property (Physprop) and Geo- chemical (Geochem) Samples (CACV-9x-xxxx)	Moisture/Matric Pot. R25-depth (ft)	Lithology	Graphic Log	Lithologic Symbol

1585	5930						PUYE FORMATION: (1567-1627') Medium light gray (N6). Medium sand to gravel derived primarily from the upper dacite of Pajarito Mountain.		
1590	5925								
1595	5920								
1600	5915								
1605	5910								
1610	5905								
1615	5900								
1620	5895								
1625	5890						PUYE FORMATION: (1627-1632') Light brownish gray (5YR 6/1). Very fine sand (<60 mesh).		
1630	5885								
1635	5880						PUYE FORMATION: (1632-1657') Light brownish gray (5YR 6/1). Medium sand to gravel. Derived primarily from the upper dacite of Pajarito Mountain.		
1640	5875								
1645	5870								
1650	5865								
1655	5860								
1660	5855						PUYE FORMATION: (1657-1870') Light brownish gray (5YR 6/1). Medium sand to coarse gravel. Derived primarily from the rhyodacite of Rendija Canyon.		
1665	5850								
1670	5845								
1675	5840								
1680	5835								

Tpf

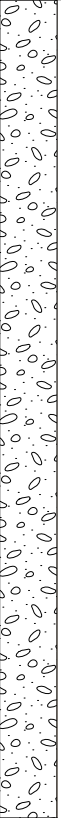

LOS ALAMOS NATIONAL LABORATORY
REGIONAL HYDROGEOLOGIC CHARACTERIZATION PROJECT
ENVIRONMENTAL RESTORATION, GROUNDWATER FOCUS AREA
BOREHOLE LOG

BOREHOLE ID: R-25				TA/OU: TA-16				Page 18 of 20			
DRILLING COMPANY: Tonto Drilling Co.				START DATE: July 22, 1998/0930				END DATE: February 24, 1999			
DRILLING EQ/METHOD: Foremost DR24				SAMPLING EQ/METHOD: Wireline core barrel sampling							
GROUND ELEVATION: 7516.1'				TOTAL DEPTH = 1942' bgs							
DRILLER: Larry Thoren				GEOLOGY P.I.: Rick Warren				SITE GEOLOGIST: Mark Everett			
Depth (ft)	Elevation (ft)	Core Run # (amt.-recov./amt. attemp.)	Core Run	Cuttings Collected	Hydrologic Property (Physprop) and Geochemical (Geochem) Samples (CAcV-9x-xxxx)	Moisture/Matric Pot. R25-depth (ft)	Lithology			Graphic Log	Lithologic Symbol

1685	5830						PUYE FORMATION: (1657-1870') Light brownish gray (5YR 6/1). Medium sand to coarse gravel. Derived primarily from the rhyodacite of Rendija Canyon.		
1690	5825								
1695	5820								
1700	5815								
1705	5810								
1710	5805								
1715	5800								
1720	5795								
1725	5790								
1730	5785								
1735	5780								
1740	5775								
1745	5770								
1750	5765								
1755	5760								
1760	5755								
1765	5750								
1770	5745								
1775	5740								
1780	5735								

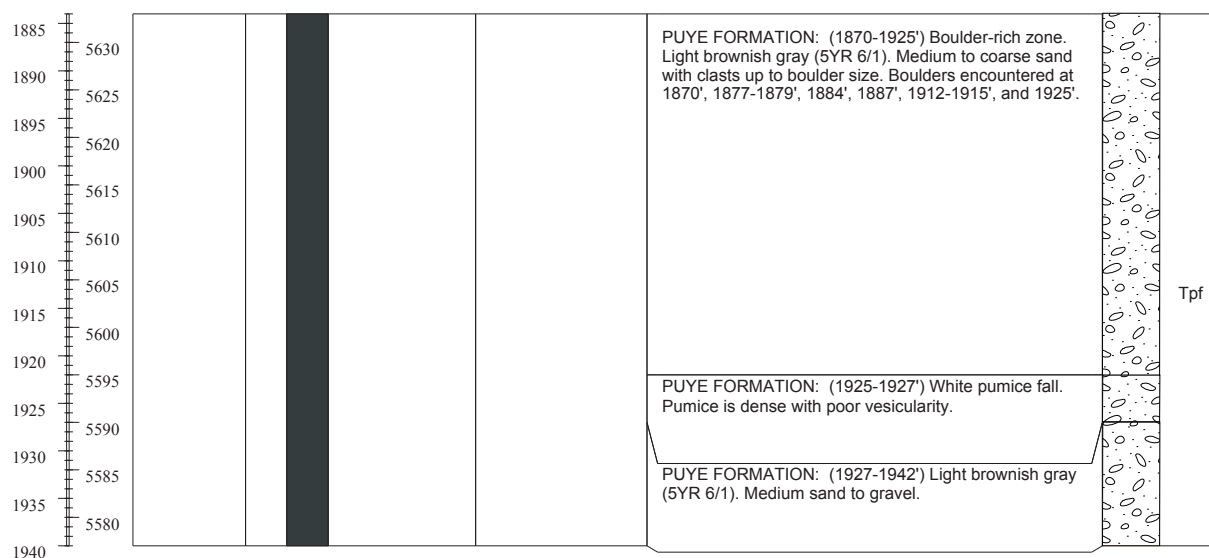
LOS ALAMOS NATIONAL LABORATORY
REGIONAL HYDROGEOLOGIC CHARACTERIZATION PROJECT
ENVIRONMENTAL RESTORATION, GROUNDWATER FOCUS AREA
BOREHOLE LOG

BOREHOLE ID: R-25				TA/OU: TA-16				Page 19 of 20			
DRILLING COMPANY: Tonto Drilling Co.				START DATE: July 22, 1998/0930				END DATE: February 24, 1999			
DRILLING EQ/METHOD: Foremost DR24				SAMPLING EQ/METHOD: Wireline core barrel sampling							
GROUND ELEVATION: 7516.1'				TOTAL DEPTH = 1942' bgs							
DRILLER: Larry Thoren				GEOLOGY P.I.: Rick Warren				SITE GEOLOGIST: Mark Everett			
Depth (ft)	Elevation (ft)	Core Run # (amt.-recov./amt. attemp.)	Core Run	Cuttings Collected	Hydrologic Property (Physprop) and Geochemical (Geochem) Samples (CACV-9x-xxxx)	Moisture/Matric Pot. R25-depth (ft)	Lithology	Graphic Log	Lithologic Symbol		

1785	5730						PUYE FORMATION: (1657-1870') Light brownish gray (5YR 6/1). Medium sand to coarse gravel. Derived primarily from the rhyodacite of Rendija Canyon.		Tpf
1790	5725								
1795	5720								
1800	5715								
1805	5710								
1810	5705								
1815	5700								
1820	5695								
1825	5690								
1830	5685								
1835	5680								
1840	5675								
1845	5670								
1850	5665								
1855	5660								
1860	5655						PUYE FORMATION: (1870-1925') Boulder-rich zone. Light brownish gray (5YR 6/1). Medium to coarse sand with clasts up to boulder size. Boulders encountered at 1870', 1877-1879', 1884', 1887', 1912-1915', and 1925'.		
1865	5650								
1870	5645								
1875	5640								
1880	5635								

LOS ALAMOS NATIONAL LABORATORY
REGIONAL HYDROGEOLOGIC CHARACTERIZATION PROJECT
ENVIRONMENTAL RESTORATION, GROUNDWATER FOCUS AREA
BOREHOLE LOG

BOREHOLE ID: R-25				TA/OU: TA-16		Page 20 of 20			
DRILLING COMPANY: Tonto Drilling Co.				START DATE: July 22, 1998/0930		END DATE: February 24, 1999			
DRILLING EQ/METHOD: Foremost DR24				SAMPLING EQ/METHOD: Wireline core barrel sampling					
GROUND ELEVATION: 7516.1'				TOTAL DEPTH = 1942' bgs					
DRILLER: Larry Thoren		GEOLOGY P.I.: Rick Warren		SITE GEOLOGIST: Mark Everett					
Depth (ft)	Elevation (ft)	Core Run # (amt.-recov./amt. attemp.)	Core Run	Cuttings Collected	Hydrologic Property (Physprop) and Geochemical (Geochem) Samples (CACV-9x-xxxx)	Moisture/Matric Pot. R25-depth (ft)	Lithology	Graphic Log	Lithologic Symbol



Appendix D

Descriptions of Geologic Samples

Sample No. ^a	Description
R25-5D cuttings	This polished thin section consists of a single, large fragment of cuttings that is vitric nonwelded tuff. Pyroclasts include common fine tube pumice to 9 mm and colorless shards. Common felsic phenocrysts are primarily sanidine, many moderately resorbed, with minor anorthoclase, plagioclase, and a single large quartz graphically intergrown with sanidine. Scarce to common mafics are mostly clinopyroxene and lesser orthopyroxene. Clinopyroxene ranges from very pale green, Mg-rich to moderately dark green, Fe-rich. Scarce to rare small lithics are argillic sediments.
R25-93.2 core	This polished thin section of core is microgranophyric, well indurated, partially welded tuff with common granospherulitic pumice to 4 mm containing moderate vapor-phase crystallization. Common felsic phenocrysts are primarily sanidine, some moderately resorbed, and quartz. Quartz is about 20% of the felsic phenocrysts. Scarce to common mafics are light green, moderately Mg-rich clinopyroxene and orthopyroxene. Rare lithics are argillite.
R25-144D cuttings	This polished thin section consists of 30 fragments of microgranophyric, vapor-phase, moderately welded tuff with common granospherulitic pumice. Common felsic phenocrysts are primarily sanidine and quartz. Quartz is about 15% of the felsic phenocrysts. Scarce to common mafics of pyroxene are mostly pseudomorphs, except for several very strongly altered grains of clinopyroxene. A single large grain of perrierite/chevkinite was observed. Scarce to rare lithics include argillite (probably Santa Fe Group) and microgranophyric and minor fine granophyric sanidine-bearing lava.
R25-165.5D cuttings	This polished thin section consists of 20 fragments of microgranophyric, vapor-phase, moderately welded tuff, close to partially welded tuff, with common granospherulitic pumice. Common felsic phenocrysts are primarily sanidine and quartz, and phenocrysts include a single small grain of altered plagioclase. Quartz is about 35% of the felsic phenocrysts. Scarce mafics are strongly altered clinopyroxene and orthopyroxene. A single large grain of perrierite/chevkinite was observed. A single large lithic observed is microgranophyric and pilotaxitic dacite with common altered plagioclase phenocrysts.
R25-188D cuttings	This polished thin section consists of 32 fragments, mostly microgranophyric, vapor phase partially welded tuff with common microgranophyric and lesser granospherulitic pumice. Common felsic phenocrysts are primarily sanidine and quartz, and phenocrysts include two small grains of plagioclase, one altered. Quartz is about 20% of the felsic phenocrysts. Scarce mafics are strongly altered clinopyroxene and orthopyroxene and a single grain of hornblende. A single large grain of perrierite/chevkinite was observed. Tiny lithics are rare. Two granospherulitic fragments with common felsic phenocrysts, primarily sanidine and quartz, represent large pumices; only a small fragment of a similar granospherulitic pumice was observed within the other 30 fragments.
R25-231.35 core	This polished thin section of core is microgranophyric moderately welded tuff, near densely welded, with minor vapor-phase alteration and highly compacted pumice with axiolitic borders, typically 2.0 mm in diameter and 0.2 mm thick. Interiors of the largest pumices, to 6 mm, are spherulitic and granophyric. Abundant felsic phenocrysts are primarily sanidine and quartz. Scarce to common mafics are mostly pseudomorphs pyroxene, but several small grains of hornblende and one small, shreddy biotite were observed. Quartz is about 40% of the felsic phenocrysts. Scarce to rare lithics are entirely microgranophyric and pilotaxitic dacitic lava with plagioclase phenocrysts, probably from the Tschicoma Formation.

Sample No. ^a	Description
R25-264D cuttings	This polished thin section consists of 16 fragments, mostly microgranophyric moderately welded tuff with minor vapor-phase alteration and common granospherulitic pumice to 7 mm. Common felsic phenocrysts are primarily sanidine and quartz, with one large plagioclase observed within a large pumice. Quartz is about 30% of the felsic phenocrysts. Mafics are scarce to common pyroxene pseudomorphs and minor, small hornblende. About half of the pyroxene occurs as a single glomerocryst within pumice. A single lithic occurs within tuff of pilotaxitic dacite to andesite lava with scarce plagioclase phenocrysts and scarce, small pseudomorphs of hornblende or orthopyroxene. One entire fragment is microgranophyric and pilotaxitic dacite to andesite lava with scarce to common small plagioclase phenocrysts and common to abundant small hornblende, certainly representing a lithic similar to the single lithic found within tuff.
R25-318D cuttings	This polished thin section consists of 12 fragments of microgranophyric, vapor-phase, moderately welded tuff with common granospherulitic pumice to 8 mm. Common felsic phenocrysts are primarily sanidine and quartz; minor plagioclase also occurs primarily as a very strongly resorbed, 2-mm phenocryst within a large, quartz-bearing pumice, and within several mafic pumices. Quartz is about 30% of the felsic phenocrysts. These mafic pumices, to 6 mm, have scarce to common plagioclase phenocrysts, and abundant groundmass plagioclase laths and hornblende. Mafics within the tuff also include scarce to common pyroxene, mostly pseudomorphic except for several very strongly altered grains of clinopyroxene. A single lithic, an argillite, was observed.
R25-352.4 core	This polished thin section of core is microgranophyric, vapor-phase nonwelded tuff with pumice to 3 mm that is filled with vapor-phase minerals, primarily tridymite. Common to abundant felsic phenocrysts are primarily sanidine and quartz, both together with rare plagioclase. Quartz is about 35% of the felsic phenocrysts. Scarce mafics are mostly moderately to entirely altered pyroxene, with some relict clinopyroxene, and include a single grain of iddingsite after olivine. One large lithic, which covers 15% of the section, is microgranophyric and pilotaxitic dacite to andesite lava with common plagioclase phenocrysts and orthopyroxene, and completely lacking clinopyroxene.
R25-373.5 core	This polished thin section consists of disaggregated fragments of core that are mostly vitric pumices with the largest length >19 mm. Common felsic phenocrysts are equally abundant sanidine and quartz. Scarce to rare clinopyroxene is medium green, moderately Fe-rich. Scarce to rare lithics include spherulitic, vapor-phase lava and microgranophyric strongly welded tuff, both with a large sanidine phenocryst.
R25-428D pumice separate from cuttings	This polished thin section exhibits 22 fragments, mostly individual vitric pumice with colorless glass, but two fragments also include the host vitric pumiceous sandy argillite. All fragments have scarce felsic phenocrysts of sanidine, plagioclase, and a single, large quartz grain. Hornblende is scarce, and no lithics were observed. Smectite partly to completely fills vesicles, and a second generation of smectite coats surfaces of pumices.
R25-456 core	This polished thin section of core is a lithic fragment of pilotaxitic and microgranophyric dacite to andesite lava with minor vapor-phase crystallization. Plagioclase phenocrysts are common, and mafics are abundant blackened hornblende and common orthopyroxene.
R25-484D pumice separate from cuttings	This polished thin section exhibits 32 fragments, mostly individual vitric pumice with colorless glass, but two fragments are the host vitric pumiceous sandy argillite and one fragment is a lithic of vesicular microgranophyric and pilotaxitic dacite of the Tschicoma Formation with common phenocrysts of plagioclase and scarce microphenocrysts of orthopyroxene. Within pumice, scarce felsic phenocrysts are sanidine, with much lesser quartz and plagioclase, and scarce mafics are clinopyroxene and orthopyroxene. Scarce smectite in two generations partly to completely fills vesicles. The rock matrix has similar proportions of felsic minerals as pumice, but felsics are common, generally tiny broken fragments. Within the two fragments of vitric pumiceous sandy argillite, no mafics and a single, tiny argillite lithic were observed.

Sample No. ^a	Description
R25-568 core	This polished thin section consists of disaggregated fragments of core that are vitric nonwelded tuff with pale brown shards and two large pumices to 6 mm that dominate. Common felsic phenocrysts are subequal sanidine and quartz. Scarce mafics are primarily pale green, moderately Mg-rich clinopyroxene, but one shredded biotite is present. Scarce lithics are entirely volcanic, and include pilotaxitic dacite to andesite lava. One large pale brown hydroclastic shard contains plagioclase phenocrysts, common groundmass plagioclase laths, and a single groundmass orthopyroxene.
R25-798DP pumice separate from cuttings	This polished thin section consists of 34 individual vitric pumice fragments. Scarce felsic phenocrysts are primarily sanidine and quartz; also included is minor plagioclase. Quartz is about 35% of the felsic phenocrysts. One grain of light green, moderately Mg-rich clinopyroxene and one large grain of perrierite/chevkinite were observed.
R25-846.1P10 pumice separate from cuttings	This polished thin section exhibits 20 individual vitric pumice fragments with colorless glass. One pumice is thick-walled, and the others are fine tube. Most vesicles are filled with smectite. Scarce to common felsic phenocrysts are equally abundant sanidine and quartz; also included is rare plagioclase. One large, dark green, Fe-rich clinopyroxene occurs. One small lithic of sandy argillite occurs at the edge of a pumice, and the largest single fragment in the section is quartzose argillic sandstone.
R25-864D10 cuttings	This polished thin section consists of 21 separated lithic fragments, mostly pilotaxitic and microgranophyric dacite lava with common plagioclase phenocrysts and abundant pyroxene with orthopyroxene strongly dominant over clinopyroxene. Two fragments with similar primary mineralogy are microlite-charged vitric with colorless glass, and one is granospherulitic to (minor) pilotaxitic. These 20 fragments were derived from the upper dacite of Pajarito Mountain. One fragment of pilotaxitic and microgranophyric rhyodacite lava, derived from the rhyodacite of Rendija Canyon, has common, large phenocrysts of plagioclase, some with extreme resorption, and quartz and biotite.
R25-1082D10 cuttings	This polished thin section consists of 20 separated lithic fragments, mostly pilotaxitic and microgranophyric dacite lava with minor vapor-phase alteration and with common plagioclase phenocrysts and abundant pyroxene that is orthopyroxene strongly dominant over clinopyroxene. Two grains of hornblende and one large biotite each occur with separate plagioclase glomerocrysts. Two fragments with similar primary mineralogy are vitric with pale brown glass, two are microlite-charged vitric with colorless glass, two are fine to medium grained granophyric, and one is argillic. All fragments were derived from the upper dacite of Pajarito Mountain.
R25-1182.3 core	This polished thin section of core is sandy argillite with 50% lithics, represented almost entirely by a single lithic. Sand consists mostly of angular, very abundant felsics, mostly plagioclase and quartz, but also including sanidine; the largest grains are quartz. Several moderate-sized biotite grains occur within the matrix, as well as smaller hornblende. The large lithic is partly vitric, partly granospherulitic and pilotaxitic lava with scarce to rare plagioclase phenocrysts, many strongly resorbed, and common orthopyroxene and clinopyroxene. One large hornblende is associated with plagioclase. This lithic might represent latite of SHB1. The three next largest lithics are all pilotaxitic and microgranophyric dacite lava with common plagioclase phenocrysts and scarce to common orthopyroxene, probably derived from the upper dacite of Pajarito Mountain.
R25-1302D10 cuttings	This polished thin section consists of 20 separated lithic fragments, mostly pilotaxitic and microgranophyric dacite lava with common plagioclase phenocrysts and abundant pyroxene with orthopyroxene strongly dominant over clinopyroxene. Three grains of strongly blackened hornblende occur, as well as one biotite with strongly resorbed plagioclase. Two fragments with similar primary mineralogy are mostly or entirely vitric with microlite-charged colorless glass. All fragments were derived from the upper dacite of Pajarito Mountain.

Sample No. ^a	Description
R25-1507D cuttings	This polished thin section consists of sand-sized fragments of dacite lava, mostly vitric but many microgranophyric, all with very abundant plagioclase phenocrysts, commonly pyroxene with orthopyroxene strongly dominant over clinopyroxene, and much lesser biotite and hornblende. All fragments were derived from the upper dacite of Pajarito Mountain. The derivation of such relatively fine material from a single source rock indicates that this section probably represents a single boulder, either mechanically weathered in place or disaggregated by drilling.
R25-1517D10 cuttings	This polished thin section consists of 20 separated lithic fragments. Seventeen of these are dacite lava with common plagioclase phenocrysts and common to abundant pyroxene with orthopyroxene strongly dominant over clinopyroxene; ten such fragments are pilotaxitic and microgranophyric, and seven are vitric with microlite-charged colorless glass. These fragments were derived from the upper dacite of Pajarito Mountain. The remaining three fragments are pilotaxitic and microgranophyric dacite lava with common plagioclase phenocrysts and hornblende and scarce orthopyroxene, possibly derived from the upper dacite of Cerro Grande.
R25-1587D10 cuttings	This polished thin section consists of 20 separated lithic fragments, all dacite lava with common plagioclase phenocrysts and common to abundant pyroxene with orthopyroxene strongly dominant over clinopyroxene, and including two blackened hornblende grains. About two-thirds of the fragments are pilotaxitic and microgranophyric; the remainder are vitric with microlite-charged colorless glass. All fragments were derived from the upper dacite of Pajarito Mountain.
R25-1647D10 cuttings	This polished thin section consists of 21 separated lithic fragments, all pilotaxitic and microgranophyric dacite lava. Most fragments were derived from the upper dacite of Pajarito Mountain and have common plagioclase phenocrysts and common to abundant pyroxene with orthopyroxene strongly dominant over clinopyroxene. One fragment, possibly derived from the upper dacite of Cerro Grande, has common plagioclase phenocrysts and common to abundant hornblende and orthopyroxene, and another has scarce to rare plagioclase phenocrysts and scarce to rare hornblende.
R25-1682D10 cuttings	This polished thin section consists of 21 separated lithic fragments, all dacite lava from three units. Nine fragments contain scarce to common plagioclase phenocrysts and pyroxene that has subequal orthopyroxene and clinopyroxene; five of these are pilotaxitic and microgranophyric and four are vitric with microlite-charged colorless glass. These were probably derived from the lower dacite of Pajarito Mountain. Eight fragments contain phenocrysts of quartz and plagioclase, some with extreme resorption, and biotite and some clinopyroxene; five of these are pilotaxitic and microgranophyric, one with minor vapor-phase alteration; one fragment is pilotaxitic and granospherulitic; and two are vitric with microlite-charged colorless glass. These were derived from the rhyodacite of Rendija Canyon. Four fragments contain scarce to common phenocrysts of plagioclase and mafics that are dominated by hornblende over clinopyroxene and orthopyroxene; two of these are pilotaxitic and microgranophyric and two are vitric with microlite-charged colorless glass. These may have been derived from the upper dacite of Cerro Grande.
R25-1802D10 cuttings	This polished thin section consists of 21 separated lithic fragments, mostly pilotaxitic and microgranophyric rhyodacite lava with phenocrysts of quartz and plagioclase, some with extreme resorption, and biotite, clinopyroxene, and a single large grain of sphene. Two such fragments have minor vapor-phase crystallization. These dominant fragments were derived from the rhyodacite of Rendija Canyon. Three fragments are pilotaxitic and microgranophyric dacite lava with scarce plagioclase phenocrysts and pyroxene that includes both clinopyroxene and orthopyroxene, probably representing the lower dacite of Pajarito Mountain. One fragment of dacite lava has scarce phenocrysts of plagioclase and abundant mafics, mostly small hornblende and much lesser orthopyroxene, possibly representing the upper dacite of Cerro Grande.
R25-1927DP pumice separate from cuttings	This polished thin section consists of 45 individual somewhat spherulitic pumice fragments that are uniform in primary mineralogy and alteration. Common felsic phenocrysts are plagioclase, quartz, and sanidine. Common biotite is entirely altered to smectite.

Sample No. ^a	Description
R25-1937D10 cuttings	This polished thin section consists of 19 separated lithic fragments. Most are silicic lava with scarce to common phenocrysts of quartz and plagioclase, some with extreme resorption, and biotite. Eleven such fragments are pilotaxitic and microgranophyric, one is spherulitic, and one is vitric with microlite-charged colorless glass. Four fragments are pilotaxitic and microgranophyric dacite lava with scarce to common phenocrysts of plagioclase and common to abundant mafics, mostly hornblende, strongly subordinate clinopyroxene and orthopyroxene, and biotite. One fragment of pilotaxitic and microgranophyric dacite lava has common to abundant plagioclase phenocrysts and pyroxene, both clinopyroxene and pseudomorph orthopyroxene. One fragment is pilotaxitic, somewhat argillic Miocene basalt with phenocrysts of scarce plagioclase, common to abundant iddingsite after olivine, and scarce to common clinopyroxene.

^a Number listed after R25- indicates depth. Drill cuttings are indicated by D and the depth listed is the top of the cuttings run, pumice is indicated by P, and all others are core. The number 10 at the end of the sample number indicates >10 mesh (>2 mm) size fraction.

Appendix E

Moisture-Content and Matric-Potential Results

Sample ID	Upper Depth (ft)	Lower Depth (ft)	Lithology	Gravimetric Moisture (%)	Activity (H ₂ O)	Temperature (°C)	Matric Potential (cm)
R25-05.0	5.00	5.00	Qbt 4	5.93	0.9925	26.11	-10588.3
R25-09.5	9.50	9.50	Qbt 4	4.11	0.987	26.32	-18417.0
R25-30.5	30.25	30.50	Qbt 4	4.92	0.9865	26.55	-19144.9
R25-35.5	35.00	35.50	Qbt 4	7.31	0.9925	26.65	-10607.3
R25-42.5	42.00	42.50	Qbt 4	3.72	0.987	26.78	-18445.0
R25-44.5	44.25	44.50	Qbt 4	5.74	0.99	26.89	-14172.2
R25-51.5	51.00	51.50	Qbt 4	5.48	0.9925	26.99	-10619.3
R25-55.5	55.00	55.50	Qbt 4	3.06	0.9915	27.16	-12048.3
R25-59.0	58.60	59.00	Qbt 4	2.82	0.9885	27.38	-16337.0
R25-66.5	66.00	66.50	Qbt 4	2.23	0.99	27.54	-14202.9
R25-74.0	73.00	74.00	Qbt 4	3.14	0.989	27.69	-15638.9
R25-79.0	78.30	79.00	Qbt 4	1.95	0.985	27.78	-21375.3
R25-84.0	83.25	84.00	Qbt 4	5.69	0.992	27.94	-11366.0
R25-93.2	93.00	93.20	Qbt 3t	1.92	0.9865	27.83	-19226.4
R25-97.8	97.50	97.80	Qbt 3t	3.07	0.996	27.57	-5664.7
R25-102.3	102.00	102.30	Qbt 3t	4.59	0.996	27.76	-5668.2
R25-106.8	106.60	106.80	Qbt 3t	4.08	0.9955	27.72	-6377.5
R25-112.0	111.70	112.00	Qbt 3t	2.65	0.9945	27.79	-7800.4
R25-121	120.25	121.00	Qbt 3t	1.75	0.978333	28.19	-31023.3
R25-126	125.80	126.00	Qbt 3t	2.88	0.9825	28.53	-25032.1
R25-131	130.52	131.00	Qbt 3t	3.64	0.9895	28.60	-14969.7
R25-134.5	134.25	134.50	Qbt 3t	2.84	0.9875	28.48	-17831.9
R25-139	138.50	139.00	Qbt 3t	2.74	0.986	28.68	-19999.8
R25-144	143.80	144.00	Qbt 3t	4.50	0.989	28.64	-15688.5
R25-146.6	146.50	146.60	Qbt 3t	7.14	0.9935	28.57	-9247.4
R25-150	149.78	150.00	Qbt 3t	6.17	0.99	28.36	-14241.9
R25-155	154.56	155.00	Qbt 3t	5.34	0.993	28.42	-9956.1
R25-161	160.65	161.00	Qbt 3	2.53	0.9875	28.25	-17818.0
R25-165.5	164.70	165.50	Qbt 3	3.07	0.9915	28.10	-12086.0
R25-174	173.46	174.00	Qbt 3	2.58	0.99	28.08	-14228.6
R25-178	177.25	178.00	Qbt 3	2.92	0.99	28.00	-14224.6
R25-183	182.25	183.00	Qbt 3	2.30	0.992	27.85	-11362.8
R25-188	187.50	188.00	Qbt 3	2.65	0.9935	27.85	-9225.1
R25-193	192.50	193.00	Qbt 3	3.64	0.9945	27.89	-7803.0
R25-198	197.15	198.00	Qbt 3	3.08	0.994	27.87	-8513.9
R25-204	203.50	204.00	Qbt 3	2.55	0.993	27.87	-9938.1
R25-208	207.20	208.00	Qbt 3	2.67	0.9935	27.87	-9225.9
R25-216	215.42	216.00	Qbt 3	1.88	0.9925	27.88	-10650.8
R25-223	222.54	223.00	Qbt 3	2.62	0.9925	27.97	-10654.0

Sample ID	Upper Depth (ft)	Lower Depth (ft)	Lithology	Gravimetric Moisture (%)	Activity (H ₂ O)	Temperature (°C)	Matric Potential (cm)
R25-228	227.58	228.00	Qbt 3	1.06	0.983	27.79	-24251.1
R25-231.35	231.00	231.35	Qbt 2	4.79	0.995	27.84	-7090.7
R25-237.25	237.00	237.25	Qbt 2	3.85	0.995	27.91	-7092.4
R25-241.7	241.40	241.70	Qbt 2	3.40	0.9955	28.08	-6385.1
R25-248	247.30	248.00	Qbt 2	1.52	0.965	28.11	-50443.8
R25-252.5	252.20	252.50	Qbt 2	1.75	0.9885	28.04	-16372.9
R25-258.5	258.00	258.50	Qbt 2	0.94	0.978667	28.08	-30529.1
R25-264	263.50	264.00	Qbt 2	2.73	0.991	28.11	-12800.6
R25-268	267.50	268.00	Qbt 2	2.31	0.9925	28.27	-10664.6
R25-272.5	272.20	272.50	Qbt 12	2.61	0.989	28.33	-15672.2
R25-277	276.60	277.00	Qbt 12	1.44	0.99	28.12	-14230.5
R25-282	281.60	282.00	Qbt 12	1.97	0.9855	28.19	-20685.7
R25-288	287.50	288.00	Qbt 12	2.64	0.9875	28.46	-17830.4
R25-293	292.00	293.00	Qbt 12	2.65	0.9915	28.55	-12104.1
R25-298	297.50	298.00	Qbt 12	2.49	0.992	27.13	-11335.4
R25-302	301.00	302.00	Qbt 12	2.34	0.992	27.36	-11344.3
R25-308	307.50	308.00	Qbt 12	2.55	0.992	27.51	-11349.9
R25-313	312.00	313.00	Qbt 12	2.53	0.992	27.54	-11351.1
R25-318	317.00	318.00	Qbt 12	1.75	0.9915	27.61	-12066.1
R25-323	322.25	323.00	Qbt 12	2.17	0.99	27.73	-14211.9
R25-328	326.25	328.00	Qbt 12	1.84	0.9885	27.70	-16354.7
R25-333	332.25	333.00	Qbt 1v	2.11	0.988	27.74	-17072.0
R25-338	337.30	338.00	Qbt 1v	1.92	0.986	27.80	-19941.5
R25-343	342.00	343.00	Qbt 1v	1.96	0.99	27.94	-14222.0
R25-348	346.00	348.00	Qbt 1v	3.40	0.992	28.00	-11368.4
R25-352.4	352.10	352.40	Qbt 1v	7.35	0.994	28.05	-8519.2
R25-361.5	361.20	361.50	Qbt 1v	10.29	0.996	28.10	-5674.7
R25-368	367.80	368.00	Qbt 1g	9.91	0.9975	28.03	-3543.2
R25-373.5	373.00	373.50	Qbt 1g	11.96	0.9995	28.20	-708.3
R25-377	376.50	377.00	Qbt 1g	11.37	0.9985	28.16	-2125.8
R25-385.5	385.20	385.50	Cerro Toledo	21.17	1	28.10	0.0
R25-399	397.70	399.00	Cerro Toledo	4.52	0.994	28.54	-8533.0
R25-404	403.40	404.00	Cerro Toledo	5.33	0.9975	28.54	-3549.2
R25-408	407.00	408.00	Cerro Toledo	4.86	0.997	28.52	-4259.8
R25-414	413.00	414.00	Cerro Toledo	8.37	0.9975	28.50	-3548.7
R25-418	417.50	418.00	Cerro Toledo	8.12	0.9965	28.59	-4972.2
R25-422	421.50	422.00	Cerro Toledo	11.05	0.999	28.62	-1419.0
R25-428	426.75	428.00	Cerro Toledo	11.91	1	28.60	0.0
R25-440	437.50	440.00	Cerro Toledo	23.93	1.0005	28.61	708.9

Sample ID	Upper Depth (ft)	Lower Depth (ft)	Lithology	Gravimetric Moisture (%)	Activity (H ₂ O)	Temperature (°C)	Matric Potential (cm)
R25-448	445.00	448.00	Cerro Toledo	8.24	0.9985	28.67	-2129.3
R25-456	455.60	456.00	Cerro Toledo	4.74	0.9975	25.35	-3511.6
R25-462	461.50	462.00	Cerro Toledo	5.16	0.9985	25.96	-2110.2
R25-468	466.00	468.00	Cerro Toledo	2.73	0.9915	26.08	-12004.7
R25-474	473.50	474.00	Cerro Toledo	6.98	0.9985	26.14	-2111.5
R25-478	477.40	478.00	Cerro Toledo	6.43	0.9995	26.20	-703.6
R25-484	483.50	484.00	Cerro Toledo	8.66	1.0005	26.37	703.7
R25-488	487.25	488.00	Cerro Toledo	8.23	0.9995	26.50	-704.3
R25-492	491.30	492.00	Cerro Toledo	5.38	0.9995	26.48	-704.3
R25-498	497.00	498.00	Cerro Toledo	8.15	1	26.47	0.0
R25-508	506.00	508.00	Cerro Toledo	6.62	0.9995	26.66	-704.7
R25-514	513.00	514.00	Otowi Member	10.26	0.9995	24.73	-700.2
R25-518	517.30	518.00	Otowi Member	8.16	0.999	24.99	-1401.9
R25-528	525.50	528.00	Otowi Member	8.77	0.9995	25.18	-701.2
R25-532	531.10	532.00	Otowi Member	8.12	0.9995	25.21	-701.3
R25-537	536.10	537.00	Otowi Member	9.23	0.999	25.25	-1403.1
R25-538.9	538.50	538.90	Otowi Member	14.27	0.9985	25.54	-2107.2
R25-543.9	543.50	543.90	Otowi Member	13.14	0.999	25.41	-1403.9
R25-548.9	548.50	548.90	Otowi Member	12.29	1.003	25.42	4203.4
R25-558	557.60	558.00	Otowi Member	13.81	0.999	25.57	-1404.6
R25-568	567.50	568.00	Otowi Member	11.77	1.0005	25.57	701.8
R25-573	572.60	573.00	Otowi Member	12.28	1	25.66	0.0
R25-588	586.00	588.00	Otowi Member	8.29	0.9965	26.75	-4941.8
R25-613	612.00	613.00	Otowi Member	16.16	0.9985	27.02	-2117.7
R25-618	617.50	618.00	Otowi Member	16.54	0.9995	27.03	-705.6
R25-627	626.00	627.00	Otowi Member	17.28	0.998	27.28	-2826.7
R25-667	664.00	667.00	Otowi Member	18.72	1.0005	27.24	705.7

Appendix F

Results of Unsaturated Hydraulic-Property Testing



Daniel B. Stephens & Associates, Inc.

Moisture Retention Data
Hanging Column/Pressure Plate/Thermocouple
(Main Drainage Curve)

Job Name: LANL
Job Number: 9958.01
Sample Number: CACV-98-0039
Ring Number: CACV-98-0039
Depth: NA

Dry wt. of sample (g): 292.43
Tare wt., screen & clamp (g): 31.06
Tare wt., ring (g): 107.52
Tare wt., epoxy (g): 0.00
Sample volume (cm³): 135.27

Saturated weight* at 0 cm tension (g): 445.63
Volume of water [†] in saturated sample (cm³): 14.62
Saturated moisture content (% vol): 10.81
Sample bulk density (g/cm³): 2.16

	Date/Time	Weight* (g)	Matric Potential (-cm water)	Moisture Content [†] (% vol)
Hanging column:	18-Oct-99 / 15:45	445.63	0.00	10.81
	21-Oct-99 / 10:30	444.72	53.20	10.14
	23-Oct-99 / 15:00	444.45	126.40	9.94
Pressure plate:	26-Oct-99 / 09:50	444.16	509.90	9.72

Dry weight* of thermocouple sample (g): 342.31
Tare weight, jar (g): 205.68
Sample bulk density (g/cm³): 2.16

	Date/Time	Weight* (g)	Matric Potential (-cm water)	Moisture Content [†] (% vol)
Thermocouple:	22-Sep-99 / 10:32	345.89	9790.1	5.66
	24-Sep-99 / 18:24	344.78	12849.5	3.91

Comments:

* Weight including tares

[†] Assumed density of water is 1.0 g/cm³

Laboratory analysis by: E. Koenig/T. Gere
Data entered by: M. Devine
Checked by: R. Smith



Daniel B. Stephens & Associates, Inc.

Moisture Retention Data
Water Activity Meter/Relative Humidity Box
(Main Drainage Curve)

Job Name: LANL
Job Number: 9958.01
Sample Number: CACV-98-0039
Ring Number: CACV-98-0039
Depth: NA

Dry weight* of relative humidity box sample (g): 86.71
Tare weight (g): 47.60
Sample bulk density (g/cm³): 2.16

	Date/Time	Weight* (g)	Matric Potential (-cm water)	Moisture Content [†] (% vol)
Relative humidity box:	20-Sep-99 / 10:15	86.80	836961	0.51

Comments:

* Weight including tares

[†] Assumed density of water is 1.0 g/cm³

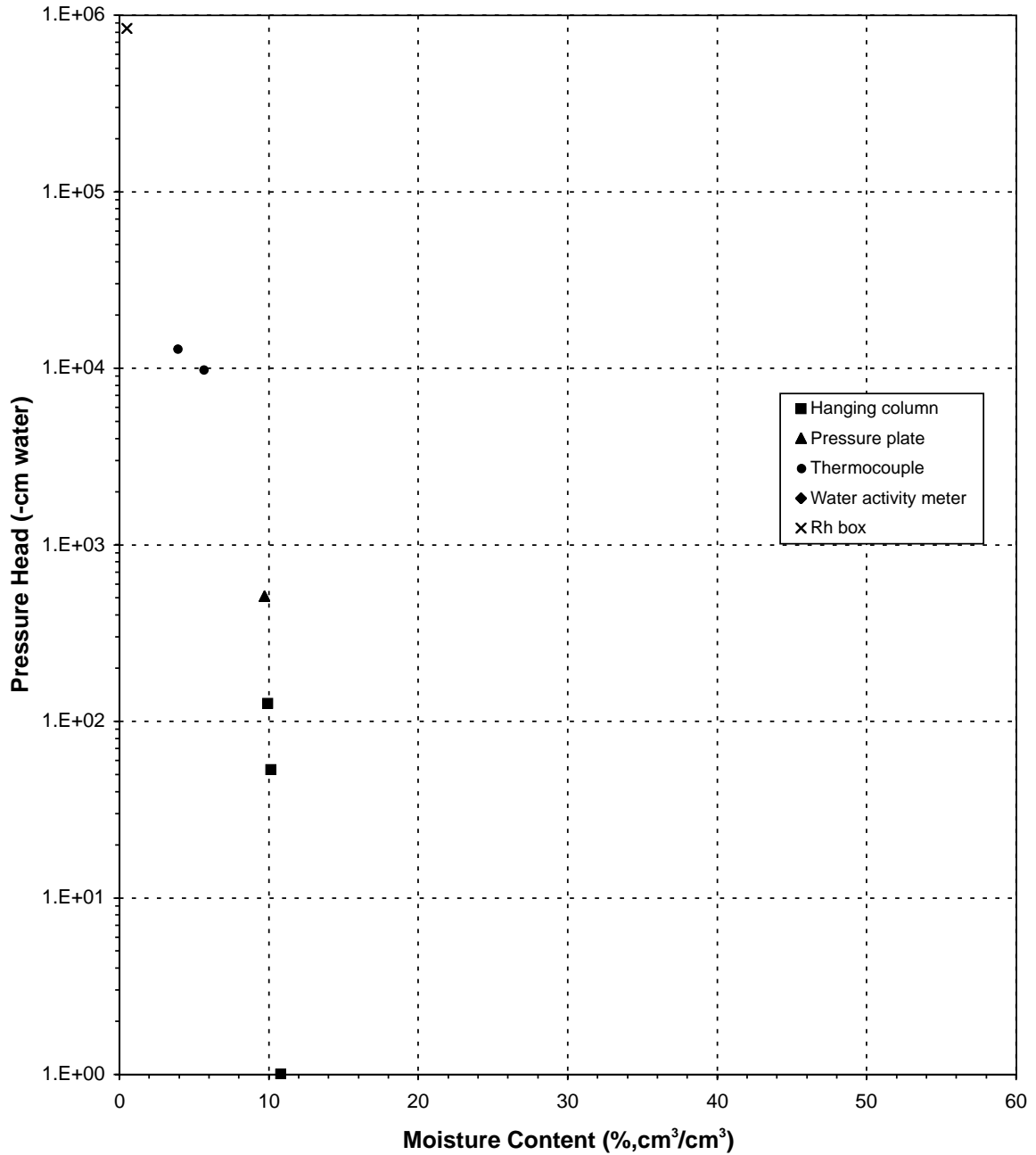
Laboratory analysis by: J. Locke/T. Gere
Data entered by: M. Devine
Checked by: R. Smith



Daniel B. Stephens & Associates, Inc.

Water Retention Data Points

Sample Number: CACV-98-0039

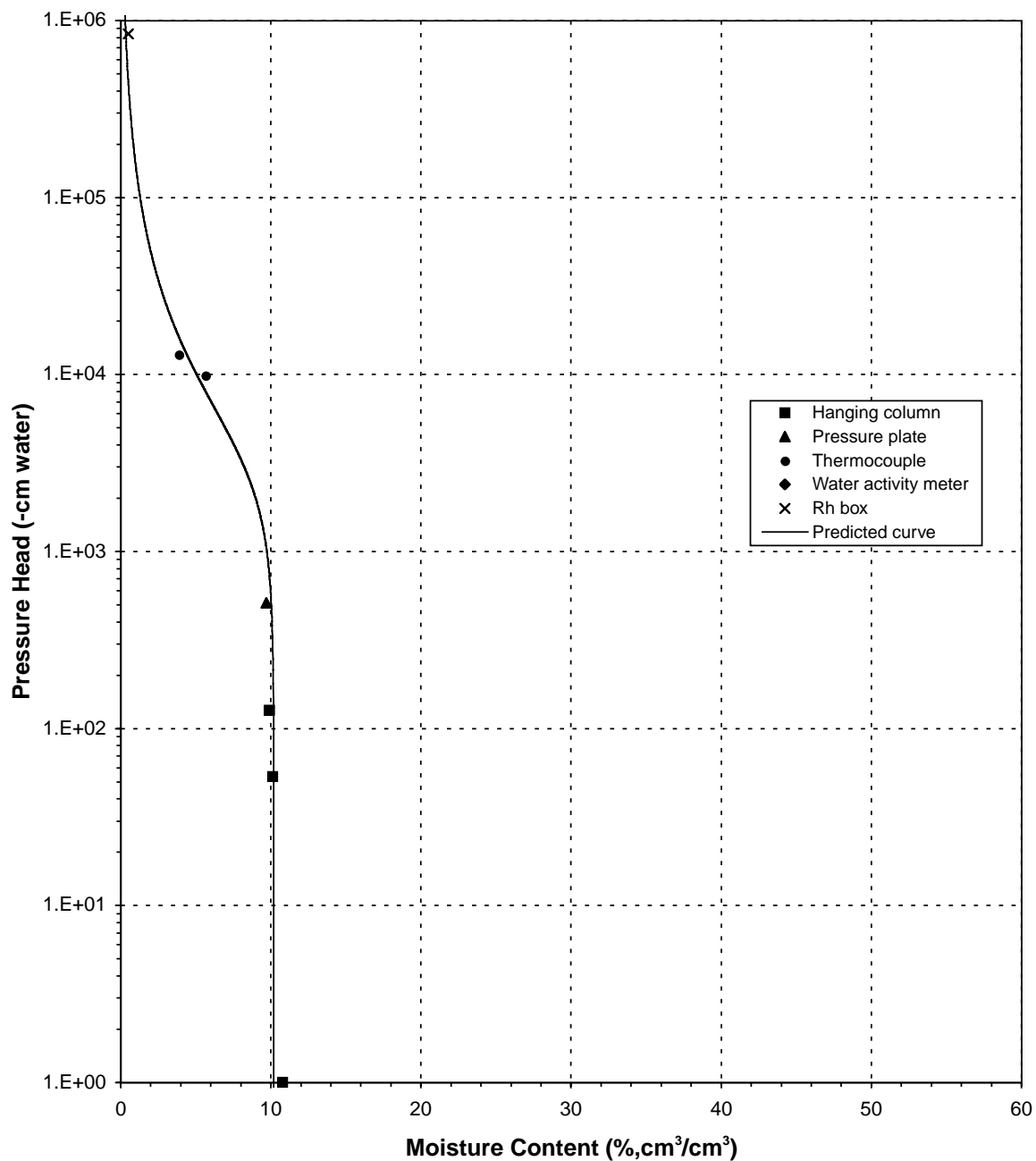




Daniel B. Stephens & Associates, Inc.

Predicted Water Retention Curve and Data Points

Sample Number: CACV-98-0039

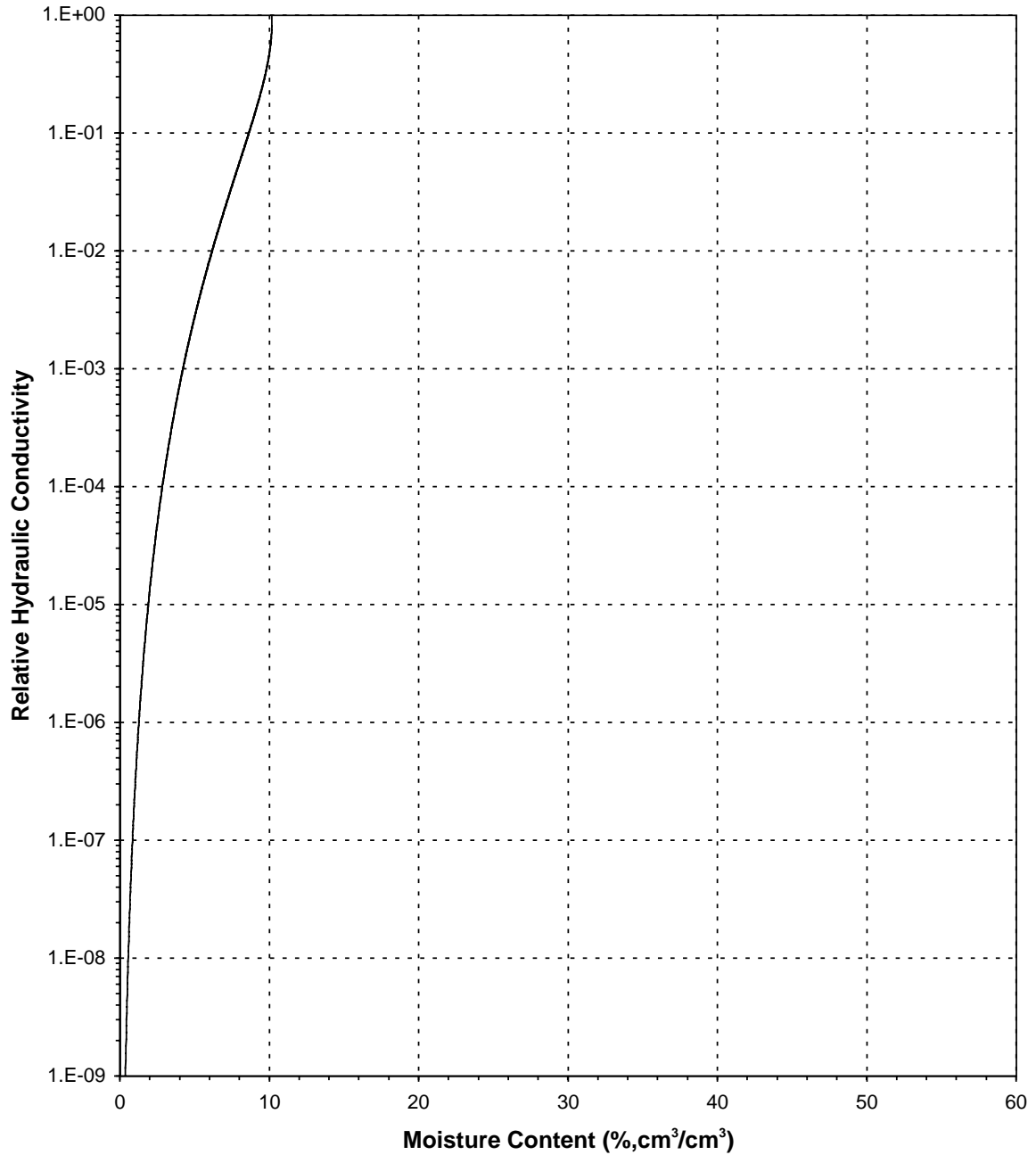




Daniel B. Stephens & Associates, Inc.

Plot of Relative Hydraulic Conductivity vs Moisture Content

Sample Number: CACV-98-0039

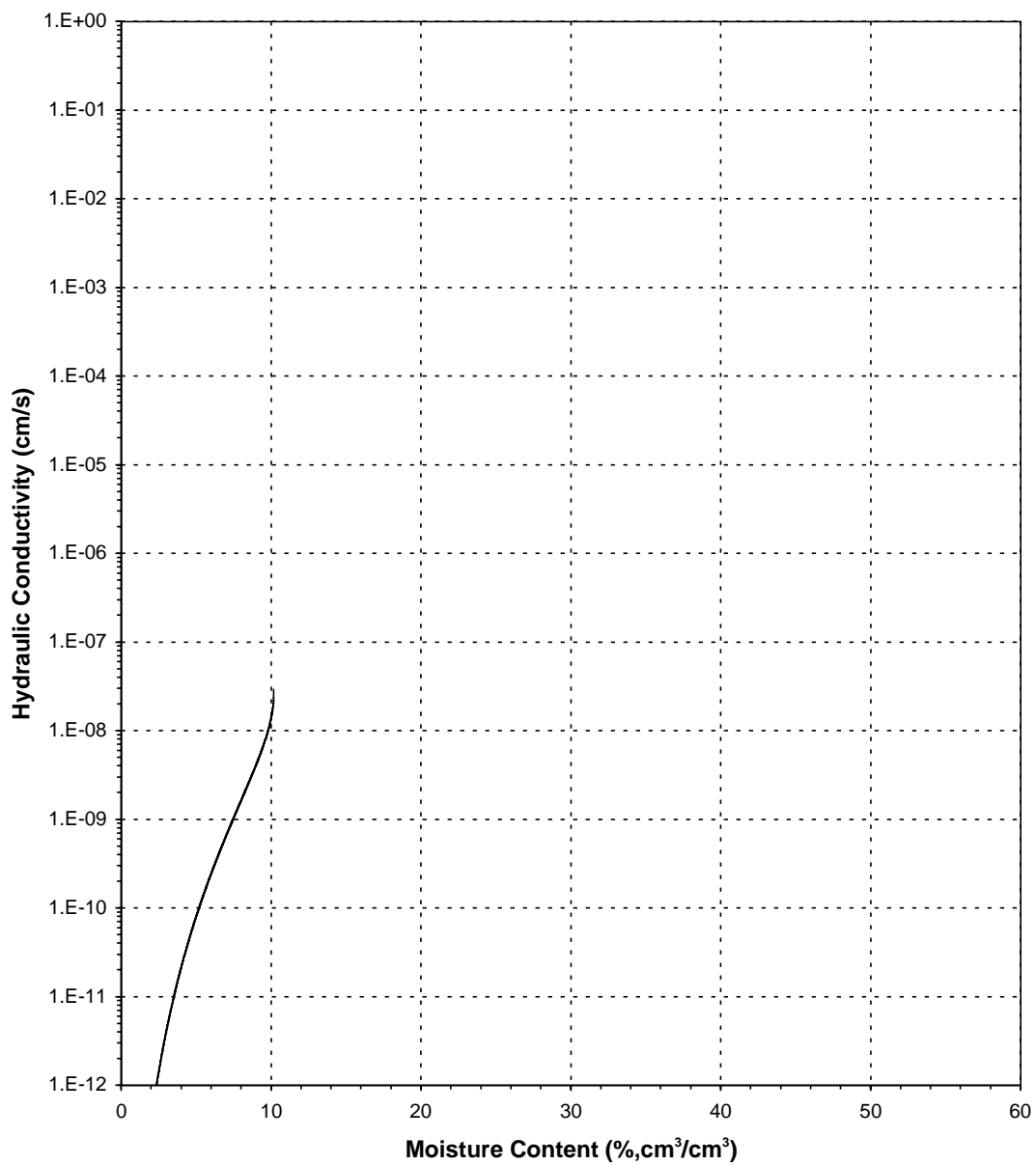




Daniel B. Stephens & Associates, Inc.

Plot of Hydraulic Conductivity vs Moisture Content

Sample Number: CACV-98-0039

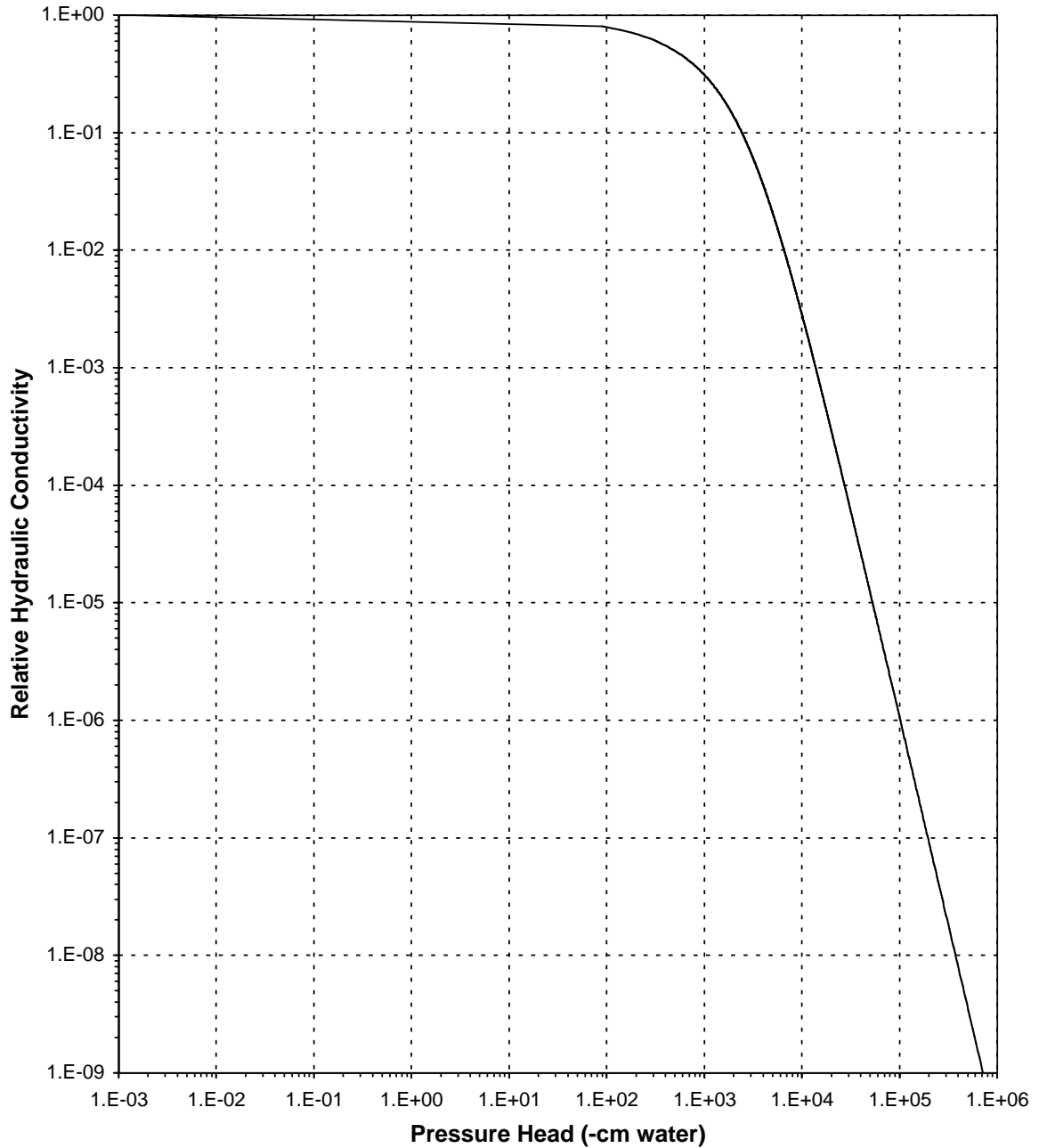




Daniel B. Stephens & Associates, Inc.

Plot of Relative Hydraulic Conductivity vs Pressure Head

Sample Number: CACV-98-0039

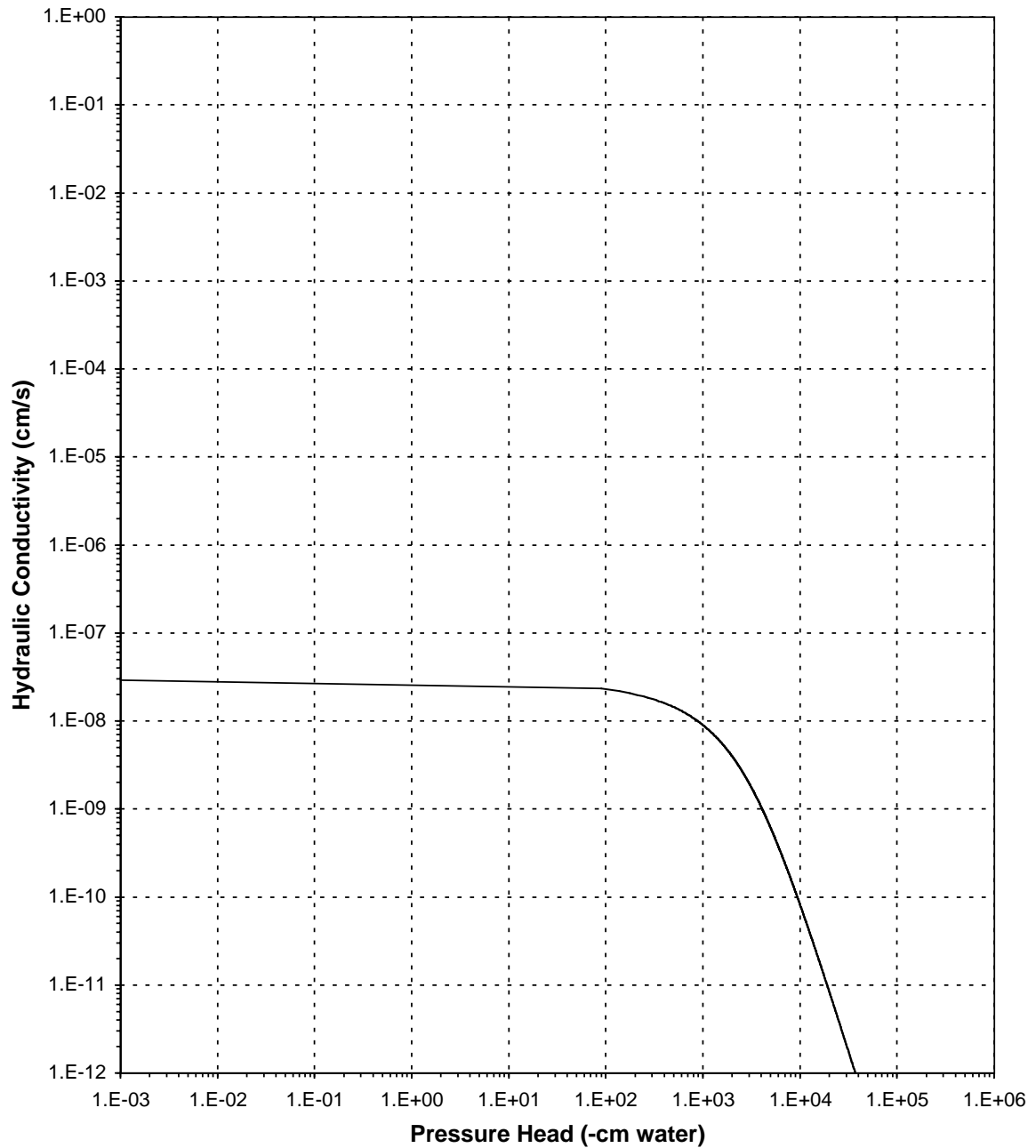




Daniel B. Stephens & Associates, Inc.

Plot of Hydraulic Conductivity vs Pressure Head

Sample Number: CACV-98-0039





Daniel B. Stephens & Associates, Inc.

Moisture Retention Data
Hanging Column/Pressure Plate/Thermocouple
 (Main Drainage Curve)

Job Name:	LANL	Dry wt. of sample (g):	109.72
Job Number:	9958.01	Tare wt., screen & clamp (g):	29.02
Sample Number:	CACV-98-0043	Tare wt., ring (g):	130.79
Ring Number:	CACV-98-0043	Tare wt., epoxy (g):	0.00
Depth:	NA	Sample volume (cm ³):	85.85

Saturated weight* at 0 cm tension (g): 326.42
 Volume of water [†] in saturated sample (cm³): 56.89
 Saturated moisture content (% vol): 66.27
 Sample bulk density (g/cm³): 1.28

	Date/Time	Weight* (g)	Matric Potential (-cm water)	Moisture Content [†] (% vol)
<i>Hanging column:</i>	01-Oct-99 / 12:00	326.42	0.00	66.27
	04-Oct-99 / 09:20	321.58	9.50	60.63
	06-Oct-99 / 15:40	316.20	38.10	54.36
	08-Oct-99 / 20:40	308.96	80.30	45.93
<i>Pressure plate:</i>	11-Oct-99 / 09:20	290.12	254.95	23.98
	13-Oct-99 / 14:25	281.90	1019.80	14.41

Dry weight* of thermocouple sample (g): 270.78
 Tare weight, jar (g): 171.22
 Sample bulk density (g/cm³): 1.28

	Date/Time	Weight* (g)	Matric Potential (-cm water)	Moisture Content [†] (% vol)
<i>Thermocouple:</i>	08-Oct-99 / 13:33	273.93	8464.3	4.04
	04-Oct-99 / 16:31	273.27	17336.6	3.20

Comments:

* Weight including tares

[†] Assumed density of water is 1.0 g/cm³

Laboratory analysis by: E. Koenig/R. Smith
 Data entered by: M. Devine
 Checked by: R. Smith



Daniel B. Stephens & Associates, Inc.

Moisture Retention Data
Water Activity Meter/Relative Humidity Box
(Main Drainage Curve)

Job Name: LANL
Job Number: 9958.01
Sample Number: CACV-98-0043
Ring Number: CACV-98-0043
Depth: NA

Dry weight* of relative humidity box sample (g): 78.72
Tare weight (g): 39.92
Sample bulk density (g/cm³): 1.28

	Date/Time	Weight* (g)	Matric Potential (-cm water)	Moisture Content [†] (% vol)
Relative humidity box:	22-Sep-99 / 08:32	79.15	836961	1.43

Comments:

* Weight including tares

[†] Assumed density of water is 1.0 g/cm³

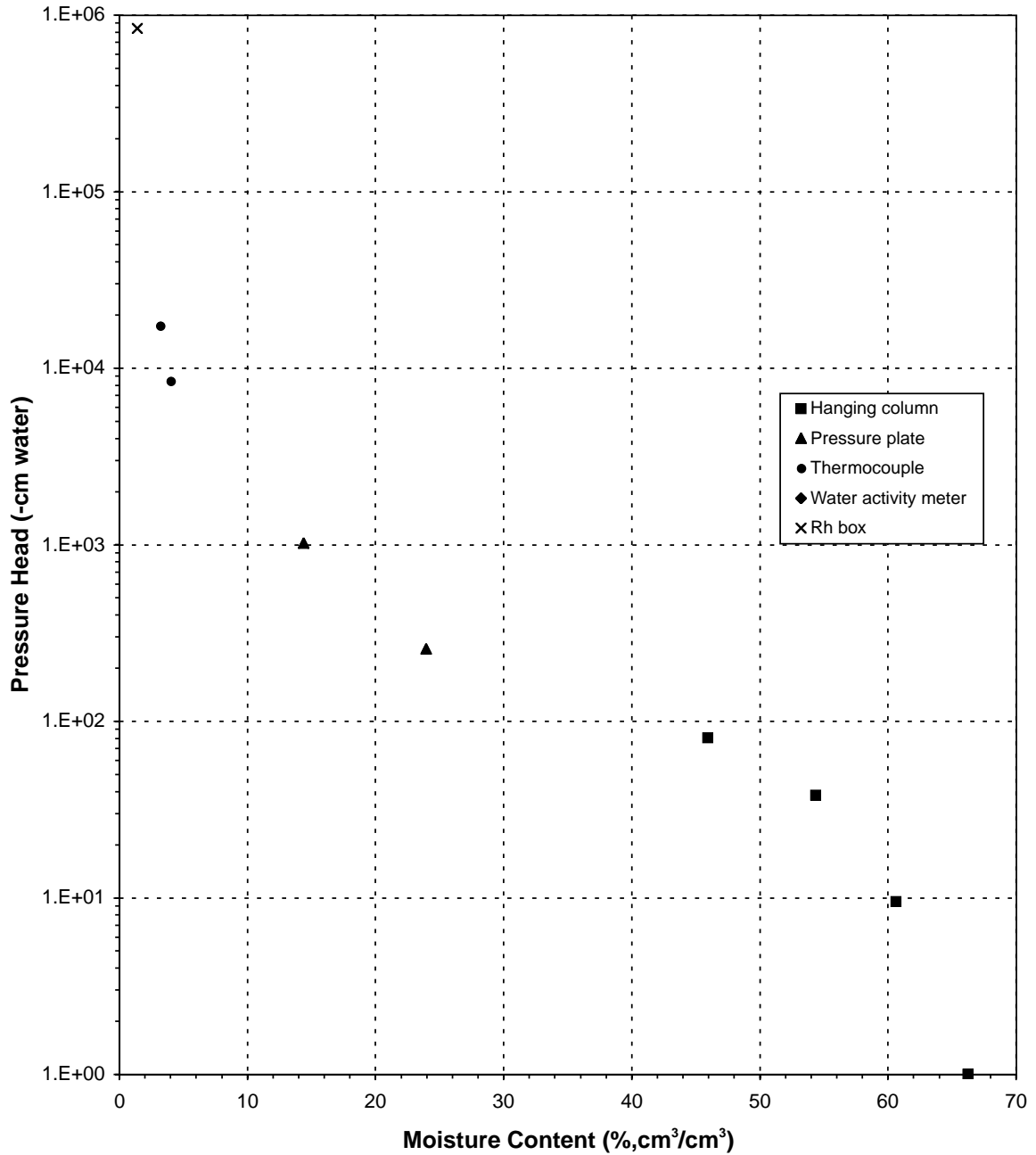
Laboratory analysis by: J. Locke/R. Smith
Data entered by: M. Devine
Checked by: R. Smith



Daniel B. Stephens & Associates, Inc.

Water Retention Data Points

Sample Number: CACV-98-0043

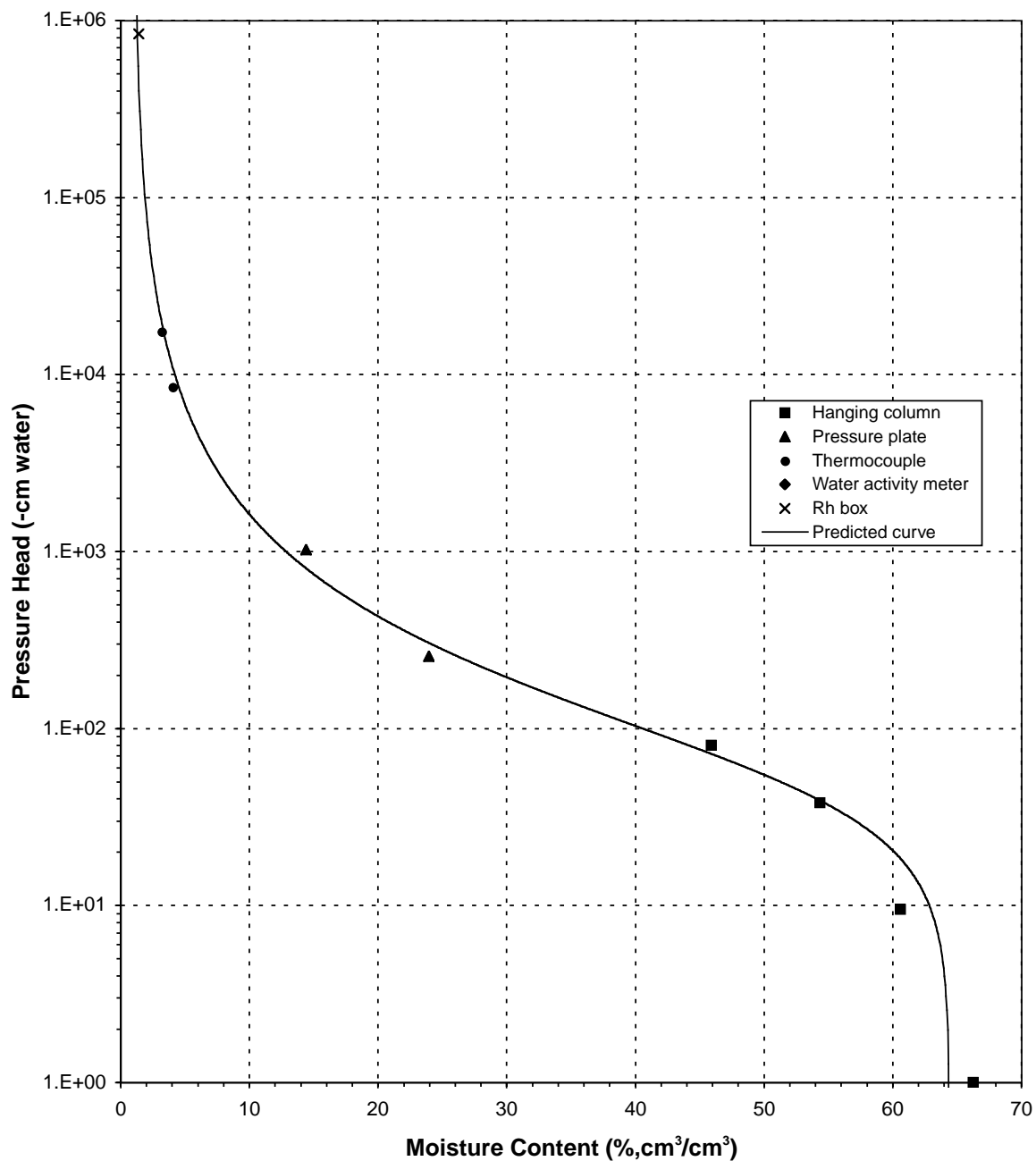




Daniel B. Stephens & Associates, Inc.

Predicted Water Retention Curve and Data Points

Sample Number: CACV-98-0043

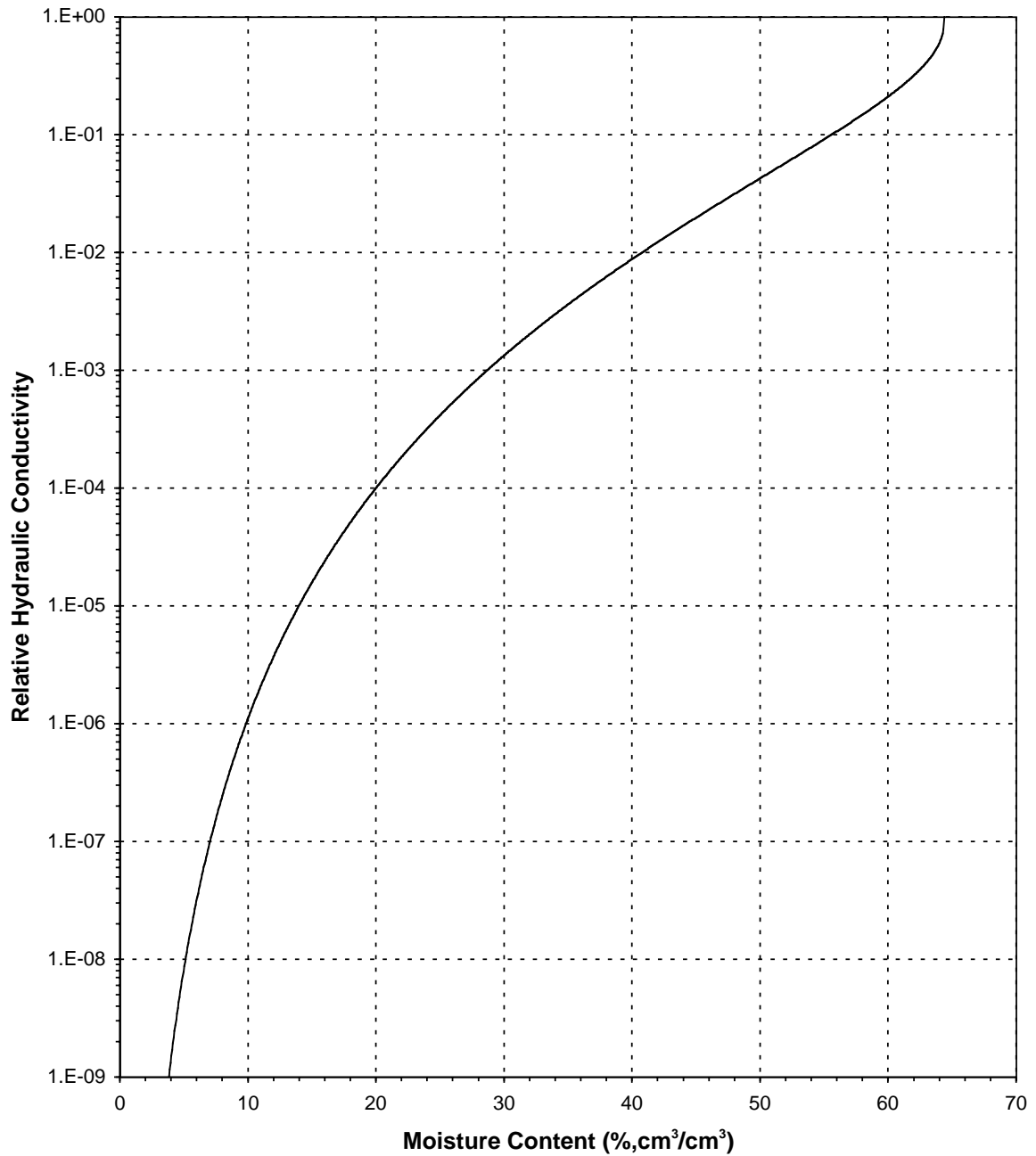




Daniel B. Stephens & Associates, Inc.

Plot of Relative Hydraulic Conductivity vs Moisture Content

Sample Number: CACV-98-0043

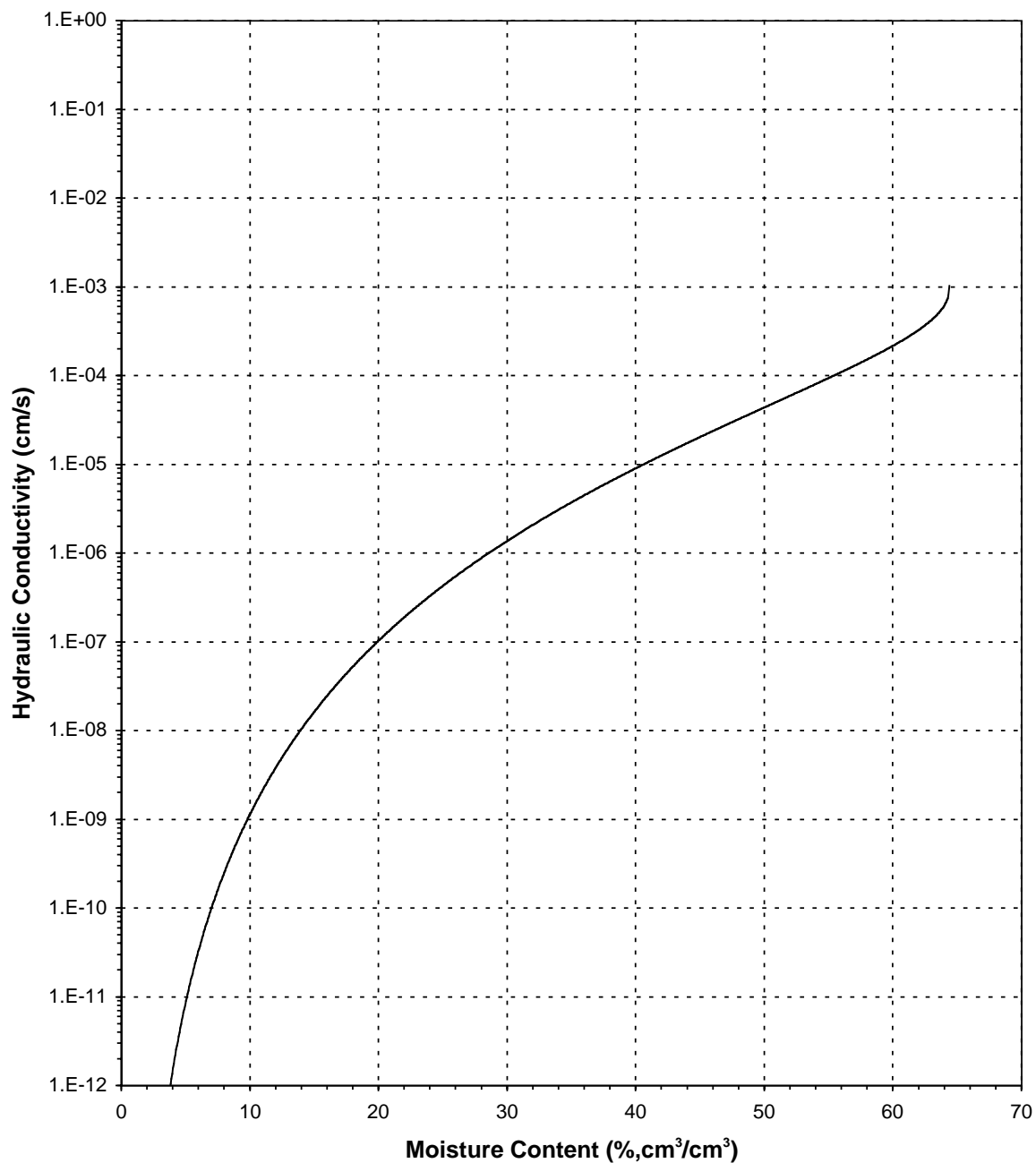




Daniel B. Stephens & Associates, Inc.

Plot of Hydraulic Conductivity vs Moisture Content

Sample Number: CACV-98-0043

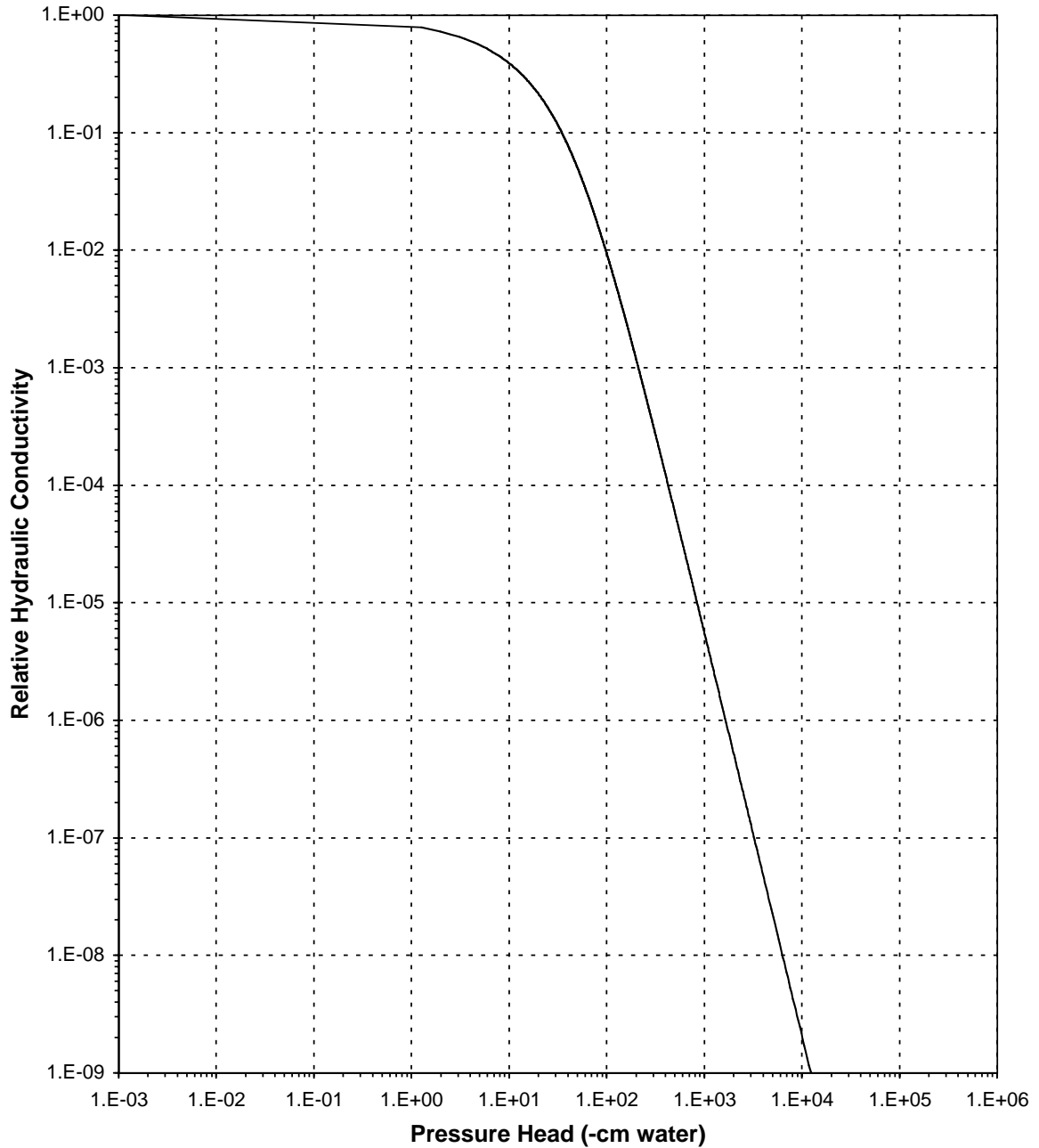




Daniel B. Stephens & Associates, Inc.

Plot of Relative Hydraulic Conductivity vs Pressure Head

Sample Number: CACV-98-0043

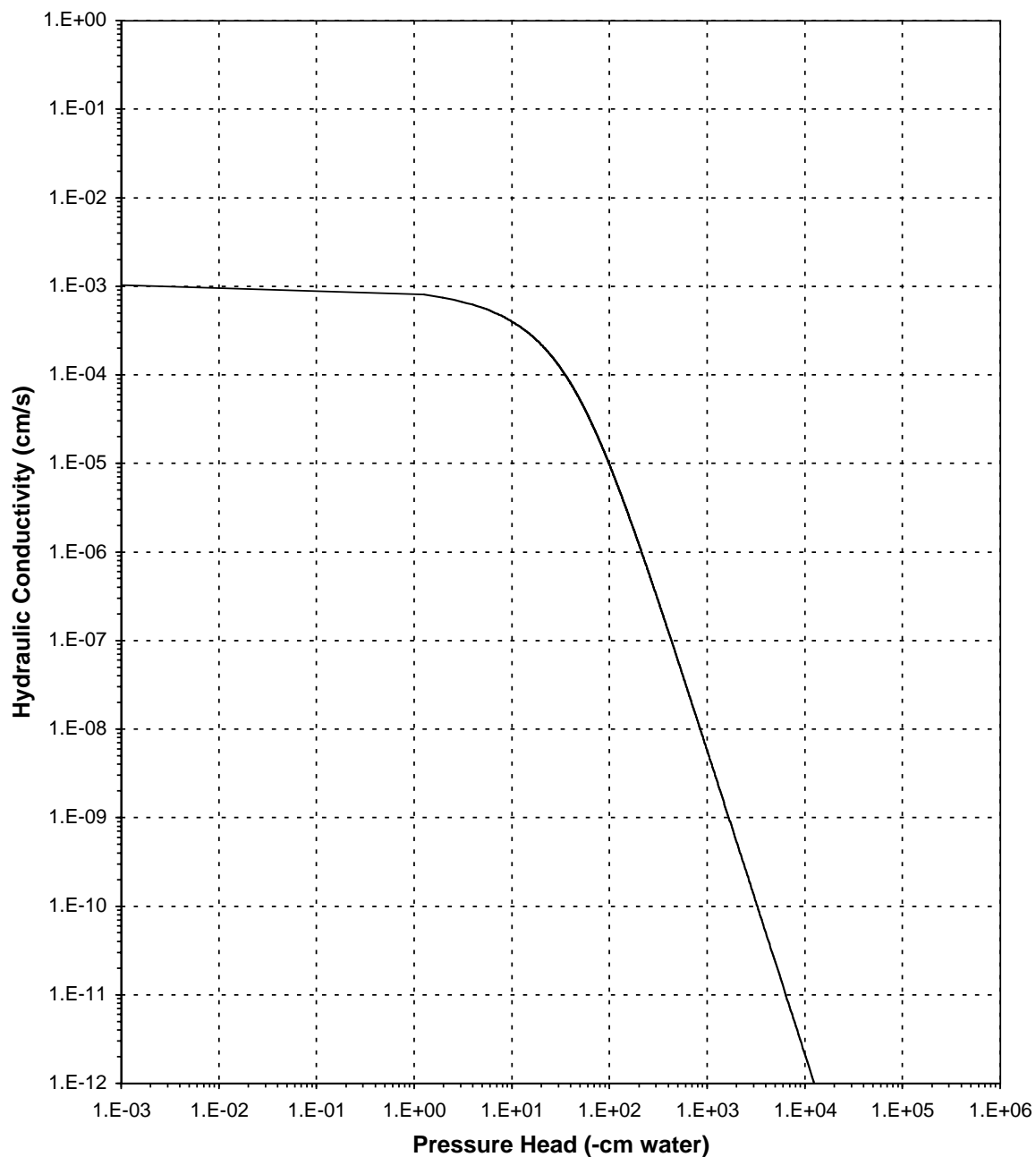




Daniel B. Stephens & Associates, Inc.

Plot of Hydraulic Conductivity vs Pressure Head

Sample Number: CACV-98-0043





Daniel B. Stephens & Associates, Inc.

Moisture Retention Data
Hanging Column/Pressure Plate/Thermocouple
 (Main Drainage Curve)

Job Name:	LANL	Dry wt. of sample (g):	53.35
Job Number:	9958.01	Tare wt., screen & clamp (g):	40.07
Sample Number:	CACV-98-0046	Tare wt., ring (g):	189.36
Ring Number:	CACV-98-0046	Tare wt., epoxy (g):	0.00
Depth:	NA	Sample volume (cm ³):	48.35

Saturated weight* at 0 cm tension (g): 327.17
 Volume of water [†] in saturated sample (cm³): 44.39
 Saturated moisture content (% vol): 91.80
 Sample bulk density (g/cm³): 1.10

	Date/Time	Weight* (g)	Matric Potential (-cm water)	Moisture Content [†] (% vol)
<i>Hanging column:</i>	01-Oct-99 / 11:40	327.17	0.00	91.80
	04-Oct-99 / 09:20	318.13	9.60	73.11
	06-Oct-99 / 15:40	312.80	38.20	62.08
	08-Oct-99 / 20:40	311.46	80.40	59.31
<i>Pressure plate:</i>	11-Oct-99 / 09:20	309.09	254.95	54.41
	13-Oct-99 / 14:23	307.26	1019.80	50.63

Dry weight* of thermocouple sample (g): 259.63
 Tare weight, jar (g): 173.72
 Sample bulk density (g/cm³): 1.10

	Date/Time	Weight* (g)	Matric Potential (-cm water)	Moisture Content [†] (% vol)
<i>Thermocouple:</i>	07-Oct-99 / 10:37	264.84	6934.6	6.69
	08-Oct-99 / 13:38	263.77	13767.3	5.32

Comments:

* Weight including tares

[†] Assumed density of water is 1.0 g/cm³

Laboratory analysis by: E. Koenig/R. Smith
Data entered by: M. Devine
Checked by: R. Smith



Daniel B. Stephens & Associates, Inc.

Moisture Retention Data
Water Activity Meter/Relative Humidity Box
(Main Drainage Curve)

Job Name: LANL
Job Number: 9958.01
Sample Number: CACV-98-0046
Ring Number: CACV-98-0046
Depth: NA

Dry weight* of relative humidity box sample (g): 75.66
Tare weight (g): 39.99
Sample bulk density (g/cm³): 1.10

	Date/Time	Weight* (g)	Matric Potential (-cm water)	Moisture Content [†] (% vol)
Relative humidity box:	22-Sep-99 / 08:31	76.09	836961	1.35

Comments:

* Weight including tares

[†] Assumed density of water is 1.0 g/cm³

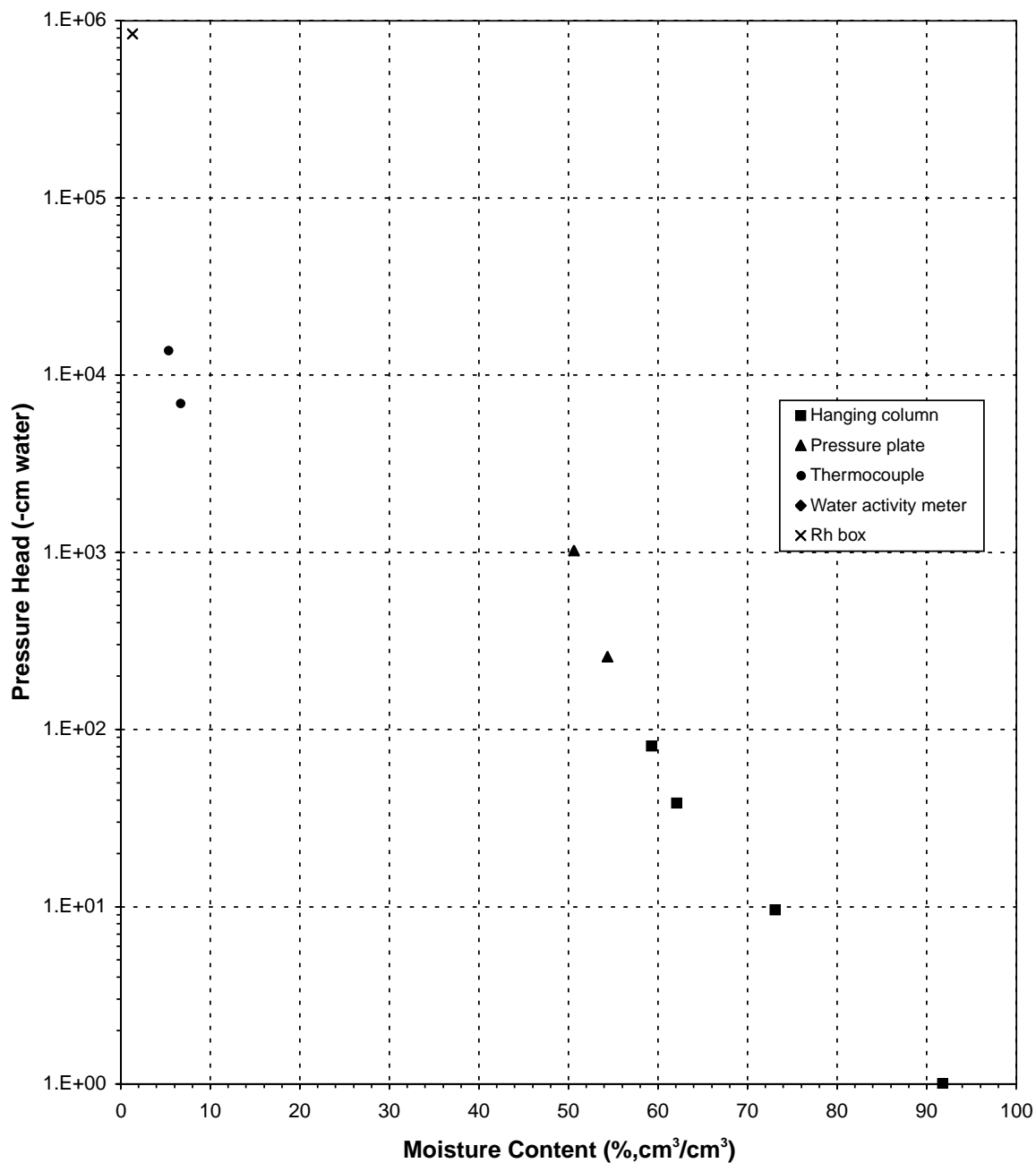
Laboratory analysis by: J. Locke/R. Smith
Data entered by: M. Devine
Checked by: R. Smith



Daniel B. Stephens & Associates, Inc.

Water Retention Data Points

Sample Number: CACV-98-0046

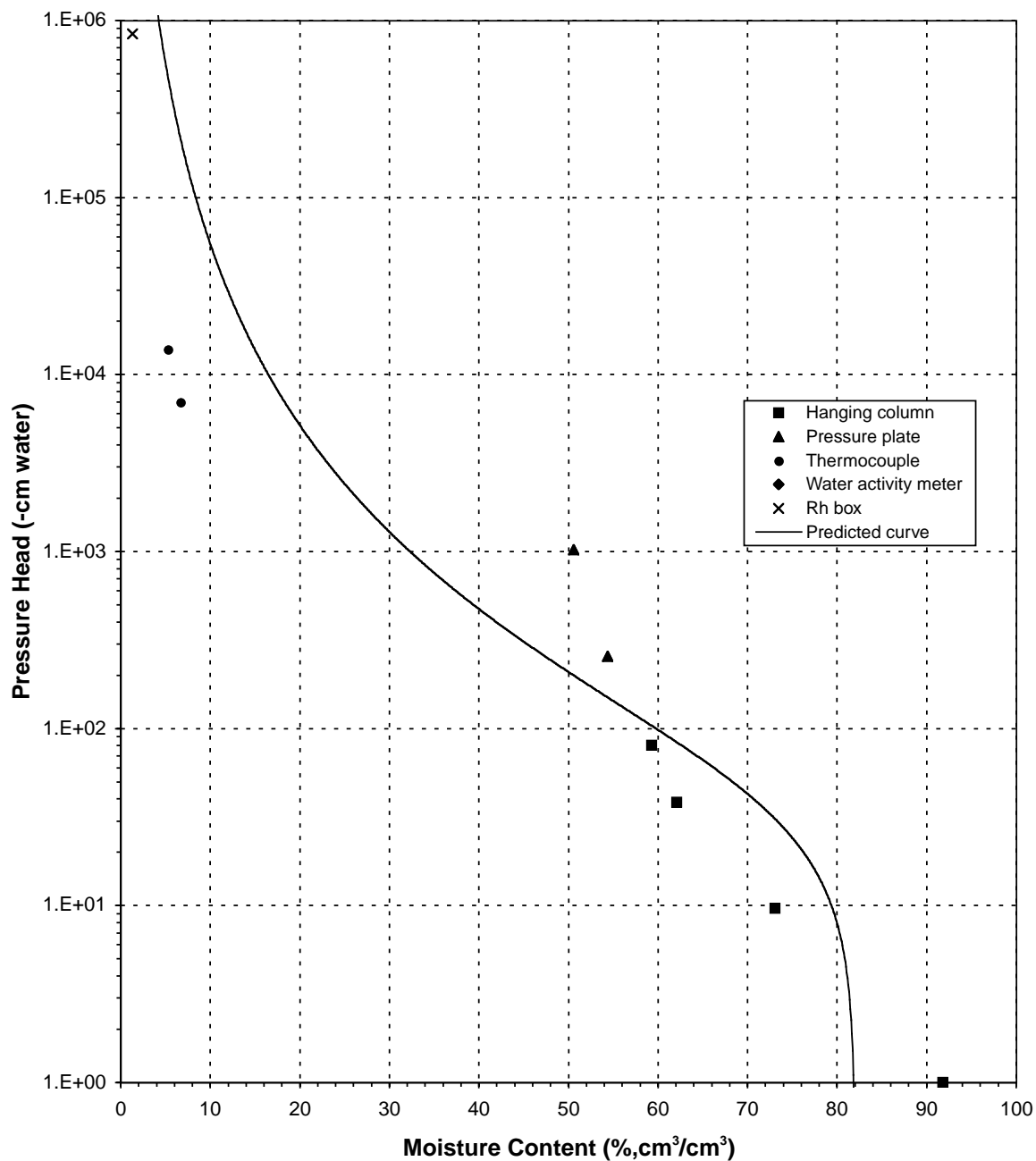




Daniel B. Stephens & Associates, Inc.

Predicted Water Retention Curve and Data Points

Sample Number: CACV-98-0046

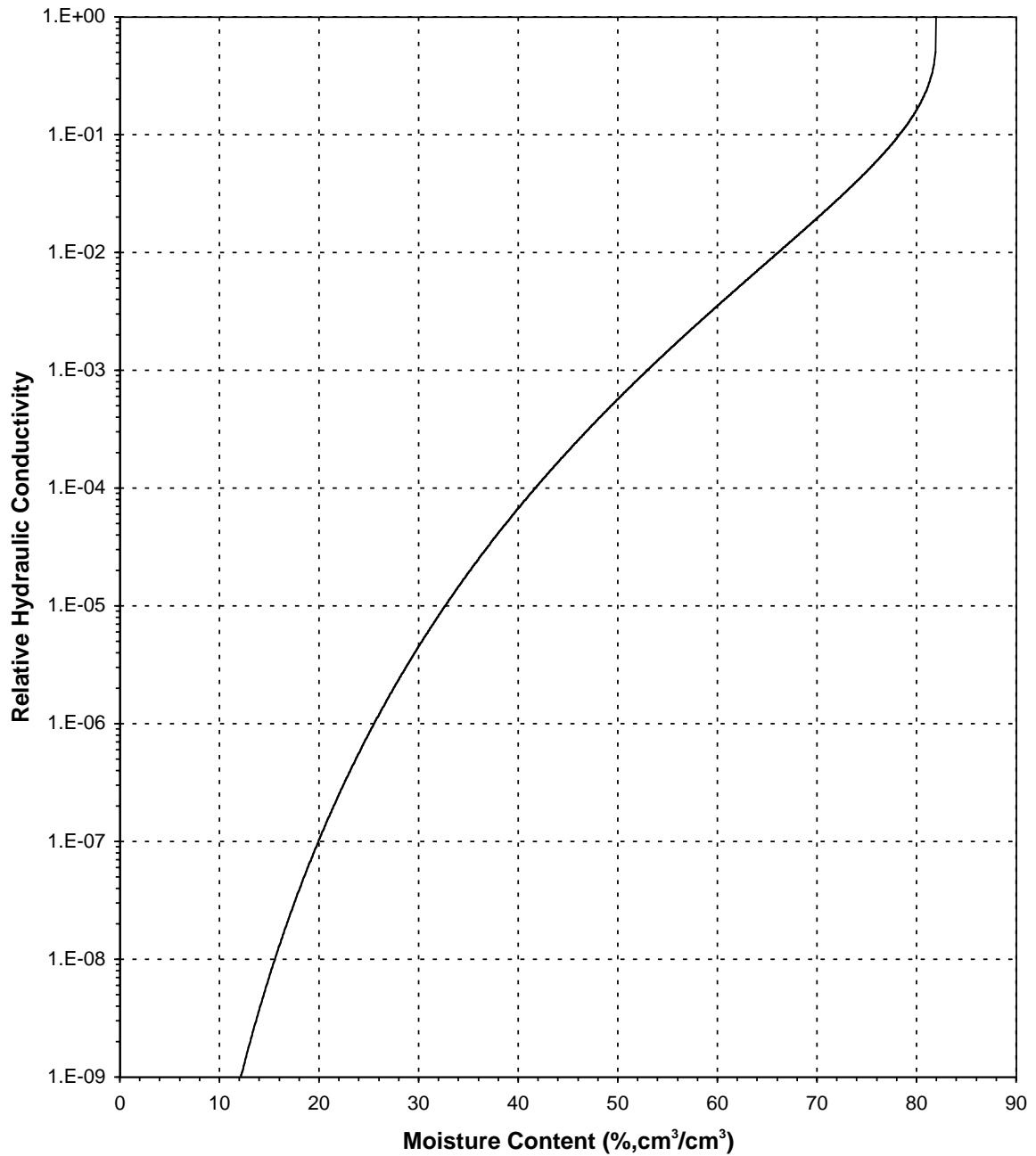




Daniel B. Stephens & Associates, Inc.

Plot of Relative Hydraulic Conductivity vs Moisture Content

Sample Number: CACV-98-0046

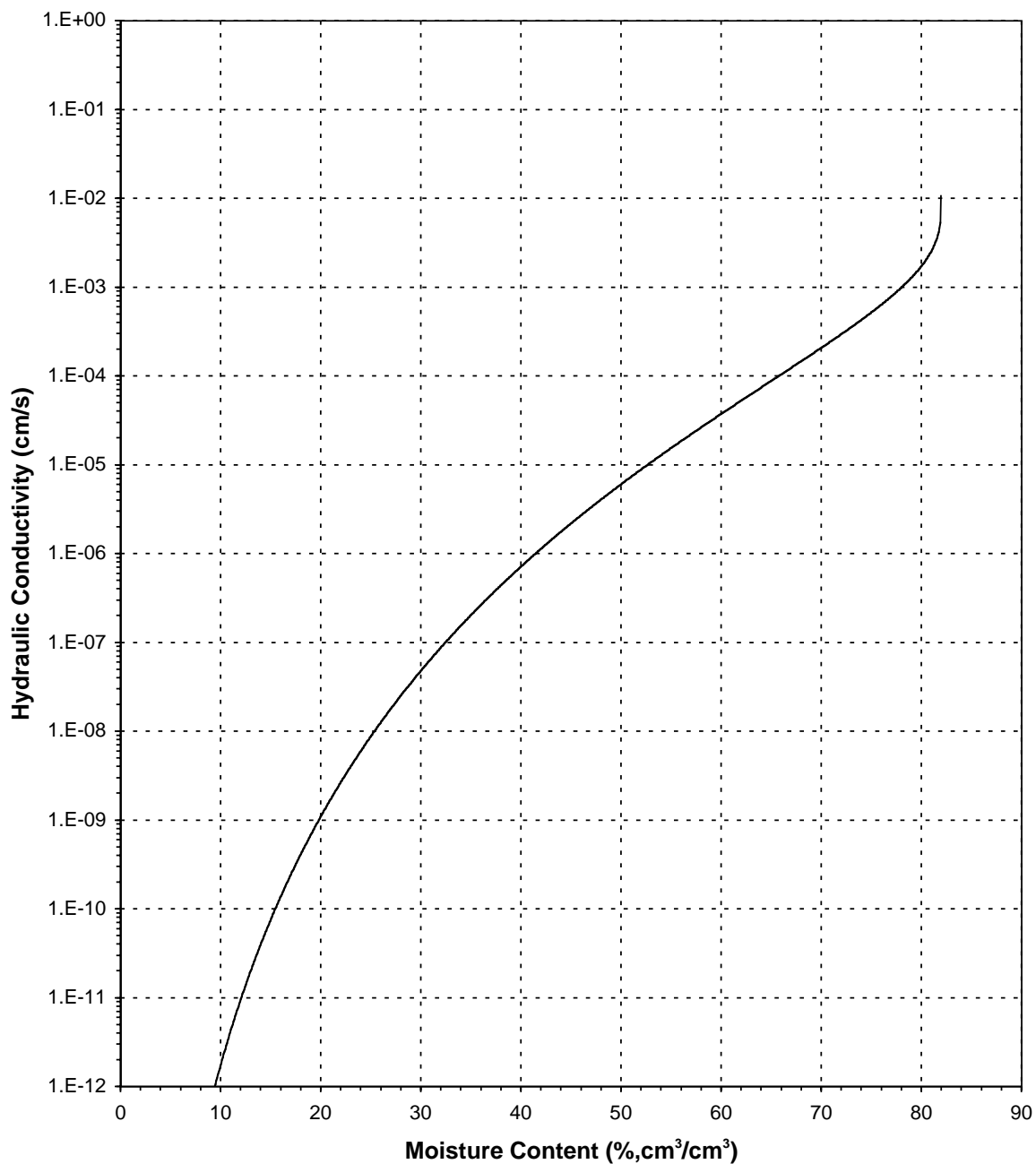




Daniel B. Stephens & Associates, Inc.

Plot of Hydraulic Conductivity vs Moisture Content

Sample Number: CACV-98-0046

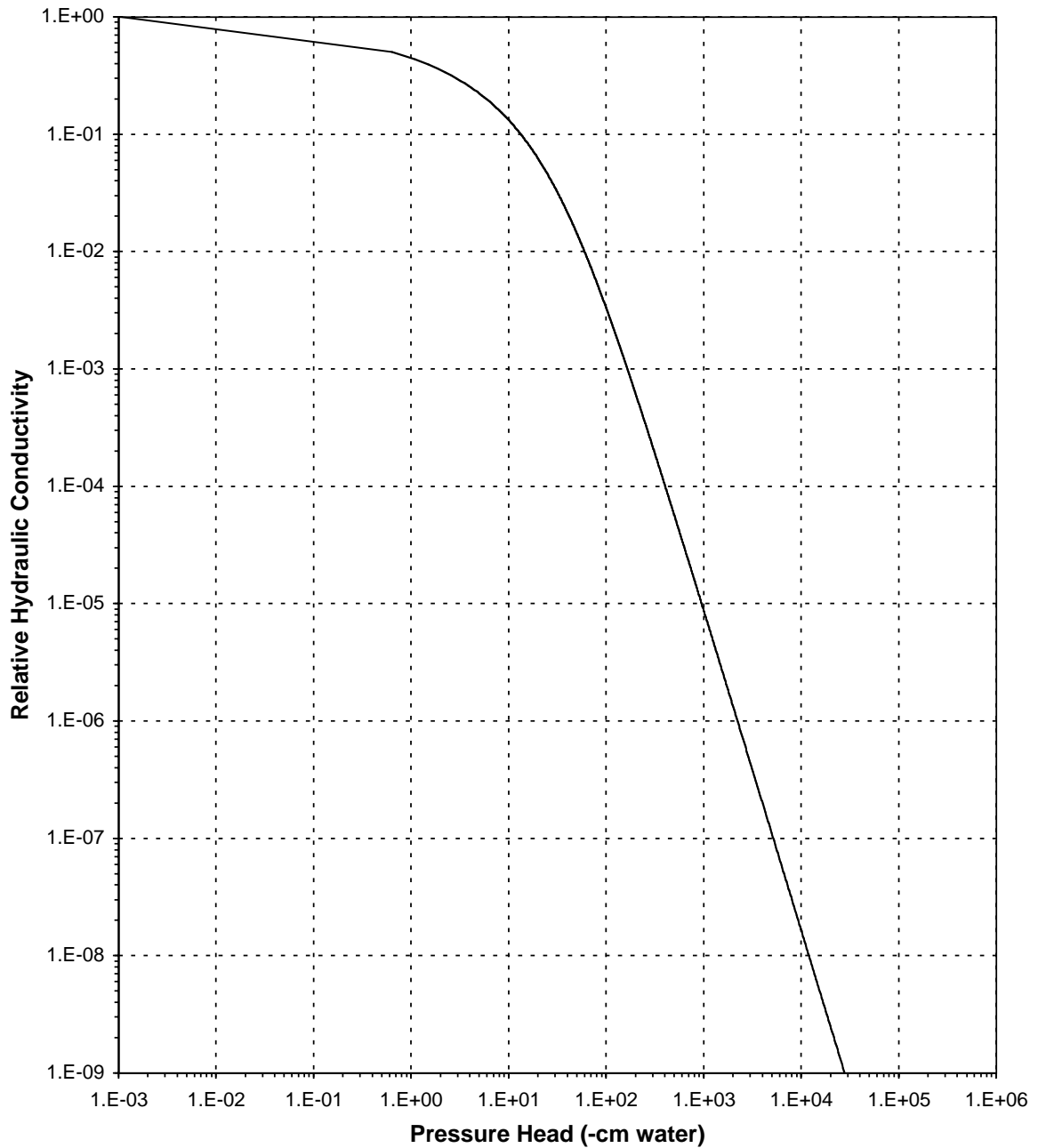




Daniel B. Stephens & Associates, Inc.

Plot of Relative Hydraulic Conductivity vs Pressure Head

Sample Number: CACV-98-0046

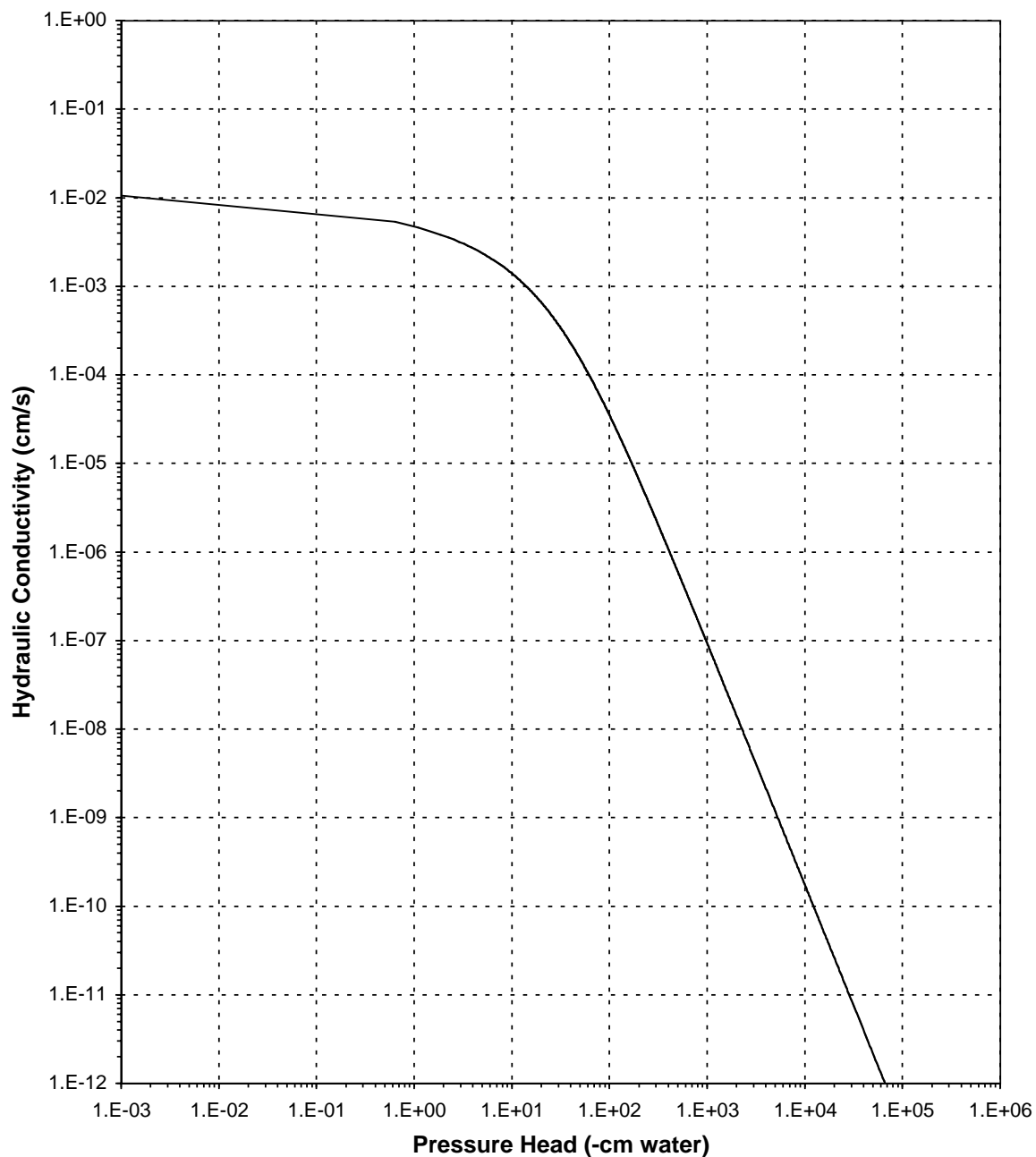




Daniel B. Stephens & Associates, Inc.

Plot of Hydraulic Conductivity vs Pressure Head

Sample Number: CACV-98-0046





Daniel B. Stephens & Associates, Inc.

Moisture Retention Data
Hanging Column/Pressure Plate/Thermocouple
 (Main Drainage Curve)

Job Name:	LANL	Dry wt. of sample (g):	207.84
Job Number:	9958.01	Tare wt., screen & clamp (g):	29.03
Sample Number:	CACV-98-0049	Tare wt., ring (g):	127.41
Ring Number:	CACV-98-0049	Tare wt., epoxy (g):	0.00
Depth:	NA	Sample volume (cm ³):	218.12

Saturated weight* at 0 cm tension (g): 451.02
 Volume of water [†] in saturated sample (cm³): 86.74
 Saturated moisture content (% vol): 39.77
 Sample bulk density (g/cm³): 0.95

	Date/Time	Weight* (g)	Matric Potential (-cm water)	Moisture Content [†] (% vol)
Hanging column:	28-Oct-99 / 11:05	451.02	0.00	39.77
	01-Nov-99 / 10:05	443.36	21.60	36.26
	03-Nov-99 / 12:15	437.36	51.60	33.50
	05-Nov-99 / 18:37	423.97	152.50	27.37
Pressure plate:	08-Nov-99 / 09:35	399.09	509.90	15.96

Dry weight* of thermocouple sample (g): 179.32
 Tare weight, jar (g): 114.62
 Sample bulk density (g/cm³): 0.95

	Date/Time	Weight* (g)	Matric Potential (-cm water)	Moisture Content [†] (% vol)
Thermocouple:	07-Nov-99 / 18:11	180.99	7036.6	2.46
	01-Nov-99 / 12:10	180.61	16724.7	1.90

Comments:

* Weight including tares

[†] Assumed density of water is 1.0 g/cm³

Laboratory analysis by: E. Koenig/R. Smith
 Data entered by: D.O'Dowd
 Checked by: R. Smith



Daniel B. Stephens & Associates, Inc.

Moisture Retention Data
Water Activity Meter/Relative Humidity Box
(Main Drainage Curve)

Job Name: LANL
Job Number: 9958.01
Sample Number: CACV-98-0049
Ring Number: CACV-98-0049
Depth: NA

Dry weight* of relative humidity box sample (g): 67.36
Tare weight (g): 40.97
Sample bulk density (g/cm³): 0.95

	Date/Time	Weight* (g)	Matric Potential (-cm water)	Moisture Content [†] (% vol)
Relative humidity box:	28-Oct-99 / 09:48	67.49	848426	0.48

Comments:

* Weight including tares

[†] Assumed density of water is 1.0 g/cm³

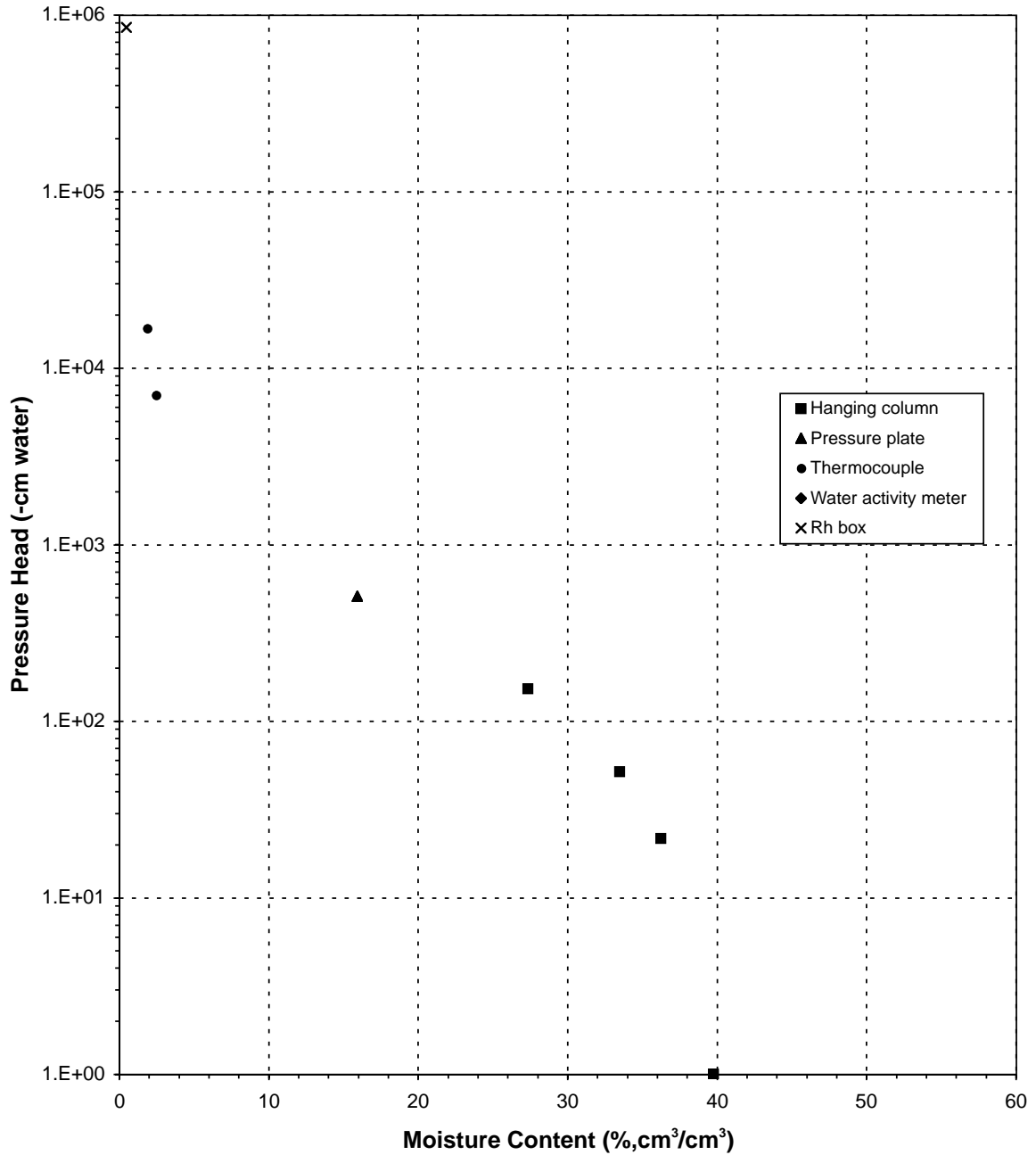
Laboratory analysis by: J. Locke/R. Smith
Data entered by: D.O'Dowd
Checked by: R. Smith



Daniel B. Stephens & Associates, Inc.

Water Retention Data Points

Sample Number: CACV-98-0049

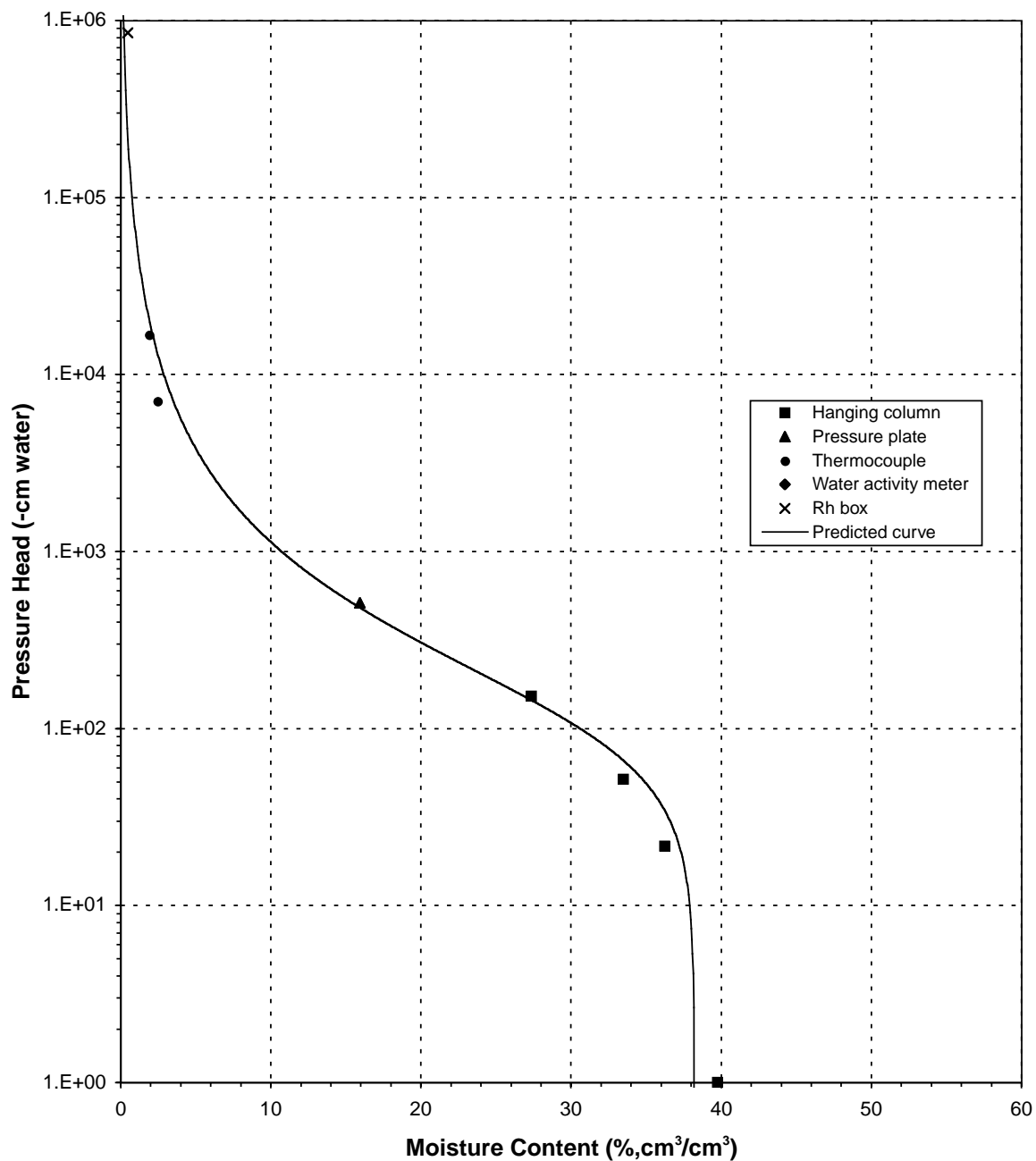




Daniel B. Stephens & Associates, Inc.

Predicted Water Retention Curve and Data Points

Sample Number: CACV-98-0049

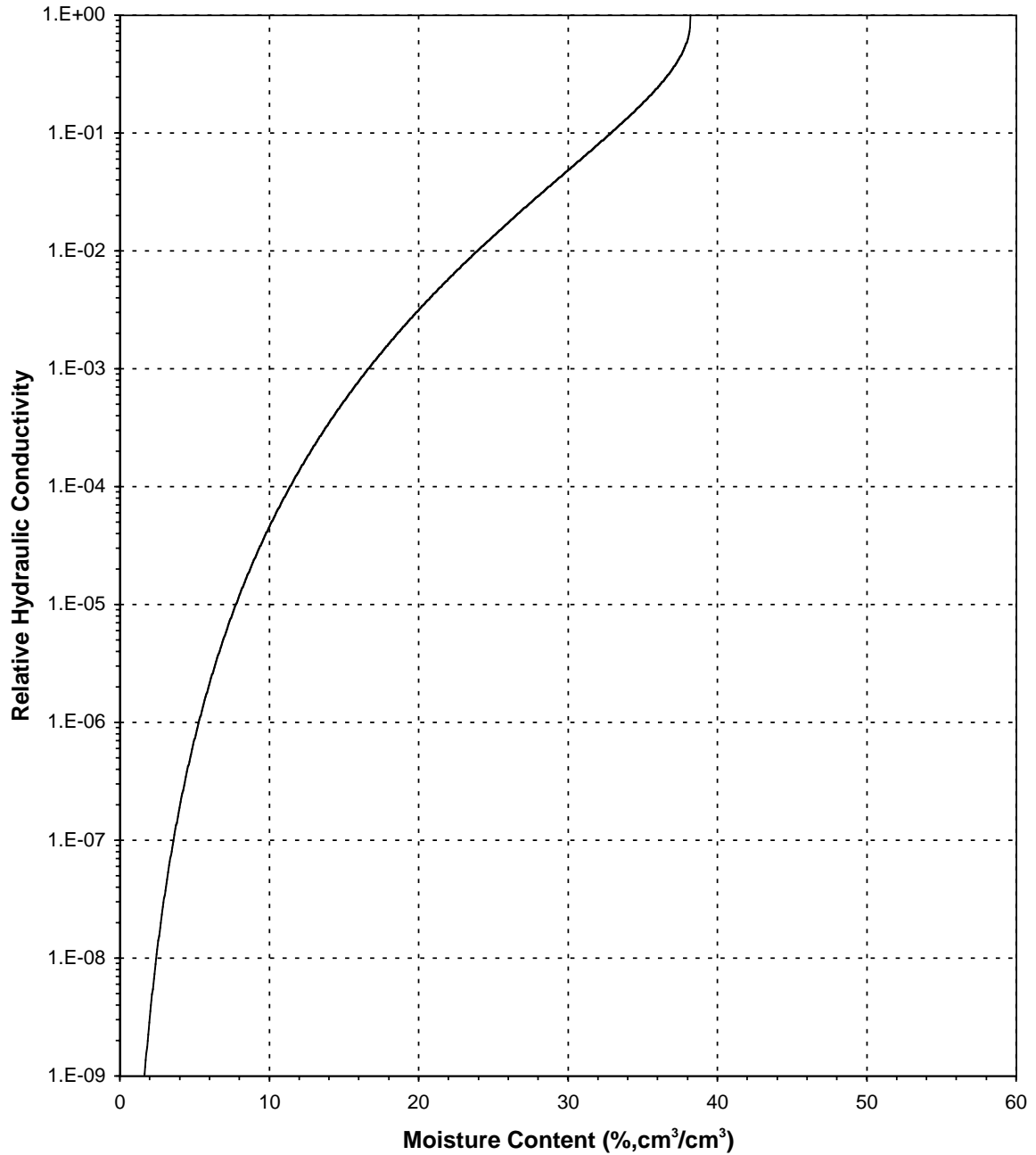




Daniel B. Stephens & Associates, Inc.

Plot of Relative Hydraulic Conductivity vs Moisture Content

Sample Number: CACV-98-0049

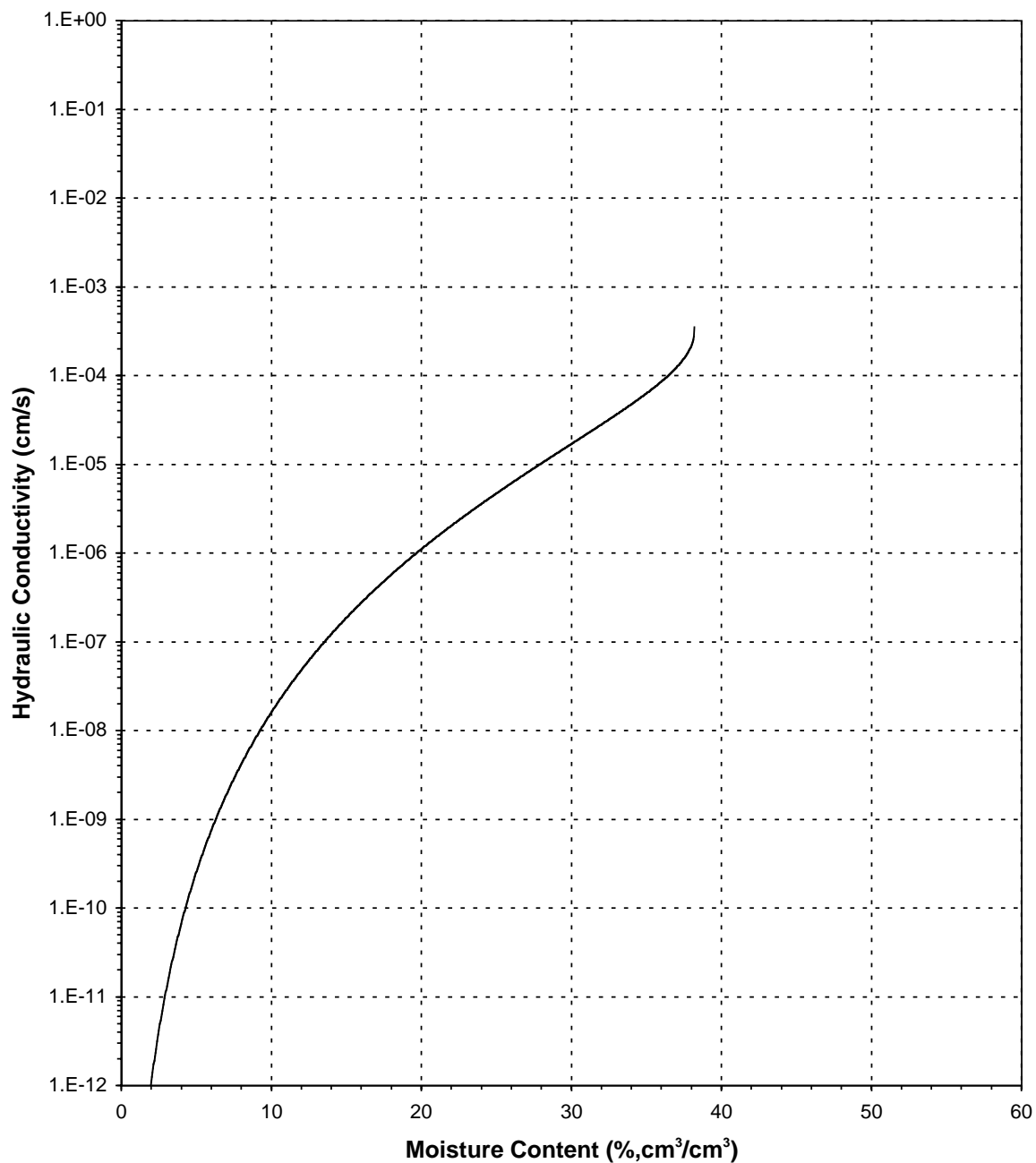




Daniel B. Stephens & Associates, Inc.

Plot of Hydraulic Conductivity vs Moisture Content

Sample Number: CACV-98-0049

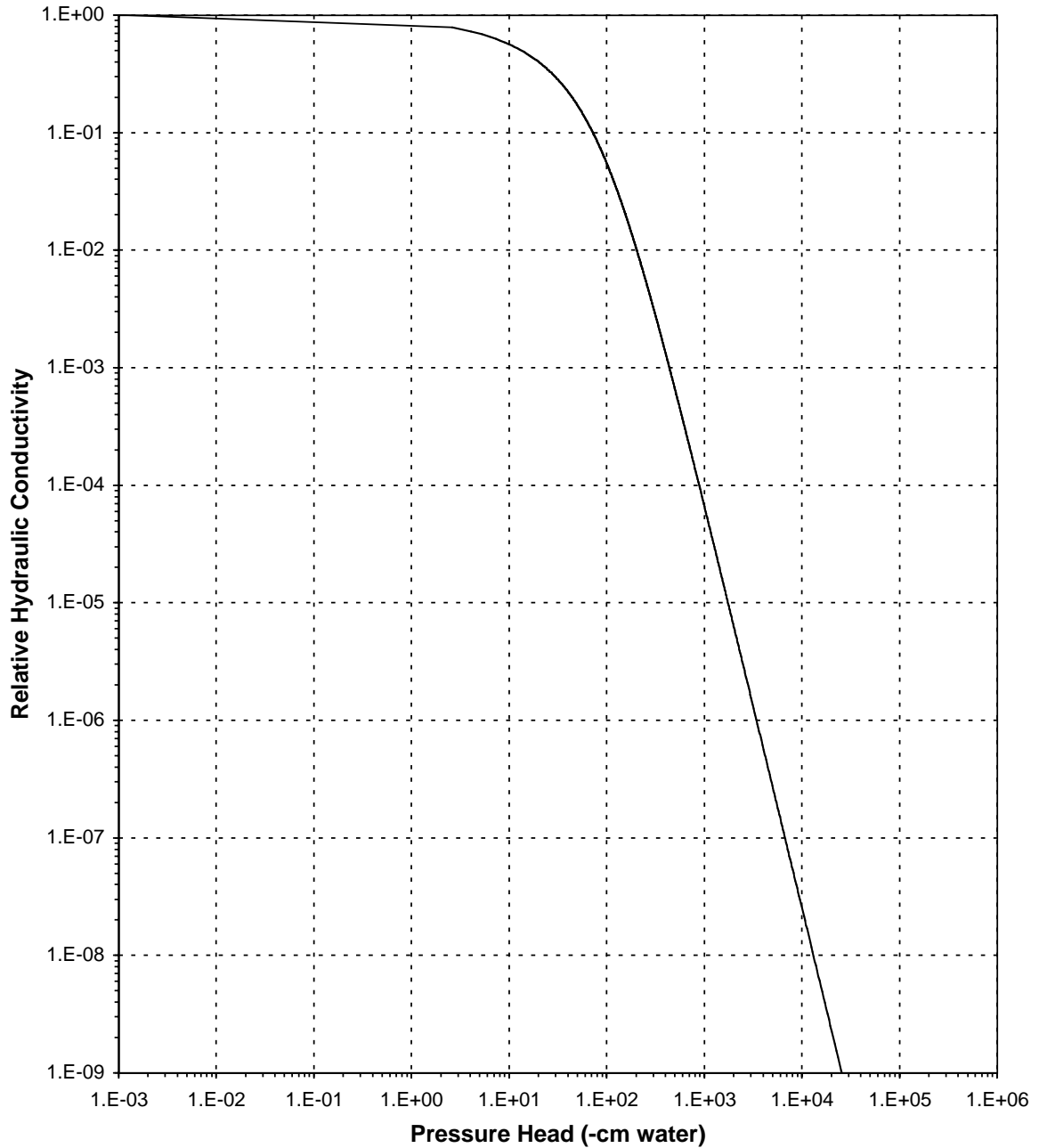




Daniel B. Stephens & Associates, Inc.

Plot of Relative Hydraulic Conductivity vs Pressure Head

Sample Number: CACV-98-0049

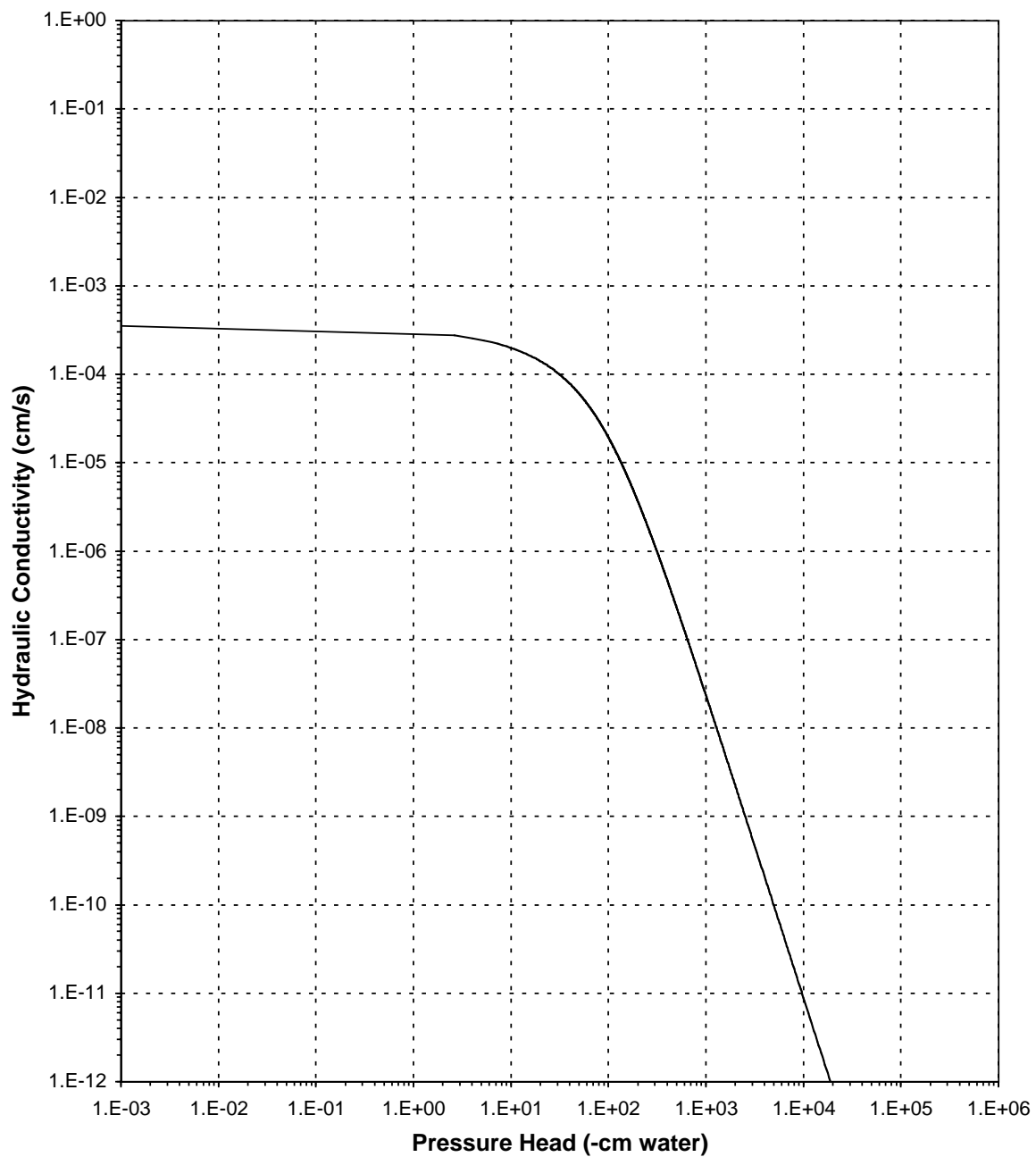




Daniel B. Stephens & Associates, Inc.

Plot of Hydraulic Conductivity vs Pressure Head

Sample Number: CACV-98-0049



Appendix G

*Groundwater Screening Samples
Collected While Drilling R-25 Borehole*

Depth	Date	Ag (ppm)	Al (ppm)	Std. D. (+/-)	Alk(Lab) (ppm CaCO ₃)	As (ppm)	B (ppm)	Std. D. (+/-)	Ba (ppm)	Std. D. (+/-)	Be (ppm)	Std. D. (+/-)	Br (ppm)	Ca (ppm)	Std. D. (+/-)
747' dissolved	09/30/98	<0.001	0.07	0.01	70.0	0.0001	0.12	0.01	0.006	0.001	<0.002	—	0.05	17.0	0.1
747' total	09/30/98	<0.001	27.3	0.1	72.4	0.0024	0.15	0.01	0.12	0.01	0.012	0.001	0.05	21.8	0.1
867' dissolved	10/09/98	<0.001	<0.02	—	58.0	<0.0001	0.058	0.003	0.005	0.001	<0.002	—	0.05	13.8	0.1
867' total	10/09/98	<0.001	10.7	0.1	59.3	0.0013	0.087	0.002	0.11	0.01	0.002	0.001	0.05	16.6	0.2
1,047' dissolved	10/28/98	<0.001	0.04	0.01	57.5	<0.0001	0.090	0.002	0.007	0.001	<0.002	—	0.07	14.6	0.1
1,047' total	10/28/98	<0.001	10.0	0.1	59.1	0.0012	0.095	0.003	0.15	0.01	0.002	0.001	0.07	18.2	0.1
1,137' dissolved	11/03/98	<0.001	0.19	0.02	60.7	0.0003	0.074	0.002	0.005	0.001	<0.002	—	0.07	6.47	0.04
1,137' total	11/03/98	<0.001	124	1	95.1	0.017	0.097	0.004	1.26	0.01	0.010	0.001	0.06	47.0	0.1
1,184' dissolved	12/02/98	<0.001	0.02	0.01	50.5	0.0003	0.027	0.002	0.008	0.001	<0.002	—	0.05	11.0	0.1
1,184' total	12/02/98	<0.001	13.2	0.1	53.0	0.0041	0.021	0.003	0.13	0.01	<0.002	—	0.05	15.4	0.1
1,286' dissolved	12/18/98	<0.001	0.03	0.01	54.7	0.0001	0.014	0.001	0.014	0.001	<0.002	—	0.02	8.70	0.02
1,286' total	12/18/98	<0.001	199	2	62.5	0.015	0.013	0.003	1.75	0.01	0.009	0.001	0.02	45.1	0.3
1,407' dissolved	01/07/99	<0.001	0.10	0.01	53.0	0.0003	0.087	0.001	0.016	0.001	<0.002	—	0.04	12.1	0.1
1,407' total	01/07/99	<0.001	45.9	0.1	57.7	0.012	0.10	0.01	0.26	0.01	0.004	0.001	0.05	31.3	0.3
1,507' dissolved	01/13/99	<0.001	0.04	0.01	46.9	<0.0001	0.037	0.001	0.010	0.001	<0.002	—	0.02	7.83	0.04
1,507' total	01/13/99	<0.001	27.7	0.1	51.6	0.0041	0.032	0.004	0.21	0.01	<0.002	—	0.02	13.4	0.1
1,607' dissolved	02/03/99	<0.001	0.05	0.01	48.1	0.0001	0.027	0.002	0.014	0.001	<0.002	—	0.03	9.53	0.04
1,607' total	02/03/99	<0.001	15.7	0.1	51.1	0.0038	0.024	0.007	0.18	0.01	<0.002	—	0.04	15.9	0.1
1,747' dissolved	02/12/99	<0.001	<0.02	—	46.5	0.0008	0.011	0.001	0.013	0.001	<0.002	—	0.01	7.32	0.07
1,747' total	02/12/99	<0.001	2.14	0.01	48.3	0.0018	0.012	0.002	0.042	0.001	<0.002	—	0.01	8.31	0.08
1,867' dissolved	02/20/99	<0.001	0.07	0.01	44.2	0.0004	0.010	0.001	0.009	0.001	<0.002	—	0.02	5.89	0.01
1,867' total	02/20/99	<0.001	3.39	0.04	45.1	0.0018	0.010	0.002	0.045	0.001	<0.002	—	0.02	7.11	0.08
1,940' dissolved	02/23/99	<0.001	0.41	0.01	52.0	0.0002	0.013	0.002	0.015	0.001	<0.002	—	0.03	10.9	0.1
1,940' total	02/23/99	<0.001	21.2	0.3	53.7	0.0025	0.014	0.003	0.17	0.01	<0.002	—	0.03	15.6	0.1
1,942' dissolved	02/26/99	<0.001	0.03	0.01	47.4	0.0004	0.016	0.003	0.006	0.001	<0.002	—	0.01	7.08	0.01
1,942' total	02/26/99	<0.001	3.67	0.03	46.8	0.0024	0.016	0.005	0.045	0.001	<0.002	—	0.01	8.23	0.02

Depth	Date	Cd (ppm)	Std. D. (+/-)	Cl (ppm)	ClO ₃ (ppm)	Co (ppm)	Std. D. (+/-)	CO ₃ (ppm)	Cond.(L) (μS/cm)	Cr (ppm)	Std. D. (+/-)	Cs (ppm)	Std. D. (+/-)	Cu (ppm)	Std. D. (+/-)
747' dissolved	09/30/98	<0.001	—	11.1	<0.02	0.005	0.002	0	197	<0.002	—	<0.002	—	0.003	0.002
747' total	09/30/98	0.0019	0.0002	11.0	<0.02	0.010	0.002	0	199	0.026	0.002	0.002	—	0.033	0.002
867' dissolved	10/09/98	0.0023	0.0002	9.80	<0.02	<0.002	—	0	171	<0.002	—	<0.002	—	0.006	0.002
867' total	10/09/98	0.0088	0.0002	9.76	<0.02	0.006	0.002	0	171	0.023	0.002	<0.002	—	0.021	0.002
1,047' dissolved	10/28/98	<0.001	—	9.13	<0.02	<0.002	—	0	166	<0.002	—	<0.002	—	0.014	0.002
1,047' total	10/28/98	<0.001	—	9.22	<0.02	0.006	0.002	0	166	0.021	0.002	<0.002	—	0.024	0.002
1,137' dissolved	11/03/98	<0.001	—	8.04	<0.02	<0.002	—	0	175	<0.002	—	<0.002	—	0.003	0.002
1,137' total	11/03/98	0.0011	0.0002	7.83	<0.02	0.028	0.004	0	202	0.17	0.01	0.013	0.002	0.56	0.02
1,184' dissolved	12/02/98	<0.001	—	5.79	<0.02	<0.002	—	0	147	<0.002	—	<0.002	—	0.013	0.002
1,184' total	12/02/98	<0.001	—	5.74	<0.02	0.008	0.002	0	155	0.072	0.005	0.006	0.002	0.20	0.01
1,286' dissolved	12/18/98	<0.001	—	1.09	<0.02	<0.002	—	0	116	<0.002	—	<0.002	—	<0.002	—
1,286' total	12/18/98	<0.001	—	1.09	<0.02	0.026	0.002	0	126	0.11	0.01	0.023	0.002	0.24	0.02
1,407' dissolved	01/07/99	<0.001	—	8.03	<0.02	<0.002	—	0	154	<0.002	—	<0.002	—	<0.002	—
1,407' total	01/07/99	<0.001	—	8.00	<0.02	0.012	0.002	0	161	0.11	0.01	0.003	0.002	0.12	0.01
1,507' dissolved	01/13/99	<0.001	—	3.80	<0.02	<0.002	—	0	117	<0.002	—	<0.002	—	0.005	0.002
1,507' total	01/13/99	<0.001	—	3.74	<0.02	0.008	0.002	0	121	0.044	0.004	0.006	0.002	0.12	0.01
1,607' dissolved	02/03/99	<0.001	—	2.49	<0.02	<0.002	—	0	117	<0.002	—	<0.002	—	0.002	0.002
1,607' total	02/03/99	<0.001	—	2.44	<0.02	0.006	0.002	0	117	0.22	0.02	<0.002	—	0.072	0.005
1,747' dissolved	02/12/99	<0.001	—	1.54	<0.02	<0.002	—	0	106	<0.002	—	<0.002	—	0.003	0.002
1,747' total	02/12/99	<0.001	—	1.53	<0.02	0.002	0.002	0	106	0.17	0.02	<0.002	—	0.026	0.002
1,867' dissolved	02/20/99	<0.001	—	1.65	<0.02	<0.002	—	0	101	<0.002	—	<0.002	—	0.004	0.002
1,867' total	02/20/99	<0.001	—	1.65	<0.02	0.003	0.002	0	101	0.089	0.004	<0.002	—	0.032	0.002
1,940' dissolved	02/23/99	<0.001	—	2.15	<0.02	0.002	0.002	0	120	<0.002	—	<0.002	—	<0.002	—
1,940' total	02/23/99	<0.001	—	2.16	<0.02	0.006	0.002	0	120	0.034	0.002	0.006	0.002	0.07	0.01
1,942' dissolved	02/26/99	<0.001	—	1.77	<0.02	<0.002	—	0	105	<0.002	—	<0.002	—	<0.002	—
1,942' total	02/26/99	<0.001	—	1.75	<0.02	0.003	0.002	0	105	0.046	0.002	0.003	0.002	0.027	0.002

March 2002

G-2

ER2001-0697

Depth	Date	F (ppm)	Fe (ppm)	Std. D. (+/-)	Hardness (ppm)	HCO ₃ (ppm)	Hg (ppm)	I (ppm)	K (ppm)	Std. D. (+/-)	Li (ppm)	Std. D. (+/-)	Mg (ppm)	Std. D. (+/-)
747' dissolved	09/30/98	0.17	0.04	0.01	70.5	85.4	0.00005	<0.01	2.59	0.01	0.02	0.01	6.82	0.02
747' total	09/30/98	0.17	30.5	0.3	96.4	88.3	0.00007	<0.01	12.8	0.1	0.26	0.01	10.2	0.1
867' dissolved	10/09/98	0.07	0.02	0.01	56.3	70.8	<0.00002	<0.01	0.77	0.04	<0.01	—	5.30	0.01
867' total	10/09/98	0.07	27.8	0.1	67.9	72.4	<0.00002	<0.01	2.24	0.01	0.02	0.01	6.43	0.01
1,047' dissolved	10/28/98	0.07	0.05	0.01	58.2	70.2	<0.00002	<0.01	0.7	0.1	0.02	0.01	5.29	0.03
1,047' total	10/28/98	0.09	16.8	0.1	70.6	72.1	<0.00002	<0.01	2.2	0.1	0.02	0.01	6.10	0.02
1,137' dissolved	11/03/98	0.12	0.13	0.01	25.8	74.1	<0.00002	<0.01	2.07	0.06	0.02	0.01	2.35	0.02
1,137' total	11/03/98	0.14	150	1	208.8	116	0.00018	<0.01	13.3	0.1	0.10	0.01	22.2	0.2
1,184' dissolved	12/02/98	0.03	<0.01	—	41.0	61.6	<0.00002	<0.01	2.17	0.01	0.04	0.01	3.29	0.01
1,184' total	12/02/98	0.04	34.3	0.2	60.4	64.7	<0.00002	<0.01	4.46	0.01	0.05	0.01	5.32	0.01
1,286' dissolved	12/18/98	0.10	0.02	0.01	33.4	66.7	0.00006	<0.01	1.54	0.01	0.02	0.01	2.84	0.04
1,286' total	12/18/98	0.12	123	1	184	76.3	0.00008	<0.01	16.0	0.1	0.17	0.01	17.4	0.1
1,407' dissolved	01/07/99	0.09	0.17	0.01	48.6	64.7	<0.00002	<0.01	1.59	0.03	<0.01	—	4.47	0.01
1,407' total	01/07/99	0.10	80.9	0.6	140	70.4	0.00005	<0.01	4.29	0.01	0.03	0.01	14.9	0.1
1,507' dissolved	01/13/99	0.06	0.07	0.01	31.6	57.2	0.00005	<0.01	1.34	0.01	0.01	0.01	2.92	0.02
1,507' total	01/13/99	0.09	95.9	0.1	60.0	62.9	0.00005	<0.01	4.03	0.01	0.03	0.01	6.44	0.03
1,607' dissolved	02/03/99	0.06	0.12	0.01	36.8	58.7	<0.00002	<0.01	1.30	0.03	0.02	0.01	3.15	0.02
1,607' total	02/03/99	0.07	47.2	0.2	59.1	62.3	<0.00002	<0.01	2.97	0.02	0.02	0.01	4.70	0.01
1,747' dissolved	02/12/99	0.12	1.75	0.02	28.6	56.7	<0.00002	<0.01	2.01	0.01	0.02	0.01	2.50	0.01
1,747' total	02/12/99	0.16	11.7	0.1	32.1	58.9	<0.00002	<0.01	2.17	0.01	0.03	0.01	2.76	0.01
1,867' dissolved	02/20/99	0.16	0.61	0.02	23.3	53.9	0.00002	<0.01	2.60	0.01	0.02	0.01	2.09	0.01
1,867' total	02/20/99	0.18	14.8	0.1	28.3	55.0	0.00005	<0.01	2.94	0.02	0.02	0.01	2.57	0.03
1,940' dissolved	02/23/99	0.06	0.76	0.01	41.8	63.5	<0.00002	<0.01	1.18	0.02	0.01	0.01	3.54	0.01
1,940' total	02/23/99	0.06	41.7	0.6	67.4	65.5	0.00005	<0.01	3.32	0.03	0.02	0.01	6.91	0.01
1,942' dissolved	02/26/99	0.14	0.52	0.01	28.4	57.8	<0.00002	<0.01	2.78	0.01	0.01	0.01	2.61	0.02
1,942' total	02/26/99	0.14	28.7	0.5	33.4	57.1	<0.00002	<0.01	3.23	0.02	0.02	0.01	3.12	0.02

ER2001-0697

G-3

March 2002

Depth	Date	Mn (ppm)	Std. D. (+/-)	Mo (ppm)	Std. D. (+/-)	Na (ppm)	Std. D. (+/-)	NH ₄ (ppm)	Ni (ppm)	Std. D. (+/-)	NO ₂ (ppm)	NO ₃ (ppm)	Oxalate (ppm)	Pb (ppm)	Std. D. (+/-)
747' dissolved	09/30/98	1.39	0.01	0.006	0.002	11.5	0.1	0.03	0.016	0.002	<0.02	4.17	<0.02	<0.002	—
747' total	09/30/98	2.27	0.01	0.018	0.002	22.0	0.1	0.04	0.032	0.002	<0.02	4.14	<0.02	0.040	0.004
867' dissolved	10/09/98	0.27	0.01	<0.002	—	12.9	0.1	0.03	0.007	0.002	<0.02	4.02	<0.02	<0.002	—
867' total	10/09/98	0.77	0.01	0.008	0.002	13.7	0.1	<0.02	0.029	0.002	<0.02	3.37	<0.02	0.008	0.002
1,047' dissolved	10/28/98	0.19	0.01	<0.002	—	12.4	0.1	0.05	0.004	0.002	<0.02	3.55	<0.02	<0.002	—
1,047' total	10/28/98	0.77	0.01	0.009	0.002	13.4	0.1	0.13	0.012	0.002	<0.02	2.93	<0.02	0.008	0.002
1,137' dissolved	11/03/98	0.11	0.01	<0.002	—	29.2	0.4	0.08	<0.002	—	<0.02	3.84	<0.02	<0.002	—
1,137' total	11/03/98	5.44	0.01	0.023	0.002	33.1	0.2	0.74	0.13	0.01	<0.02	<0.02	<0.02	0.18	0.01
1,184' dissolved	12/02/98	0.18	0.01	0.002	0.002	13.9	0.1	0.18	0.018	0.002	<0.02	3.32	0.82	<0.002	—
1,184' total	12/02/98	0.49	0.01	0.022	0.002	15.0	0.1	0.19	0.083	0.004	<0.02	3.37	0.81	0.028	0.002
1,286' dissolved	12/18/98	0.25	0.01	0.046	0.004	11.9	0.1	<0.02	0.002	0.002	<0.02	1.70	0.05	<0.002	—
1,286' total	12/18/98	2.14	0.03	0.055	0.004	28.6	0.3	0.02	0.19	0.01	<0.02	1.41	0.10	0.089	0.005
1,407' dissolved	01/07/99	0.21	0.01	0.007	0.002	12.6	0.1	<0.02	0.005	0.002	<0.02	2.38	<0.02	<0.002	—
1,407' total	01/07/99	0.95	0.01	0.044	0.002	15.2	0.1	0.04	0.072	0.004	0.05	2.25	<0.02	0.056	0.004
1,507' dissolved	01/13/99	0.19	0.01	0.017	0.002	12.5	0.1	<0.02	0.003	0.002	<0.02	1.31	0.16	0.002	0.002
1,507' total	01/13/99	0.96	0.01	0.048	0.004	13.3	0.1	<0.02	0.050	0.004	<0.02	1.22	0.13	0.028	0.002
1,607' dissolved	02/03/99	0.19	0.01	0.014	0.002	9.98	0.04	<0.02	0.009	0.002	<0.02	1.86	0.06	<0.002	—
1,607' total	02/03/99	0.51	0.01	0.048	0.004	12.7	0.1	<0.02	0.12	0.01	<0.02	1.82	0.05	0.083	0.005
1,747' dissolved	02/12/99	0.10	0.01	0.007	0.002	11.0	0.1	<0.02	0.011	0.002	<0.01	1.86	0.07	0.061	0.004
1,747' total	02/12/99	0.17	0.01	0.018	0.002	10.9	0.1	<0.02	0.078	0.002	<0.01	1.35	0.02	0.089	0.005
1,867' dissolved	02/20/99	0.11	0.01	0.006	0.002	10.9	0.1	<0.02	0.020	0.002	<0.02	1.93	0.11	0.004	0.002
1,867' total	02/20/99	0.20	0.01	0.019	0.002	11.1	0.1	<0.02	0.050	0.004	0.13	0.88	<0.02	0.11	0.01
1,940' dissolved	02/23/99	0.14	0.01	0.003	0.002	9.35	0.03	<0.02	<0.002	—	<0.02	1.81	<0.02	<0.002	—
1,940' total	02/23/99	0.69	0.01	0.024	0.002	10.7	0.1	<0.02	0.027	0.002	<0.02	1.69	<0.02	0.021	0.002
1,942' dissolved	02/26/99	0.30	0.01	0.030	0.002	10.1	0.1	<0.02	0.003	0.002	<0.01	1.53	<0.02	<0.002	—
1,942' total	02/26/99	0.54	0.01	0.062	0.002	10.3	0.1	<0.02	0.017	0.002	0.12	1.11	<0.02	0.020	0.002

March 2002

G-4

ER2001-0697

Depth	Date	pH (Lab)	PO ₄ (ppm)	Rb (ppm)	Std. D. (+/-)	Sb (ppm)	Se (ppm)	Si (ppm)	Std. D. (+/-)	SiO ₂ (ppm calc)	SO ₄ (ppm)	S ₂ O ₃ (ppm)	Sn (ppm)	Std. D. (+/-)
747' dissolved	09/30/98	7.69	<0.05	0.012	0.002	0.0005	<0.0001	20.7	0.1	44.3	9.66	<0.01	<0.005	—
747' total	09/30/98	7.35	<0.05	0.12	0.01	0.0006	0.0002	78.5	0.1	168	9.61	<0.01	0.014	0.005
867' dissolved	10/09/98	7.52	<0.05	0.005	0.002	0.0001	<0.0001	18.4	0.1	39.4	8.93	<0.01	<0.005	—
867' total	10/09/98	7.37	<0.05	0.018	0.002	0.0004	<0.0001	41.6	0.1	89.0	8.90	<0.01	<0.005	—
1,047' dissolved	10/28/98	7.74	<0.05	0.003	0.002	0.0002	<0.0001	25.1	0.2	53.7	7.87	<0.01	<0.005	—
1,047' total	10/28/98	7.29	<0.05	0.018	0.002	0.0002	<0.0001	41.0	0.1	87.7	8.00	<0.01	<0.005	—
1,137' dissolved	11/03/98	7.92	<0.05	0.004	0.002	0.0008	<0.0001	21.1	0.1	45.2	10.8	<0.01	<0.005	—
1,137' total	11/03/98	7.63	<0.05	0.12	0.01	0.0008	0.0001	122	1	261	11.1	<0.01	<0.005	—
1,184' dissolved	12/02/98	7.38	0.07	0.002	0.002	0.0002	<0.0001	20.2	0.2	43.2	7.49	<0.01	<0.005	—
1,184' total	12/02/98	7.14	0.07	0.031	0.002	0.0008	<0.0001	46.6	0.1	99.7	7.51	<0.01	<0.005	—
1,286' dissolved	12/18/98	7.12	<0.05	0.002	0.002	0.0003	<0.0001	15.9	0.2	34.0	4.17	<0.01	<0.005	—
1,286' total	12/18/98	7.38	<0.05	0.13	0.01	0.0008	0.0001	66.6	0.4	143	4.42	<0.01	<0.005	—
1,407' dissolved	01/07/99	7.40	<0.05	0.002	0.002	0.0002	<0.0001	20.7	0.1	44.3	7.44	<0.01	<0.005	—
1,407' total	01/07/99	6.96	<0.05	0.028	0.002	0.0006	<0.0001	116	1	248	7.56	<0.01	<0.005	—
1,507' dissolved	01/13/99	7.39	<0.05	0.002	0.002	0.0001	<0.0001	5.29	0.01	11.3	4.64	<0.01	<0.005	—
1,507' total	01/13/99	7.43	<0.05	0.026	0.002	0.0007	<0.0001	63.9	0.1	137	4.63	<0.01	<0.005	—
1,607' dissolved	02/03/99	7.24	<0.05	0.002	0.002	0.0003	<0.0001	17.5	0.1	37.5	3.77	<0.01	<0.005	—
1,607' total	02/03/99	6.80	<0.05	0.013	0.002	0.0057	<0.0001	45.7	0.1	97.8	3.80	<0.01	<0.005	—
1,747' dissolved	02/12/99	7.14	<0.02	0.003	0.002	0.0010	<0.0001	28.1	0.1	60.1	1.50	<0.01	<0.005	—
1,747' total	02/12/99	6.94	<0.02	0.006	0.002	0.0073	<0.0001	32.4	0.1	69.3	1.49	<0.01	<0.005	—
1,867' dissolved	02/20/99	7.40	<0.05	0.005	0.002	0.0007	<0.0001	28.4	0.2	60.8	1.55	<0.01	<0.005	—
1,867' total	02/20/99	6.83	<0.05	0.007	0.002	0.0069	<0.0001	36.6	0.3	78.3	1.59	<0.01	<0.005	—
1,940' dissolved	02/23/99	7.45	<0.05	0.004	0.002	0.0001	<0.0001	28.1	0.1	60.1	3.56	<0.01	<0.005	—
1,940' total	02/23/99	7.48	<0.05	0.013	0.002	0.0008	0.0004	75.5	0.1	162	3.58	<0.01	<0.005	—
1,942' dissolved	02/26/99	7.46	<0.02	0.007	0.002	0.0003	<0.0001	25.0	0.1	53.5	2.45	<0.01	<0.005	—
1,942' total	02/26/99	6.98	<0.02	0.009	0.002	0.0008	0.0001	36.0	0.1	77.0	2.49	<0.01	<0.005	—

ER2001-0697

G-5

March 2002

Depth	Date	Sr (ppm)	Std. D. (+/-)	Ti (ppm)	Std. D. (+/-)	TI (ppm)	Std. D. (+/-)	V (ppm)	Std. D. (+/-)	Zn (ppm)	Std. D. (+/-)	TDS (ppm)	Cation Sum	Anion Sum	Percent Balance
747' dissolved	09/30/98	0.12	0.01	<0.002	—	<0.002	—	<0.002	—	<0.01	—	265.1	2.044	1.996	+2.34
747' total	09/30/98	0.20	0.01	0.42	0.01	<0.002	—	0.011	0.001	0.19	0.01	n/a ^a	8.017	2.041	n/a
867' dissolved	10/09/98	0.10	0.01	<0.002	—	<0.002	—	<0.002	—	<0.01	—	222.6	1.720	1.695	+1.49
867' total	10/09/98	0.15	0.01	0.23	0.01	<0.002	—	0.009	0.001	0.08	0.01	n/a	4.731	1.710	n/a
1,047' dissolved	10/28/98	0.11	0.01	<0.002	—	<0.002	—	<0.002	—	0.02	0.01	236.4	1.744	1.638	+6.26
1,047' total	10/28/98	0.17	0.01	0.28	0.01	<0.002	—	0.009	0.003	0.14	0.01	n/a	4.111	1.666	n/a
1,137' dissolved	11/03/98	0.051	0.001	0.003	0.001	<0.002	—	0.011	0.001	<0.01	—	208.7	1.880	1.739	+7.79
1,137' total	11/03/98	0.60	0.01	1.84	0.01	0.003	0.002	0.10	0.01	0.60	0.01	n/a	28.074	2.365	n/a
1,184' dissolved	12/02/98	0.079	0.001	<0.002	—	<0.002	—	<0.002	—	0.34	0.01	194.7	1.517	1.387	+8.90
1,184' total	12/02/98	0.15	0.01	0.33	0.01	<0.002	—	0.010	0.001	1.67	0.01	n/a	5.373	1.438	n/a
1,286' dissolved	12/18/98	0.056	0.001	<0.002	—	<0.002	—	<0.002	—	<0.01	—	166.7	1.243	1.245	-0.16
1,286' total	12/18/98	0.57	0.01	7.85	0.02	<0.002	—	0.075	0.001	0.33	0.01	n/a	34.195	1.403	n/a
1,407' dissolved	01/07/99	0.11	0.01	<0.002	—	<0.002	—	<0.002	—	0.01	0.01	207.1	1.591	1.490	+6.57
1,407' total	01/07/99	0.35	0.01	0.49	0.01	<0.002	—	0.034	0.002	0.34	0.01	n/a	13.066	1.585	n/a
1,507' dissolved	01/13/99	0.048	0.003	<0.002	—	<0.002	—	<0.002	—	0.02	0.01	135.1	1.227	1.168	+4.97
1,507' total	01/13/99	0.12	0.01	0.80	0.01	<0.002	—	0.012	0.001	0.10	0.01	n/a	10.155	1.259	n/a
1,607' dissolved	02/03/99	0.057	0.001	<0.002	—	<0.002	—	<0.002	—	0.03	0.01	165.7	1.226	1.146	+6.77
1,607' total	02/03/99	0.15	0.01	0.39	0.01	<0.002	—	0.007	0.001	0.43	0.01	n/a	6.128	1.204	n/a
1,747' dissolved	02/12/99	0.045	0.001	<0.002	—	<0.002	—	0.003	0.001	0.08	0.01	175.4	1.060	1.041	+1.74
1,747' total	02/12/99	0.058	0.001	0.064	0.001	<0.002	—	0.007	0.002	0.28	0.01	n/a	2.058	1.071	n/a
1,867' dissolved	02/20/99	0.039	0.001	0.002	0.001	<0.002	—	<0.002	—	0.02	0.01	165.8	1.055	1.003	+5.10
1,867' total	02/20/99	0.054	0.001	0.11	0.01	<0.002	—	0.005	0.003	0.18	0.01	n/a	2.314	1.009	n/a
1,940' dissolved	02/23/99	0.071	0.001	0.019	0.001	<0.002	—	<0.002	—	<0.01	—	199.5	1.367	1.209	+12.22
1,940' total	02/23/99	0.13	0.01	0.69	0.01	<0.002	—	0.012	0.002	0.08	0.01	n/a	6.532	1.241	n/a
1,942' dissolved	02/26/99	0.040	0.001	<0.002	—	<0.002	—	<0.002	—	<0.01	—	169.2	1.123	1.082	+3.80
1,942' total	02/26/99	0.056	0.001	0.12	0.01	<0.002	—	0.005	0.004	0.04	0.01	n/a	3.172	1.066	n/a

Note: The data in this table should be used only for screening purposes. All analyses performed at EES-6 aqueous chemistry laboratory. Std. D. means a one sigma standard deviation. Dissolved means filtered through 0.45-µm membrane. Total means nonfiltered.

^a n/a = not applicable.

March 2002

G-6

ER2001-0697

Appendix H

Geochemical Calculations and Constraints

H-1.0 MOBILITY OF RDX AND TNT

Concentrations of RDX and TNT found in the upper saturated zone and possibly in the regional aquifer in the R-25 borehole exceeded EPA HA limits for drinking water. The EPA HA limits for RDX and TNT are 0.61 µg/L and 2.2 µg/L, respectively (EPA 2000, 70122). The mobility of these two compounds is predicted to be nearly equal to the rate of groundwater movement at the R-25 site. This appendix provides the basis for that prediction, including calculations for distribution coefficients and retardation factors, sources of estimated values, and constraints on the implications of the calculations.

H-1.1 Distribution Coefficients

The amount or fraction of solid organic carbon (foc) and an organic compound's organic carbon partition coefficient (Koc) (Schwarzenbach et al. 1993, 71318) largely control the adsorption of that compound onto solid organic matter. The Koc values for RDX and TNT are 100 cm³/g and 525 cm³/g, respectively (Burrows et al. 1989, 71319). The foc value for the Otowi Member is estimated to be 0.0005 (0.05 wt%), based on the amount of solid organic carbon measured at R-25 (0.05 wt%). Distribution coefficients (Kd) for RDX and TNT are calculated as follows:

$$K_d = (K_{oc})(f_{oc}) \quad \text{Equation H-1}$$

$$K_{d_{RDX}} = (100 \text{ cm}^3/\text{g})(0.0005) = 5.00 \times 10^{-2} \text{ cm}^3/\text{g} \quad \text{Equation H-2}$$

$$K_{d_{TNT}} = (525 \text{ cm}^3/\text{g})(0.0005) = 0.26 \text{ cm}^3/\text{g} \quad \text{Equation H-3}$$

These coefficients are small, implying that RDX and TNT do not readily adsorb to aquifer material. This is mainly a function of the low amount of solid organic carbon present.

H-1.2 Retardation Factors

The rate of movement of a contaminant relative to the rate of groundwater flow is determined by calculating a retardation factor (Rf) for the contaminant of interest. Non-sorbing chemicals have a retardation factor of unity. Contaminants that adsorb on aquifer material have Rf values greater than unity. Retardation factors for RDX and TNT are calculated from the following equation (Freeze and Cherry 1979, 64057):

$$(Rf) = 1 + \rho K_d / n_e$$

where ρ is the bulk density, and n_e is the effective porosity. Average bulk density and effective porosity values for the Otowi Member were determined by Rogers and Gallaher (1995, 49824) as $1.18 \pm 0.10 \text{ g/cm}^3$ and 0.47 ± 0.05 , respectively. Retardation factors for RDX and TNT are calculated as follows:

$$Rf_{RDX} = 1 + [(1.18 \text{ g/cm}^3)(5.00 \times 10^{-2} \text{ cm}^3/\text{g})/(0.47)] = 1.13 \quad \text{Equation H-4}$$

$$Rf_{TNT} = 1 + [(1.18 \text{ g/cm}^3)(0.26 \text{ cm}^3/\text{g})/(0.47)] = 1.65 \quad \text{Equation H-5}$$

These retardation factors are near unity, implying that RDX and TNT move at nearly the same rate as groundwater.

H-1.3 Implications

The low K_d values for RDX and TNT coupled with the retardation factors near unity imply that these compounds are very mobile in aqueous systems with small amounts of solid organic carbon. Adsorption onto clay minerals, through hydrogen bonding, is also possible, however, but this process is not accounted for with this calculation. The HE compound TNT binds more strongly to clay minerals than does RDX (Spain et al. 2000, 71317)

The travel time for groundwater (regional aquifer) between R-25 and a distance equal to that of the nearest water supply well, PM-2, is estimated to be between 50 and 200 years. This is based on plateau-wide average groundwater flow rates of between 95 and 345 ft per year determined by Purtymun (1995, 45344). However, neither groundwater flow rates nor flow direction in the vicinity of R-25 are yet known.

If groundwater flow from R-25 is in the direction of water supply well PM-2, and RDX or TNT neither adsorb onto aquifer material nor hydrolyze or biodegrade, these contaminants may potentially reach PM-2 within 50 to 200 years.

H-1.4 Constraints on Implications

The K_{oc} values for RDX and TNT are laboratory-derived values taken from published literature and are limited in their application to actual field conditions occurring at the R-25 site.

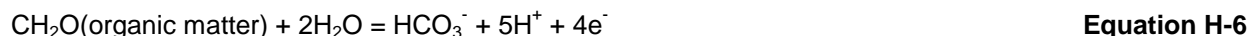
The f_{oc} value was estimated from the solid organic carbon content of one core sample from the Otowi Member of the Bandelier Tuff collected from the R-25 borehole. However, 22 other samples from the Bandelier Tuff collected from the R-15 borehole showed f_{oc} values less than detection (<0.05 wt%). Ideally, f_{oc} values would be obtained for the saturated Puye Formation as well.

The R_f value calculated uses average bulk density and porosity values for the Otowi Member. Ideally, R_f values would be calculated for the regional aquifer materials of the Puye Formation as well.

The implication that RDX or TNT would reach water supply well PM-2 does not take into account hydrolysis reactions, biodegradation, or mixing, which are dependent on site-specific conditions at R-25.

H-2.0 OXIDATION-REDUCTION CHEMISTRIES OF CARBON, IRON, MANGANESE, AND HE COMPOUNDS

This section presents a discussion on the oxidation-reduction chemistry of TNT, RDX, carbon, manganese, and iron. Elevated concentrations of manganese and iron were observed in R-25, probably as a result of the oxidation of DOC, which also enhances reduction (biotransformation) of TNT and possibly RDX. Biotransformation of TNT and RDX occurs through reduction of nitro (R-NO₂) functional groups to amino (R-NH₂) functional groups (Spain et al. 2000, 71317). This reduction of TNT and RDX requires a source of electrons, which may be provided by the oxidation of DOC to bicarbonate. The oxidation half reaction for DOC is given by the following equation:



The E_h of this reaction, at a pH of 7, is equal to -482 mV (Langmuir 1997, 56037).

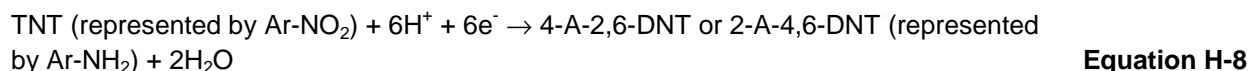
Concentrations of DOC are within the mg/L range, which are sufficient to provide electrons needed for the reduction of TNT and RDX. Concurrently, Mn(IV) solids become reduced to form aqueous Mn(II) species,

which results in elevated concentrations of dissolved manganese (Table 7.2-4). This process is represented by the following reaction:



The Eh for the Mn(IV)/Mn(II) half-cell reaction is equal to +544 mV at a pH of 7 and 1 ppm dissolved manganese (Langmuir 1997, 56037). Mn(II) species dominate at Eh values of +544 mV or less at a pH of 7.

The Eh for the TNT/4-A-2,6-DNT half-cell reaction is equal to -430 mV at a pH of 7 (Hofstetter et al. 1999, 71307). The Eh for the TNT/2-A-4,6-DNT half-cell reaction is equal to -390 mV at a pH of 7 (Hofstetter et al. 1999, 71307). This reduction is represented by the following:



Because the oxidation of DOC to bicarbonate and the transformation of TNT to 4-A-2,6-DNT or 2-A-4,6-DNT occurs at much lower Eh values than does the reduction of Mn(IV) solids to aqueous Mn(II) species, both DOC and HE (TNT) may act as reducing agents (sources of electrons) for Mn(IV). The HE compound TNT initially biodegrades to 4-A-2,6-DNT or 2-A-4,6-DNT followed by the formation of diaminonitrotoluene compounds including 2,4-DA-6-NT or 2,6-DA-4-NT under more reducing conditions (2,4-DA-6-NT, Eh = -515 mV at a pH of 7; 2,6-DA-4-NT, Eh = -495 mV at a pH of 7) (Hofstetter et al. 1999, 71307). Mono amino toluene compounds are present at R-25 (Table 7.2-2) and di amino compounds have not been identified at the R-25 site using the EPA 8330 method.

More analyses for RDX reductive intermediates will be conducted to evaluate the presence or absence of these compounds at the R-25 site. These intermediates include hexahydro-1-nitroso-3,5-dinitro-1,3,5-triazine (MNX), hexahydro-1,3-dinitroso-5-nitro-1,3,5-triazine (DNX), and hexahydro-1,3,5-trinitroso-1,3,5-triazine (TNX).

Based on free energy yields associated with reduction by DOC, the following sequence represents the order of reduction (most oxidizing to most reducing): Mn(IV) \rightarrow Mn(II)(+544 mV); Fe(III) \rightarrow Fe(II)(+14 mV); TNT \rightarrow 2-A-4,6-DNT (-390 mV); and TNT \rightarrow 4-A-2,6-DNT (-430 mV). Reduction of 2-A-4,6-DNT and 4-A-2,6-DNT to 2,4-DA-6-NT and 2,6-DA-4-NT requires even more reducing conditions, such as those produced by hydrogen gas. These conditions do not occur at the R-25 site.

The same reductive process may affect the dissolution of Fe(III) solids by the following reaction:



The Eh for this half-cell reaction is equal to +14 mV at a pH of 7 and 1 ppm dissolved iron (Langmuir 1997, 56037). Ferrous iron is stable below an Eh value of +14 mV at a pH of 7 and one ppm Fe^{2+} .

Dissolved iron concentrations increase with depth in R-25 in both saturated zones (Appendix G), suggesting that iron solids have increasing solubility with depth. It is possible that the solubility of Fe(OH)_3 is controlled by the above redox couple.

This report has been reproduced directly from the best available copy. It is available electronically on the Web (<http://www.doe.gov/bridge>).

Copies are available for sale to U.S. Department of Energy employees and contractors from—

Office of Scientific and Technical Information
P.O. Box 62
Oak Ridge, TN 37831
(865) 576-8401

Copies are available for sale to the public from—

National Technical Information Service
U.S. Department of Commerce
5285 Port Royal Road
Springfield, VA 22616
(800) 553-6847



Los Alamos NM 87545